An Assessment of miRNA Manipulation on Senescence and Ageing Phenotypes *in vitro* and *in vivo*

Submitted by Emad Mohammed O Manni to the University of Exeter as a thesis for the degree of Doctor of Philosophy in Medical Studies, January 2023.

I certify that all material in this thesis which is not my own work has been identified and that any material that has previously been submitted and approved for the award of a degree by this or any other University has been acknowledged.

Signature……

Declaration

I declare that this thesis was authored by myself and has not been submitted for another degree or professional certification. I declare that the work I submitted to the University of Exeter is all my original work, with the exception of a publication in which the study was co-authored. My contribution to this work, as well as the contributions of the other writers, is fully stated here. Co-authors have been explicitly acknowledged in the submitted manuscript for their efforts. The experimental work is almost entirely my own, except for the generation of miRNA profiles and whole transcriptome microarrays (Clariom D), which was performed at UK Bioinformatics by David Chambers.

Abstract

Ageing has been widely described as a progressive functional deterioration of tissues that causes diminished organ function and increased mortality risk. It has been established that the proportion of senescent cells in tissues rises with age in many organs and in age-related illnesses, suggesting that cellular senescence plays a significant role in the functional decline related to ageing. Correspondingly, it has previously been shown in animal models that eliminating senescent cells might mitigate the deleterious consequences of ageing. As a key regulator of several cellular mechanisms, there are microRNAs (miRNAs) known to be associated with senescence. However, miRNAs that may directly trigger or reverse senescence remain to be elucidated.

Here, the first goal of thesis was to identify the miRNA profile of proliferating, senescent, and rescued senescent endothelial cells to determine miRNAs that may be causal or influential of cellular senescence. I found that miR-361-5p not only associated with senescence but also reduced the load of senescent cells *in vitro* in human endothelial cells upon induction in late passage cells. Secondly, *C. elegans* was used to examine the role of miR-361-5p targeted genes on ageing *in vivo.* I found that 56% of genes which were dysregulated *in vitro* adversely affected healthspan and/or lifespan *in vivo*. Finally, a previous finding from our lab (Holly *et al.*, 2015) identified three miRNAs-associated with human ageing and senescence in human primary fibroblasts of which miR-15b-5p may reduce senescence markers and secretory phenotypes (SASP) in the human dermal fibroblast cells.

This thesis presents new miRNAs (miR-361-5p and miR-15b-5p) which may be involved in the aetiology of senescence and may be used in future in ageing intervention.

Table of Contents

List of Figures

List of Tables

List of Abbreviations

Abbreviation	
3'	3-prime end of a nucleic acid molecule
5'	5-prime end of a nucleic acid molecule
AD	Alzheimer's disease
AMPK	AMP-activated protein kinase
ANOVA	Analysis of variance
AS	Alternative splicing
BSA	Bovine serum albumin
C. elegans	*Caenorhabditis elegans*
CDK2	Cyclin dependent kinase 2
CDKN2A	Cyclin Dependent Kinase Inhibitor 2A
cDNA	Complementary DNA
daf2	Insulin-like receptor subunit beta
DDR	DNA damage response
DMEM	Dulbecco's modified eagle medium
DMSO	Dimethylsulfoxide
dNTPs	Deoxyribonucleotide triphosphates
DPBS	Dulbecco's phosphate buffered saline
DR	Dietary restriction
FOXO	Forkhead box O
GO	Gene ontology

H. sAPIENS	*Homo sapiens*
HAoECs	Human aortal endothelial cells
hnRNP	Heterogeneous nuclear ribonucleoproteins
IGF-1	Insulin-like growth factor-1
IIS	Insulin/insulin-like growth factor-1 signalling
lncRNAs	Long non-coding RNAs
miRNA	microRNA
mTOR	Mechanistic target of rapamycin
NAD	Nicotinamide adenine dinucleotide
ncRNAs	Non-coding RNAs
NF-κB	Nuclear factor kappa-light-chain-enhancer of activated B cells
NGS	Next generation sequencing
nHDF	Normal human dermal fibroblast
nt	Nucleotides
PBS	Phosphate buffered saline
PCR	Polymerase chain reaction
PD	Population doubling
PI3K	Phosphatidylinositol-4,5-bisphosphate 3-kinase
piRNA	piwiRNA
pre-miRNA	Pre-micro RNA
pri-miRNA	Pre-micro RNA
PTEN	Phosphatase and tensin homolog

RB 1	Retinoblastoma transcriptional corepressor 1
RBPs	RNA-binding proteins
RIN	RNA Integrity Number
RISC	RNA-induced silencing complex
ROS	Reactive oxygen species
RT	Reverse transcription
RT-qPCR	Real-time quantitative polymerase chain reaction
SAHF	Senescence-associated heterochromatin foci
SASP	Senescence-associated secretory phenotype
SA-β-Gal	Senescence-associated beta-galactosidase
SFs	Splicing factors
SIRT1	Sirtuin-1
snRNA	Small nuclear RNA
TGF-β	Transforming growth factor beta
TUNEL	Terminal deoxynucleotidyl transferase dUTP nick-end labelling
UTRs	Untranslated regions
VEGF	Vascular endothelial growth factor
VEGFR	Vascular endothelial growth factor receptor
ΔCT	Delta threshold cycles value

Acknowledgments

First and foremost, I express my gratitude to Almighty Creator for everything that He has given to me and treated me well, and I am grateful that He is giving me the perseverance, talent, and strength necessary to finish my PhD.

I must express my deep gratitude to Professor Lorna Harries, who serves as my principal supervisor, for her unwavering support and endurance. I also appreciate her for giving me a job in her lab and for being sincere, kind, and supportive of me when I was studying in Exeter. I must also express my profound appreciation to my secondary supervisors, Dr. Timothy Etheridge and Professor Matt Whitemann, for their insightful criticism and contributions. I'd also want to express my gratitude to Dr. Mark Russell for serving as my PGR pastoral tutor. He has consistently offered assistance and helped during my study.

There aren't enough words to adequately explain how grateful I am to the TeamRNA members who helped me immensely throughout my PhD programme at Exeter. Many thanks to Dr. Shahnaz Haque, Dr. Eva Latorre, Dr. Laura Bramwell, Ryan Frankum, Merlin Davies-Abraham, and Zhuofan Mou (Fred), who have all been incredibly helpful colleagues. Dr. Nicola Jeffery is also to be thanked for her explanations and training on cell culture, TAC 4.0 software, and immunocytochemistry. Dr. Ben Lee is also to be thanked for his training and advice on RT-qPCR. Thanks to all of the members of SENISCA Ltd team for their support specially Dr. Sam Gould and ….

In Canada, I started my first PhD in 2017. However, it was unfortunate that a political crisis happened between Saudi Arabia, my scholarship provider, and Canada. Consequently, Saudi students including myself had to relocate to other countries to

complete their studies. During this time, I had learned and professionalized several experiments in cell culture and proteomics thanks to members of professor Ilka Heinemann and Professor Patrick O'Donoghue teams, Matthew Turk, Christina Chung, and Yumin Bi.

Additionally, I would like to thank the Medical School Department staff at the University of Exeter for providing a fantastic and well-run facility for me to do my study. They did a fantastic job, even at a challenging period when the COVID-19 outbreak was in full swing.

Without the financial assistance from Aljouf University in Saudi Arabia, completing my PhD would not have been achievable. I appreciate your kindness and generousness.

Due to the political issue with Saudi Arabia in 2018, I was fortunate to have Professor Ilka Heinemann as my supervisor during my Canadian PhD, which I had to abandon. Her guidance allowed me to get a great deal of lab experience, and because of my work in her lab, I was swiftly able to land another PhD job.

There were many ups and downs when I was pursuing my PhD, but I had a lot of friends who were really helpful when I needed to unwind or deal with stress. Mohammed Baity, who unfortunately passed away a few months before receiving his PhD degree from the Medical School Department. Thanks, also, to Mohammed Sharaheily and Adnan Almasoudy from Exeter University's physics department for the continuous great support, encouragement, and appreciation.

Lastly, I can never be grateful enough to my parents, Mohammed and Fatema. In addition, I want to express my gratitude to my entire family, especially my wife Alanoud, my children

Mohammed, Aylla, and Elias and all of my siblings and sisters, for their support during my PhD journey. From the bottom of my heart, THANK YOU.

Chapter 1

Introduction

1.1 Introduction

The population of older people is increasing worldwide, especially in developed countries like the USA and Europe (United Nations, 2017). This can be attributed to human adaptation and the development of medicines such as vaccination against life-threatening diseases. However, an ageing population results in increases in diseases such as diabetes mellitus, cancer, and many infectious diseases which affect mainly older people. A recent example is the COVID-19 pandemic where thousands of deaths have occurred, predominantly among older people (Lewis *et al.*, 2021). Older people are more susceptible to diseases and one reason may possibly be decline in health and immunity.

1.1.1 Ageing and senescence

Ageing is characterized by a decline in the functioning of tissues and organs, and it is the major leading cause of death worldwide (Armanios *et al.*, 2015). As an ageing person's body systems become less efficient in their functions, a variety of potentially deadly diseases can easily be fatal. Ageing and death are inevitable, but people could reduce the effect of ageing and age well. Mainly, dividing or somatic cells also age and this phenomenon is called senescence; senex means old in Latin (Gorgoulis *et al.*, 2019). The accumulation of senescent cells increases with age, leading to organ dysfunctions. The mechanisms of ageing and senescence are similar yet distinct from one another. The steady decline of how well the body is able to operate is a characteristic of ageing. This may involve both apparent changes like hair loss and wrinkles and internal changes like a higher risk of a chronic diseases.

Senescence serves as an essential cell during development and wound healing (Gorgoulis *et al.*, 2019). Senescence was discovered by Hayflick in relation to the finite proliferative lifespan of dermal fibroblasts in culture. (Hayflick, 1965). Researchers remained sceptical about this discovery for decades and designated it an *in vitro* artifact. Senescence is the state of stable cell cycle arrest as a result of internal and external stress factors (Suh, 2018). Replicative senescence is primarily caused by the shortening of telomeres due to repeated DNA replication and the absence of the enzyme that protects the end of chromosomes, telomerase (Shay & Wright, 2000). The shortening of telomeres stimulates DNA damage response (DDR) and expression of senescence-associated secretory phenotype (SASP), a cocktail of pro-inflammatory cytokines and remodelling proteins. Oncogene-induced senescence, also known as OIS, can stimulate the DDR and cause the cell cycle to be arrested. DDR, however, is not required to drive cells into senescence. Senescence is also known to be caused by epigenetic changes and mitochondrial dysfunction (Campisi *et al.*, 2019). As a defence mechanism, this response is intended to keep cells from transforming into cancerous cells. However, abundance of senescent cells can contribute to the ageing of tissues. For example, paracrine effects of ageing cells drive adjacent cells into senescence, and this leads to the enhancement of multiple age-related diseases (ARD) (Borodkina *et al.*, 2018).

1.1.2 Ageing-Related Diseases (ARD)

Ageing increases the risk of developing and worsening the outcomes of diseases such as cancer, cardiovascular disease, diabetes, osteoarthritis, and neurodegenerative diseases. It was long thought that every age-related disorder was caused by a unique set of triggers, but it has become clear that this may not be the case, and that most

age-related diseases are caused by the progressive failure of a relatively small number of basic health maintenance mechanisms. In elderly patients with ARDs, dysfunction of these pathways occurs, and are also shared in many conditions of premature ageing, such as Hutchinson Gilford Progeria and Werner syndrome (Campisi *et al.*, 2019; López-Otín *et al.*, 2013; Partridge *et al.*, 2018). These observations in diverse tissues and organ systems suggest that ARD share common underpinning mechanisms and pathways (Niccoli & Partridge, 2012).

1.2 Hallmarks of ageing at cellular level

As advances in techniques of molecular biology have emerged in the past few years, several phenomena believed to control the process of ageing have been identified which collectively have been described as the 'hallmarks' of ageing (López-Otín *et al.*, 2013). The hallmarks of ageing have been categorized into primary, antagonistic and integrative markers. Primary hallmarks are direct triggers of ageing processes, whereas antagonistic markers relate to processes or phenotypes that are efficient in early life but are later associated with detrimental effects in late life. The third category are evolved from primary or antagonistic hallmarks and are designated integrative hallmarks. These hallmarks have been reviewed in detail elsewhere (López-Otín *et al.*, 2013). It has been a decade now since this paper was published; hence, several researchers suggested to review and update these hallmarks. In a recent conference, some scientists in the ageing field published the article "New hallmarks of ageing: a 2022 Copenhagen ageing meeting summary" which explained the new evolving hallmarks of ageing compromised autophagy, microbiome disturbance, altered mechanical properties, splicing dysregulation, and inflammation (see figure 1.1)

(Schmauck-Medina *et al.*, 2022). In this thesis, cellular senescence and the hallmarks that are interconnected with it will be discussed in detail in subsections 1.2.1 to 1.2.3.

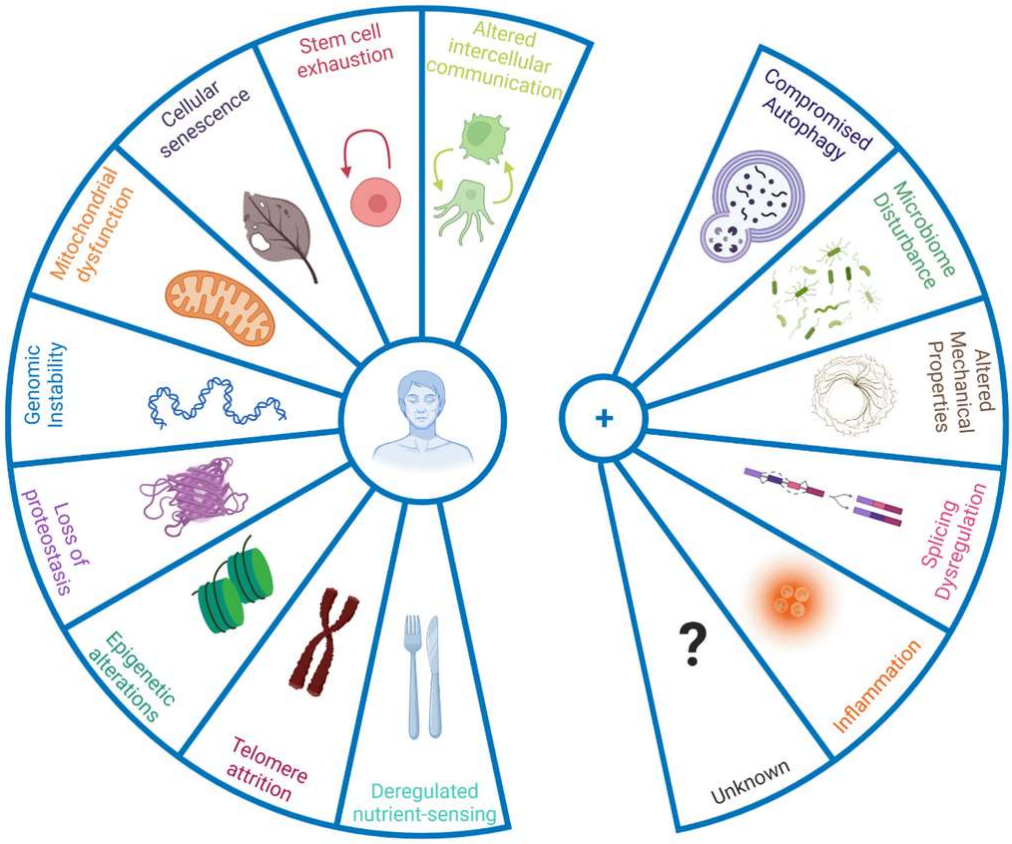

Figure 1.1: Hallmarks of ageing.

The figure includes the original hallmarks of ageing published in (López-Otín *et al.*, 2013) on the lift side as well as the five additional suggested hallmarks discussed in the new paper (Schmauck-Medina *et al.*, 2022) on the right side. The new hallmarks are considered as they serve in ageing intervention that targeting these hallmarks are supposed to, at a minimum, prevent more negative features of aging and enhance phenotypes linked with aging.

1.2.1 Alteration in genome stability and epigenetics

Significant changes to the human genome may occur between birth and old age, for a variety of reasons including environmental stresses and mutation; this is mainly due to modifications of genome during development and also effects on the genome from environmental stressors. Several players affect the accessibility of genes with consequent effects on gene expression including but not limited to DNA methylation and acetylation, chromatin remodelling, post-transcriptional and post-translational modifications, and transcription of noncoding RNAs (ncRNAs) (Harries, 2014; O'Sullivan & Karlseder, 2012). Progeroid diseases that cause people to age faster than normal such as Werner syndrome, and Bloom syndrome have been demonstrated to be caused by accumulation of DNA damage (López-Otín *et al.*, 2013). One main reason was that these patients have compromised DNA repair mechanisms which results in an increased rate of molecular ageing. DNA damage and lesions accumulate through lifespan leading to impairment of tissue functions (López-Otín *et al.*, 2013). Interventions that support proper DNA repair mechanism have consequences for lifespan, as demonstrated by the observation that transgenic mice with overexpression of *BubR1*, a mitotic checkpoint component that supports proper chromosomal segregation and result in increased DNA repair activity in response to double-strand breaks in DNA (Komura *et al.* 2021), have longer healthy lifespans than control mice (Baker *et al.*, 2013).

Epigenetic alterations block the accessibility to genes through changes in DNA methylation, post-translational histone modification, and chromatin remodelling. Age-associated epigenetic markers include increased histone *H4K16* acetylation, *H4K20* trimethylation, or *H3K4* trimethylation, as well as reduced *H3K9* methylation or *H3K27* trimethylation (López-Otín *et al.*, 2013). Another example showing that epigenetics

factors may affect ageing in animals is that nematode worms (histone demethylases, H3K4) and flies (histone demethylases, H3K27) had been longer lived when histone methylation complex components were eliminated. The lifespan of worms can be enhanced by targeting the Insulin/IGF-1 signalling system and suppression of histone demethylases (H3K27) (Jin *et al.*, 2011). Overexpression of *Sir2* (a deacetylase enzyme) has also been demonstrated to improve longevity in *Saccharomyces cerevisiae.* Later studies have shown that higher expression of the worm and fly *Sir2* orthologs may extend lifespan (Wood *et al.*, 2004). These examples suggest that manipulation of crucial genes regulating epigenetics could influence the DNA damage response that accumulate during ageing.

1.2.2 Telomere attrition

Telomere length is also altered during ageing due to the sequential loss of telomere repeat sequences every time the cell divides. Telomeres are a repetitive sequence of $(TTAGGG)_n$ which lie on the terminal arms of human chromosomes. Telomeres are protective shield sequences capping chromosome ends and the lengths of which may indicate the number of cell divisions. At birth, telomere lengths may range from 5,000 to 15,000 bp (Harley *et al.*, 1990). The shelterin complex, a multimer made up of the six protein components *TRF1*, *TRF2*, *TPP1*, *POT1*, *TIN2*, and *RAP1*, is a group of specialised proteins that covers the telomere (O'Connor *et al.*, 2006). The telotypes of people may be determined by the lengths of their parents' telomeres (Aubert & Lansdorp, 2008). Telomerase is an enzyme that increases the length of telomere. Since its discovery by Greider and Blackburn in 1985, which led to the name "telomerase," a new enzyme activity has been discovered that may add DNA repeat sequences to the ends of chromosomes and therefore increase telomere length.

Telomerase is an enzyme that binds to the terminal region of chromosomes and has a catalytic component in addition to an RNA template. Telomerase extends the DNA strand by adding complementary RNA nucleotides to the 3′ end. Once the 3′ end of the lagging strand template has been sufficiently extended, the enzyme DNA polymerase attaches complementary sequences to the ends of the chromosomes, resulting in the replication of the ends of the chromosomes. It was subsequently demonstrated that short telomeres underpin the Hayflick limit and that telomere attrition occurs concurrently with the cell cycle division in *in vitro* cell culture (Harley *et al.*, 1990).

Interestingly, there have been several studies on telomeres and telomerase in the last few decades, and outcomes from these investigations are currently being examined in clinical trials related to cancer. Telomerase is highly expressed in 85 to 90% of human tumours, and it is thought to be an important therapeutic target in the cancer field (Relitti *et al.*, 2020). P53 is encoded by *TP53* gene, and the main role of this protein is the induction of apoptosis and cell cycle regulation through DNA damage response and repair pathways (Mijit *et al.*, 2020). Beauséjour *et al.*, (2003) showed that senescence was not reversed by the restoration of telomerase expression alone *in vitro*. However, upon p53 inactivation, cells with low p16 levels during senescence resumed vigorous growth. On the other hand, when p53 was inactivated or *RAS* was expressed, senescent cells with high p16 levels failed to proliferate (Beauséjour *et al.*, 2003). The relationship between telomere disruption and the manifestations of ageing, the incidence of age-related disorders, and the emergence of hereditary and acquired degenerative pathologies has attracted attention in telomerase restoration therapy as a possible intervention of the ageing process. Preclinical mouse models with long telomeres showed that *Tert* expression improved longevity by 40%, but these animals

also had more p53, p16, and Arf copies, which made them more resistant to cancer (Bernardes *et al.*, 2012). Therefore, it is unknown if the prolonged life span and disease-preventing effects of forced *Tert* expression are related to *Tert* 's effects on telomeres or to its stimulation of Wnt (a core signal transduction protein that involves in Wnt signaling pathway and regulates some transcription factors), which may augment stem cell reserves (Park *et al.*, 2009). Finally, telomere shortening has been linked to premature ageing syndromes, age-related diseases, and normal ageing (Aubert & Lansdorp, 2008); therefore the telomere attrition hallmark is one of the main therapeutic target in the ageing intervention research and ARDs such as cancer.

1.2.3 Dysregulation of Spliceosome and Protein Homeostasis

Ageing cells demonstrate dysregulation of splicing events (Harries *et al.*, 2011; Holly *et al.*, 2013; Latorre *et al.*, 2017) and elevate the degradation of misfolded proteins (Morimoto & Cuervo, 2014). There are several mechanisms regulating the processes of protein maturation and degradation including splicing, chaperone mediating proteins, and proteasomal degradation. Alternative splicing is a key approach for gene expression regulation. This enables gene level responses to intracellular and external stimuli. Human genes are alternatively spliced in more than 95% of cases, and some of these alternative isoforms will differ from their parent isoform in terms of their UTR sequences (Vitulo *et al.*, 2014). Mice and other animals have shown that splicing regulatory factor gene expression is connected to longevity as well as predictively linked to human ageing characteristics in population studies (Lee *et al.*, 2020). Cell proliferation is closely regulated by the expression of splicing factors, and cancers typically have mutant versions of these factors (Lee *et al.*, 2020). *In vitro* studies employing aged human primary cells and small compounds or focused genetic

treatments have shown that restoring splicing factor expression may correct various aspects of senescence (Latorre *et al.*, 2017; Latorre *et al.*, 2018).

Some of the chaperone systems that have been linked to the ageing process are *HSP40*, *HSP70*, *HSP72*, and *HSP90* (Harries, 2014). Numerous animal models suggest that the reduction in chaperones has a causal effect on lifespan. Transgenic worms and flies that overexpress chaperones in particular have a long lifespan (Morrow *et al.*, 2004). Heat shock genes like *HSP70* are activated more effectively when SIRT1 deacetylation of HSF-1 occurs, but SIRT1 deacetylation decreases the heat shock response in mammalian cells (Westerheide *et al.*, 2009). This makes recovery of chaperones expression level a potential target in the ageing intervention. Deterioration in proteasome function is linked to the development of age-related pathologies. A reduction in the prevalence of age-related diseases may be achieved through mechanisms that maintain proteasome activity. For instance, autophagy-promoting processes may lengthen lifespan (Saez & Vilchez, 2014).

1.2.4 Cellular senescence

Cellular senescence is defined as a stable arrest of the cell cycle due to intrinsic or extrinsic factors. These cells could be both reversible or irreversible to division depending on the level of cellular damage (Hernandez-Segura *et al.*, 2018; López-Otín *et al.*, 2013). Cellular senescence is often characterized by flattened and enlarged morphology, an altered transcriptome and splicing patterns, senescence-associated secretory phenotype (SASP), and elevation of DNA damage response (DDR) (shown in figure 1.2). In their 1961 paper, Leonard Hayflick and Paul Moorhead showed cessation of cell division experimentally and coined the term "cellular senescence"

(Hayflick & Moorhead, 1961). Nevertheless, senescence gained more attention after the discovery of the possible triggering mechanism of senescence in 1990 through shortening of telomere length *in vitro* (Harley *et al.*, 1990) and *in vivo* (D'Adda Di Fagagna et al., 2003). However, repeated cycles of cell division, the protective cap on the telomeres shortens over time, producing a DNA damage response and eventually leading to cell cycle arrest and senescence (Hernandez-Segura *et al.*, 2018); and this is known as the Hayflick limit.

There are several categories of senescence based on the stimulus. 1) Replicative senescence is a term used to describe the decline in proliferative capability that occurs after repeated cell divisions and eventually results in cell cycle arrest. Multiple cell divisions in non-transformed cells shorten telomeres, which drive replicative senescence. 2) Stress-induced senescence can result from many stimuli including DNA damage, oxidative stress and expression of oncogenes. Stress-induced senescence (also known as premature senescence) results from regulation of cell cycle pathways, p53/p21 and/or p16/Rb (Hernandez-Segura *et al.*, 2018). More recent data reveal that the pathways to replicative and stress-induced senescence are not mutually exclusive, leading researchers to conclude that both types of senescence share a large number of biomarkers (Hernandez-Segura *et al.*, 2018; López-Otín *et al.*, 2013).

Senescent cells play an important role in a variety of biological processes, including suppression of tumours, healing of wounds, repair of damaged tissue, and the formation of embryonic tissue (presented in figure 1.2). In these circumstances the presence of senescent cells is temporary, and the SCs are eventually eradicated by the immune system. However, during ageing, a build-up of senescent cells occurs, and this is regarded to be a cause of more damage in late-life (van Deursen, 2014).

This is due to persistent expression of SASP factors which has been proven to cause senescence in neighbouring non-senescent cells and to promote chronic inflammation and tissue malfunction (Acosta *et al.*, 2013). Consequently, accumulation of senescent cells leads to an acceleration of the ageing process. Hence, senescent cells have been linked to a range of age-related disorders, including cardiovascular disease (Shimizu & Minamino, 2019).

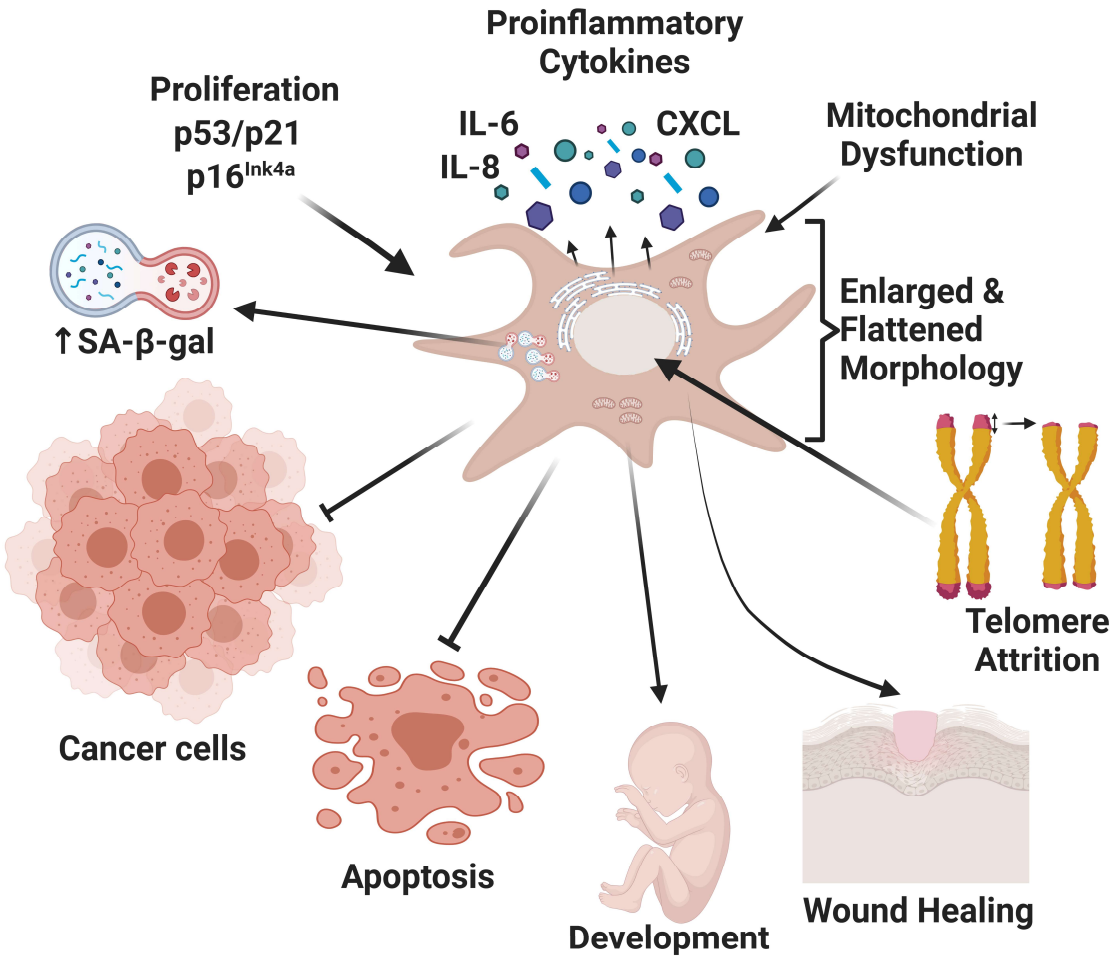

Figure 1.2 Senescence biomarkers and their associated phenotypes and functions.

Markers of senescent cells. Indirect markers characterizing cellular senescence (which may vary between tissues and cells) are as follows: (1) Enlarged and flat morphology, (2) cell cycle arrest (elevated p53/p21, $p16^{Ink4a}$ expression), (3) DNA damage response (γH2AX, p53, and MAPK signals are elevated), (4) exit from cell cycle, (5) high senescence-associated beta-galactosidase (SA-β-gal) activity, (6) telomere attrition, (7) telomere dysfunction.

Senescent cells have an impact on both tissue healing and embryonic development. Cellular senescence, a common tumor-suppressing process, prevents the development of abnormal cells. In contrast, senescent cells are accompanied by producing inflammation factors in the body such as cytokines/chemokines (CXCL1, CXCL2, CXCL5, IL-6, and IL-8), and the continuous inflammation may cause tissue degradation and harmful acute inflammation, hence exacerbating ageing-related disorders. Detail of this figure was adopted from (Shimizu & Minamino, 2019) and created with BioRender.com.

1.2.4.1 SA-β-Gal

SA-β-Gal uses a chromogenic substrate to stain senescent cells with an X-Gal (5-bromo-4-chloro-3-indolyl β-D-galactopyranoside) and is used to visualize the increase of beta galactosidase activity in mammalian cells and tissues. It was reported in 1995 by Dimri and colleagues that SA-β-Gal activity accumulates in old animals and humans, which suggests cellular senescence is a characteristic of the elderly (Dimri *et al.*, 1995). From that point on, this method has been the most used indicator of senescence, both *in vitro* and *in vivo*. SA-β-Gal activity in senescent cells is detectable at pH 6.0, unlike the activity in normal cells which is detectable at lower pH. This activity, however, is not necessary for senescence and therefore it is not present in all senescent cells (Lee *et al.*, 2006). In HeLa cells, knocked out of the *GLB1* gene, which codes for the lysosomal β-D-galactosidase, senescence phenotypes were still apparent. On the other hand, proliferating cells at high density *in vitro* exhibited SA-β-Gal activity at pH 6.0 (N. C. Yang & Hu, 2005). It is not clear why SA-β-Gal activity is increased in senescent cells and this remains to be further studied. Figure 1.3 shows senescent cells stained with SA-β-Gal.

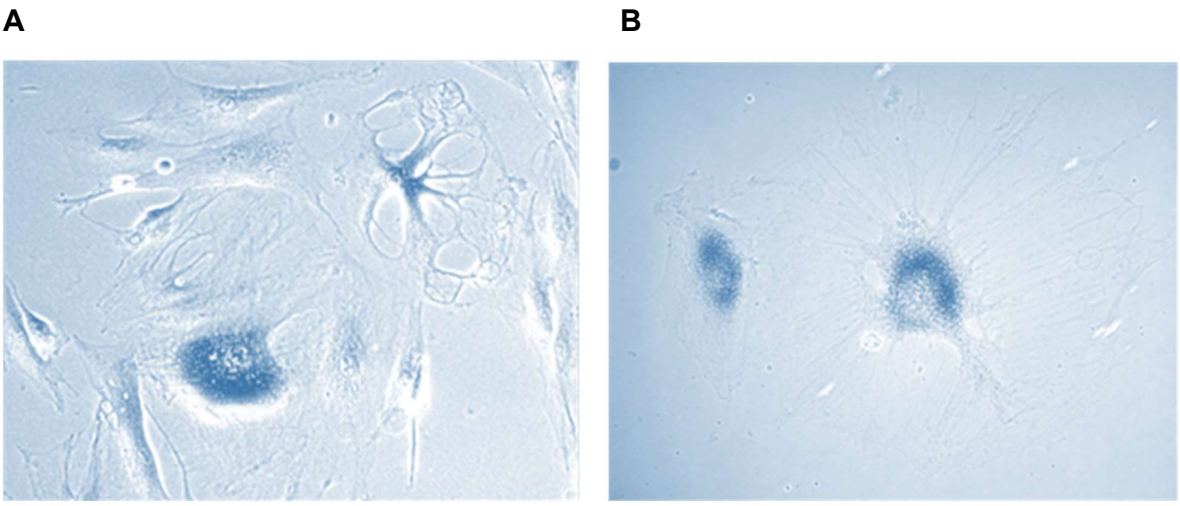

Figure 1.3 Senescent cells show a SA-β-Gal staining at pH 6.

SA-β-Gal assay to identify senescent cells in late passage of (A) normal human dermal fibroblast (NHDF) and (B) human aortic endothelial cells (HAoECs). Images were captured by brightfield microscope 20X objective lens and processed using the imageJ software.

1.2.4.2 Senescence and theory of antagonistic pleiotropy

In his 1957 paper, George Williams proposed the antagonistic pleiotropy hypothesis of ageing (G. C. Williams, 1957), a concept Peter Medawar had previously discussed and stated as unresolved problem in biology (Austad & Hoffman, 2018). Interestingly, animals possess genes that boost fitness early in life but diminish it as they age, and choosing to preserve these genes can favour them because natural selection is stronger in early life, while the ageing phenotype emerges later (Austad & Hoffman, 2018). Serving as a protective mechanism against cancer (Zhang *et al.*, 2021) and playing a role in the human development (Muñoz-Espín *et al.*, 2013; Storer *et al.*, 2013), senescence is also harmful as we progress in life since it causes tissue dysfunction in the older organisms (McHugh & Gil, 2018). Senescence can be considered a positive feature in youth because it serves as an anti-cancer mechanism,

through inhibiting the proliferation of damaged cells. A supporting fact is that genes involved in tumor suppression are also involved in senescence. Cancer incidence is increased in mice whose senescence effectors have been knocked out, including p53 and p16 (Zhang *et al.*, 2021). For instance, Collado and colleagues showed that $p16^{INK4a}$, $p15^{INK4b}$, *Dec1* and *Dcr2* demonstrated higher expression in benign lung tumour samples but were not expressed in malignant tissue in mouse models (Collado *et al.*, 2005). It is also important to note that knockout of $p21^{CIP1/WAF1}$ increased replication without contributing to transformation (Brown *et al.*, 1997) while loss of p53 along with telomerase resulted in an increased incidence of transformation to cancer (Chin *et al.*, 1999).

Accumulation of senescent cells have been demonstrated to negatively impact aged organisms (He & Sharpless, 2017; Deursen, 2014). As more senescent cells build up, more SASP is secreted, which eventually leads to an unbalanced tissue homeostasis. For example, premalignant epithelial cells transformed to tumours in mice when exposed to SASP factors produced by neighbouring senescent cells (Krtolica *et al.*, 2001). Also, senescence has been demonstrated to contribute to cancer cell radioresistance in non-small cell lung cancer (NSCLC). Targeting and removing senescent fibroblast cells using FOXO4-DRI (this will be discussed in senotherapeutic section 1.2.4.4) reduced NSCLC cells' radio-resistance (Meng e*t al.*, 2021). The theory of antagonistic pleiotropy may define the seemingly conflicting roles of senescence at young and old ages. Figure 1.4 summarizes the roles of senescent cells at both ages.

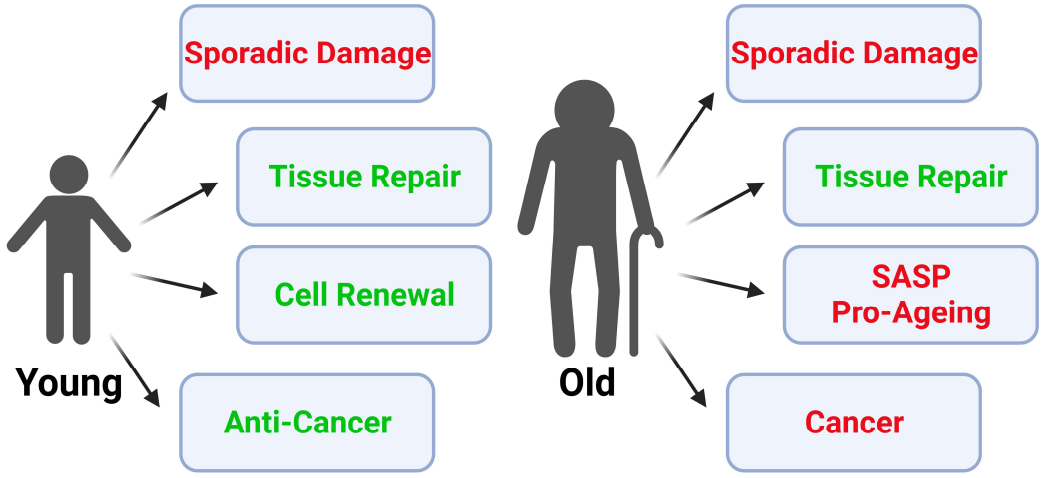

Figure 1.4: Senescent cells and theory of antagonistic pleiotropy.

In younger adults, senescence mainly prevents uncontrolled proliferation of damaged cells by inhibiting their proliferation, they involve in cellular renewal, and tissue repair (green). On the other hand, ageing leads to the accumulation of senescent cells which accelerates ageing and can even promote tumours and increase tissue damages (red) (Adopted and modified from (López-Otín *et al.*, 2013)). The figure was created in BioRender.com.

1.2.4.3 Senescence and alteration in the spliceosome

The process of alternative splicing is now recognised as a crucial modulator in cellular senescence and ageing (Latorre *et al.*, 2019). Spliceosomes are huge ribonucleoprotein complexes that carry out alternative RNA splicing. *HNRNPs* (heterogeneous nuclear ribonucleoprotein particles) and *SRSFs* (serine-arginine rich splicing factors) are the two groups of splicing factors (SFs) that enable a variety of

RNA splicing actions (Cartegni *et al.*, 2002). Ageing has recently been strongly linked to changes in spliceosomes in the human brain and many other animal tissues. (Lee & Harries, 2021; Tollervey *et al.*, 2011). Splicing factor expression diminishes with age probably due to a consequence of the *AKT* and *ERK* signalling pathways activation, as well as associated downstream effects of genes *FOXO1* and *ETV6* activity (Latorre *et al.*, 2018). A novel hallmark of ageing is the dysregulation of alternative splicing, and disruption of this cellular process is linked to cellular senescence and critical ageing outcomes. Interestingly, the recovery of more juvenile splicing patterns and the recovery of splicing factor expression using genetic or small chemical methods provide a potential new senotherapeutic technique for cellular rejuvenation (Lee & Harries, 2021).

1.2.4.4 Senotherapeutic strategies and rejuvenation

Eliminating senescent cells has gained more attention in recent years as it clearly shows improvement in health span in model organisms and reduction in ageing associated disorders (Baker *et al.*, 2016; Amor *et al.*, 2020). These can be accomplished by two ways either 1) senomorphics which act by clearance of SASP (senescence-associated secretory phenotypes) cytokines overproduced by senescent cells or 2) senolytics, which are defined as small molecules or drugs that selectively kill senescent cells by inducing the apoptotic pathways (Bramwell & Harries, 2021).

Other approaches have attempted to clear senescent cells through an antibody-conjugated mechanism, applied previously to kill cancer cells. Here, an antibody-drug conjugate (ADC) against B2M, a new marker of senescent cells, was used to selectively kills senescent cells by distributing duocarmycin into them, an isotype

control ADC had no effect (Poblocka *et al.*, 2021). Moreover, the senomorphic drugs JH1, JH4, and JH13 when administered to cells isolated from an individual with premature ageing disease Hutchinson-Gilford progeria syndrome (HGPS) and normal ageing cells showed a reduction in nuclear deformation and senescence markers, extending the lifespan of HGPS-progeroid mice, and reducing age-related diseases (Lee *et al.*, 2016). A summary of current promising and potential senotherapeutic agents along with their effects are presented in table 1.1.

UBX1325 (Bcl-xL inhibitor) has been examined in clinical trials including Phase II (NCT04129944) for osteoarthritis patients, patients with age-related macular degeneration (NCT04537884), and on patients with diabetic macular oedema (NCT04857996). Dasatinib a tyrosine kinase inhibitor has been used in clinical trials in scleroderma patients and healthy old individuals (NCT00764309) and (NCT04313634), respectively. Another senotherapeutics in clinical trials is fisetin which works on the PI3K/AKT inhibition pathway. Several clinical trials are currently being investigated and expected to finish in the next few years. These clinical trials are being investigated in multiple diseases and on healthy old people including patients with osteoarthritis of the knee (NCT04815902), patients with frailty (NCT04733534), healthy participants (NCT04537299), and patients with COVID-19 (NCT04771611) (Raffaele & Vinciguerra, 2022).

Table 1.1 A table to show and summarize the current senotherapeutics approaches in research and clinical trials. Potential agents to be used therapeutically to clear senescent cells or its SASP secretions. Approaches for demonstrating the mechanism of actions were given and clinical trials of these agents were indicated as italics.

Approaches	**Agents**	**Mechanism of Actions/*Clinical Trials***
Senolytics	Dasatinib (D)	• Pan-receptor tyrosine kinases (including ephrin B1)
	Quercetin (Q)	• PI3K/AKT pathway inhibitor
	D+Q	• Pan-receptor tyrosine and kinase/Multiple pathways • *Clinical Trial Phase II, (NCT02848131) for chronic kidney disease, phase II (NCT04313634) for skeletal health, phase II (NCT04063124) for Alzheimer disease*
	Fisetin	• PI3K/AKT/mTOR pathway inhibitor • Act on senescent cells and SASP in progeroid and aged mice • *Phase I/II (NCT04210986) for osteoarthritis of the knee*
	FOXO4-DRI peptide	• p53/p21/serpine
	an antibody-drug conjugate (ADC)	• B2M
	UBX0101	• MDM2/p32 • *Phase II (NCT04129944) for osteoarthritis*
	ABT-263 (navitoclax)	• BCL-2, BCL-XL and BCL-W
	ABT-737	• BCL-2, BCL-XL and BCL-W
	Panobinostat	• Chemotherapy-induced senescent NSCLC and HNSCC cells
Senomorphics	JH4	• Efficiently block progerin/lamin A/C.
	Rapamycin	• Destabilizing the mTOR-Raptor complex
	uPAR	• Senescent hepatocytes *in vivo*, senescent cells from lung adenocarcinoma and CCl4-dependent liver fibrosis mouse model
	CD199	• Senescent bladder carcinoma cells (EJp16)
	Mmu-miR-291a-3p	• TGFBR2/p21 pathway through Inhibition of senescence phenotypes of HDFs and HUVECs Acceleration of the excisional skin wound healing in aged mice.
	SH-6	• AKT
	Resveratrol	• SIRT1 activation and regulation of splicing factors
	H2S	• Regulation of splicing factors

1.2.4.4.1 Resveratrol

Several studies have reported the efficacy of resveratrol, a polyphenolic compound (3,5,4′-trihydroxy-trans-stilbene, resveratrol, structure is shown figure 1.5), in animals as a senomorphic molecule (Guan *et al.*, 2019; Latorre *et al.*, 2017; Novelle *et al.*, 2015). Red grapes, cranberries, and blueberries are rich sources of the antioxidant resveratrol. Resveratrol was discovered to possess cardioprotective, anti-cancer, anti-inflammatory, and longevity extending properties (Baur & Sinclair, 2006; Novelle *et al.*, 2015; Salehi *et al.*, 2018). This molecule gained more attention when scientists showed that resveratrol can improve the healthspan in mice and model organisms even with high calorie diet (Baur *et al.*, 2006). Regarding the mechanisms of action and its use in ARDs, resveratrol remains controversial. Studies have suggested that it is supposed to act by activating the *SIRT1* gene. However, it appears that resveratrol acts directly or indirectly via sirtuins, which are NAD+-dependent deacetylases that contribute to stress resistance and survival (Baur & Sinclair, 2006). Resveratrol promotes good health by inhibiting inflammatory and stress-related responses and by stimulating sirtuins (Latorre *et al.*, 2017; Novelle *et al.*, 2015). In a previous report from our lab, resveratrol and its paralogs were shown to have a senomorphic effect and reverse senescent fibroblast cells independently to SASP modulation or *SIRT1* stimulation. Given the importance of resveratrol, in this thesis, resveratrol was used to reverse senescent cells and study the miRNAome in endothelial cells as a response to reversal (chapter 3).

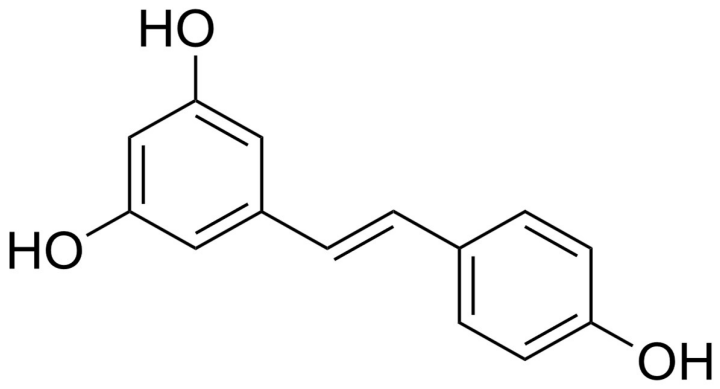

Figure 1.5: Structure of resveratrol

Chemical structure of the resveratrol compound (5-[(E)-2-(4-hydroxyphenyl)ethenyl]benzene-1,3-diol).

1.3 Pathways and Cellular Mechanisms to Maintain Cellular Senescence

Growth arrest is distinct from quiescence that senescence occurs in the G1 or G2 phase of the cell cycle, whereas quiescence develops in the G0 phase of the cell cycle (Kumari & Jat, 2021). Senescent cells are evoked in response to stimuli and stresses that induce tumor suppressor pathways p53/p21$^{WAF1/CIP1}$ and p16$^{INK4A/pRB}$. Upon activation and prolonged high expression of the effectors of these pathways, SASP, SAHF, and antiapoptotic genes play major roles in senescence survival and avoiding clearance by immunity (Muñoz-Espín & Serrano, 2014). These will be discussed in the following section.

1.3.1 The p53-p21 pathway

p53 is a master regulator protein of cell cycle fate and is known as the guardian of the genome. p53 and its downstream effector gene p21 are stimulated in response to DNA damage resulting from telomere attrition or other stimuli leading cells to block the

progression of cell cycle (see figure 1.5) (Mijit *et al.*, 2020). P53 is regulated by ubiquitination. In the absence of stressors, p53 is quickly ubiquitinated by one of the E3 ligases, such as *MDM2*, *MDM4*, *TOPORS*, and *ARF-BP1*, and then it is broken down in the proteasome. Conversely, stress signals cause covalent alteration by interrupting the interaction of p53 with the E3 ubiquitin ligases, which halts the degradation of the protein. For instance, oncogenic stress activates the INK4a locus' alternative reading frame product (p14ARF), which stabilises p53 by interacting with and suppressing its antagonistic regulator MDM2 (Fagagna, 2008). Additionally, p53 has been shown to have a direct effect on the expression of a number of cell cycle-related proteins. Only around 3% of the genes are directly interacted with p53, as a result it has an indirect effect on several pathways (Fischer *et al.*, 2014).

The *CDKN1A* gene encodes the 21 KDa protein known as $p21^{WAF1/CIP1}$. This protein belongs to the CIP/KIP family of CDK inhibitors. $p21^{WAF1/CIP1}$ has the ability to deactivate all CDKs and halt the progression of the cell cycle. Cell cycle progression is inhibited by high concentrations of $p21^{WAF1/CIP1}$, but low concentrations of $p21^{WAF1/CIP1}$ function as an assembly factor for cyclinD/CDK4,6 complex and promote its activation, which induces cellular proliferation (Mijit *et al.*, 2020). As a key player in the ageing process, $p21^{CIP1}$ is critical because of its ability to slow cell death by inhibiting apoptosis. A number of apoptotic agents, including caspases, have been shown to interact with $p21^{CIP1}$. In senescent cells, $p21^{CIP1}$ deletion induces the activation of cascade caspases and apoptosis (Yosef *et al.*, 2017).

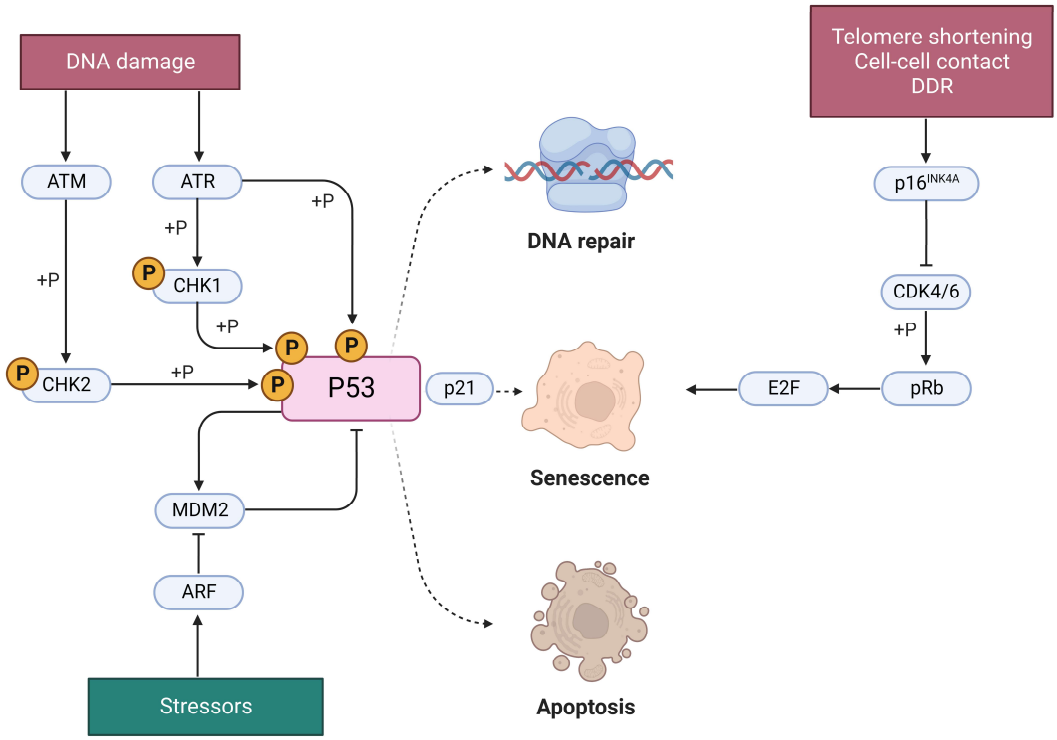

Figure 1.6: Control of cell growth and senescence by p53 or p16 pathways

Many stimuli, both internal and external, activate the p53 and/or $p16^{INK4A}$ pathways in response to DNA damage and other stressors. Cell cycle arrest and senescence are both caused by $p16^{INK4A}$, a protein that prevents *Cdk4/6* from activating, as well as the formation of phosphorylated pRB. Both *ATM-Chk2* and *ATR-Chk1* pathways govern the cell's response to DNA damage, which activates p53 and $p21^{CIP1}$ in response to these stressors. In addition, $p21^{CIP1}$ protein levels may limit *Cdk4/6* function, which contributes to the G1 arrest or senescence of the cell cycle (Marei *et al.*, 2021). The figure was created in BioRender.com.

1.3.2 The p16-pRB pathway

All RB pocket family proteins have in common an LXCXE motif-containing 2-dimensional pocket domain in general to engage in direct protein-protein interactions. The RB pocket protein family consists of three members: *RB1* (pRB), *RBL1* (p107), and *RBL2* (p130). Their most well-known action is deactivation of E2F complexes, which repress the transcription of E2F target genes (Dyson, 1998). The *E2F-RB* complex is formed by dephosphorylation of pRB, which results in inhibition of cell cycle progression. Histone deacetylases and the histone methyltransferase are recruited to increase and strengthen transcriptional repression (Fischer & Müller, 2017). This inhibition is eliminated at the restriction point hyperphosphorylation of RB by cyclinE-CDK2, which results in the release of E2Fs and promotes the transcription of genes involved in the S phase, and promotes entry into cell cycle (Zhang *et al.*, 2000). Furthermore, it has been proposed that crosstalk between the pRB and mitogenic AKT signalling pathways plays an important role in the quiescence to senescence transition by modulating the overlapping roles of *FOXO3a* and *FOXM1* (Marthandan *et al.*, 2014).

p16INK4A is a 16 KD protein that binds to CDK4/6 directly and prevents cyclin D from forming complexes with CDK4/6. This prevents RB from being phosphorylated and enhances the activity of *E2F* (Serrano *et al.*, 1993). Activation of the *CDKN2A* gene is also connected to replicative senescence. The *CDKN2A* locus is ordinarily expressed at a very low undetectable level in young tissues, but is derepressed as we age, resulting in a high level of expression (Hara *et al.*, 1996; Krishnamurthy *et al.*, 2004). In contrast to DNA damage-induced senescence, which primarily depends on $p21^{WAF1/CIP1}$, epigenetically induced senescence predominantly occurs by increasing $p16^{INK4A}$ expression (Petrova *et al.*, 2016).

Numerous crosstalk mechanisms, some of which have been partially explained, seem to impact the p53/p21 and p16/pRB pathways. Ablation of p53 before overexpression of p16, for example, may prevent senescence induction (Campisi, 2005). However, downregulation of p53 is unable to restore cell cycle arrest if p16 is abundantly expressed. Cellular senescence was produced in virtually all human cervical cancer cells when p53 and pRB were revived to normal levels concurrently in a study on the cross-talk between the two proteins (Kapić *et al.*, 2006).

1.3.3 Senescence-Associated Secretory Phenotype (SASP)

Despite the lack of cell division, senescent cells are still metabolically active. Predominant among the acquired functions of senescent cells is the secretion of the SASP (Gorgoulis *et al.*, 2019). Through secretion of SASP factors, senescence has the capacity to impact the environment and interact with adjacent cells, and this may influence the behaviour of normal dividing cells in the surroundings which leads to impairment of tissue homeostasis and organ dysfunction (Lopes-Paciencia *et al.*, 2019; Sun *et al.*, 2018). Growth regulators, pro-inflammatory cytokines, chemokines, extracellular matrix components, and matrix metalloproteinases (MMPs) are among the substances that have been identified as SASP (Juan Carlos Acosta *et al.*, 2013; Lopes-Paciencia *et al.*, 2019). They include the following: growth factors (vascular endothelial growth factor (VEGF), platelet-derived growth factor (PDGF), hepatocyte growth factor (HGF)), interleukins (IL-1α, IL-6, IL-8, IL-10, IL-13, IL-15), matrix metalloproteinases (MMP3, MMP9) and cytokines/chemokines (CXCL1, CXCL2, CXCL5, CXCL11, CXCL12, CCL2, CCL20). Due to diversity of senescence triggering stimuli and downstream affected pathways, none of these indicators may be attributed solely to the senescence phenotype (Chambers *et al.*, 2021). The main elements of

SASP are NF-kB dependent pro-inflammatory factors, with IL-6 and IL-8 being the most persistent and robustly produced cytokines (Chambers *et al.*, 2021; Sun *et al.*, 2018). Studies have shown that IL-6 and IL-8 have autocrine actions that control cell cycle arrest and maintain senescence (Acosta *et al.*, 2008). It is important to mention that several senescence biomarkers are needed to confidently define and identify senescent cells.

Inflammageing is a term used to describe a state of chronic inflammation that occurs as a result of age-related decline associated with senescence. Inflammageing results in the amplification of the SASP (Lopes-Paciencia *et al.*, 2019). Clearing SASP has been shown to improve tissue function without removal of the source, senescent cells (Kim & Kim, 2019). For instance, Y-27632 molecule has been shown to inhibit ROCK, which lowers the amounts of *IL-1*, *IL-6*, and *IL-8* released by senescent cells without affecting the irreversible cell growth arrest (Niklander *et al.*, 2020). Also, the FOXO4 peptide, a senomorphic compound, when administered to mice with an accelerated ageing phenotype, restored their fitness, fur density and kidney function (Baar *et al.*, 2017).

1.3.4 Senescence-Associated Heterochromatin Foci (SAHF)

SAHF, a condensed region of the genome and consist of inaccessible genes, is a consequence of major changes in chromatin structure in senescent cells. The p16-pRB pathway is essential in controlling how chromatin is organized and it helps formation of SAHF (Narita *et al.*, 2003). SAHF has been proven to be different from other types of heterochromatin since centromeres, telomeres, and other heterochromatin components are not present in SAHF; hence, it is a marker for senescent cells (Narita *et al.*, 2003). pRB inhibits E2F which is a transcription factor

facilitates the activation of genes essential for cell cycle progression. DNA foci in senescent cells are assembled by the pRb-E2F complex, which recruits heterochromatin proteins and methylated histone at position 9 (K9M-H3) (Takahashi *et al.*, 2000). Also, the translocation of histone repressor A (HIRA, a histone chaperone), to promyelocytic leukemia nuclear (PML) bodies appears to be another critical step in the formation of SAHF. Other factors necessary to formation of SAHF are *LMNB1*, *HIRA/ASF1A* complex, and *HMGA1* (Narita *et al.*, 2006). *LMNB1* is downregulated in senescence and it has been shown to be associated with the formation of SAHF. Without completely rescuing cells from senescence, ectopic *LMNB1* expression resulted in a decrease in SAHF positive cells in senescence (Sadaie *et al.*, 2013). Interestingly, downregulation of *ASF1A* or *HMGA1* led to partially bypassing senescence (Zhang *et al.*, 2005).

1.3.5 Resistance to apoptosis

Senescent cells secrete SASP as a recognition marker for immune cells for clearance through triggering apoptosis. Nonetheless, owing to the declining of immunological function associated with ageing, senescent cells persist in local tissues and contribute to tissue malfunction and chronic inflammation (Schroth *et al.*, 2020). Senescent cells become resistant to apoptosis throughout upregulation of *Bcl-2*, *Bcl-xL*, or *Bcl-w* and downregulation of pro-apoptotic gene, *Bax* (Sasaki *et al.*, 2001; Yosef *et al.*, 2016). Persistent activation of transcription factor cAMP response element-binding protein was found to be connected with senescent cells' ability to maintain *Bcl-2* expression (Ryu *et al.*, 2007). Also, Sanders and colleagues found that production of the proapoptotic protein *Bax* was limited by the repressive histone marker *H4K20me3* in senescent fibroblast cells (Sanders *et al.*, 2013). Genes that regulate apoptosis in

senescence are potential therapeutic targets to clear senescent cells and a few targets are being investigated.

Senescent cells are known to have increased FOXO4 expression, which inhibits apoptosis by trapping p53 in the nucleus (Baar *et al.*, 2017). This led to discovery of a senolytic peptide, fork head box O transcription factor 4-D-Retro-Inverso (FOXO4-DRI) which has been used to disturb the interaction between p53 and FOXO4 that leads to p53-dependent apoptosis (Huang *et al.*, 2021). The Bcl-2 family of antiapoptotic proteins is another viable target that regulates senescent cells through blocking apoptosis. In particular, the Bcl-2 family proteins Bcl-xl and Bcl-w are essential for the maintenance of senescent cells. Elimination of these proteins by siRNA induced apoptosis in senescent mouse epidermal cells *(Yosef et al.*, 2016). Furthermore, researchers have shown that p21 is necessary for both senescence and cell death. Elevation of p21 under conditions of ongoing DNA damage prevents JNK and caspase signalling pathways to allow senescent cells to avoid apoptosis (Yosef *et al.*, 2017)**.** Medicines that control several survival pathways implicated in senescence resistance to apoptosis such as the Bcl-xl inhibitor navitoclax and the combination of dasatinib and quercetin have shown promising preclinical outcomes (Zhu *et al.*, 2016).

One important regulator of the genes involved in senescence is noncoding RNA (ncRNA) regulation. These processes are a fundamental component of the gene regulatory machinery, and have potential to serve as diagnostic or prognostic biomarkers or as the basis for future therapeutics in the field of ageing (Harries, 2014, 2019).

1.4 Regulation of gene expression by non-coding RNAs

RNAs are classified into coding RNAs, RNAs that translate into proteins, and non-coding RNAs, which are mainly used to regulate the expression of coding RNAs. There are long non-coding RNAs (lncRNAs) and short non-coding RNAs (piwi (piRNAs) or microRNAs). The long non-coding RNAs have more than 200 nucleotides (nts) whereas the short non-coding RNAs are shorter than 200 nts (Majeed Shah et al., 2022). There are nearly 22 000 proteins encoded in the human genome. However, this number rises to 70,000 different proteins when considering the fact that many coding genes has multiple splice variants (Aebersold *et al.*, 2018). This accounts for less than a third of the human genome. In the past, most of the genome's non-coding parts have been ignored and treated as junk RNA. However, the genes that encode for proteins (messenger RNA) are largely controlled by noncoding genes such as microRNAs. MicroRNAs (hereafter will be referred to as miRNAs) are mature, small, genome-encoded, highly conserved RNA molecules consisting of 18-25 nucleotides long. miRNAs control the expression of genes through partially complementary binding sites located mainly in the 3'-untranslated regions (3'-UTR) or coding regions of target mRNAs that eventually will result in repression or degradation of mRNAs (Bueno & Malumbres, 2011).

1.4.1 miRNA biogenesis

All human chromosomes, except for the Y chromosome, contain miRNA genes. In terms of their genomic locations, miRNAs fall into three categories: intergenic, intronic, and exonic (Rodriguez *et al.*, 2004). Intergenic miRNAs are found in genomic regions that are distinct from the known functional transcription units, and they are mainly transcribed by RNA Pol II promoters. A few experimental observations and

bioinformatic predictions have demonstrated that the primary transcript of an intergenic miRNA is approximately 4 kb in length and carries the cap and poly(A) signaling sequences. MiRNAs present in intron regions of host genes have the same promoter, while exonic miRNAs are much less common, as they often overlap an exon and an intron of a noncoding gene (Rodriguez *et al.*, 2004). It is important to note that miRNA biogenesis involves multiple steps in the maturation process. There are two major types of miRNA biogenesis pathways, canonical and noncanonical. The next section will discuss these topics in more detail.

1.4.1.1 Canonical pathway

MiRNAs are synthesised mainly in the nucleus by transcription by RNA polymerase II, which produces long primary miRNAs (pri-miRNAs) (figure 1.7). Pri-miRNAs are cleaved by RNase III *Drosha*, along with *DGCR8*, to yield a hairpin-shaped precursor miRNA (pre-miRNA) (Lee *et al.*, 2003). The pre-miRNAs are then exported from the nucleus to the cytoplasm through a protein known as exportin-5. A short 3′ overhang of about 8 nt on the pre-miRNA is recognized by exportin-5 along with the long dsRNA stem of >14 bp (Yi *et al.*, 2003).

The next step is the cleavage of pre-miRNAs by dicer and TAR RNA protein (*TRBP*), cytoplasmic endonucleases. The mature miRNA duplex consists of approximately 22 nucleotides (Chendrimada *et al.*, 2005). The RISC active complex (RNA-induced silencing complex) is formed by attaching an argonaute (*Ago*) protein to the 22-nt RNA duplex. Ago typically keeps one strand of the 22nts miRNA duplex as mature miRNA (the guide strand) while degrading the second strand, potentially due to its thermodynamic stability. RISC is formed by the interaction between *Dicer* and *TRBP*

and *PACT* which leads to the formation of RISC. Upon unwinding, however, each of these strands can target mRNA through incorporation into RISC complex with help of the endonuclease argonaute to form miRISC (Matranga *et al.*, 2005).

Furthermore, *Ago1*, *Ago3*, and *Ago4* proteins do not possess the slicer activity preventing the cleavage of miRNA, unlike siRNA duplexes. The stability of the miRNA is often determined by 1-2 nt insertions or deletions, which are often the cause of the heterogeneity at the end of miRNAs. The terminal uridyl/adenyl transferases add untemplated nucleotides (mostly uracil and adenine) to the 3′ end of RNA sequences in order to stabilize them or to degrade them in case of several addition of these residues (Turk *et al.*, 2018).

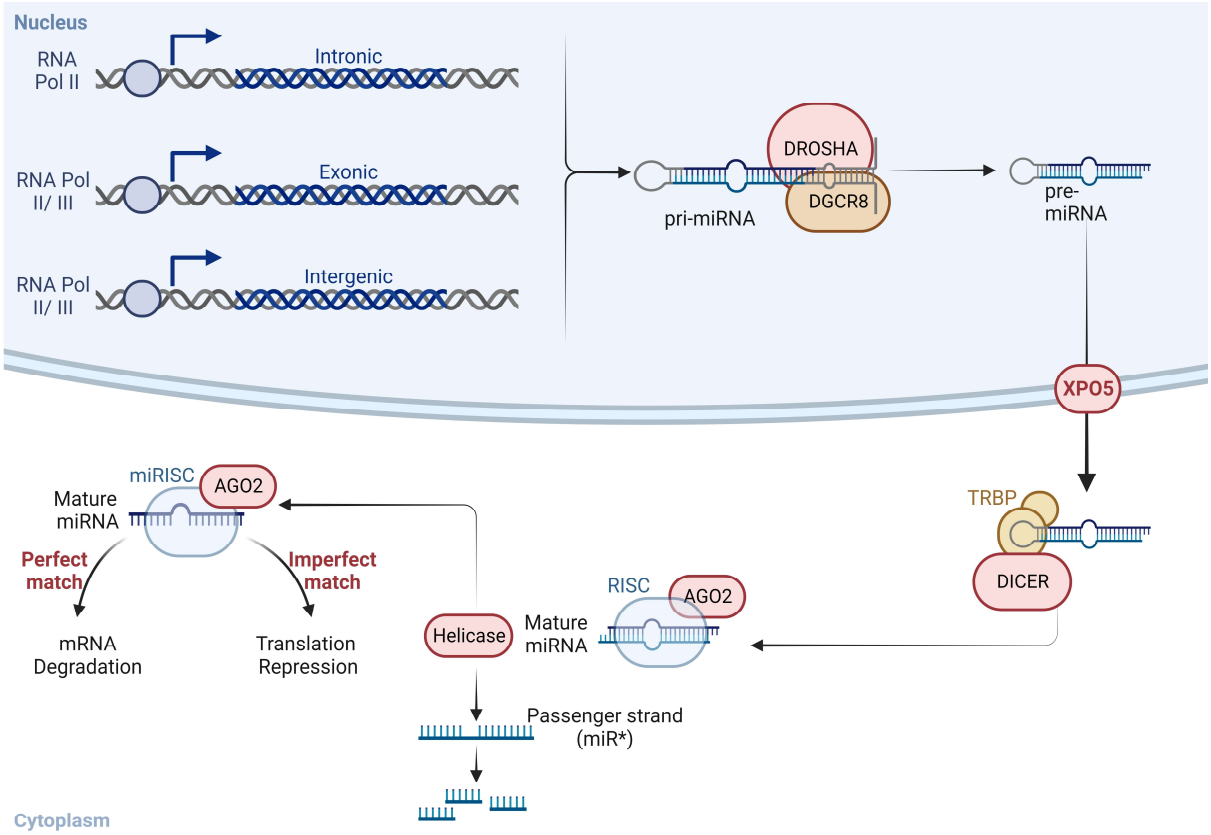

Figure 1.7: Biogenesis of miRNAs

Biogenesis of miRNAs is a multi-step process that includes transcription of a pri-miRNA, nuclear processing by *Drosha* and *DGCR8*, nuclear export of the pre-miRNA by exportin 5, and final unwinding of the mature miRNA duplex by helicase-mediated unwinding. To mediate either translational inhibition or mRNA degradation, the mature miRNA strand is either degraded or incorporated into the RNA-induced silencing complex (RISC). This is dependent on the degree of complementarity between the miRNA and its intended target. This image was created in BioRender.com. Detail was obtained from (Bronze-Da-Rocha, 2014).

1.4.1.2 Non-canonical pathway

The non-canonical synthesis of miRNAs takes place by bypassing some of the microprocessor step of miRNAs maturation discussed in section 1.4.1.1. This pathway is also involved in the progression of ageing diseases such as cancer (Stavast & Erkeland, 2019). miRNAs are produced non-canonically through two mechanisms: pathways that are dependent on Dicer and pathways that are independent of Dicer (Bronze-Da-Rocha, 2014).

Recent studies identified some miRtrons as non-canonical pri-miRNAs. miRtrons encoded in introns of coding genes despite being a commonly found source of canonical miRNAs (Stavast & Erkeland, 2019). MiRtrons, similar to introns, are spliced primarily in the nucleus, forming stable hairpins with shorter stem loop compared to canonical pri-miRNAs (Stavast & Erkeland, 2019). Due to its short sequence in the stem loop, DROSHA/DGCR8 cannot process miRtrons thus bypassing the microprocessor of canonical pathway. Conversely, debranching enzyme 1 (*DBR1*) cleaves the stem loop of miRtrons. Then, pre-miRNAs are exported and processed similarly as in the canonical pathway. miRNAs are still a gene expression regulator in cells that are not expressing *DROSHA*/*DGCR8*. Recently, based on the hairpin length and GC content of miRNAs, a highly accurate predictive modelling tool was developed (Rorbach *et al.*, 2018).

In Drosha/DGCR8-Dependent/Dicer-Independent pathways, there is only one miRNA, miR-451. Drosha/DGCR8 cleaves pri-miR-451 into an 18-bp duplex stem, which is too short to be used as a Dicer substrate. As a result, pre-miR-451 is directly loaded into *Ago2* protein. This finding has helped in improvement of RNA interference or RNAi tools especially in DICER-mutant tumor cells (Herrera-Carrillo & Berkhout, 2017).

Small interfering RNAs (siRNAs) maybe loaded preferentially into AGO2 with DICR-independent processing of small hairpin RNAs (shRNAs).

The main function of miRNAs is to target mRNA by complementary base pairing. This will result in either mRNA cleavage and degradation when the seed region of miRNAs is exactly matching to targeted mRNA or translation repression when seed region is imperfectly matching base pairing to targets (figure 1.7). Consequently, miRNA regulates the gene expression patterns and is necessary in both normal and abnormal cellular mechanisms including the ageing process and senescence.

1.4.2 miRNAs as diagnostic and prognostic biomarkers

More than 200 clinical studies are registered at clinicaltrials.gov in which a miRNA or miRNA signature is being investigated for a variety of clinical applications from early disease detection and diagnosis to treatment response and prognosis (ClinicalTrials.gov, 2022). Research on the significance of miRNAs in a variety of biological processes has shown that they have a substantial role in metabolic processes as well as cell proliferation, cell death, and many cellular roles. In this thesis, the well-documented miRNAs known to be involved in ARDs especially, cardiovascular disease, cancer, and diabetes mellitus were discussed.

1.4.3 Therapeutic potential of miRNAs

Up to date, the vast majority of miRNAs are in their early phase of clinical trials; therefore, the outcomes of miRNAs-based therapy that are undergoing clinical trials for human use remain to be seen, particularly in terms of efficacy and toxicity. miRNAs can directly target genes that cause diseases as oncogenes. For example, knockout

of miR-15a-miR-16-1 gene cluster of leukemic models identified a first miRNA gene that links to the causality of human cancer (Calin *et al.*, 2002). Another study showed that treating mice model of malignant pleural mesotheliomas with dsRNA miR-16 mimic overcame the resistance to chemotherapy (Reid *et al.*, 2013). The positive and promising findings led to a phase 1 clinical trial (NCT033689198; miR-16 mimic targomiR or mesomiR-1) which was designed to assess its safety and tolerability in patients with malignant pleural mesothelioma resistant to chemotherapy (van Zandwijk *et al.*, 2017). Results of the phase 1 of mesomiR-1 continued to show good preliminary results in term of safety and efficacy (van Zandwijk *et al.*, 2017). This study provides inspiring results that will support the plan to conduct a phase 2 clinical study to determine whether mesomiR-1 is effective as a single or in combination with chemotherapy.

miR-21 plays a role in tissue fibrosis, and inflammation (Borja-Gonzalez *et al.*, 2020), and it is one of the most highly expressed miRNAs reported in many cancer types (Bautista-Sánchez *et al.*, 2020; Feng & Tsao, 2016). Downregulation of critical cell cycle progression and/or apoptotic genes such *PTEN*, *PDCD4*, *RECK*, *ERK/MAPK*, *AKT* and *Sprouty1/2* drives the oncogenic activity of miR-21 in cancer cells (Feng & Tsao, 2016). For example, cancer development was delayed when knocking out miR-21 activity in two cancer models, lung adenocarcinoma (Hatley *et al.*, 2010) and lymphoma (Ma *et al.*, 2013). Also, miR-21 may possibly have a role in the development of resistance to chemotherapy in women with breast cancer. Tamoxifen and fulvestrant were shown to be more effective against breast cancer *in vitro* when miR-21 was silenced, boosting autophagic cell death and decreasing the PI3K-AKT-mammalian target of rapamycin pathway inhibition (Yu *et al.*, 2016). Currently, miR-21 is being investigated in two clinical trials (NCT03373786) and (NCT02581098).

The miR-17-92 cluster is another promising biomolecule in ARD targeting oncogenes and cell cycle regulating factors. Among the seven mature miRNAs in the major transcript are miR-17-3p, miR-17-5p, miR-18a, miR-19b, miR-20a, and miR-92a (Nikolajevic *et al.*, 2022). In B-cell lymphoma, a shortened variant of the cluster (lacking miR-92) was shown to be expressed ectopically, and as a result, this cluster was called (oncomiR-1) (He *et al.*, 2005; Ota *et al.*, 2004). MiR-17-92 was shown to be able to disrupt oncogenic Ras-induced senescence in human primary fibroblasts by directly targeting p21 in animal models of age-associated heart failure. Though there is currently a lack of data to support its significance in the onset of non-oncogenic senescence (Nikolajevic *et al.*, 2022). Furthermore, both embryonic and postnatal cardiac development was shown to be dependent on miR-17-92. MiR17-92 has been shown to suppress apoptosis directly through the MAPK/ERK and PI3K/Akt signalling pathways (Zhou *et al.*, 2013). Some miRNAs from miR-17-92 cluster have been investigated in clinical trials studies.

1.4.4 miRNA in senescence and ageing

There are numerous miRNAs that act as senescence and ageing modulators. Pathways that miRNAs control include sirtuins, mammalian target of rapamycin (mTOR), AMP-activated protein kinases (AMPKs), and other important pathways of the ageing process. Also, several miRNAs have been identified to regulate key genes in the nine hallmarks of ageing and also in the new evolving hallmark, dysregulation of alternative splicing (see figure 1.7). miRNAs are emerging as key regulators of senescence and ageing processes. In this part, various miRNAs that have been shown to have an impact on senescent cells and the lifespan of organisms will be discussed.

Cellular senescence occurs in response to the shortening of telomeres, the signalling of DDR, ROS, and the high expression of oncogenes. Senescent cells have also been linked to certain miRNAs. Among them are miR-34, miR-24, the miR17-92 cluster and its paralogues the miR-106a and the miR-106b cluster, all of which control DNA damage checkpoints (Harries, 2014). Additional miRNAs, such as miR-29, have also been linked in previous studies to ageing muscle and cellular senescence in HeLa/E6 cells (Hu *et al.*, 2014). The miR-29 interacted with the 3'-UTR of B-myb RNA (myeloblastosis-related protein B) and was up-regulated when cells entered the senescence state. A recent study reported that miR-29b-5p expression in osteoarthritis cartilage was shown to be greatly reduced, and upregulating miR-29b-5p level of expression might suppress the production of *Mmp* and ageing-related genes ($p16^{INK4A}$/p21); and as a consequence osteoarthritis articular cartilage was reduced and ageing phenotypes delayed in treated mice (Zhu *et al.*, 2022). Also, Igfbp5, which is a target gene of miR-143, being upregulated is linked to an increase in cellular senescence enhancing the ageing characteristics in skeletal muscle (Soriano-Arroquia *et al.*, 2016). miR-21 is another miRNA known to affect ageing of muscle *in vitro* through controlling *IL6R*, *PTEN*, and *FOXO3* signalling to decrease myogenesis (Borja-Gonzalez *et al.*, 2020). In senescent cells, expression of miR-21 was elevated, and its overexpression was linked to cell-cycle arrest and inflammation (Tyczewska *et al.*, 2016).

The expression level of miRNA has been reported in several studies to be associated with ageing processes. miRNA can regulate factors controlling the transcription and translation of genes involved in molecular pathways that related to human lifespan (Hamdan *et al.*, 2021). Studies have already show that human miRNAs were expressed differentially according to ageing and ARD in blood (Elsharawy et al., 2012;

Holly et al., 2015; Majidinia et al., 2020), serum (Smith-Vikos *et al.*, 2016), and plasma (Ameling et al., 2015; Olivieri et al., 2014; S. Wu et al., 2016) body fluids. Furthermore, some miRNAs have been shown to substantially vary between those who live long compared to individuals who lived short life (Huan *et al.*, 2018; Kinser & Pincus, 2020; Zhang *et al.*, 2015). (Islam *et al.*, 2021) explains the biological process by which three blood miRNAs (miR-181a-5p, miR-146a-5p, and miR-148a-3p) contribute to cognitive impairment. These three miRNAs may help maintain brain homeostasis in addition to providing information about changes in cognitive state (Islam *et al.*, 2021). Additional animal studies supported the finding that silencing these three miRNAs might improve cognitive function in old mice as well as AD models (Wang *et al.*, 2022). These reports have shown a strong correlation between ageing or ARD and miRNA in human.

p16 (*CDKN2A*), p53 (*TP53*), and p21 (*CDKN1A*) are all crucial actors in senescence and they are regulated by miRNAs (Harries, 2014). For instance, the activation of the DNA damage checkpoint's *CDKN2A-ARF* and p53 components in embryonic fibroblasts was discovered to be triggered by the loss of DICER and the subsequent influence on miRNA synthesis. Also, several miRNAs may influence p53 expression, including miR-20, miR-106a, miR-22, and miR-33 (Hu *et al.*, 2014). A further study has discovered 22 senescence-associated miRNAs that are found in human breast epithelial cells. It includes miR-26b, miR-181a, miR-210, and miR-424, which decrease polycomb group proteins *CBX7*, *EED*, *EZH2*, and *SUZ12*, and activate p16, a key regulator of cellular senescence (Caravia & López-Otín, 2015). Since most of these miRNAs target genes listed in several miRNA databases, it remains difficult to understand the physiological processes involved in the ageing and lifespan.

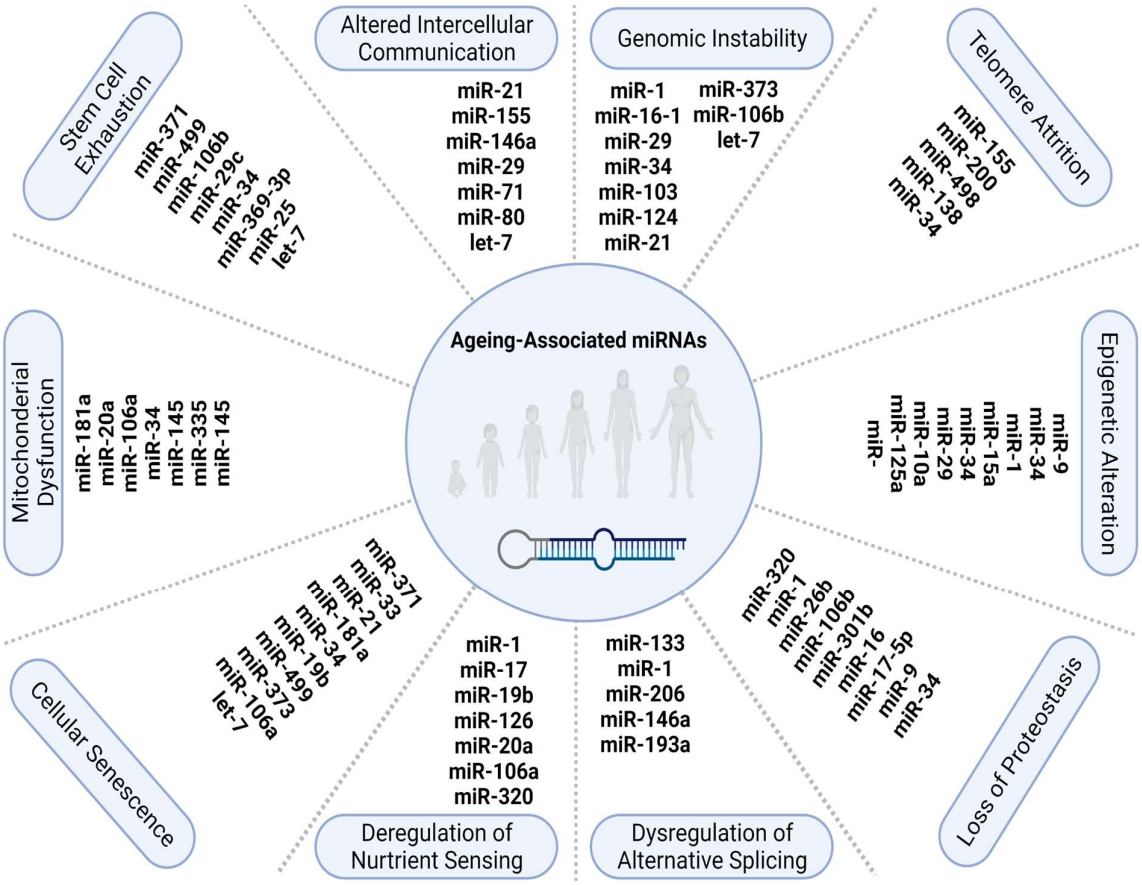

Figure 1.8: miRNAs influencing the hallmarks of ageing

The figure illustrated miRNAs that control over the nine hallmarks of ageing: genomic instability, telomere ageing, epigenetic regulation loss of proteostasis nutritional sensing deregulation mitochondrial malfunction stem cell fatigue and altered intercellular communication. Also, the new evolving hallmark, dysregulation of alternative splicing may be controlled by miRNA. Detail in figure was adopted from (Caravia & López-Otín, 2015; Harries, 2014). This figure was created in BioRender.com.

In normal mice, miR-146a-5p increases with age, while in long-living Ames dwarf mice, it remains constant (Victoria *et al.*, 2015). The miR-146a-5p mimic treatment promoted cellular senescence and inflammation in the visceral adipose tissue of df/df mice, while decreasing pro-apoptotic markers. This was also examined *in vitro* on 3T3-L1 cultured cells and it showed that miR-146a-5p mimics had similar influence on promoting senescence phenotypes as in df/df mice (Nunes *et al.*, 2021). These result suggest that miR-146a-5p may modulate senescent cells through increasing the production of SASP factors.

There are numerous miRNAs that have been linked to senescence and the ageing process (figure 1.8), but few of them have been suggested as directly causing and triggering senescence or its rescue. It is possible that miRNAs may act as a biomarker and potentially as a senotherapeutic target, leading to improve diagnosis and treatment of ageing-related diseases.

1.5 Research hypothesis:

MicroRNAs (miRNAs) play significant roles in numerous processes of cell development, growth, apoptosis, as well as ageing and senescence. In this thesis, I aimed to identify and examine miRNA with potential causal involvement in the ageing and senescence processes in human primary cell models and *in vivo* using *C. elegans* as an animal model.

The objectives of my thesis are to:

1. Identify miRNAs that might be causally involved in driving ageing phenotypes by determining those which demonstrate differential expression in early and late passage human primary endothelial cells, but also in response to small molecule reversal of senescent cell phenotypes, and test these for causality by targeted miRNA manipulation in late passage human primary endothelial cells.
2. Identify targets of dysregulated miRNAs that could be causally involved in ageing phenotypes by assessing effects of target gene knockdown on lifespan and ageing phenotypes in an invertebrate animal model system, *C. elegans*.
3. Assess whether targeted manipulation of miRNAs or their targets previously identified in the literature to be associated with senescence is able to rescue aspects of cellular senescence in aged primary human dermal fibroblasts, or to attenuate ageing and lifespan in an animal model system *C. elegans*.

These objectives will be investigated and presented as an individual chapter as mentioned below in details:

1.5.1 Chapter 3: Identification of miRNA may contribute to senescence in human primary endothelial cells.

The first aim of my thesis is to identify and evaluate miRNAs that were not only associated with senescence, but also with response to rescue. This was addressed through treatment of senescent human primary endothelial cells with a small molecule (resveratrol), previously demonstrated to attenuate aspects of the senescent cell phenotype in several primary human cell lineages (Latorre *et al.*, 2017). Whole miRNome expression profiling was then carried out in early passage, senescent and rescued human primary endothelial cells using the GeneChip™ miRNA 4.0 Array (Thermo Fisher Scientific, Applied Biosystems™) to identify differentially expressed miRNA. Those demonstrating differential expression were then assessed for effects on senescent cell phenotypes by the use of miRNA mimics and miRNA inhibitors in proliferating or senescent human primary endothelial cells. We found three miRNAs which were significantly differentially expressed between senescent and rescued cells of which one, miR-361-5p demonstrated antagonistic patterns of expression. Targeted manipulation with a miRNA mimic brought about a reduction in senescent cell load as measured by senescence-associated beta galactosidase (SA-β-Gal) staining, but in the absence of re-entry to cell cycle as assessed by Ki67 staining. This showed that miR-361-5p plays a role in senescent cells reversal.

1.5.2 Chapter 4: Determination of the role of miR-361-5p target genes in cellular senescence phenotypes *in vitro*, and on ageing and healthspan measures in *C. elegans*.

Manipulation of the orthologue genes targeted by miR-361-5p should yield effects on healthspan phenotypes in *C. elegans*. The objective of this aim is to prove that the targets of miR-361-5p, identified to be associated with being rescued a senescent state, in the previous chapter, play roles in improving the healthspan or lifespan *in vivo*. The assessment of the effects on healthspan and movement phenotypes in *C. elegans* upon knocking down targets of miR-361-5p using the Ahringer RNAi library (Kamath & Ahringer, 2003). Lifespan and healthspan assessed by using microfluidic chips (Rahman et al., 2020) (Infinity Chips, NemaLife Inc., TX, USA).

1.5.3 Chapter 5: miR-15b-5p, miR-92a-3p, miR-125a-3p miRNAs may have senescence maintenance roles

Targeted manipulation of senescence-related miRNAs may influence senescence phenotypes in the primary cells of NHDF. Our second *in vitro* model is the normal human dermal fibroblast NHDF. It has been shown in our lab that several types of fibroblasts had three common miRNAs has-miR-15b-5p, has-miR-92a-3p, has-miR-125a-3p that are downregulated at late passages (Holly et al., 2015). Therefore, here we hypothesize that miR-15b, miR-92a, and miR-125a miRNAs are necessary in the regulation, maintenance, and probably rescuing from senescence in fibroblasts. This is addressed by measuring the following cell kinetics SA-β-Gal assay, Ki67, yH2AX, and TUNEL upon knocking down or knocking in of miRNAs.

These 3 miRNAs have been validated to target *ZMPSTE24*, *INMT*, *LHFPL2*, and *LYST* (Holly *et al.*, 2015). In *C. elegans, ZMPSTE24* and *INMT* have orthologues namely *fce-1* and *anmt-3*, respectively. Here I assessed the effect on healthspan and movement phenotypes in *C. elegans* upon knocking down *fce-1* and *anmt-3* using the Ahringer RNAi library (Kamath & Ahringer, 2003). Lifespan and healthspan was assessed by using the microfluidic chips (Rahman *et al.*, 2020) (Infinity Chips, NemaLife Inc., TX, USA).

Chapter 2

Materials and Methods

2.1 Cell culture and treatment

In this thesis, two primary human cell types were used, Normal Human Dermal Fibroblast donated from a 36 year-old male (C-12302, PromoCell, Germany) (henceforth, referred as NHDF) and Human Aortic Endothelial Cells donated from a 45 year-old male (C-12271, PromoCell, Germany) (henceforth, referred as HAoECs). Propagation of cells were place in whole growth medium (C-23020 for NHDF or C-22022 for HAoECs media; Promocell, Germany) at 37°C with 1% penicillin and 1% streptomycin in ambient oxygen and 5% CO_2. Cell number was determined by either a hemacytometer chamber and/or the TC20™ automated cell counter (Bio-Rad, 1450102). Trypan blue was used to assess the percentage of living cells at cell passaging. To obtain the population doubling time (PD) of cells, the following formula was applied:

$$DoublingTime = \frac{duration * \log(2)}{\log(FinalConcentration) - log(InitalConcentration)}$$

Where "log" is the logarithm to base 2.

2.1.1 Human Primary Aortic Endothelial (HAoECs) Cells

The endothelial cells is a single layer of cells lining the blood vessels and has several functions in homeostasis, maintenance, and regulation of blood fluids and immune response (Jia *et al.*, 2019). With ageing, endothelial cells may influence many ARD such as cardiovascular diseases, arterial stiffness, atherosclerosis, hypertension, and cancer. Understanding how this cells maintain their senescence phase could lead to discovery of drugs to reduce ageing phenotypes associated with HAoEC senescence.

HAoECs cells can reach up to passage (P) 17; however, throughout this study P <7 (PD = 36) was considered as proliferating or non-senescent cells and P 14 to 16 (PD = 84) as senescent cells. While NHDF maybe sub-cultured up to about P 24; nonetheless, here, I used P <8 (PD = 38) for non-senescent and P 18 – 19 (PD = 96) for senescent cells as the cultures had ceased proliferating.

HAoECs senescent cells were treated with 5 μM of resveratrol (Sigma Aldrich, UK) for 48 hours to reverse senescent cells according the protocol described in (Latorre *et al.*, 2017). In a previous study, we showed that 5 μM resveratrol was sufficient to rescue human primary fibroblast senescent cells (Latorre *et al.*, 2017). Briefly, cells were seeded in a 6-well plate at a concentration of 4.0×10^5 cell/cm^2 and propagated until 70% - 80% confluent prior to treatment with resveratrol or DMSO. After 48 hours, cells were washed twice with 1X Dulbecco's phosphate-buffered saline (DPBS) followed by harvesting for RNA extraction or fixation for cell kinetics assays (these will be discussed in section 2.2).

2.1.2 Normal Human Dermal Fibroblast (NHDF) Cells

Fibroblast cells were the first to be discovered of having the hayflick limit (Hayflick, 1965) and hence, it is the most type of cells used by most researchers in *in vitro* work in ageing research due to the ease of isolation and manipulation. Fibroblasts are important in skin integrity and the physical immune barrier to the outside world of human body. Senescence in fibroblast reduces its main functions and leads to progression in ARD. Lago and Puzzi studied ageing phenotype changes in young and elderly fibroblasts from three different donors (Lago & Puzzi, 2019). Fibroblast cells remain an excellent *in vitro* model for ageing research and intervention.

2.1.1 Transfection of siRNAs, mimics, and miRNA inhibitors

To investigate the influences of hit genes and miRNAs on senescence phenotype, I used TriFECTa® Dicer-Substrate siRNA (DsiRNA) (Integrated DNA Technologies, USA) to knockdown genes of interest, miRNA MirVana mimic (Thermo Fisher, Waltham, MA, USA) to increase the level of miRNAs of interest, or MirVana miRNA inhibitor (Thermo Fisher, Waltham, MA, USA) to inhibit miRNA of interest. Lipofectamine® 3000 and Optim-MEM® (Life Technologies, Foster City, USA) were used to transfect small RNAs to cells; details are presented in table 2.1. Controls used to validate the transfection are negative control DS, TYE™ 563 DS transfection efficiency control, and HPRT-S1 DS positive duplex control (Integrated DNA Technologies, USA). A transfection efficiency control tye^{563} (IDT DNA Technology, INC) was transfected into the cells to quantify the transfection efficiency at a same dosage of siRNAs (30 pmol); scramble-treated cells were also included to check for effects caused by the transfection procedure itself.

Cells were cultured in a 6-well plate at a density of 1.5×10^6 and maintained at optimal culturing conditions until reaching 70% - 80% confluency. A day prior to transfection, cells were washed twice with 1X DPBS and growth medium was added without the 1% penicillin and 1% streptomycin. Reagents and transfections were prepared and performed as described in the Lipofectamine™ 3000 protocol. Cells were incubated at 37°C in ambient oxygen and 5% CO_2 for 24 hours. Followed by subsequent analysis.

Table 2.1 Summary of the DsiRNAs, miRNAs mimics, and inhibitor for indicated miRNAs used in this thesis. Sequence of these short RNAs is given or in case of DsiRNA targets of DsiRNA are indicated.

Name	Sequence and Target	Provider
DsiRNAs INMT	hs.Ri.INMT.13.1: target Exon 3 hs.Ri.INMT.13.2: target Exon 3 hs.Ri.INMT.13.3: target Exon 3	Integrated DNA Technologies, Inc.
DsiRNAs LHFPL2	hs.Ri.LHFPL2.13.1: target Exon 5 hs.Ri.LHFPL2.13.2: target Exon 5 hs.Ri.LHFPL2.13.3: target Exon 4	Integrated DNA Technologies, Inc.
DsiRNAs LYST	hs.Ri.LYST.13.1: target Exon 3 hs.Ri.LYST.13.2: target Exon 3 hs.Ri.LYST.13.3: target Exon 3	Integrated DNA Technologies, Inc.
DsiRNAs ZMPSTE24	hs.Ri.ZMPSTE24.13.1: target Exon 10 hs.Ri.ZMPSTE24.13.2: target Exon 4 hs.Ri.ZMPSTE24.13.3: target Exon 8	Integrated DNA Technologies, Inc.
miRNA Inhibitor hsa-miR-92a-3p	mA/ZEN/mC mAmGmG mCmCmG mGmGmA mCmAmA mGmUmG mCmAmA mU/3ZEN/	Integrated DNA Technologies, Inc.
miRNA Inhibitor hsa-miR-125a-3p	mG/ZEN/mG mCmUmC mCmCmA mAmGmA mAmCmC mUmCmA mCmCmU mG/3ZEN/	Integrated DNA Technologies, Inc.
miRNA Inhibitor hsa-miR-15b-5p	mA/ZEN/mC mAmGmG mCmCmG mGmGmA mCmAmA mGmUmG mCmAmA mU/3ZEN/	Integrated DNA Technologies, Inc.
mirVana™ miRNA Mimic hsa-miR-92a-3p	UAUUGCACUUGUCCCGGCCUGU	Thermo Fisher Scientific
mirVana™ miRNA Mimic hsa-miR-15b-5p	UAGCAGCACAUCAUGGUUUACA	Thermo Fisher Scientific
mirVana™ miRNA Mimic hsa-miR-125a-3p	ACAGGUGAGGUUCUUGGGAGCC	Thermo Fisher Scientific
mirVana™ miRNA Mimic hsa-miR-361-5p	UUAUCAGAAUCUCCAGGGGUAC	Thermo Fisher Scientific
mirVana™ miRNA Mimic hsa-miR-3665	AGCAGGUGCGGGGCGGCG	Thermo Fisher Scientific
mirVana™ miRNA Mimic hsa-miR-5787	GGGCUGGGGCGCGGGGAGGU	Thermo Fisher Scientific

mirVana™ miRNA Inhibitor hsa-miR-361-5p	N/A	Thermo Fisher Scientific
mirVana™ miRNA Inhibitor hsa-miR-3665	N/A	Thermo Fisher Scientific
mirVana™ miRNA Inhibitor hsa-miR-5787	N/A	Thermo Fisher Scientific

2.2 Cell kinetics

Cellular senescence does not possess a singular marker; therefore, multiple biomarkers are needed to assess the phase of cellular senescence. In this thesis, five different assays were used to assess cellular senescence: These were: Senescence associated β-Galactosidase (SA-β-Gal) staining to identify senescent cells on the basis of their high lysosomal content, ki67 staining to assess proliferation, γH2AX to assess DNA damage, and TUNEL assays to identify the cells undergoing apoptosis. Also, RT-qPCR was used to confirm changes of senescence-association genes.

2.2.1 SA-β-gal assay

SA-β-Gal staining assay kit was performed according to manufacturer's instructions (SigmaAldrich, CAT number: CS0030). Briefly, cells were seeded into 6-well plate until the desired confluency achieved, 70% - 80%. Cells were then washed twice with 1X DPBS and fixed with 4% paraformaldehyde diluted in 1X PBS for 10-15 minutes at room temperature. X-gal solution mixture 40 mM citric acid/sodium phosphate pH 6.0, 150 mM NaCl, 2 mM MgCl2, 5 mM potassium ferrocyanide, 5 mM potassium ferricyanide, 1 mg/ml X-gal in Dimethylformamide) then applied on cells for 20 – 22 hours in humidifier chamber at 37 ˚C . Images were acquired using a brightfield microscope and with magnification 10X and 20X objective lenses. Cells staining as blue were counted as positive then divided by whole number of cells to obtain the percentage of senescent cells. A minimum of 300 cells per replicate were assessed and at least three biological replicates was performed for each condition.

2.2.2 Determination of Ki67 and γH2AX positive cells through immunocytochemistry

Briefly, cells were seeded at 1 x 10^4 cells per 14 mm glass coverslip and after 10 days were treated with 5 μM resveratrol compound or vehicle DMSO or transfected with miRNAs mimics/inhibitors for 24 hours in 3 biological replicates. DDR were assessed using the antibody against γH2AX (Abcam, ab26350) and cessation of proliferation was confirmed using a commercially-available antibody against Ki67 (Abcam, ab16667). Cells were fixed for 10 min with 4% PFA and permeabilized with 0.025 % Triton and 5 % serum in PBS for 1 hour. Cells were then incubated with a rabbit monoclonal anti-Ki67 antibody (ab16667, Abcam, UK) at 1:400 overnight at 4 °C followed by FITC-conjugated secondary goat anti-rabbit (1:400) for 1 hour, and nuclei were counterstained with DAPI. Coverslips were mounted on slides in DAKO fluorescence mounting medium (S3023; Dako). Images were obtained with an Olympia microscope using the proper fluorescent channels. In each case, a minimum of 400 cells were assessed per replicate. Significance was determined by Students t-test in GraphPad Prism 8.

2.2.3 Apoptosis assays

The assessment of apoptosis in *in vitro* takes place by TUNEL assays and the transcriptional expression of apoptotic marker genes (*CASP1*, *CASP3*, *CASP7*, and *BCL2*).

For TUNEL Assay, the Click-iT TUNEL Alexa Fluor 488 Imaging Assay Kit (Thermo Fisher Scientific®, Catalogue number: C10245) was used. Cells were grown to less than

90% confluence on 14 mm round coverslips. Cells washed twice with DPBS then fixed by 4% paraformaldehyde for 10 – 15 minutes. TUNEL staining was performed by permeabilizing cells for 10 minutes with 0.1% Triton X-100 in 1X PBS. This was followed by incubating the coverslip for 60 minutes in a humidified chamber with TdT reaction mixture. This mixture is to incorporate an EdUTP into dsDNA stand breaks. Coverslips were washed three times with DPBS. Then incubated with the fluorescent detection of EdUTP with click chemistry for 30 minutes. Next, coverslips were washed three times with DPBS and stained the nucleus with DAPI for 5 minutes. The positive control was untreated cells were incubated with DNase1 after the permeabilization step and followed the protocol above. Images were acquired by Olympia microscope with a 40-objective lens using appropriate fluorescent channels. The TUNEL positive cells were counted if they exhibit DAPI signal as well.

The level of gene expression of *CASP1*, *CASP3*, *CASP7*, and *BCL2* were determined by RT-qPCR method (explained in detail elsewhere). The probes used in this experiment are listed in table 2.2

2.3 RNA extraction from cultured cells

Confluent cell cultures were seeded in 6-well plates at a density of 1.5 x 10^6. Cells were maintained in their optimal culture conditions unless otherwise mentioned until desired confluency. Prior to RNA extraction, cells were washed twice with DPBS. RNA was extracted using 1 mL of TRI Reagent® (Sigma-Aldrich, Steinheim, Germany), 10 µL $MgCl_2$ (ThermoFisher Scientific, Waltham, MA, USA) and 200 µL chloroform

(ThermoFisher Scientific, Waltham, MA, USA). Phenol and guanidine thiocyanate, two ingredients in TRI Reagent®, help to lyse cells, enable rapid inhibition of RNase activity, and partition RNA into the aqueous phase. During precipitation, $MgCl_2$ stabilises RNA-RNA interactions and enable longer biological RNAs to function as 'carriers' for small RNAs (Kim *et al.*, 2012) thus this extraction method is used also for the miRNAs extraction as well. The mixture was centrifuged for 45 minutes at 4°C at 14,800 x *g*. The top aqueous phase was carefully transferred to a new Eppendorf tube (~ 300 µL). 500 mL of absolute isopropanol were added to the tube alongside with 1.2 µL of GlycoBlue™ (Thermo Fisher, Waltham, MA, USA) to facilitate the precipitation overnight at -20°C. After precipitation, samples were centrifuged for an hour at 14,800 x g at 4°C to pellet the RNA. The pellet was washed in 75% ethanol to remove any remaining phenol-chloroform, then dried for about 15 minutes, and resuspended in RNase-free dH_2O.

2.4.1 RNA clean, concentration, and measurement

RNA samples intended for downstream analysis were purified using a RNA Clean & Concentrator kit (Zymo Research, CA, USA) according to the manufacturer's instructions. All of the RNA samples were measured using a spectrophotometer made by NanoDrop (NanoDrop, Wilmington, DE, United States), and where necessary, they were diluted to a final concentration of 300 ng/µL (using the appropriate diluent) in order to ease the normalisation of the RNA input amounts in the subsequent experiments.

2.4 Gene expression microarray

For microarray data, several analysis techniques for gene expression have been developed during the last 20 years. In this thesis, two microarray techniques were used: Clariom D and miRNA GeneChip microarrays.

2.4.1 Clariom D to analyze the whole transcriptome

Affymetrix released two versions of the Clariom™ array: Clariom™ S (shallow) and Clariom™ D (deep). In this study, I used the Clariom™ D. The Clariom™ D gives an extremely thorough picture of the transcriptome, which opens the possibility of conducting analysis of gene expression and alternative splicing processes not just in genes that code for proteins but also in lengthy non-coding genes. This version uses a database of more than 6.5 million probes to determine the expression of more than 130,000 genes and 540,000 transcripts. Affymetrix relied on more than 15 distinct sources of annotation in order to build such a comprehensive transcriptome. The Clariom™ array is available for human, rat, and mouse species in both versions. The Clariom™ D was used here to determine the genes expression in both young proliferating and old senescent cells in 3 biological replicates of each condition.

2.4.2 GeneChip® miRNA 4.0 Array

This technique measures the changes in miRNA expression, and it requires only 130 ng total RNA. Sample preparation and gene chip cartridge arrays were performed by a commercial subcontractor (UK Bioinformatics Ltd, Caterham, UK). Arrays are Coupled with the Affymetrix® FlashTag™ Biotin HSR RNA Labeling Kit for detection. Data

underwent quality control for probeset mean for hybridisation intensity, probeset residual mean which compares probeset signal to residual signal, poly-A positive spike in controls as control genes and positive versus negative area under the curve. SST-RMA was selected to reduce background and normalize intensity (Wu *et al.*, 2013). Data analysis of Affymetrix' miRNA Arrays generated CEL files that are compatible with transcriptomic Analysis Console (TAC) (Applied Biosystems) software (TAC 4.0.2.10) using the default settings (Ling & He, 2021; Rani *et al.*, 2017). Differences between two groups were identified by one-way ANOVA. Data analysis and statistical significance were completed using GraphPad Prism 8.0 software (GraphPad Software, La Jolla, CA, USA). Data were adjusted for false discovery rate by Benjamini Hochberg correction.

2.4.2 Bioinformatics

All Raw data of Clariom™ D and miRNAs 4.0 microarray were generated from a commercial subcontractor (UK Bioinformatics Ltd, Caterham, UK) and pre-analysed with the TAC software (TAC 4.0.2.10). Gene Ontology (GO) enrichment analysis was performed to explore the functions for each differentially expressed gene sets. Using R software the function *enrichGO* from *clusterprofiler package* (Yu *et al.*, 2012) was conducted and adjusted p value (FDR) <0.05 was considered as the cut-off for the significant enrichment. Enrichment results of GO biological process (BP), GO molecular function (MF) and GO cellular component (CC) were analysed for miR-361-5p and miR-15b-5p and their validated targets.

miRNAs demonstrate tissue specificity, so even genuine targets may not be present in the cells of interest. We identified 839 validated targets of miR-361-5p and 429 validated

targets of miR-15b-5p using the DNA intelligent analysis (DIANA) mirPath v3.0 database and miR-TarBase (Paraskevopoulou *et al.*, 2013; Vlachos *et al.*, 2015), which includes only experimentally validated target genes (Huang *et al.*, 2020). Thresholds were set at the default of -1.0. Gene Set enrichment analysis (GSEA) was carried out using EnrichR (Chen *et al.*, 2013) to identify pathways that were enriched in validated target genes of miR-361-5p and miR-15b-5p. EnrichR is a webtool designed to determine whether candidate genes from a user-supplied list are present in specific GO biological function processes than one would expect by chance, based on the adjusted p value (ranking derived from Fisher exact test for gene sets) significance.

2.5 Reverse transcription

Reverse transcription is used to create complementary DNA (cDNA) of RNA samples in order to measure the level of gene expression. Similar to standard PCR protocol, the reaction mixture includes dNTPs, a buffer solution, and $MgCl_2$, which functions as a cofactor for the *Taq* polymerase enzyme.

In this thesis, we used EvoScript Universal cDNA Master kit (Roche LifeScience, Burgess Hill, West Sussex, UK) for RT of longer than 200 nucleotides transcripts. While for shorter RNA sequences (miRNAs), Applied Biosystems™ TaqMan™ Advanced MicroRNA Reverse Transcription Kit was used.

2.5.1 EvoScript universal cDNA reverse transcription

The two-tube EvoScript Universal cDNA Master kit contains an "Enzyme mix" tube that contains a combination of exclusive enzymes as well as Protector RNase Inhibitor. Random primers, tethered oligo(dT), dNTP, and $Mg(OAc)_2$ are all present in a second "Reaction buffer" tube. In order to make it easier for PCR primers to attach to the cDNA, EvoScript reverse transcriptase maintains its RNase H activity, which eliminates the RNA template following cDNA synthesis. As a result, additional care must be made to administer the "Enzyme mix" before incubation in order to prevent digestion. After being normalised to 300ng/µL, RNA samples were added in 1 µL increments to an RT reaction using 1X "Reaction buffer" and RNase-free dH_2O, resulting in a total volume of 18 µL. The samples were then kept on ice for 5 minutes to enable the primers to anneal to the RNA. Next, 2 µL of "Enzyme mix" was added to the samples, resulting in a final volume of 20 µL that had a 1X concentration. Reactions were put on a thermal cycler and incubated at 42 °C for 30 minutes, 85 °C for 5 minutes, 65 °C for 15 minutes, and 4 °C for a final hold. To ensure there was enough cDNA for subsequent analysis, samples were then diluted 1:5.

2.5.2 TaqMan™ Advanced microRNA reverse transcription

The Taqman® Advanced miRNA Assay kit was used to create the cDNA for the miRNA expression measurements (Thermo Fisher, Waltham, MA USA). Before beginning the reverse transcription process, the sample concentration was adjusted to 5 ng/µL. This assay comprises a 4-step processes to elongate the mature miRNA sequence and a miR-Amp reaction prior to RT-qPCR. First, a polyA tail is added to the 3' end of the miRNA

sequence through addition of 2 µL RNA sample and 3 µL of Poly(A) Reaction Mix followed by 45 minutes of cycling at 37 ^{o}C and a final 10 minutes at 65 ^{o}C to finish the reaction. The second step involves adding a 5' adapter ligation for 60 minutes at 16 ^{o}C to extend the mature miRNAs already present in the sample. The third step is the reverse transcription process that is carried out using universal primers, which are able to detect the universal sequences on the 5' and 3' ends of the miRNAs, after these preparatory reactions. For this reaction, the cycling conditions are 42 ^{o}C for 15 minutes, followed by a 5-minute cycle at 85 ^{o}C to halt the reaction. The fourth step is to amplify miRNA targets that lowly expressed; the product of the reverse transcription reaction is amplified in the miR-Amp reaction. Figure 2.1 provides an illustration of these 4 steps. The finished product is then diluted at 1:10 for RT-qPCR experiments.

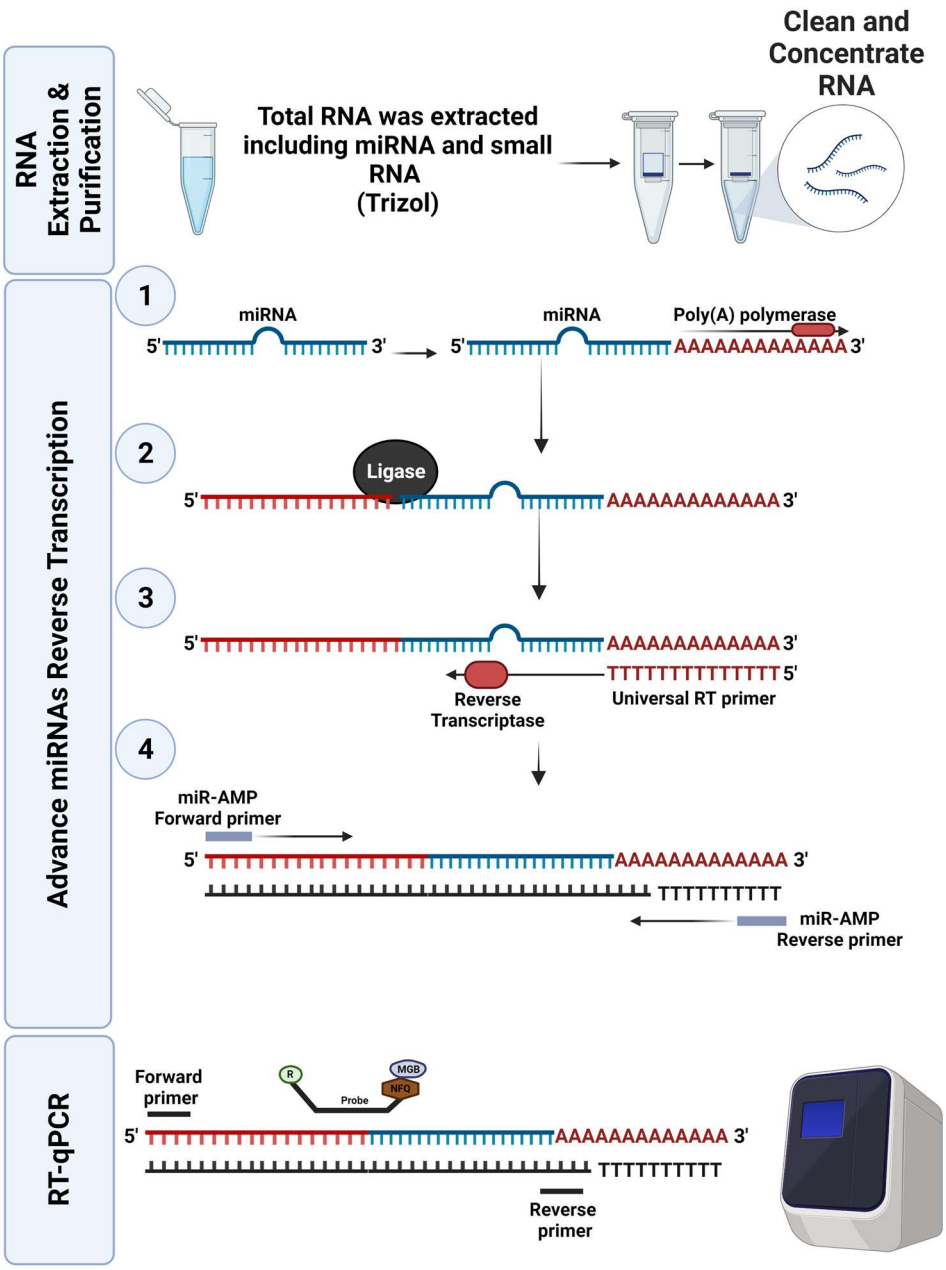

Figure 2.1 TaqMan™ Advanced miRNA Assay

TaqMan® advanced miRNA assay is 4 a step-processes. (1) Poly(A) tailing reaction that starting with a total RNA sample, poly(A) polymerase is used to add a 3' adenosine tail to the miRNA. (2) Adaptor ligation reaction where the miRNA with poly(A) tail undergoes adaptor ligation at the 5' end. The adaptor acts as the forward-primer binding site for the miR-Amp reaction. (3) Reverse transcription (RT) reaction occurs by a Universal RT primer bind to the 3' poly(A) tail and the miRNA is reverse transcribed. The resulting cDNA is suitable for all TaqMan Advanced miRNA Assays. (4) miR-Amp reaction process uses universal forward and reverse primers to increase the number of cDNA molecules. RT-qPCR reaction. This figure was created in BioRender.com based on the protocol provided by manufacturer.

2.6 Quantitative Real-Time Polymerase Chain Reaction (RT-qPCR)

In this thesis, I used the oligonucleotide probes designed in (ThermoFisher, Waltham, MA, USA) TaqMan™ assays (probes, used in this thesis, are summarized in table 2.2). The hydrolysis probes used in TaqMan™ assays have a Minor Groove Binding (MGB) domain linked through a flexible linker at the 5' end, a non-fluorescent quencher (NFQ) at the 3' end, and a reporter fluorophore covalently coupled to the 5' end. The shorter oligonucleotides may be synthesized, which results in better specificity and less background fluorescence. The MGB enhances probe binding to its complementary sequence and increases the melting temperature (Tm) of the probe. *Taq* polymerase has 5' to 3' exonuclease activity which cleaves the probe during the PCR extension phase, that causes the fluorophore and quencher to become uncoupled. The outcome is a fluorescent signal proportionate to the number of cleaved probes and consequently the number of amplification products in the reaction since these are no longer close together for quenching to occur.

Experiments with these assays were carried out in manually loaded 384-well plates and the reactions taken place using Applied Biosystems™ QuantStudio 12K Flex Real-Time PCR System. To measure the gene expression in samples, the following components were mixed: cDNA, TaqMan™ Universal Master Mix II, no UNG, RNase-free dH_2O, and TaqMan™ Assay were combined in suitable amounts to provide a 15 µL final reaction volume. This is enough for 3 technical replicates, and they were combined into a single big volume before being put onto the 384-well plate to reduce pipetting error. A single cycle of 95°C for 10 minutes, followed by 45 cycles of 95°C for 15 seconds and 60°C for one minute, comprised the cycling conditions. The following elements were used to

measure the expression of miRNA in samples: an appropriate mixture of cDNA, TaqMan™ Fast Advanced Master Mix, TaqMan™ Advanced miRNA Assay (20X), and RNase-free dH_2O was used to create a final reaction volume of 15 µL. A single cycle of 95°C for 20 seconds, followed by 45 cycles of 95°C for 3 seconds and 60°C for 30 seconds, comprised the cycling conditions.

Table 2.2 RT-qPCR probes used in this thesis.

Transcript Name	Transcript ID	Role
CDKN1A	Hs00355782_m1	Senescent marker
CDKN2A	Hs00923894_m1	Senescent marker
LMNB1	Hs01059205_m1	Senescent marker
CXCL8 (IL8)	Hs00174103_m1	SASP factor
IL6	Hs00174131_m1	SASP factor
CXCL1	Hs00236937_m1	SASP factor
CXCL10	Hs00171042_m1	SASP factor
BCL2	Hs04986394_s1	Apoptotic marker
CASP1	Hs00354836_m1	Apoptotic marker
CASP3	Hs00234387_m1	Apoptotic marker
CASP7	Hs00169152_m1	Apoptotic marker
ARPC5L	Hs00229649_m1	Targeted by miR-361-5p
EZR	Hs00931646_m1	Targeted by miR-361-5p
HNRNPM	Hs01115690_m1	Splicing and Targeted by miR-361-5p
INMT	Hs04233979_m1	Targeted by miR-15b-5p
ZMPSTE24	Hs00195298_m1	Targeted by miR-15b-5p
LYST	Hs00915889_m1	Targeted by miR-15b-5p
LHFPL2	Hs00299613_m1	Targeted by miR-15b-5p
ETV6	Hs00231101_m1	Targeted by miR-3665
ALCAM	Hs00977641_m1	Targeted by miR-3665
CXorf36	Hs01126375_m1	Targeted by miR-3665
HNF1A-AS1	Hs00703760_s1	Targeted by miR-3665
FAM107A	Hs00200376_m1	Targeted by miR-3665
ZNF675	Hs00603247_m1	Targeted by miR-3665
HPRT1	Hs02800695_m1	House keeping
TUBB4A	Hs00760066_s1	House keeping
ACTR1B	Hs00194899_m1	House keeping
GAPDH	Hs02786624_g1	House keeping
GUSB	Hs00939627_m1	House keeping

2.6.1 Relative quantification

Relative quantification of gene expression levels from RT-qPCR data could be done by $2^{-\Delta\Delta CT}$ method, the Pfaffl method (Pfaffl, 2001), and sigmoidal (Rutledge, 2004). The $2^{-\Delta\Delta CT}$ approach is the most straightforward and popular way to calculate relative quantification. In this thesis, the relative expression of both the gene expression and miRNA expression experiments were determined using the comparative $2^{-\Delta\Delta CT}$ technique and calculations were performed in Excel.

This approach employs the CT value, which is the PCR cycle at which fluorescence exceeds the background threshold. This method is simple to apply, however it makes the assumption that the transcript amplification efficiency is 100% which is the case for all TaqMan™ used in this thesis. Each sample's CT values for the genes of interest (GOI) and Housekeeping (HK) genes are acquired. It is important to note that many HKs are often included into experimental designs, and it is important to apply an average (or geometric mean) of the Ct values of these genes. The first step in calculating $2^{-\Delta\Delta CT}$ is within-sample normalisation, which uses the HK gene(s) to adjust for any difference in cDNA products. This is measured by deducting the HK CT value by the GOI CT value to get a ΔCT value. In the following step, calculation of the change in the ΔCT value relative to calibration samples. The calibrators are variable based on the experimental design. For each sample, subtracting sample's ΔCT value from the calibrator's ΔCT value produces each sample's ΔΔCT value. Also, essentially zeros out the calibrators. The ΔΔCT value measures how each sample's expression has changed in relation to the calibrator, but since it currently depends on the number of cycles between samples, it must be transformed to provide a fold-change measurement that is easier to comprehend.

Using the formula $2^{-\Delta\Delta CT}$, each value is transformed into a fold-change value, which may then be utilised for statistical analysis. The expression of each gene or miRNA was measured and normalised relatively to the geomean.

2.7 *Caenorhabditis elegans* as a systemic model organism for miRNA and ageing studies

Caenorhabditis elegans (*C. elegans*) was isolated and characterised by Émile Maupas, a librarian and biology enthusiast. With the intention of using it as a model for reproduction. Maupas' publications from 1899 and 1900 describe for the first time *C. elegans* life cycle. He studied how *C. elegans* reproduces from embryonic development to the formation of larvae 2, which could live for several months. Sections 2.8.1 and 2.8.2 are mainly from the wormbook (Dreisbach, 2022) unless otherwise indicated.

2.7.1 The life cycle of *C. elegans*

C. elegans, like many other nematodes, has a life cycle that includes an embryonic stage, four larval stages, and an adult stage. *C. elegans* undergoes moults as it transitions between larval and adult stages, noted by shedding of the outer cuticle and temporary cessation of the pharyngeal pump, which is used to consume food. In general, worms have a lifespan of between two and three weeks, although it can differ based on genetics and environmental conditions. The first day after they turn into adults, worms begin to lay eggs. In order of development, the larval stages are L1, L2, L3, and L4. Each of these stages differs in duration based on the temperature. At higher temperatures, worms

develop more rapidly, while lower temperatures result in slower development. A worm's development depends on its temperature, as higher temperatures allow it to develop more rapidly. Experimental culturing typically takes between eight and fourteen hours, depending on the temperature (16-25°C). In severe conditions such as starvation, overcrowding, and extreme temperatures, *C. elegans* L1 and L2 larvae can go through an alternative developmental mode known as the Dauer stage ("dauer," German which means duration). Dauer stage worms have thickened cuticles and are generally much harder to kill, thus permitting them to persist in a kind of stasis for several months. DAF-7/TGF-β and the Insulin-like pathways control switching to the dauer stage. A graph summarizing the life cycle of the worm at 22°C is depicted in figure 2.2.

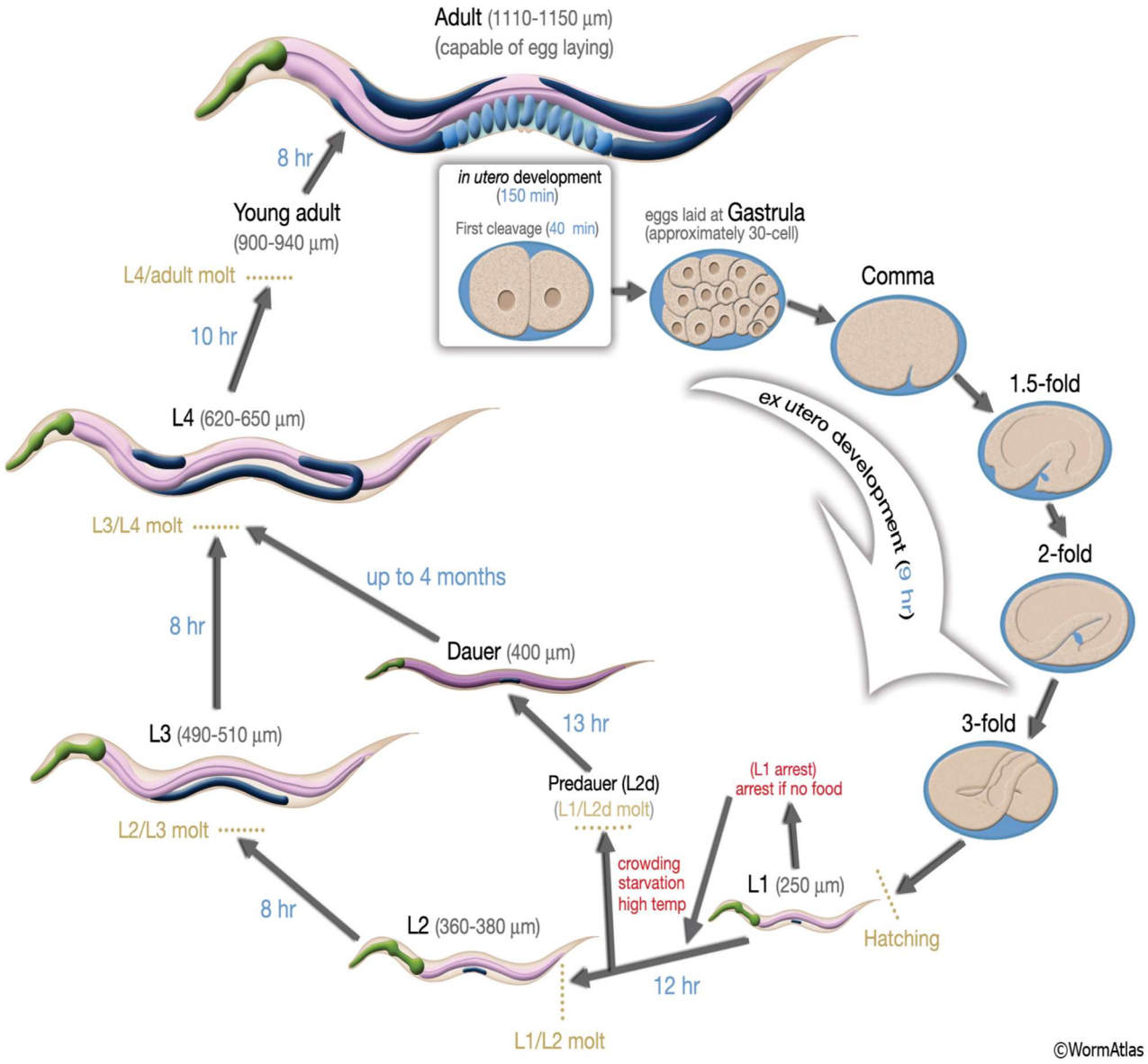

Figure 2.2 *C. elegans* Life Cycle

The figure illustrates the life cycle of C. elegans at 22 °C. There are four larval stages (L1, L2, L3, and L4) in the life cycle of C. elegans prior to adulthood. The dauer larval stage, characterised by fat buildup and extended life, may be triggered by starvation or other environmental stresses and at this stage C. elegans could live for several months. When stressors are removed from an organism's environment, the worm may depart the dauer stage and become an adult, but transcriptional alterations may continue. Figure reproduced from WormAtlas.

2.7.2 Genome and genetics of the *C. elegans*

In *C. elegans*, the genome is made up of 100 megabases, which are distributed among five autosomes and one allosome. Shermaphrodites have two X chromosomes, while males have only one X chromosome. Despite being extremely information-rich, the *C. elegans* genome is very small. Twenty-five percent of the DNA is protein-coding but 40% of the genome is made up of genes (including introns and other regulatory sections). A total of 20,470 genes have been identified in *C. elegans*, with 35% having orthologs in humans. Its sequence and detailed annotation have also made it a perfect model for molecular biology and genetics since the worm is easy to manipulate genetically and can be sequenced completely.

2.8 *C. elegans* growth and conditions

Wild-type Bristol nematodes (N2 Bristol) were maintained on nematode growth media (NGM) plates planted with Escherichia coli OP50 at 20°C. The strain was maintained according to the previously described methods (Brenner, 1974). Briefly, they were kept at 20 ℃ on 6cm plates (Greiner Bio One) containing nematode growth media (NGM) (50 mM NaCl, 0.25% (w/v) bacto peptone, 1.7% (w/v) agar, 1 mM CaCl2, 1 mM MgSO4, 25 mM KH2PO4, 12.9 μM cholesterol) which was seeded with the E. Coli OP50 strain.

2.8.1 RNAi library

The RNA interference (RNAi) library from Ahringer was used in this study (Kamath & Ahringer, 2003). In spite of the fact that RNAi was first observed in plants in the early

1990s, the mechanism for its activity was not elucidated until the experiments conducted by Craig C. Mello and Andrew Fire on *C. elegans* in 1998 (Fire *et al.*, 1998). The RNAi treatments were carried out by feeding *C. elegans* with *E. coli* bacteria expressing dsRNA against targeted mRNAs. This strain of bacteria does not possess the enzyme ribonuclease III, which is required to degrade dsRNA. Any cloned DNA sequence can be inserted into the bacteria containing the L4440 vector (empty vector) and it has been used in this study as a control.

C. elegans were synchronised by gravity using M9 solution (3 g KH_2PO_4, 6 g Na_2HPO_4, 5 g NaCl, 1 mL 1 M $MgSO_4$, H_2O to 1 litre). Afterwards, synchronised L1 larvae were plated on RNAi NGM plates containing (50 mM NaCl, 0.25% (w/v) bacto peptone, 1.7% (w/v) agar, 1 mM $CaCl_2$, 1 mM $MgSO_4$, 25 mM KH_2PO_4 (pH 6), 12.9μM cholesterol, 1 mM IPTG, 50 μg/mL ampicillin. The RNAi were plated with bacteria expressing L4440 or the genes of interest as dsRNA. A comprehensive list of the RNAi clones used in this study can be found in the table 2.3 below.

Table 2.3: A comprehensive list of the RNAi clones used in this study.

Gene Name *(Hs)*	Gene ID *(Hs)*	Gene Name *(C. elegans)*	Sequence ID *(C. elegans)*	Genetic position *(C. elegans)*	Protein Sequence Similarities
ARPC5L	ENSG00000136950	*C46H11.3*	C46H11.3	I:-0.42 +/- 0.000 cM (interpolated)	38.41 %
EZR	ENSG00000092820	*erm-1*	C01G8.5	I:-0.16 +/- 0.005 cM	59.34 %
AMFR	ENSG00000159461	*hrdl-1*	F26E4.11	I:3.91 +/- 0.001 cM	22.91 %
HNRNPM	ENSG00000099783	*sup-46*	C25A1.4	I:4.72 +/- 0.000 cM	33.65 %
IQGAP1	ENSG00000140575	*pes-7*	F09C3.1	I:24.15 +/- 0.021 cM	26.91 %
FN1	ENSG00000115414	*let-805*	H19M22.2	III:-10.86 +/- 0.073 cM	22.01 %
DIAPH1	ENSG00000131504	*cyk-1*	F11H8.4	III:-0.83 +/- 0.009 cM	30.38 %
PRPF8	ENSG00000174231	*prp-8*	C50C3.6	III:-0.37 +/- 0.000 cM	86.61 %
TGFBR1	ENSG00000106799	*daf-1*	F29C4.1	IV:-26.90 +/- 0.008 cM	34.14 %
WASL	ENSG00000106299	*wsp-1*	C07G1.4	IV:3.66 +/- 0.003 cM	35.48 %
VCL	ENSG00000035403	*deb-1*	ZC477.9	IV:3.29 +/- 0.000 cM	46.52 %
RHOA	ENSG00000067560	*rho-1*	Y51H4A.3	IV:15.09 +/- 0.001 cM	88.02 %
ACTN4	ENSG00000130402	*atn-1*	W04D2.1	V:4.31 +/- 0.022 cM	61.88 %
TWIST1	ENSG00000122691	*hlh-8*	C02B8.4	X:-0.53 +/- 0.011 cM	36.28 %
VIM	ENSG00000026025	*ifa-1*	F38B2.1	X:2.87 +/- 0.001 cM	29.00 %
SDC4	ENSG00000124145	*sdn-1*	F57C7.3	X:2.31 +/- 0.010 cM	27.92 %
DAG1	ENSG00000173402	*dgn-2*	F56C3.6	X:-18.21 +/- 0.052 cM	21.68 %
INMT	ENSG00000241644	*anmt-3*	T07C12.9	V:2.22 +/- 0.000 cM	41.82 %
ZMPSTE24	ENSG00000084073	*fce-1*	C04F12.10	I:3.86 +/- 0.001 cM	25.00 %

2.8.2 Microfluidic Chips for *C. elegans* motility and lifespan studies

Microfluidics is a recently developed technique that has enhanced *C. elegans* research which has helped to answer several biological and genetics questions. Numerous investigations that would not be conducted using traditional techniques have been made possible. Examples available now that highlight the key benefits of employing microfluidics for *C. elegans* research, including the ability to create exact environmental conditions, simplify worm handling and imaging. In this thesis, I used the NemaLife Microfluidic Device (Infinity chip, NemaLife Inc.) to investigate the involvement of top hit miRNAs from *in vitro* studies on the healthspan and lifespan of *C. elegans.*

2.8.3 Loading *C. elegans* into microfluidic chips

The microfluidic chip, described in figure 4.1 in details, (Infinity chip, NemaLife Inc.) were sterilized by immersion in 70% ethanol for five minutes before using for lifespan experiments. Basal S-complete solution was then rinsed 4–5 times over the microfluidic chip. For 30 minutes, chips were treated with 5 wt% Pluronic F127 (Sigma-Aldrich) to prevent bacterial and protein build-up. Additionally, pluronic treatment helps to remove trapped air bubbles. Using basal S-complete, excess Pluronic was removed after 1 hour incubation at room temperature. The Pluronic-treated chips were stored in moist petri dishes at 20 °C for immediate use and at 4 °C for future use. 60 - 70 worms were loaded into each device following the protocol suggestion (Rahman *et al.*, 2020).

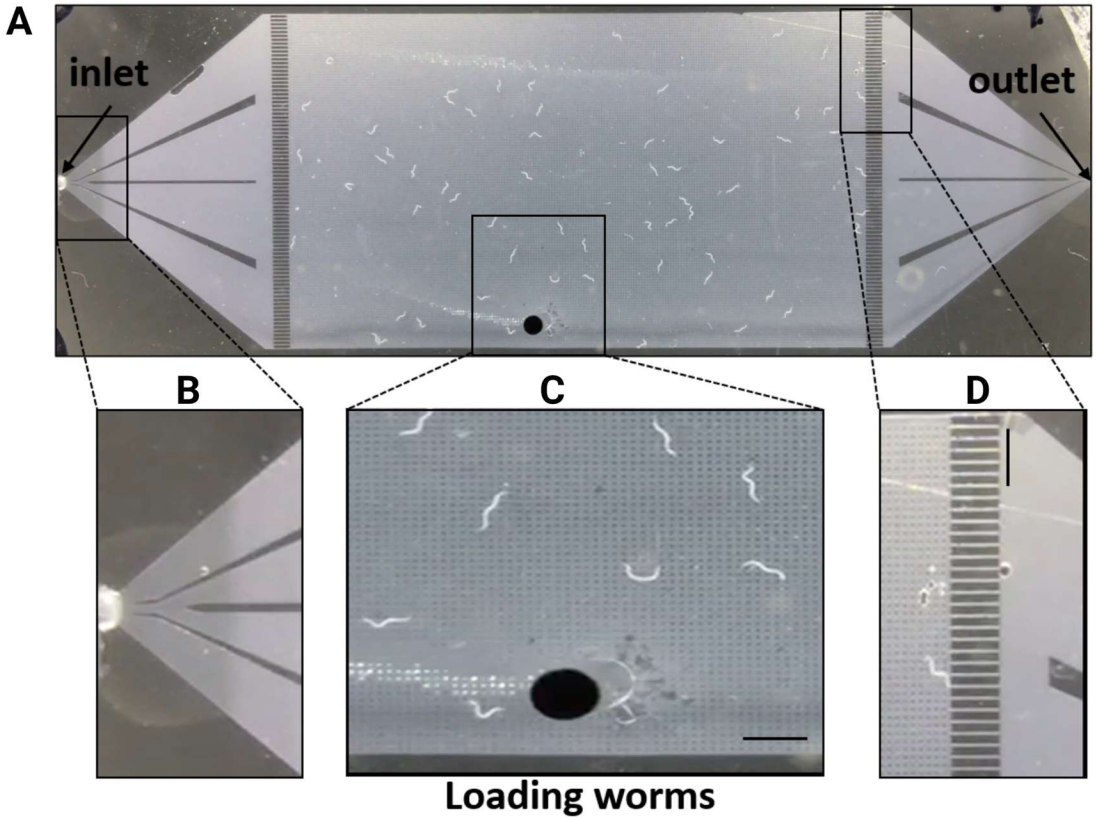

Figure 2.3 NemaLife chip design and description.

A microfluidic device for lifelong studies of crawling *C. elegans*. Devices contain ports ((B) inlet, (D) outlet, and main port for loading worms) for connecting 1-mL syringes for fluid manipulation. (A) Micropillars compose the habitat arena. (C) A view of the lattice structure arrangement and the micropillars. Scale bar is 1 mm.

2.8.4 Analysis of *C. elegans* lifespan and healthspan

Microfluidics-based Infinity Screening System was used to conduct lifespan and healthspan assays (NemaLife Inc.). Worms were raised to the start of adulthood according to protocol instructions (Ellwood *et al.*, 2021). From the first day of adulthood until death, survival analysis was repeated daily. We imaged the microfluidic culture chips daily for 180 seconds and washed them to remove progeny. The initial 90 seconds is used to monitor *C. elegans* while washing and the later 90 seconds is to score the lifespan and healthspan. We then fed the chips 20 mg/mL of *E. coli* OP50 in liquid NGM containing RNAi clone. The chips were stored at 20 °C in Petri dishes with damp tissue wrapped in parafilm until subsequently used. Using the Infinity Code software, the acquired videos were scored for live/dead animals (NemaLife Inc.).

2.8.5 The NemaLife software for assessment of lifespan and healthspan *C. elegans* video

The Infinity Code Analysis System (NemaLife Inc.) was used for imaging analysis. The first 90 seconds taking during washing is used to score for loss of worms. The post-wash segment of the movie, which is 90 seconds, containing 900 frames, were processed and analysed in the software. The software has three processing stages, optimization, process, and storyboard (illustrated in figure 2.4). The optimization step performs cropping, thresholding, and measurement of vitality. The main operation is the processing step that can be used to perform batch processing of movies including naming and frames selection. Experiment parameters were measuring from the 900 till 1800 frames and the skip rate is 280 frames. The last step is the storyboard step which is allowing for manual

validation and annotation of objects and exporting the processed excel file. The heatmap guideline showed very active worms as red and less active or inactive worms as blue.

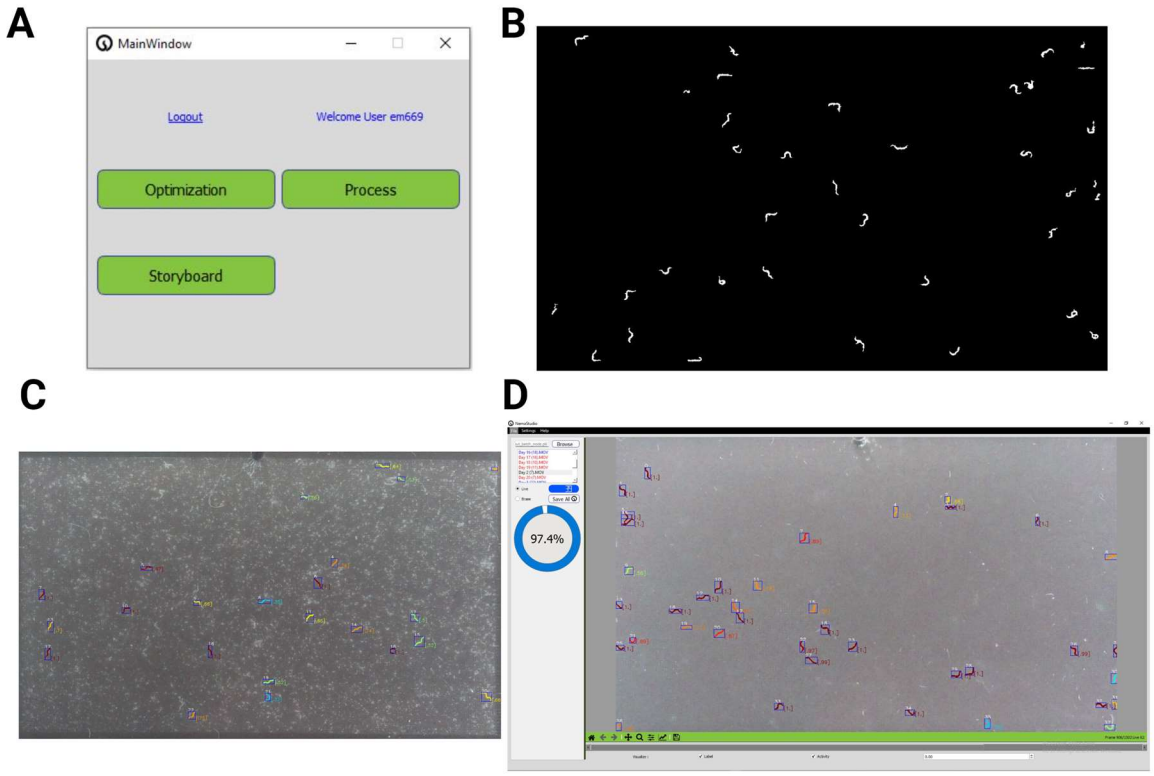

Figure 2.4 NemaLife software and the process of Imaging analysis of *C. elegans* lifespan and healthspan.

(A) The analysis process of *C. elegans* video occurs at 3 stages: optimization, process, and storyboard. (B) The optimization module performs cropping, thresholding, and measurement of vitality (live, dead, and activity assays). (C) The processing step is to perform batch processing of movies (D) Storyboard and exporting the analysis file.

2.9 Statistical methods

All *in vitro* experiments were performed in minimum of three biological replicates, unless indicated otherwise. Data are shown as mean and standard deviation and analyses were calculated using GraphPad Prism version 9.0. Differences between two groups were identified by one-way ANOVA in case of miRNAome data analysis. Also, to compare two groups the Student's t-test was performed, and survival was analysed by using Kaplan–Meier curves, with Bonferroni-corrected multiple comparisons in case of multiple comparison test. A *p-value* below 0.05 was considered statistically significant (* $p<0.05$, ** $p<0.01$, *** $p<0.001$, **** $p<0.0001$).

Chapter 3
miR-361-5p: A resveratrol-responsive miRNA associated with rescue from cellular senescence

3.1 Abstract

The accumulation of senescent cells is a key regulator of ageing. MicroRNAs are a key component of the molecular machinery which are emerging as crucial regulators of cellular senescence. Here, we have carried out a whole miRNome characterisation of the patterns of miRNA expression in early and late passage human primary endothelial cells, as well as late passage cells that have undergone cellular rejuvenation following treatment with the polyphenol resveratrol, to identify miRNAs associated with both senescence and reversal. We have identified a miRNA (miR-361-5p) that demonstrates an association with both conditions following correction for multiple testing, and exhibits an antagonistic pattern of expression in senescence and rescue. Validated target genes of miR-361-5p were demonstrated to be enriched in pathways that regulate proteostasis and mRNA processing by gene ontology biological process pathways analysis. Treatment of aged endothelial cells with a miR-361-5p mimic caused a 24% decrease in the senescent load of the culture, but in the absence of effects on proliferation. These data indicate that dysregulation of miR-361-5p may contribute to cellular senescence in human primary endothelial cells, and pathways enriched in its targets may include those involved in known hallmarks of ageing.

3.2 Introduction

Organismal ageing and its associated biochemical and cellular changes are major risk factors for the development of common and/or complex disease (Fougère *et al.*, 2019). It was initially assumed that each age-related disorder was associated with a unique and specific set of triggers, but it is now becoming increasingly apparent that this may not be the case, and that many share common disease processes (Kenessary *et al.*, 2013). The factors leading to such as the hallmark of ageing remain elusive and require further investigation. However, there are consistent changes in cell biology that occur in ageing cells, which are known collectively as the 'hallmarks of ageing'. These include alteration of intracellular communication, stem cell exhaustion, genomic instability, shortening of telomere length, loss of proteostasis, epigenetic alteration, dysregulation of nutrient sensing, malfunction of mitochondria, and cellular senescence (López-Otín *et al.*, 2013); also another five new hallmarks of ageing have been added to this list which are compromised autophagy, microbiome disturbance, altered mechanical properties, splicing dysregulation, and inflammation (Schmauck-Medina *et al.*, 2022).

Cellular senescence is defined as the irreversible exit from cell cycle that occurs at the end of the replicative lifespan of a cell. Senescent cells are alive and metabolically active, but exhibit characteristic differences to their non-senescent counterparts (Childs *et al.*, 2017). These include morphological and functional changes, which in most cases include the secretion of the senescence-associated secretory phenotype (SASP), a cocktail of cytokines and remodelling proteins (Watanabe *et al.*, 2017). The most compelling evidence for senescent cells as drivers of ageing involve selective ablation of senescent cells in transgenic mice demonstrated elegantly that the presence of such cells shortened healthy lifespan (Baker *et al.*, 2016) and the removal

of these is able to prevent several age-associated diseases (Baker *et al.*, 2011). Follow on work has since demonstrated links between the presence of senescent cells and multiple ageing phenotypes (Bussian *et al.*, 2018; Ogrodnik *et al.*, 2017; van Willigenburg *et al.*, 2018). Accordingly, approaches to selectively ablate or regenerate senescent cells *in vivo* (senotherapeutics) are now the subject of intense study as future therapeutics which are already demonstrating promise in human systems (Justice *et al.*, 2019; Paez-Ribes *et al.*, 2019). Features of senescence can be reversed at least *in vitro* by low dose small molecules (polyphenols, ERK/AKT inhibitors or by treatment with donors of the gasotransmitter hydrogen sulfide (Latorre *et al.*, 2017; Latorre *et al.*, 2018a; Latorre *et al.*, 2018b).

Cellular senescence can arise from repeated and unresolved cellular stress (S. He & Sharpless, 2017). Cells have a battery of molecular responses to stress, one of which is the microRNA (miRNA) response (Du *et al.*, 2019; LaPierre *et al.*, 2017). MicroRNAs are small RNA molecules of approximately 22 nucleotides in length that are pivotal regulators of gene expression and have roles in many aspects of cell development, proliferation, and apoptosis (Bartel, 2004). In accordance with their fundamental importance in complex cellular processes and in systemic ageing, studies have reported associations between miRNA profiles and age-related phenotypes (Grillari *et al.*, 2010; Li *et al.*, 2016; Rani *et al.*, 2017), and between individual miRNA and cellular senescence itself (Y. L. Chen et al., 2020; Pitto et al., 2009). The small size of miRNA, the relative ease of high throughput methods for measuring them and the ready availability of reagents for their evaluation *in vitro* has highlighted them as a promising therapeutic avenue (Chakraborty *et al.*, 2017).

In this study, the aim was to identify and evaluate miRNA that were not only associated with senescence, but also with response to senescence-reversing small molecules in

human primary endothelial cells, a cell type relevant to many human diseases. Assessment of senescence profiles alone reveals both causes and effects of senescence, whereas other miRNAs not involved in reversal of senescence may be altered by drug treatment. Juxtaposition of the two datasets however may aid identification of miRNAs with potential roles in senescence. Three miRNAs (miR-5787, miR-3665 and miR-361-5p) demonstrated dysregulated expression in both datasets, but only one, miR-361-5p, exhibited opposing directionality. Biological process GO terms analysis of experimentally-validated targets of miR-361-5p revealed that these were enriched in pathways involved in protein and mRNA processing, and with cell projection, differentiation and morphogenesis. Finally, increasing the levels of miR-361-5p in senescent endothelial cells using an miR-361-5p mimic brought about a 24% reduction of the number of senescent cells present in the culture, but in the absence of renewed proliferation or increased cell death.

3.3 Materials and methods

3.3.1 Cell culture conditions, senescence kinetics and resveratrol treatment

Primary human aortic endothelial cells (HAoECs; C-12271, PromoCell, Germany) were used for this study. Cells were cultured and propagated in C-22022 medium (Promocell, Germany) with 1% penicillin and 1% streptomycin at 37°C, ambient oxygen and 5% CO2. Senescent cells were produced by continuous culture as previously described until growth slowed to less than 0.5 population doublings per week (Holly *et al.*, 2013; Latorre, *et al.*, 2018) and were assessed in 3 biological replicates at PD = 84. Early passage cells for comparison were also assessed in 3 biological replicates and were at PD = 36. Cells were assessed at 80% confluence to ensure that cessation of growth was not due to contact inhibition. Senescence was

confirmed by senescence-associated beta galactosidase (SA-β-Gal) positivity and γH2AX activity using commercial kits (Sigma, Aldrich, UK and CS0030 for SA-β-Gal and Abcam, ab26350 for γH2AX respectively). Cessation of proliferation was confirmed using a commercially-available antibody against Ki67 (Abcam, ab16667). Briefly, cells were seeded at 1 x 10^4 cells/coverslip and then after 10 days were treated with 5 μM of resveratrol compound or vehicle for 48 hours in 3 biological replicates. Cells were fixed for 10 min with 4% PFA and permeabilized with 0.025 % Triton and 10 % serum in PBS for 1 hour. Cells were then incubated with a rabbit monoclonal anti-Ki67 antibody (ab16667, Abcam, UK) at 1:200 overnight at 4 °C followed by FITC-conjugated secondary goat anti-rabbit (1:400) for 1 hour, and nuclei were counterstained with DAPI. Coverslips were mounted on slides in DAKO fluorescence mounting medium (S3023; Dako). In each case, at least 400 cells were assessed per replicate. For assessment of miRNA response to resveratrol treatment, cells were seeded at a density of 4.0×10^5 cell/cm^2 in 6-well plates and left to settle for 24 hr, after which they were treated with 5 μM of resveratrol (a concentration previously demonstrated by ourselves to elicit reversal of senescence (Latorre *et al.*, 2017) or with DMSO carrier alone for 48 hours, after which senescence kinetics were established as described above. Significance was determined by Students t-test in GraphPad Prism 8.

3.3.2 RNA extraction and Purification

Early and late passage cells as well as late passage cells in the presence of treatment or vehicle alone were washed in Dulbecco's phosphate-buffered saline (DPBS) and harvested. Total RNA was then extracted from each replicate using 1 mL of Tri reagent® (Thermo Fisher, Waltham, MA, USA) according to the manufacturer's

instructions. RNA samples destined for GeneChip miRNome and whole transcriptome analysis were purified further using an RNA Clean & Concentrator kit (Zymo Research, CA, USA) according to the manufacturer's instructions.

3.3.3 Whole miRNome profiling

Transcriptome-wide miRNA patterns of miRNA expression were assessed in early passage (PD = 36), late passage (PD = 84) cells, and in resveratrol or vehicle (DMSO) treated late passage cells (PD = 84) in 3 biological replicates using the GeneChip™ miRNA 4.0 system (Thermo Fisher, Waltham, MA, USA) which allows simultaneous assessment of all miRNAs in miRBase release 20. A detailed explanation could be found in section 2.4.2.

3.3.4 Gene Ontology pathway analysis of dysregulated miRNA target genes

MicroRNA binding sites may demonstrate tissue specificity, so even genuine targets may not be present in the cells of interest. We identified 839 validated targets of miR-361-5p using the DNA intelligent analysis (DIANA) mirPath v3.0 database and miRTarBase (Paraskevopoulou *et al.*, 2013; Vlachos *et al.*, 2015), which includes only experimentally validated target genes (Huang *et al.*, 2020). Thresholds were set at the default of -1.0. Gene Set enrichment analysis (GSEA) was carried out using EnrichR (Chen *et al.*, 2013) to identify pathways that were enriched in validated target genes of miR-361-5p. EnrichR is a webtool designed to determine whether candidate genes from a user-supplied list are present in specific Gene Ontology (GO) biological function processes than one would expect by chance, based on the adjusted p value (ranking derived from Fisher exact test for gene sets) significance.

3.3.5 Manipulation of miR-361-5p levels using a miRNA mimic

To determine whether restoring miR-361-5p levels in senescent primary endothelial cells was capable of attenuating senescence, aged cells at PD80 were seeded into 12 well plates at a density of 2 x 10^5 cells/well and maintained until 70% confluence. Cells were then transfected with 50pmol of a MirVana mimic (Thermo Fisher, Waltham, MA, USA) to miR-361-5p for 24hrs. Transfections were carried out using Lipofectamine 3000 (Thermo Fisher, Waltham, MA, USA) and a lipofectamine-only control was also performed. The percentage of senescent cells in the culture was then assessed by senescence-associated beta galactosidase staining in duplicate fields of each of 3 biological replicates, with >450 cells per condition assessed. Changes to cell proliferation and the occurrence of DNA damage foci were assessed by Ki67 and γH2AX staining as described above. Differences between treated and control cultures assessed for statistical significance by unpaired t-test in GraphPad Prism 8.0 software (GraphPad Software, La Jolla, CA, USA).

3.3 Results

3.3.1 Senescence kinetics of early passage, late passage and rejuvenated primary human endothelial cells

Early passage HAoECs (PD = 36) demonstrated an average level of 10% SA-β-Gal positive cells, whereas late passage cells (PD = 84) demonstrated 64% positivity ($p = 0.0001$). This was accompanied by a 25% decrease in the number of cells staining positive for the cell proliferation marker Ki67 ($p = 0.0008$) and a 28% increase in the number of cells demonstrating γH2AX foci indicating increased levels of DNA damage ($p = 0.016$; figure 3.1). We have previously reported that resveratrol and other related polyphenols bring about a rescue from senescence in late passage human primary dermal fibroblasts and other cell types (Latorre *et al.*, 2017). We observed a similar effect in human primary endothelial cells; treated cells demonstrated an approximate 33% decrease in the number of cells staining positive for SA-β-Gal activity ($p = 0.002$; figure 3.2), but no significant increase in cell proliferation or decrease in DNA damage foci (figure 3.2).

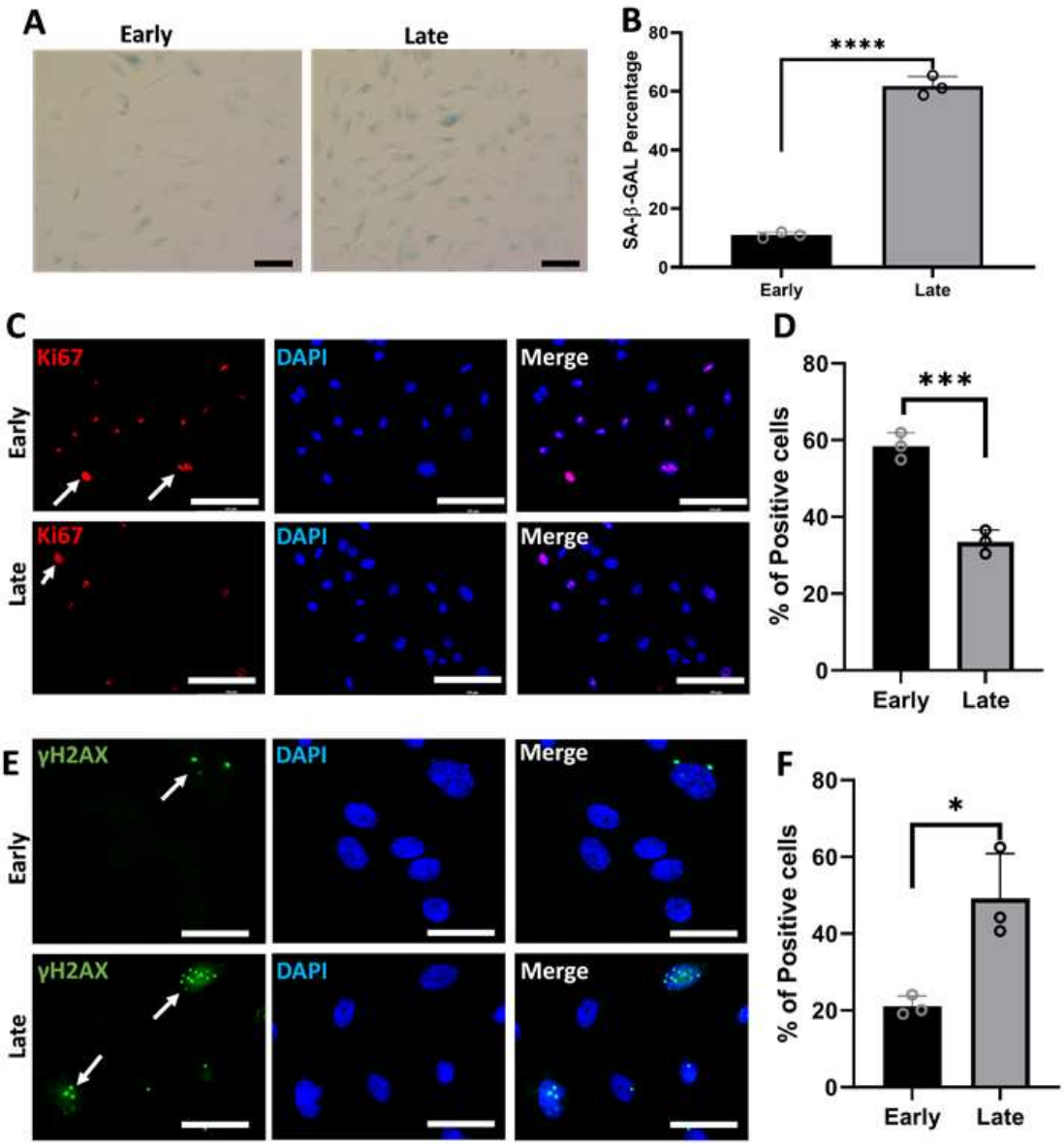

Figure 3.1: Senescence kinetics of early and late passage human primary endothelial cells. (A) Microscope fields illustrating representative senescence-associated beta galactosidase (SA-β-Gal) activity in early (PD = 36) and late passage (PD = 84) human primary endothelial cells. **(B)** Graph showing change in SA-β-Gal activity in early and late passage human primary endothelial cells. **(C)** Proliferation kinetics in early (PD = 36) and late passage (PD = 84) human primary endothelial cells stained for Ki67 activity.

Continuation of legend of figure 3.1: (D) Graph showing change in Ki67 staining in early and late passage human primary endothelial cells. **(E)** DNA damage foci as identified by γH2AX staining in early and late passage human primary endothelial cells. **(F)** Graph showing change in γH2AX staining in early and late passage human primary endothelial cells. Early passage cell counts are shown in black, late passage cell counts are given in grey. Cell counts were obtained by manual counting of multiple fields in 6-well plates from 3 biological replicates in case of SA-β-Gal and on coverslips for Ki67 and γH2AX. N > 300 cells for each replicate. Error bars represent standard deviation of measurement. Statistical significance was determined by one-way ANOVA with * = $p \leq 0.05$, *** = ≤ 0.001 and **** = $p \leq 0.0001$. Scale bars are 50 µm for A and C and 100 µm for E.

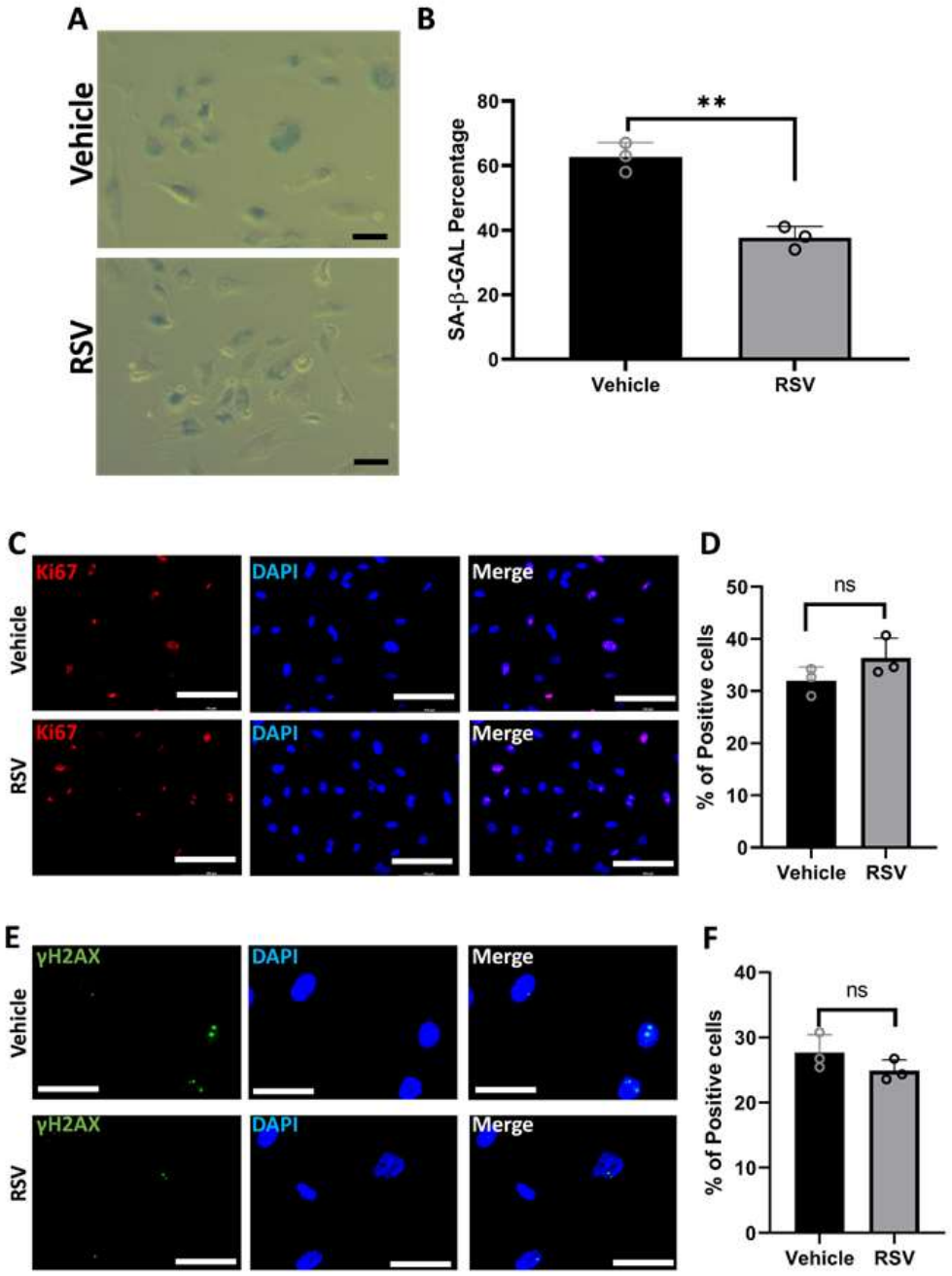

Figure 3.2: Senescence-associated beta galactosidase activity in late passage (PD = 84) human primary endothelial cells treated with 5mM resveratrol for 48 hours. **(A)** Microscope fields illustrating representative senescence-associated beta galactosidase (SA-β-Gal) activity in late passage (PD = 84) human primary endothelial cells treated with resveratrol (RSV) or with vehicle (DMSO) alone.

Continuation of legend of figure 3.2: (B) Graph showing change in SA-β-Gal activity in early and late passage human primary endothelial cells. **(C)** Proliferation kinetics late passage (PD = 84) and RSV treated human primary endothelial cells stained for Ki67 activity. **(D)** Graph showing change in Ki67 staining in late passage (PD = 84) and RSV treated human primary endothelial cells. **(E)** DNA damage foci as identified by γH2AX staining in late passage (PD = 84) and RSV treated human primary endothelial cells. **(F)** Graph showing change in γH2AX staining in late passage (PD = 84) and RSV treated human primary endothelial cells. Vehicle treated cells are shown in black, resveratrol treated cells in grey. Cell counts were obtained by manual counting of multiple fields in 6-well plates from 3 biological replicates. N > 400 cells for each replicate. Error bars represent standard deviation of measurement. Statistical significance was determined by one-way ANOVA with ** $p = \leq 0.001$. Scale bars are 50 μm for A and C and 100 μm for E.

3.3.2 244 miRNAs are dysregulated in senescent human primary endothelial cells

Whole miRNome profiling of early and late passage human primary endothelial cells revealed that 404 miRNAs were expressed in early and/or late passage primary human endothelial cells. Of these, 244 miRNAs demonstrated nominal significance for an association with senescence, and 202 demonstrated significance following adjustment for false discovery rate (figure 3.3a; appendix I). The most dysregulated miRNA were miR-6850-5p (fold change = -38.69; FDR adjusted p value = 0.0002), miR-4687-3p (fold change = -29.59; FDR adjusted p value = 0.0005; appendix I and II), miR-7108-5p (fold change = -28.03; FDR adjusted p value = 0.0007), miR-4632-5p (fold change = -10.49; FDR adjusted p value = 0.001) and miR-4530 (fold change = -16.12; FDR adjusted p value = 0.001). We have previously demonstrated that low dose resveratrol is capable of bringing about reversal of multiple senescent cell phenotypes in human primary dermal fibroblasts (Latorre *et al.*, 2017). Accordingly, treatment of late passage human primary endothelial cells also showed a rescue phenotype when treated with low dose (5 μM) resveratrol (figure 3.2a&b). We identified 202 miRNAs were expressed in senescent primary human endothelial cells, but far fewer demonstrated associations with resveratrol treatment. 35 demonstrated nominal associations with senescence, and 3 met multiple testing criteria (figure 3.3b and c; appendix II). These were miR-5787 (fold change -1.76; FDR adjusted p value = 0.0005), miR-3665 (fold change -3.36; FDR-adjusted p value = 0.001) and miR-361-5p; fold change 1.41; FDR adjusted p value = 0.001). MiRNA differentially regulated with senescence comprise a mix of those that may induce senescence and those that are a result of it. Resveratrol may also induce some changes unrelated to the reversal response, due to the pleiotropic nature of the molecule. To focus our analysis on those

miRNAs which may be directly involved in the reversal response, from the small number of altered miRNAs we identified, we identified a single miRNA (miR-361-5p) that was present at the juxtaposition of both datasets, but with opposite direction of effect ($p = 0.0015$; figure 3.3d).

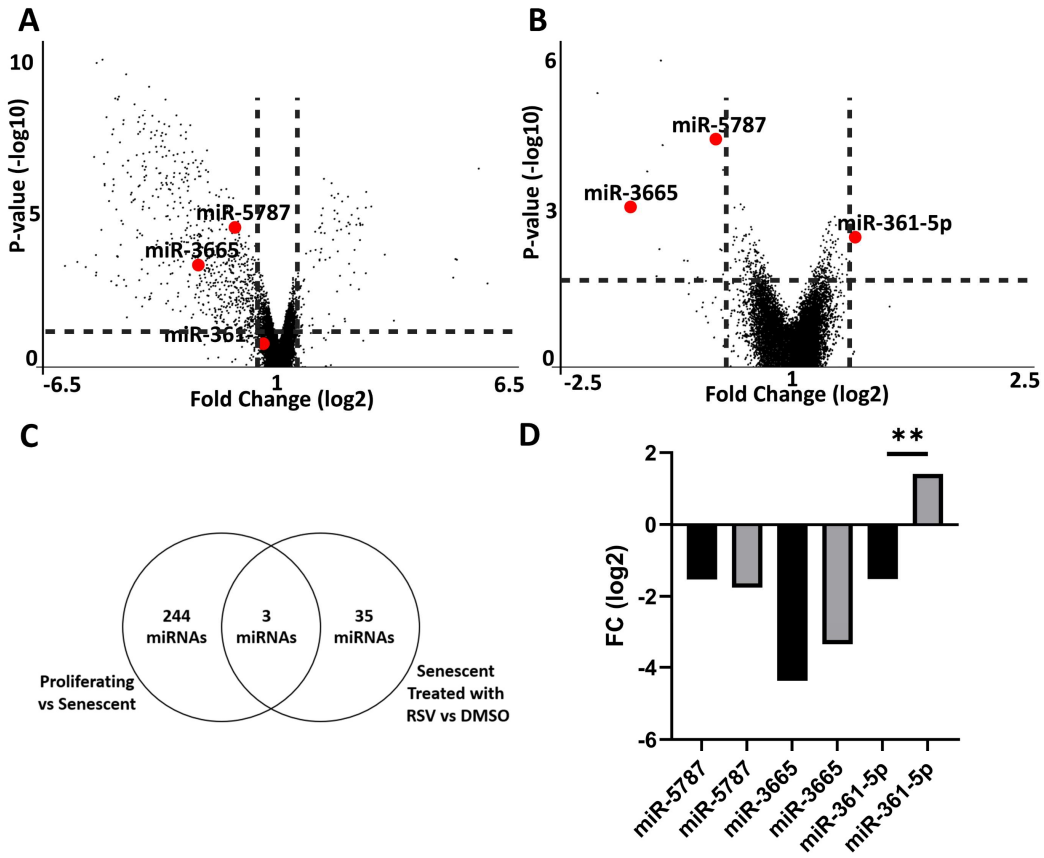

Figure 3.3: Analysis of miRNAs expression profiles associated with endothelial cell senescence and rescue. (A) Volcano plot illustrating differentially-expressed miRNAs in senescent human primary endothelial cells. (B) Volcano plot illustrating differentially-expressed miRNAs in rejuvenated senescent human primary endothelial cells. (C) Venn diagram to summarize overlap between miRNA datasets differentially expressed in senescence and those differentially expressed in rejuvenation. (D) Expression pattern of miR-361-5p in senescent (black bars) and rejuvenated (grey bars) human primary endothelial cells expressed as a fold change compared with young or vehicle treated cells. Cut-off was adjusted to 1.5. Statistical significance was determined by Benjamini FDR. ** p = ≤0.001.

3.3.3 Pathway analysis of restored miRNA and their target genes

We carried out a Biological Processes GO terms analysis of the 839 experimentally validated miR-361-5p target genes (table 1). We identified that the cellular function pathways that were enriched in miR-361-5p target genes were involved with the transport, localisation or catabolism of proteins (protein localization to organelle; $p = 0.0006$, cellular protein catabolic processes; $p = 0.0007$, protein catabolic processes; $p = 0.002$, intracellular protein transport; $p = 0.003$), with the metabolism or splicing of mRNA (regulation of mRNA metabolic process; $p = 0.002$, RNA splicing via transesterification reactions involving adenosine; $p = 0.003$, mRNA splicing via spliceosome; $p = 0.003$, mRNA metabolic processes; $p = 0.004$, RNA splicing, via transesterification reactions; $p = 0.004$) or with cellular morphology or differentiation (cell junction organization; $p = 0.005$, regulation of cell projection organization; $p = 0.005$, cell morphogenesis; $p = 0.007$, positive regulation of cell projection organization; $p = 0.008$).

Table 3.1: Gene Ontology (GO) biological process enriched in miR-361-5p target genes (839). Adjusted p values have been derived from Fisher exact test for gene set enrichment in each pathway. Pathways involved in deregulated proteostasis are marked in bold type, whilst those associated with mRNA processing are marked by grey shading. These involved in cellular morphology or differentiation are marked in italics.

Cellular component	Adj p value
Biological Process	
protein localization to organelle (GO:0033365)	**0.0006**
cellular protein catabolic process (GO:0044257)	**0.0007**
cell division (GO:0051301)	0.0012
protein catabolic process (GO:0030163)	**0.0016**
regulation of mRNA metabolic process (GO:1903311)	0.0022
regulation of cellular response to stress (GO:0080135)	0.0022
intracellular protein transport (GO:0006886)	**0.0026**
microtubule-based process (GO:0007017)	0.0030
RNA splicing, via transesterification reactions with bulged adenosine (GO:0000377)	0.0033
mRNA splicing, via spliceosome (GO:0000398)	0.0033
regulation of protein kinase activity (GO:0045859)	0.0038
mRNA metabolic process (GO:0016071)	***0.0039***
RNA splicing, via transesterification reactions (GO:0000375)	0.0040
regulation of cellular component biogenesis (GO:0044087)	0.0044
cell junction organization (GO:0034330)	0.0048
regulation of cell projection organization (GO:0031344)	0.0052
cell morphogenesis involved in differentiation (GO:0000904)	0.0072
positive regulation of cell projection organization (GO:0031346)	0.0081
covalent chromatin modification (GO:0016569)	0.0082
mitotic cell cycle process (GO:1903047)	0.0090

3.3.4 Restoration of miR-361-5p levels in aged cells causes a decrease in senescent cell load.

To determine whether miR-361-5p influences cellular senescence phenotypes, we treated primary senescent human endothelial cells with a miR-361-5p mimic. Transfection efficiencies were >90% and we achieved an approximate 75% upregulation of miR-361-5p. We identified that increasing levels of miR-361-5p in aged endothelial cells resulted in a 24% drop in the percentage of senescent cells in the culture (the percentage of senescent cells in cells treated with carrier only was 49.9% (SD = 7.4%) compared with 38.1% (SD = 8.5%) in mimic treated cells; ($p = 0.013$) (figure 3.4 A&B). The drop in senescent cell load was however not associated with increased proliferation or a reduction in DNA damage foci. We saw no evidence in support of an increase in Ki67 (figure 3.4 C&D) or a decrease in γH2AX staining (figure 3.4 E&F). No differences were noted in cell count between scramble control and mimic-treated cells ($p = 0.14$).

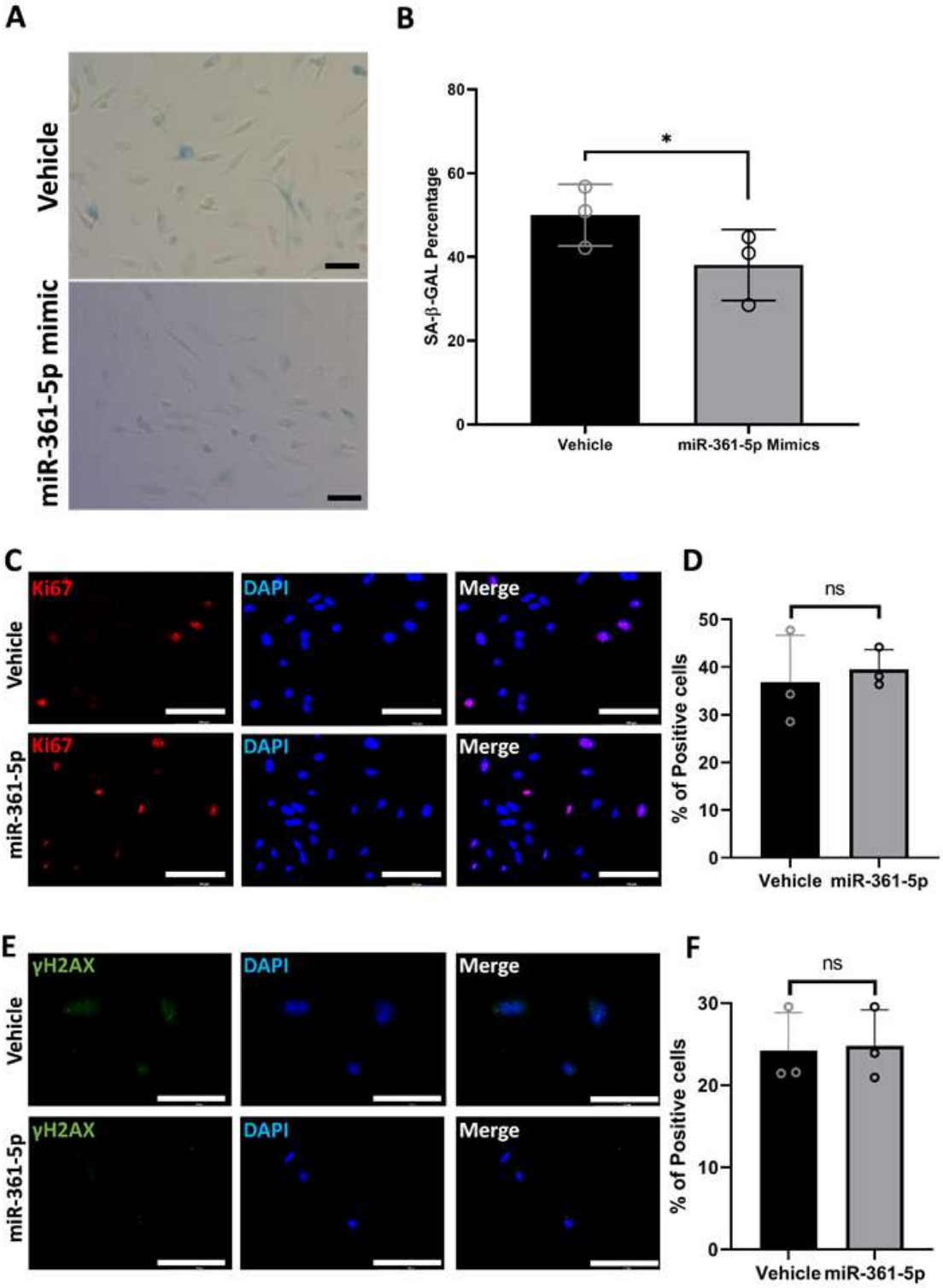
A
Vehicle
miR-361-5p mimic
B
SA-β-GAL Percentage
80
60
40
20
0
*
Vehicle
miR-361-5p Mimics
C
Ki67
DAPI
Merge
Vehicle
miR-361-5p
D
ns
% of Positive cells
50
40
30
20
10
0
Vehicle
miR-361-5p
E
γH2AX
DAPI
Merge
Vehicle
miR-361-5p
F
ns
% of Positive cells
30
20
10
0
Vehicle
miR-361-5p

Figure 3.4: Attenuation of cellular senescence in aged endothelial cells using a mimic to miR-361-5p. The percentage of SA-β-Gal positive cells in cultures of senescent primary human endothelial cells treated with a mimic to miR-361-5p, or with scrambled negative control (vehicle) are presented above. (A) Microscope fields illustrating representative senescence-associated beta galactosidase (SA-β-Gal) activity in scramble-treated late passage (PD = 84) human primary endothelial cells or late passage cells treated with a mimic to miR-361-5p. (B) Graph showing change in SA-β-Gal activity in scramble-treated late passage (PD = 84) human primary endothelial cells or late passage cells treated with a mimic to miR-361-5p. (C) Proliferation kinetics in scramble-treated late passage (PD = 84) human primary endothelial cells or late passage cells treated with a mimic to miR-361-5p. Cells were stained for Ki67 activity. (D) Graph showing change in Ki67 staining in scramble-treated late passage (PD = 84) human primary endothelial cells or late passage cells treated with a mimic to miR-361-5p. (E) DNA damage foci as identified by γH2AX staining in scramble-treated late passage (PD = 84) human primary endothelial cells or late passage cells treated with a mimic to miR-361-5p. (F) Graph showing change in γH2AX staining in scramble-treated late passage (PD = 84) human primary endothelial cells or late passage cells treated with a mimic to miR-361-5p. The black bars represent senescent cell load in vehicle treated cells, whilst the grey bars represent senescent cell load following treatment with a miR-361-5p mimic. Transfection efficiency was >90%, and we achieved >75% induction of miR-361-5p. Error bars indicate standard deviation of measurement. Statistical significance of effect as determined by independent t-test is indicated by a star * = <0.02. Scale bars are 50 μm for A and C and 100 μm for E.

3.4 Discussion

MicroRNAs are key components of the cellular stress response and are pivotal to a multitude of cellular processes. Here, we report the miRNA profiles associated with cellular senescence and those associated with polyphenol induced rescue from senescence, in human primary endothelial cells. We have identified one miRNA, miR-361-5p, which demonstrates antagonistic patterns of expression in response to senescence and rescue. GO terms analysis reveals that targets of this miRNA are enriched in pathways involved in protein transport, localisation or catabolism and with metabolism and splicing of RNA. Finally, manipulation of miR-361-5p levels using a miRNA mimic to miR-361-5p resulted in a 24% reduction of the senescent cell load in aged primary endothelial cells, in the absence of renewed cell division. We have previously noted such an uncoupling of proliferative responses from senescence rescue in our previous work, whereby restoration of splicing regulation caused cellular rejuvenation in the absence of renewed cell division (Latorre *et al.*, 2018a; Latorre *et al.*, 2018b). We did not note any differences in cell count between the scramble-treated control and the mimic-treated cells, indicating that the reduction in senescent cells we have observed is not due to senolysis. This is in accordance with previous data that senescence induced by splicing dysregulation is senostatic rather than senolytic. Our data suggest that miR-361-5p may contribute to the development of senescence in human primary endothelial cells.

Cancer and senescence are often regarded as opposite sides of the same coin. Deduction of causality from association data is of course not possible, but there are some good reasons to predict that the disruption of miR-361-5-p targets may be associated with senescence. The two most prominent pathways identified in the GO terms analysis were involved with the transport, localisation or catabolism of proteins,

and with mRNA processing. Disrupted proteostasis is one of the nine documented hallmarks of ageing (López-Otín *et al.*, 2013). A direct role for this in cellular ageing in *C. elegans* has been extensively described (Ben-Zvi *et al.*, 2009), but evidence for a causal role in humans has remained elusive until recent work has demonstrated that whilst stressed human cells were able to properly sense cellular stress (an important trigger for senescence), they were unable to activate the unfolded protein response to moderate transcriptional function. Proteasome function was also compromised (Sabath *et al.*, 2020). These data suggest that deregulated proteostasis is an active hallmark in human ageing, and our finding that genes involved in these processes are targets of miR-361-5p adds evidence to suggest a role for this miRNA in this process. A growing body of evidence also implicates dysregulation of splicing as a new hallmark of ageing. Pathways involved in mRNA processing are amongst the most dysregulated in human ageing (Harries *et al.*, 2011), and splicing factor expression (the effectors of splicing decision making) are disrupted in human primary senescent cells of multiple subtypes (Holly *et al.*, 2013; Latorre *et al.*, 2018b; Lye *et al.*, 2019). Furthermore, splicing factor expression levels in human peripheral blood are predictive of multiple human ageing outcomes in a longitudinal population study (Lee *et al.*, 2019a), and are associated with lifespan (Lee *et al.*, 2016) and response to calorific restriction (a well know lifespan extension pathway) (Lee *et al.*, 2019b) in mice. Restoration of splicing factor expression using polyphenols and other small molecules, or targeted genetics, has been demonstrated to lead to the rejuvenation of aged cells (Latorre *et al.*, 2017; Latorre *et al.*, 2018a; Latorre *et al.*, 2018b). Interestingly, the FOXO1 gene has been demonstrated to be a target of miR-361-5p in human chondrocytes (Wang *et al.*, 2019). FOXO1 has been demonstrated to be a negative regulator of splicing factor expression in primary human senescent fibroblasts, where ablation of its expression

was demonstrated to restore splicing factor levels and reverse aspects of the senescent cell phenotype (Latorre *et al.*, 2019).

Our study does of course have limitations. We identified differences between the number of miRNAs expressed in the senescent vehicle-treated cells compared with the untreated senescent cells in our initial comparison. Expression thresholds were identically set for both datasets, so this does not represent a threshold issue. Both probesets underwent identical normalisation (SST-RMA), which equilibrates background and normalises signal based on probe intensity. These differences are most likely a reflection of the fact that the two cell populations are not equivalent, since one has been exposed to no treatment, whilst the other has been exposed to the vehicle, DMSO. It is not uncommon for there to be differences between vehicle and untreated datasets, which is why comparison to the same set of untreated controls would not have been appropriate. It is also not unexpected that we identified fewer dysregulated miRNAs under conditions of resveratrol treatment than we did between early and late passage cells. The reduction in senescent cell load was modest, and the cultures still contained a significant proportion of non-rejuvenated cells which might be expected to have similar miR profiles to the untreated population, particularly at the relatively low doses we have used. It is also possible that the effects we have noted are specific to endothelial cells. However, increased expression of miR-361-5p has previously been associated with multiple diseases with an age-related component in multiple tissue types. These include acute coronary syndrome (Zhang *et al.*, 2021) and coronary artery disease (Su *et al.*, 2020), osteoarthritis (Wang *et al.*, 2019), rheumatoid arthritis (Romo-García *et al.*, 2019), hepatosteatosis (Zhang *et al.*, 2018), hypertension (Qi *et al.*, 2017), Alzheimer Disease (Mendes-Silva *et al.*, 2016) and macular degeneration (Grassmann *et al.*, 2014). MicroRNA miR-361-5p also has

known roles in epithelial-to-mesenchymal cell transition (Wu *et al.*, 2013; Yin *et al.*, 2020; Zhang *et al.*, 2017) which may underpin its associations with the development or progression of multiple cancers, including those of the reproductive (Ling & He, 2021; Yang & Xie, 2020; Zheng *et al.*, 2021), respiratory (Othman & Nagoor, 2019; Zhuang *et al.*, 2016), digestive (Cui *et al.*, 2016; Qian *et al.*, 2020), skeletal (Shen *et al.*, 2019) and nervous systems (Zhou *et al.*, 2020).

We report here the identification of a miRNA (miR-361-5p) that displays opposite directionality of effect in response to cellular senescence and resveratrol-induced cellular rejuvenation in human primary endothelial cells, and with mimics transfection is able to attenuate some features of cellular senescence in senescent primary human endothelial cells. We have demonstrated that several of its target genes are enriched in cellular and molecular function pathways associated with a known hallmark of ageing (deregulated proteostasis) and a phenomenon that is emerging as a potential new hallmark, dysregulated mRNA processing. We suggest that increased miR-361-5p expression in response to resveratrol may explain some of the potential senotherapeutic effects reported for this compound, and position miR-361-5p as a potential modifier of aspects of senescence in human cells.

Chapter 4
Determination of the role of miR-361-5p target genes on ageing and healthspan measures in *C. elegans*

4.1 Abstract

The process of ageing is linked to the degeneration and destruction of tissues and organs and contributes to the health defects that are associated with ageing. *C. elegans* has been extensively used as a model organism to study genes that influence ageing, benefiting from a short lifespan and similar, but less complex, genome compared to humans. MicroRNAs (miRNAs) are key players in the ageing process. I identified a potential role for miR-361-5p in suppression of senescence phenotypes in human endothelial cells cultured *in vitro* (see chapter 3). MiR-361-5p has 839 validated target genes in humans. A transcriptome-wide analysis of endothelial cells showed that 32 genes were differentially expressed in late passage versus early passage human endothelial cells. To determine the effect of these genes on systematic ageing, I used a commonly used invertebrate model, *C. elegans*. The effects of RNAi knockdown of orthologues of 16 validated miR-361-5p target genes were then evaluated in relation to lifespan and healthspan. 9/16 verified miR-361-5p target genes demonstrated effects on lifespan and 12/16 on healthspan parameters, but these were negative rather than positive effects. These findings suggest that although miR-361-5p may influence some aspects of the senescence phenotype in human primary endothelial cells *in vitro*, several of its validated target genes play crucial roles in the cell. Many of the validated target genes are involved in the regulation of the cytoskeletal network or its interaction with the extracellular matrix, processes which are important for cell survival and cell function. My findings suggest that although miR-351-5p may represent a future senotherapeutic target, simply attenuating its expression *in vivo* is unlikely to be useful in the clinic.

4.1 Introduction

Caenorhabditis elegans (*C. elegans*) is a small nematode worm species which is commonly used as a model organism for genomic studies (Weinhouse *et al.*, 2018). It is a self-fertilizing hermaphrodite that only survives for a few weeks when grown at 20 °C, its normal growth environment (Gershon, 1970). Some of the first longevity genes were discovered in this species; decreased expression of genes such as *daf-2* and *age-1* in the insulin-like signalling pathway causes increased longevity (Guarente & Kenyon, 2000) (Morris *et al.*, 1996) (Hamilton *et al.*, 2005). Similarly, the forkhead (FOXO) transcription factor *daf-16*, which is the primary effector of *daf-2*/insulin-like control of *C. elegans* lifespan, is antagonized by signalling from the *daf-2*/insulin-like receptor (Hamilton *et al.*, 2005) and plays a part in controlling lifespan (Honda & Honda, 1999). Modifications in insulin-like signalling pathways also affect lifespan in higher organisms up to and including humans, suggesting that this pathway is a fundamental regulator of longevity (Clancy *et al.*, 2001; Holzenberger *et al.*, 2003; Wrigley *et al.*, 2017). On the contrary, various genes and pathways have been described to shorten the lifespan of *C. elegans* upon manipulation, including *aak-2*, a regulator protein of the AMP-activated protein kinase (AMPK) pathway (Uno & Nishida, 2016). *C. elegans* is a small organism, easy to manipulate in the lab, and shares many genes with human, which makes it a good model system for genomic studies (Zhang *et al.*, 2020).

MicroRNA (miRNA) were firstly discovered in *C. elegans* (Lee *et al.*, 1993). Furthermore, the first link between miRNA and ageing phenotypes was also discovered in this species. (Boehm & Slack, 2005). The miRNA *lin-4* targets the putative transcription factor lin-14, which regulates the period of larval development in *C. elegans*. The life span of animals with a *lin-4* loss-of-function mutation was noticeably lower than that of the wild type, indicating that *lin-4* is necessary to avoid early mortality.

The lifespan of wild type worms was seen to be increased by RNAi-mediated reduction of the *lin-4* target gene *lin-14* during the last larval moult, a comparable increase to that seen when animals were treated with RNAi targeting *lin-14* just after hatching (Boehm & Slack, 2005). Using an RNAi library, Curran and Ruvkun (2007) investigated other genes influencing lifespan and ageing in *C. elegans* (Curran & Ruvkun, 2007). Many of these genes are modulators and factors in the insulin/insulin-like growth factor-1 signaling (IIS), mechanistic target of rapamycin (mTOR) and AMPK pathways (Elder & Pasquinelli, 2022; Hamilton *et al.*, 2005) which are known to affect the ageing process in animals and in humans (Laplante & Sabatini, 2009; López-Otín *et al.*, 2013; Pan & Finkel, 2017; Shin *et al.*, 2014; Guarente & Kenyon, 2000).

GeromiRs are a diverse group of miRNAs that have been shown to play an important regulatory role in ageing and longevity (Caravia & López-Otín, 2015; Harries, 2014). MiRNAs have been shown to be differently expressed with age in cells, organs, and body fluids (Gerasymchuk *et al.*, 2020). For instance, in a recent study, microRNA expression was studied in 5221 people, yielding the identification of 127 microRNAs whose expression levels varied with age and age-related illness. These miRNAs were shown to regulate processes fundamental to ageing, including genomic regulation and immunological responses (Huan *et al.*, 2018). This group also proposed an epigenetic age prediction model based on complementary mRNA:miRNA profiling.

I showed in chapter 3 that miRNA may play a reversal role in endothelial cells. MiR-361-5p may also have a regulatory role in age-related diseases. MiR-361-5p is an oncogenic suppressor miRNA that is dysregulated in various types of cancer (Cui et al., 2016; Ling & He, 2021; D. Liu et al., 2014). It is known to suppress carcinogenesis and epithelial-mesenchymal transition (EMT) in hepatocellular carcinoma (HCC) by targeting *TWIST1*, which is implicated in tumour development and metastasis (Yin *et*

al., 2020). Furthermore, miR-361-5p has been shown to regulate the maternally expressed 3 (*MEG3*) gene and contribute to cell proliferation, suppress cell apoptosis, and prevent extracellular matrix (ECM) breakdown in chondrocytes in a rat model for osteoarthritis, an ageing-associated disorder (A. Wang et al., 2019).

In this chapter, I aimed to define the molecular mechanisms by which miR-361-5p may exert some of its effects on ageing and senescence phenotypes. Downstream targets of miR-361-5p were identified using miRTarBase, a database of validated miRNA:target interactions (Huang *et al.*, 2022). The expression level of each miR-361-5p target gene was then assessed in senescent human primary endothelial cells in relation to early passage cells. Where miR-361-5p target genes demonstrated altered expression in aged cells, a search for *C. elegans* orthologues was then carried out. Finally, the *C. elegans* orthologues of miR-361-5p target genes were evaluated for effects on lifespan and healthspan parameters in *C. elegans,* using RNAi-mediated targeted knockdown *in vivo.* I identified 839 validated miR-361-5p target genes, of which 32 demonstrated evidence of altered expression in senescent human primary endothelial cells. 16 validated miR-361-5p target genes had orthologues in *C. elegans*, and of these, 9 genes reduced lifespan and 12 genes affected healthspan parameters following manipulation. This shows that although miR-361-5p may play roles in the development or maintenance of cellular senescence in human primary endothelial cells, knockdown of its target genes systemically in *C. elegans* may be more detrimental rather than beneficial *in vivo*.

4.2 Materials and methods

4.2.1 Identification of miR-361-5p target genes

MiR-361-5p target genes were identified using a bioinformatics tool miRTarBase version 9.0, a database containing only experimentally validated miRNA target genes using the default setting (https://mirtarbase.cuhk.edu.cn/~miRTarBase/miRTarBase_2022/php/index.php) (Huang *et al.*, 2022).

4.2.2. Assessment of miR-361-5p target gene expression in senescent primary human endothelial cells

Endothelial cells play important roles in cardiovascular diseases as they are the building blocks of the single layer lining of the blood vessel wall (Nikitenko & Boshoff, 2006). Senescence–related endothelial dysfunction contributes to a number of vascular disorders, including atherosclerosis, diabetes mellitus, and hypertension (Yamakuchi & Hashiguchi, 2018) as well as progression of cancer (Yang *et al.*, 2021). Rescuing endothelial cells from the senescent state is an interesting proposition, raising questions over whether it may be possible to regain blood vessel homeostasis and vascular integrity by targeting this pathway. MiR-361-5p target genes identified through bioinformatics may represent genuine targets of the miRNA in question, but be unrelated to senescence phenotypes. Predicted target genes were therefore assessed for transcriptome-wide senescence-associated expression changes in 3 biological replicates of early and late passage human primary endothelial cells (PDs 36 and 84 respectively) using the Clariom D Pico GeneChip platform (Thermo Fisher, Waltham, MA, USA) as described in chapter 2 section 2.4. Sample preparation and

gene chip cartridge arrays were performed by a commercial subcontractor (UK Bioinformatics Ltd, Caterham, Surrey). Data underwent QC including RNA integrity, hybridization, washing, staining, and scanning to ensure data normality and clustering. Associations between the expression of a set of bioinformatically-predicted target genes and cellular senescence was then analysed using TAC 4.0.2.10 (Applied Biosystems, Thermo Fisher, Waltham, MA, USA).

4.2.2 Gene Ontology pathway analysis of the 32 dysregulated genes

Gene Set enrichment analysis (GSEA) was carried out using PANTHER (Protein ANalysis THrough Evolutionary Relationships) (Mi & Thomas, 2009) to identify pathways that were enriched in validated target genes of miR-361-5p that were associated with senescence. PANTHER is a comprehensive, open-source software system for linking the evolution of protein sequences to the development of particular protein activities and biological roles. I identified miR-361-5p target genes demonstrating significant associations with cellular senescence in human endothelial cells and queried these for enrichment in Gene Ontology (GO) Reactome, cellular, molecular or biological function pathways based on the FDR adjusted p value (ranking derived from Fisher exact test for gene sets).

4.2.2 Identification of *C. elegans* orthologues of miR-361-5p target genes

Not every human gene has an orthologue in *C. elegans*. *C. elegans* orthologues corresponding to validated mRNA targets of miR-361-5p were therefore identified from comparison of three different databases to maximise the chances of identifying the correct orthologue if present. Firstly, orthologues of validated miR-361-5p target genes

demonstrating dysregulated expression in senescence were identified using the NCBI HomoloGene database (ncbi.nlm.nih.gov/homologene; Release 68). This provides a platform for the computational identification of homologues and orthologues among annotated genes of genomes from different species. Secondly, orthologues of miR-361-5p target genes were identified from the Ortholist 2 database (ortholist.shaye-lab.org), which is based on a meta-analysis of six different orthology-prediction algorithms (Kim *et al.*, 2018). Then, these were validated in the database for *C. elegans* (https://wormbase.org).

4.2.3 *C. elegans* growth and conditions

Wild-type Bristol nematodes (N2 Bristol) were maintained on nematode growth media (NGM) plates planted with Escherichia coli OP50 at 20°C. The strain was maintained according to the previously described methods (Brenner, 1974). Briefly, they were maintained at 20 ℃ on 6cm plates (Greiner Bio One) containing nematode growth media (NGM) (50 mM NaCl, 0.25% (w/v) bacto peptone, 1.7% (w/v) agar, 1 mM CaCl2, 1 mM MgSO4, 25 mM KH2PO4, 12.9 μM cholesterol) which was seeded with the *E. Coli* OP50 strain. RNAi clones were procured from the Ahringer repository (Kamath & Ahringer, 2003). All RNAi clones used in this study were present in Ahringer RNAi library, which were the kind gift of Dr Tim Etheridge. The RNAi treatments were carried out by plating *E. coli* bacteria expressing dsRNA against targeted mRNAs. This strain of bacteria does not possess the enzyme ribonuclease III, which is required to degrade dsRNA. Any cloned DNA sequence can thus be inserted into the bacteria containing the L4440 vector (empty vector). Empty vector alone was used as a control. *C. elegans* were synchronised by gravity using M9 solution (3 g KH_2PO_4, 6 g Na_2HPO_4, 5 g NaCl, 1 mL 1 M $MgSO_4$, H_2O to 1 litre). Afterwards, synchronised L1 larvae were plated on

RNAi NGM plates containing (50 mM NaCl, 0.25% (w/v) bacto peptone, 1.7% (w/v) agar, 1 mM CaCl2, 1 mM MgSO4, 25 mM KH2PO4 (pH 6), 12.9μM cholesterol, 1 mM IPTG, 50 μg/mL ampicillin. The RNAi were plated with bacteria expressing L4440 or the genes of interest as dsRNA. A comprehensive list of the RNAi clones used in this study can be found in (appendix VI).

4.2.4 Microfluidic assessment of *C. elegans* lifespan and healthspan

The microfluidic chip was sterilized by immersion in 70% ethanol for five minutes before using for lifespan experiments. Basal S-complete solution was then rinsed 4–5 times over the microfluidic chip. For 30 minutes, chips were treated with 5% (w/v) Pluronic F127 (Sigma-Aldrich) to prevent bacterial and protein build-up and to remove trapped air bubbles. Using basal S-complete, excess Pluronic was removed after 1 hour incubation at room temperature. The Pluronic-treated chips were stored in moist petri dishes at 20 °C for immediate use or at 4 °C for future use. 60 - 70 worms were loaded into each device according to manufacturer's instructions (Rahman *et al.*, 2020).

4.2.5 Analysis of *C. elegans* lifespan and healthspan data

A microfluidics-based Infinity Screening System (NemaLife Inc.) was used to assess effects of target gene knockdown on lifespan and healthspan, as measured by movement. Worms were raised to the start of adulthood according to stablished protocols (Ellwood *et al.*, 2021). From the first day of adulthood until death, survival analysis was repeated daily. We imaged the microfluidic culture chips daily for 180 seconds and washed them to remove progeny. The initial 90 seconds is used to

monitor *C. elegans* from washing out during the washing step and the later 90 seconds is to score the lifespan and healthspan. RNAi clones were then delivered to the worms in 20 mg/mL of *E. coli* OP50 bacteria in liquid NGM. The chips were stored at 20 °C in Petri dishes with damp tissue wrapped in parafilm until needed. Using the Infinity Code software (NemaLife Inc, Texas), the acquired videos were scored for live/dead animals (NemaLife Inc.).

4.3 Results

4.3.1 Identification of miR-361-5p target genes and expression patterns of targets in early and late passage human primary endothelial cells

C. elegans lack an ortholog to the human miR-361-5p, therefore, the approach was to identify the genes targeted by miR-361-5p, I used the miRTarBase version 9 database (Huang *et al.*, 2022). 839 genes known to be regulated by miR-361-5p were identified in this database. 65 of these were found to be expressed in human primary endothelial cells, according to our analysis, 32 of which remained significant below a Benjamini Hochberg adjusted FDR p value threshold of 0.05 (figure 4.1; appendix III). Nonetheless, most miR-361-5p target genes showed lower, rather than higher, expression in senescent primary endothelial cells compared to early passage counterparts, which was contrary to expectations. The most dysregulated miR-361-5p target genes in senescent endothelial cells included *TMEM43* (fold change >-1000; FDR adjusted p value = 0.002), *LPAR1* (fold change = -136.53; FDR adjusted p value = 0.003), *RECK* (fold change = -44.98; FDR adjusted p value = 0.02), *RAD23B* (fold change = -18.2; FDR adjusted p value = 0.008), *RAD23A* (fold change = -16.1; FDR adjusted p value = 0.02) and *TGFBR1* (fold change = -15.92 FDR adjusted p value = 0.006). Only *EZR* (fold change 19.35; FDR adjusted p value = 0.02) and *ARPC5L* (fold change 3.92; FDR adjusted p value = 0.035) demonstrated an increase in senescent cells, which would be consistent with the most predominant mode of miRNA regulation. For the complete analysed data please see the supplementary I file.

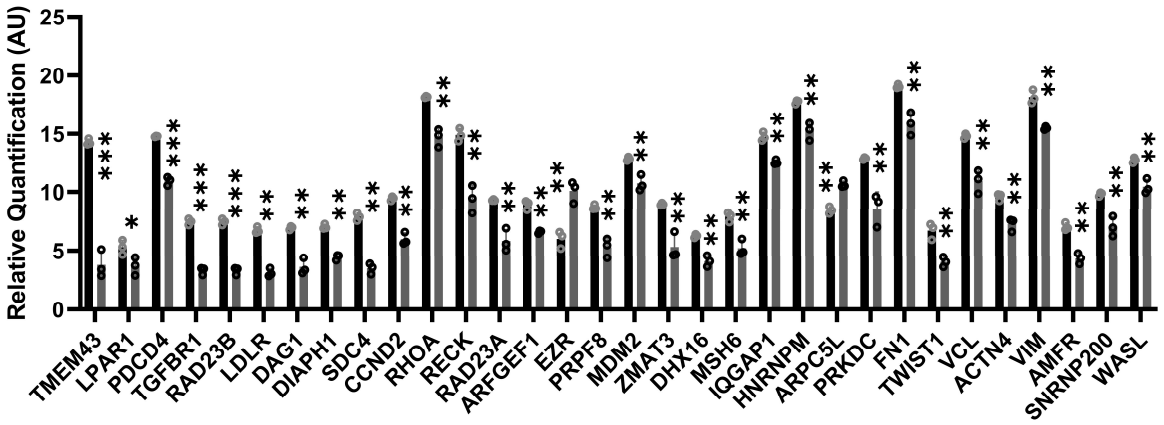

Figure 4.1 Differential expression of miR-361-5p targets in early and late passage human primary endothelial cells. The expression patterns of 32 bioinformatically-predicted miR-361-5p target genes in early (PD = 36) and late (PD = 84) passage human primary endothelial cells are given. Black bars indicate early passage cells, grey bars indicate late passage cells (n = 3 biological replicates). Error bars represent SD. Statistical significance was determined by *t test* and * = p = <0.05, ** = p = <0.001 and *** = p = <0.0001.

4.3.2 Pathway assessment of miR-361-5p and their target genes

I then assessed the Reactome, Cellular and Molecular Function, and Biological Processes GO pathways enriched for the 32 miR-361-5p target genes with differential expression in senescent human primary endothelial cells. Reactome top hits pathways of these genes were Nephrin family interactions (R-HSA-373753) FDR p value = 0.011, Signaling by moderate kinase activity BRAF mutants (R-HSA-6802946) FDR p value = 0.013, Signaling by RAS mutants (R-HSA-6802949) FDR p value = 0.014, Signaling by RAF1 mutants (R-HSA-9656223) FDR p value = 0.014, and MAP2K and MAPK activation (R-HSA-5674135) FDR p value = 0.016.

While the molecular function GO included protein containing complex binding (GO:0044877) FDR p value = 0.0000012 protein domain specific binding (GO:0019904) FDR p value = 0.000011 actin binding (GO:0003779) FDR p value = 0.00062 enzyme binding (GO:0019899) FDR p value = 0.0012 cytoskeletal protein binding (GO:0008092) FDR p value = 0.0019, and RNA binding (GO:0003723) FDR p value = 0.0033.

GO cellular component analysis involved cell-substrate junction (GO:0030055) FDR p value = 0.000016 focal adhesion (GO:0005925) FDR p value = 0.000027 protein-containing complex (GO:0032991) FDR p value = 0.000033 ribonucleoprotein complex (GO:1990904) FDR p value = 0.00042, and cortical cytoskeleton (GO:0030863) FDR p value = 0.00047.

In the GO biological process, the 32 genes were enriched in cellular response to organic substance (GO:0071310) FDR p value = 0.000016 regulation of cell morphogenesis (GO:0022604) FDR p value = 0.000097 regulation of cell motility (GO:2000145) FDR p value = 0.00012 regulation of locomotion (GO:0040012) FDR p

value = 0.00013 cellular response to chemical stimulus (GO:0070887) FDR p value = 0.00013E regulation of protein metabolic process (GO:0051246) FDR p value = 0.00012 regulation of supramolecular fiber organization (GO:1902903) FDR p value = 0.00014 regulation of cytoskeleton organization (GO:0051493) FDR p value = 0.00015 cell development (GO:0048468) FDR p value = 0.00016, and regulation of cell migration (GO:0030334) FDR p value = 0.00016.

4.3.2 Knockdown of the orthologues of miR-361-5p targeted genes reduced *C. elegans* lifespan and healthspan

From the 32 genes that were targeted by miR-361-5p and dysregulated in endothelial cells, 16 had known orthologues in *C. elegans* (table 4.1). To examine the effects of targeted knock down of miR-361-5p target genes on lifespan and healthspan of *C. elegans*, the expression of orthologues of each candidate was assessed following exposure to double stranded RNAi targeting the gene of interest, along with PL4440 empty vector as a negative control and *daf-16* and *age-1* as positive controls. Attenuation of the expression of 9 the validated miR-361-5p target genes, resulting in reduction of mean lifespan to 7 days (p = 0.0001), 8 days (p = 0.0001), 16 days (p = = 0.0001), 18 days (p = 0.0001), 15 days (p = 0.0001), 20 days (p = 0.0002), 15 days (p = 0.001), 17 days (p = 0.01) and 18 days (p=0.03) for *rho-1*, *deb-1*, *daf-1*, *ifa-1*, *cyk-1*, *hlh-8*, *erm-1*, *atn-1* and *let-805* respectively (figure 4.2, A-I). *C. elegans* treated with empty vector had a mean lifespan of 20 days, whereas knockdown of the *daf-16* and *age-1* positive control genes resulted in reduction of lifespan of 16 days and increased lifespan 26 days respectively. Knockdown of the remaining *C. elegans* miR-361-5p target gene orthologues had no effect on mean lifespan (figure 4.2, J-P).

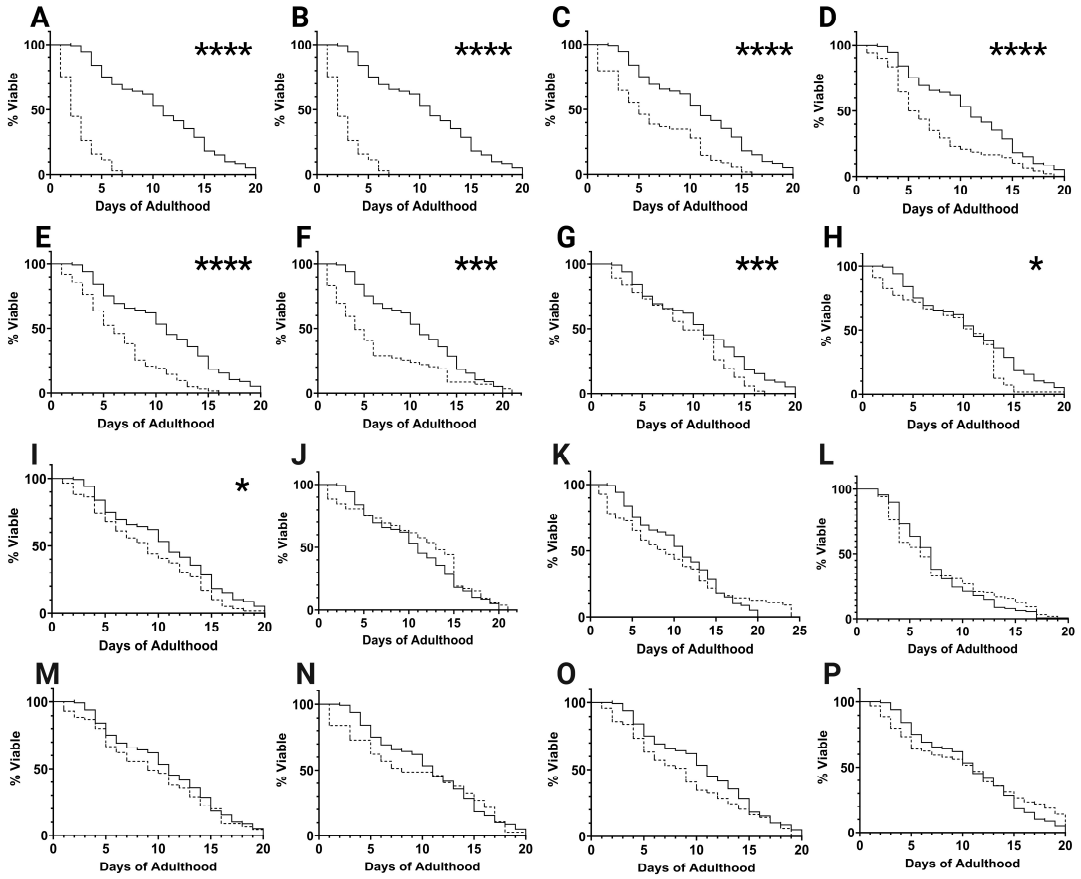

Figure 4.2: Attenuation of miR-361-5p target genes in a *C. elegans* model system altered their lifespan. Survival curves illustrating the effect of targeted RNAi knockdown of 16 validated miR-361-5p target genes with known C. elegans orthologues. Probability of survival is given on the Y axis and days from start of analysis is given on the X axis. Data from control animals is given by solid black lines, data from treated animals is given by dashed grey lines. A = *rho-1/RHOA*, B = *deb-1/VCL*, C = *daf-1/TGFBR1*, D = *ifa-1/VIM*, E = *cyk-1/DIAPH1*, F = *hlh-8/TWIST*, G = *erm-1/EZR*, H = *atn-1/ACTN4*, I = *let-805/FN1*, J = *sdn-1/SDC4*, K = *wsp-1/WASL*, L = *C46H11.3/ARPC5L*, M = *dgn-2/DAG1*, N = *pes-1/IQGAP1*, O = *hrdl-1/AMFR* and P = *sup46/HNRNPM*.

Increased lifespan does not necessarily infer a healthy longer life. To determine the role of miR-361-5p on healthspan parameters, movement rates were assessed following gene knockdown relative to empty vector controls (table 4.1). The first 12 days were analysed due to that *C. elegans* feeding on RNAi PL4440 clone or negative control had very weak movement after day 12 of adulthood. RNAi knockdown of the *rho-1/RHOA* (p value = 0.0002), *deb-1/VCL* (p value = 0.0012), *daf-1/TGFBR1* (p value = 0.0016), *ifa-1/VIM* (p value = 0.0005), *cyk-1/DIAPH1* (p value = 0.0016), *hlh-8/TWIST* (p value = 0.0005), *erm-1/EZR* (p value = 0.0047), *let-805/FN1* (p value = 0.0035), *wsp-1/WASL* (p value = 0.0260), *C46H11.3/ARPC5L* (p value = 0.0194), *hrdl-1/AMFR* (p value = 0.0032), and *sup46/HNRNPM* (p value = 0.0184) reduced the movement of worms reflecting adverse effects on healthspan (p values and days of changes in movement were summarized in table 4.1). In contrast, knockdown of the *wsp-1* gene induced a slight increase in lifespan mean = 22 days (p = 0.0949), but no alteration to healthspan. Knockdown of the remaining miR-361-4p target genes resulted in no change to degree of movement in comparison to PL4440 empty vector fed worms. 9/16 orthologues revealed impacts on longevity, whereas 12/16 orthologues indicated effects on healthspan, as measured by movement activity. However, in all cases, targeted knockdown was linked with a negative consequence; reduction in target gene expression was related with lower, not enhanced, longevity and healthspan (figure 4.3).

Table 4.1: This table shows the effect on worm survival and movement upon knocking down the target genes of miR-361-5p in comparison to empty vector (PL4440) treated worms.

Gene Name *(Hs)*	Gene Name *(C. elegans)*	Last day last worms Died	Survival (Control vs. RNAi clone) *P value*	Movement (Control vs. RNAi clone) *Days with significant change in movement*
Negative Control		19 ± 2	-	-
RHOA	*rho-1*	7	0.0001	Days 1 - 7
VCL	*deb-1*	8	0.0001	Days 1 - 8
TGFBR1	*daf-1*	16	0.0001	Days 2, 5, 6, 7, 8
VIM	*ifa-1*	18 ± 1	0.0001	Days 5-10, 12
DIAPH1	*cyk-1*	15 ± 2	0.0001	Days 2-10, 12
TWIST1	*hlh-8*	20 ± 2	0.0002	Days 2-9
EZR	*erm-1*	15 ± 2	0.0008	Days 2 and 8
ACTN4	*atn-1*	17 ± 2	0.0101	Days 3 and 10
FN1	*let-805*	18 ± 2	0.0229	Days 5, 7, 8, 9, 12
SDC4	*sdn-1*	20 ± 3	0.2491	Day 8
WASL	*wsp-1*	22 ± 3	0.0949	ns
ARPC5L	*C46H11.3*	20 ± 1	0.7599	ns
DAG1	*dgn-2*	21 ± 1	0.3449	ns
IQGAP1	*pes-7*	21	0.2502	Day 8
AMFR	*hrdl-1*	19	0.0616	Day 8
HNRNPM	*sup-46*	20 ± 2	0.2754	Days 5 and 8

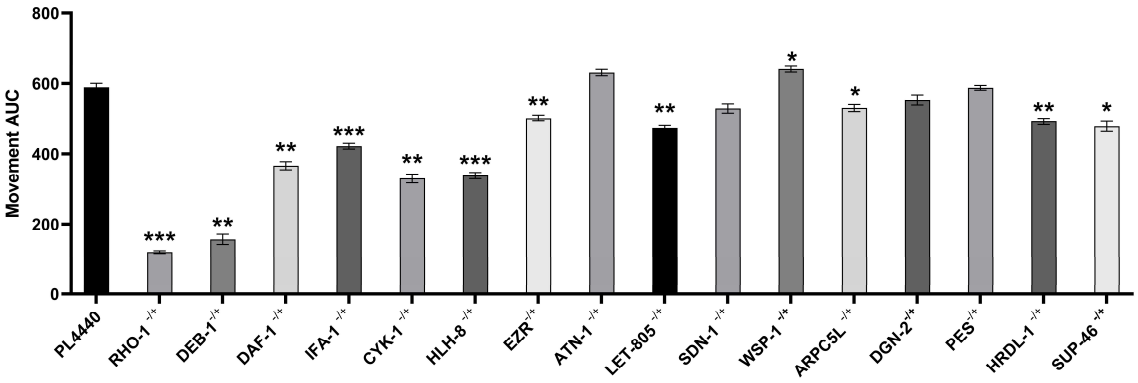

Figure 4.3: Attenuation of miR-361-5p target genes in a *C. elegans* model system. Area under the curve (AUC) measurements for a measure of healthspan (animal movement) following targeted RNAi knockdown of 16 validated miR-361-5p target genes with known C. elegans orthologues are given on the Y axis, and the identity of the gene on the X axis. Error bars represent standard deviation of measurement. In each case, data are from 3 biological replicates of 60-70 animals per replicate. * = $p \leq 0.05$, ** = ≤ 0.01, *** = $p \leq 0.001$ and **** = $p \leq 0.0001$.

4.4 Discussion

MicroRNA are emerging as powerful regulators of ageing and senescence phenotypes, as they are for other cellular processes. In work presented in chapter 3, miR-361-5p emerged as a potential regulator of senescence phenotypes in primary human endothelial cells. I found that miR-361-5p exhibits antagonistic expression patterns in response to senescence and resveratrol, a senotherapeutic compound. Here, I aimed to shed light on the mechanistic basis by which this specific miRNA may exert its effects on senescence and ageing parameters, in an *in vivo* model organism, *C. elegans*. 839 genes were identified as validated miR-361-5p targets, and 32 of these were expressed in human endothelial cells and demonstrated senescence-associated differences in expression. 16 of the 32 differentially-expressed miR-361-5p target genes had verified *C. elegans* orthologues and of these, 9 demonstrated effects negatively on lifespan and 12 on healthspan parameters. These results suggest that miR-361-5p target genes are crucial in cellular processes and reducing its expression adversely influences ageing in *C. elegans*.

Targeted manipulation of validated miR-361-5p target genes in a *C. elegans* animal model was not able to extend lifespan or healthspan parameters systemically when manipulated in adulthood. Although *C. elegans* do not undergo replicative senescence in the conventional sense due to the post-mitotic nature of their adult somatic cells, they do undergo other forms of senescence (Benedetto & Gems, 2019). Interventions designed to attenuate senescence phenotypes therefore have potential to extend healthspan and lifespan in this system. We identified two target genes (*erm-1/EZR* and *C46H11.3/ARPC5L)* that demonstrated up-regulation of expression change, consistent with the action of a down-regulated miRNA in senescence. The direction of change for most of the other miR-361-5p targets observed in senescent primary

human endothelial cells however was inconsistent with the proposed action of a miRNA; the majority of validated targets demonstrated reduced rather than elevated expression in senescent cells (Hong *et al.*, 2020). Although there are examples where miRNA can upregulate their targets in the context of senescence, this probably indicates that the majority of miR-361-5p targets are regulated by factors other than miR-361-5p in senescence.

Senescence is a key driver of ageing phenotypes. Reduction of senescent cells by senolysis or senostasis have been shown to benefits animals and reduce the ageing related diseases as cancer and neurodegenerative disease (Amor *et al.*, 2020; Baker *et al.*, 2016; Barnes *et al.*, 2019). MiR-361-5p target genes included several key players already known to be implicated as causal drivers of senescence, including serine arginine rich (SR) proteins and heterogeneous nuclear ribonucleoprotein particles (hnRNPs) (Holly *et al.*, 2013; Latorre *et al.*, 2019; Latorre *et al.*, 2018; Lee *et al.*, 2019). However, due to lack of validated orthologues of these genes in *C. elegans* or the lack of RNAi in the RNAi library, it was only possible to assess the effect of *sup-46,* which is the *C. elegans* orthologue of *HNRNPM.* The *sup-46* protein is known to contribute to the preservation of transgenerational germline immortality in *C. elegans* (Johnston *et al.*, 2017). No changes on lifespan were noted but healthspan was reduced upon knockdown of *sup-46. HNRNPM* is a member of a gene family encoding multifunctional proteins involved in alternative splicing and other aspects of mRNA processing (Geuens *et al.*, 2016). Dysregulation of mRNA processing has been suggested as a new hallmark of ageing (Schmauck-Medina *et al.*, 2022), and dysregulation of *HNRNPM* expression has been associated with ageing, senescence and age-related phenotypes in humans and other species (Latorre *et al.*, 2017; Lee *et al.*, 2019, 2016).

Of the 16 validated *C. elegans* orthologues of the validated miR-361-5p target genes identified, 14 are directly involved in the regulation or formation of the cytoskeletal network, or its interaction with the extracellular matrix. *rho-1/RHOA*, *sdn-1/SDC4*, *wsp-1/WASL, pes-7/IQGAP1*, and *hrdl-1/AMFR* are involved in transducing signals from the exterior of the cell to the interior to regulate cell motility, morphology, and survival (Chiu *et al.*, 2008; Choi & Anderson, 2016; Dart *et al.*, 2012; Elfenbein & Simons, 2013; Kempers *et al.*, 2021). *Deb-1/VCL, ifa-1/VIM, cyk-1D/IAPH1, C46H11.3/ARPC5L, erm-1/EZR, hlh-8/TWIST1* and *atn-1*/*ACTN4* are involved with formation or regulation of microtubules, intermediate filaments or other cytoskeletal components to facilitate cell attachment, cell:cell or cell:matrix interactions and EMT (Boujemaa-Paterski *et al.*, 2020; García-Palmero *et al.*, 2016; Hsu *et al.*, 2022; Schneider *et al.*, 2023; Tentler *et al.*, 2019; Yang et al., 2021). *let-805*/*FN1* and *dgn-2*/*DAG1* are extracellular matrix glycoproteins involved in cell adhesion, migration and survival (Barresi & Campbell, 2006; Owens & Baralle, 1986). The cytoskeleton and the actin filament network are widely known to regulate many aspects of cellular behaviour, particularly in the nervous system (Schneider *et al.*, 2023), and has known involvement in the ageing process and its diseases (Kim *et al.*, 2022). The remaining two miR-361-5p target genes we assessed *sup-46/HNRNPM* and *daf-1/TGFBR1* are also known to have associations with ageing and senescence. *TGFBR1* is part of the TGF signalling network and a major inducer of cell cycle arrest and senescence (Vander Ark *et al.*, 2018). The GO pathway analysis also suggested that various affected pathways are within cytoskeleton and motility; hence, this supported that several of studied genes in *C. elegans* affected the healthspan upon knockdown.

Signalling pathways and alteration in cellular communication is another hallmark of ageing. These signals may modulate major cellular fates such as apoptosis or

proliferation. The *daf-1*/*TGFBR1* is involved in TGF signalling. This gene encodes a signal receptor necessary for converting environmental stimuli into the appropriate developmental response (Georgi *et al.*, 1990). Knockout of *daf-1* resulted in the constitutive production of dauer larvae even in the presence of sufficient feeding (Georgi *et al.*, 1990). However, here knockdown of *daf-1* in adult worms reduced both the lifespan and healthspan of worms, suggesting that its effects may be life stage specific, and in adulthood may work in similar pathways to its paralog *daf-16.* Other cell signalling components were identified as contributory to lifespan and healthspan in *C. elegans* in this study, *rho-1*. The *rho-1* gene encodes a Rho GTPase, which is the sole representative of this family in *C. elegans*. A previous report has shown that *rho-1* is necessary for normal living progression of *C. elegans*. McMullan & Nurrish (2011) showed that inducing or inhibiting the activity of the only Rho GTPase in larval *C. elegans*, *rho-1*, causes changes in neural activity, fertility, defecation, and cell shape, and ultimately leads to mortality. Accordingly, knockdown of the single *rho-1* gene at L4 stage in the work presented here resulted in defects in healthspan and lifespan parameters, indicating that this gene is important not only in early life, but also in adulthood.

C. elegans represents an excellent model organism due to high genetic similarities (60-80%) with humans, a transparent body for anatomical analysis, and simplicity of maintenance in the experiment (Zhang *et al.*, 2020). This model also has a short generation time and a small size, which together with wide availability of easy molecular biology approaches for whole animal and targeted gene knockdown compared to higher organisms. Using the NemaLife microfluidic device allowed us to score for healthspan and lifespan effectively avoiding using chemicals and compounds to remove progeny and infections which were known to influence these results

(Rahman *et al.*, 2020). Even though *C. elegans* has a number of characteristics that are useful for research on the ageing process, it still has some limitations as a model organism. These include the absence of important anatomical features, such as the blood circulation system and the liver's metabolic process, compared to other mammals (Weinhouse *et al.*, 2018). It is also unsuitable for studying the relevant process in other animal species due to the absence of complex range transcriptional regulation; yet, it is advised as a simplified model for research on signal mapping mechanisms and genes influencing ageing processes (Corsi *et al.*, 2015). Other weaknesses in this work include that *C. elegans* senescence is post-mitotic, an adult worm is made up of 959 terminally differentiated post-mitotic cells (Raices *et al.*, 2005). It doesn't undergo replicative senescence but is still susceptible to other forms of senescence. Finally, this work presented here reported only loss-of-function analysis; hence, gain-of-function analysis could lead to alteration in ageing phenotypes in *C. elegans*.

In conclusion, I have validated predicted target genes of miR-361-5p, a miRNA with roles in rescue from senescence, and demonstrated that several display dysregulated expression in senescent primary human endothelial cells. Although targeted manipulation of miR-361-5p was able to bring about reversal of some aspects of the senescence phenotype in human primary endothelial cells *in vitro*, the consequences of unintended attenuation of other critical target genes *in vivo* such as those involved in maintenance of the cytoskeletal network renders it unsuitable as a future senotherapeutic target.

Chapter 5

Assessing the role of senescence-associated-miRNAs miR-15b-5p, miR-92-5p, and miR-125a-3p on senescence and ageing phenotypes *in vitro* and *in vivo*

5.1 Abstract

The accumulation of senescent cells in tissues results in systemic ageing, and ageing-related diseases. Senescent immune cells do not effectively eliminate senescent cells from tissues leading to the over production of proinflammatory cytokines, chemokines, and other inflammatory factors. Removal of senescent cells or clearance of the senescence–associated secretory phenotype (SASP) may improve and prolong the normal function of tissue. One potential serotherapeutic agent for manipulation of senescent cells is microRNAs (miRNAs). Previous work from the Harries lab has identified three miRNAs known to be dysregulated in senescent dermal fibroblast cells (miR-15b-5p, miR-92a-3p, and miR-125a-3p). Here, I showed that induction of miR-15b-5p in late passage primary normal human dermal fibroblasts cells (NHDF) using a miRNA mimic reduced the load of senescence-associated-beta-galactosidase (SA-β-Gal) positive cells and increased proliferation index (Ki67), whilst manipulation of miR-92a-3p and miR-125a-3p expression levels had no effect on senescence kinetics. Moreover, miR-15b-5p induction led to significant reduction in several components of SASP. miR-15b-5p was bioinformatically predicted to target 1800 genes, but only 16 genes were found to be differentially expressed in senescent human fibroblasts compared with early passage cells. These genes play key roles in cellular senescence, and in the FOXO, p53, and the PI3K-AKT signaling pathways. These data suggest that miR-15b-5p requires more investigation to determine whether it may represent a potential new senotherapeutic target.

5.2 Introduction

The process of ageing is intricate and is characterised by a progressive decline in cellular, tissue, and organismal function. People age at various rates and the reduction in function increases the burden of age-related disease. The hallmarks of ageing, originally described by (López-Otín *et al.*, 2013) summarized the mechanisms that may trigger and worsen the deterioration of ageing process. Recent papers have updated these hallmarks with the emerging mechanisms that affect ageing (Schmauck-Medina *et al.*, 2022; López-Otín *et al.*, 2023). One of the main hallmarks is cellular senescence, which has been demonstrated to promote the ageing process in animals (Baker *et al.*, 2016, 2011; Chang *et al.*, 2016; Hernandez-Segura *et al.*, 2018).

Cellular senescence is a phenomenon that occurs in all cell types and has been observed in almost all high eukaryotes (Wei & Ji, 2018). Senescent cells, whilst transiently present in tissue in youth, play helpful roles in wound healing (Demaria *et al.*, 2014) and also have important roles in embryogenesis (Muñoz-Espín *et al.*, 2013). It has been demonstrated that mice accumulate senescent cells during adulthood, resulting in age-dependent changes in several organs (Baker, Childs, Durik, Wijers, Sieben, Zhong, A. Saltness, et al., 2016). The persistent presence and accumulation of senescent cells that comes with ageing has a deleterious effect on the local tissue due to the chronic production of proinflammatory cytokines known as the senescence-associated secretory phenotype (SASP) (He & Sharpless, 2017; Wei & Ji, 2018). Senescent fibroblasts in the dermis contribute to skin ageing due to an arrest of cell division, dysregulated tissue homeostasis, and an increase in secretion of the SASP (de Magalhães & Passos, 2018). Fibroblasts are the main component of connective tissue; and are present and contribute to the function of organs in nearly all body

systems (Wlaschek *et al.*, 2021). In a recent study, researchers reported that the presence of fibroblast senescent cells in human breast led to increases in the expression of syndecan 1, a poor prognostic factor in breast cancer (Liakou *et al.*, 2016). Reducing the load of senescent fibroblasts cells may delay organ ageing and ameliorate the deleterious effects and disease arising from the persistence of these dysfunctional cells.

Non-coding RNAs such as miRNAs can regulate cellular mechanisms and ultimately control the fate of cells, committing them to apoptosis, senescence, or proliferation (Caravia & López-Otín, 2015; Harries, 2014). miRNAs control transcript stability by interacting with targeted messenger RNAs (mRNAs) via complementary base pairing, causing endonuclease-mediated cleavage, or silencing of protein synthesis (Chung *et al.*, 2017). In mammals, miRNA binding sites usually reside in the 3' untranslated regions (UTR) of their target mRNAs, although binding sites have also been reported in other regions of the transcript (Lewis *et al.*, 2003; Loganantharaj & Randall, 2017). Despite the fact that miRNA translational research has until recently focused mainly on cancer, dysregulation of miRNA expression and resultant effects on mRNA stability is relevant to numerous ageing related disorders including breast cancer (Mulrane *et al.*, 2013), ovarian cancer (Yoshida *et al.*, 2020), Alzheimer's disease (Provost, 2010), and diabetes (Hagiwara *et al.*, 2013). Hence, miRNAs have been emphasised as a viable therapeutic target owing to their small size, the relative simplicity of high throughput techniques for measuring them, and the availability of reagents for their *in vitro* and *in vivo* assessment.

In a recent study, our lab identified miRNAs dysregulated during senescence in more than one tissue type, dermal and lung fibroblasts (Holly *et al.*, 2015). MiRNAs were evaluated in early and late passage human primary lung and skin fibroblasts as well as in human peripheral blood from elderly participants in the InCHIANTI study (Holly *et al.*, 2015). The results showed that three miRNAs Hsa-miR-15b-5p, Hsa-miR-92a-3p, and Hsa-miR-125a-3p were commonly downregulated in skin and lung senescent fibroblasts, and also in blood samples from ageing individuals (Holly *et al.*, 2015). These three miRNAs target genes including *INMT*, *LYST*, *LHFPL2*, and *ZMPSTE24,* which have been linked to ageing related diseases such as progeria (Holly *et al.*, 2015; Messner *et al.*, 2020). However, the impact of miRNA-mediated dysregulation of the expression of these genes in senescence remains to be determined.

Here, I studied the roles of miR-15b-5p, miR-92a-3p, and miR-125a-3p in senescence phenotypes by manipulation of miRNA level in primary human fibroblasts. Assessment of senescent cells load was initially carried out through evaluation of cell kinetics including senescence-associated beta galactosidase assay (SA-β-Gal) (senescence), Ki67 (proliferation index), γH2AX (DNA damage marker), and TUNEL assay (apoptosis assay). Senescence parameters were assessed following knockdown or knock-in of miRNAs using miRNA inhibitors or mimics, respectively, depending on the directionality of the change in senescence. The effect of siRNA-mediated knockdown of the *INMT*, *LYST*, *LHFPL2*, and *ZMPSTE24* genes*,* known targets of miR-15b-5p, miR-92-3p or miR-125a-3p, were also assessed in senescent primary fibroblasts. The expression of validated miRNA target genes was also assessed. Finally, to assess the roles of these genes on ageing *in vivo*, lifespan and healthspan were assessed in an invertebrate animal model *C. elegans,* following knockdown of orthologues of the

ZMPSTE24 and INMT genes*, fce-1* and *anmt* respectively, sourced from the Ahringer RNAi library (Kamath & Ahringer, 2003).

5.3 Materials and Methods

5.3.1 Tissue culture

Primary human dermal fibroblast cells isolated from an adult donor (NHDF; C-23020, PromoCell, Germany) were used for this study. Cells were cultured and maintained in NHDF Promocell medium (C-23020, Germany) with 1% penicillin and 1% streptomycin at 37°C, ambient oxygen and 5% CO2. Senescent cells were produced by continuous culture as previously described until growth slowed to less than 0.5 population doublings per week (Holly *et al.*, 2013; Latorre, *et al.*, 2018) and were assessed in a minimum of 3 biologically independent replicates at PD = 95. Early passage cells for comparison were also assessed in 3 biological replicates and were at PD = 38. Cells were assessed at 80% confluence to ensure that cessation of growth was not due to contact inhibition.

5.3.1.1 Manipulation of miRNA expression levels

To determine whether restoring miR-15b-5p, miR-92a-3p, or miR-125a-3p levels in senescent primary dermal fibroblast cells was capable of attenuating senescence, aged cells at PD = 95 were seeded into 12 well plates at a density of 2 x 10^5 cells/ well and maintained until 70%-80% confluence. Cells were then transfected with 50pmol of a MirVana mimic (Thermo Fisher, Waltham, MA, USA) to miR-15b-5p, miR-92a-3p, or miR-125a-3p for 24hrs. To reveal whether validated miR target genes *INMT*, *LHFPL2*, *LYST*, and *ZMPSTE24* influenced senescence, late passage (PD = 95) NHDF was transfected with 30 pmol dsiRNAs (TriFECTa® Dicer-Substrate siRNA; IDT, Inc.), to knockdown the genes of interest. Transfections were carried out using Lipofectamine 3000 (Thermo Fisher, Waltham, MA, USA) and a lipofectamine-only

control was also performed to ensure that any changes observed is not due to the transfection reagent. The percentage of senescent cells in the culture was then assessed by senescence-associated beta galactosidase staining in duplicate fields of each of 3 biological replicates, with >300 cells per condition assessed. Changes to cell proliferation and the occurrence of DNA damage foci were assessed by Ki67 and γH2AX staining as described above. Differences between treated and control cultures assessed for statistical significance by unpaired t-test (GraphPad Prism 8).

5.3.2 Immunohistochemistry to determine cellular kinetics

Senescence was confirmed by senescence-associated beta galactosidase (SA-β-Gal) positivity and γH2AX activity using commercial kits (Sigma, Aldrich, UK and CS0030 for SA-β-Gal and Abcam, ab26350 for γH2AX respectively). Cessation of proliferation was confirmed using a commercially-available antibody against Ki67 (Abcam, ab16667). In brief, cells were fixed for 10 min with 4% PFA and permeabilized with 0.025 % Triton and 10 % serum in PBS for 1 hour. Cells were then incubated with a rabbit monoclonal anti-Ki67 antibody (ab16667, Abcam, UK) at 1:200 overnight at 4 °C followed by FITC-conjugated secondary goat anti-rabbit (1:400) for 1 hour, and nuclei were counterstained with DAPI. Coverslips were mounted on slides in DAKO fluorescence mounting medium (S3023; Dako). In each case, at least 300 cells were assessed per replicate. For assessment of miRNA response to each treatment, cells were seeded at a density of 4.0×10^5 cell/cm^2 in 6-well plates and left to settle for 24 hr, after which they were transfected with 50 pmol in case of miRNA mimics or 30 pmol in case of siRNAs or with negative control alone for 48 hours, after which senescence kinetics were established as described. Significance was determined by Students t-test in GraphPad Prism 8.

5.3.3 RNA extraction and Purification

Early (PD = 38) and late (PD = 95) passage cells, as well as those treated with scramble controls, a short double RNA sequence that target no genes in human and used as a negative control, were harvested by centrifugation, and rinsed in Dulbecco's phosphate-buffered saline (DPBS). Total RNA including the small RNA was extracted from each replicate using Tri reagent® (Thermo Fisher, Waltham, MA, USA) according to the manufacturer's instructions. RNA samples destined for whole transcriptome analysis were then purified further using an RNA Clean & Concentrator kit (Zymo Research, CA, USA) according to the manufacturer’s instructions.

5.3.4 Whole transcriptome profiling and differential gene expression analysis of early and late NHDF passages

An analysis of transcriptome-wide gene expression patterns of NHDF cells was conducted in early passage (PD = 38) and late passage (PD = 95) in 3 biological replicates using ClariomD pico system (Thermo Fisher, Waltham, MA, USA). The Clariom D assay identifies genes, exons, and alternative splicing events that give rise to coding RNA and lncRNA isoforms, making it the most detailed transcriptome-wide gene analysis. RNA samples were prepared and sent to (UK Bioinformatics Ltd, King’s college London, UK). Differential expression analyses were performed using the Transcriptomic Analysis Console (TAC) software (TAC 4.0.2.10) using the default settings suggested by the supplier (Applied Biosystems). Differences between two groups were identified by one-way ANOVA. Data analysis and statistical significance were completed using GraphPad Prism 8.0 software (GraphPad Software, La Jolla, CA, USA). Data were adjusted for false discovery rate by Benjamini Hochberg correction.

5.3.5 mRNA and miRNA reverse transcription and quantification (qRT-PCR)

Experiments were carried out in three biological replicates in NHDF cells using verified Silencer dsiRNAs chosen to provide the optimum coverage for the target gene (Integrated DNA Technologies, USA). The Assay Identifiers are listed in table 2.2 in chapter 2 materials and methods. NHDF cells were seeded into six-well plates at a density of 1 X 10^6 cells per mL when they were at passage 18 and PD = 95. The cells were then maintained until 70% to 80% confluence. SiRNAs were transfected at a concentration of 30 pmol in a final volume of 100 µL using Lipofectamine 3000 and incubated for 48 hours in the optimal culturing condition (Thermo Fisher, Waltham, MA). A transfection efficiency control tye^{563} (IDT DNA Technology, INC) was transfected into the cells to quantify the transfection efficiency at a same dosage of siRNAs (30 pmol); scramble-treated cells were also included to check for effects caused by the transfection procedure itself. To determine the effectiveness of the target knockdown, RNA was extracted after 48 hours using Tri-Reagent from Thermo Fisher, Waltham, USA, and then cleaned and concentrated using the RNA clean & concentratorTM-5 from Zymo Research, USA. EvoScript universal cDNA master (Roche Life Science, Burgess Hill, UK) was used for cDNA synthesis in accordance with the manufacturer's instructions. 5 µL reactions consisted of, 2.5 µL TaqMan® Universal PCR Mastermix II (no AmpErase® UNG) (Thermo Fisher, Waltham, MA, USA), 1.75 µL dH_2O, 0.5 µL cDNA, and 0.25 µL TaqMan® gene assay (Thermo Fisher, Foster City, USA) in a 5µL reaction volume. Conditions for cycling were 50 °C for 2 minutes, 95 °C for 10 minutes, and 45 cycles of 15 seconds at 95 °C for 30 seconds, followed by 1 minute at 60 °C. All reactions were run in three biological replicates and three technical replicates. Statical analysis for significance was performed in GraphPad Prism 9.0 using student unpaired *t-test*.

For miRNA quantification, cDNA was produced using the TaqMan advanced microRNA cDNA synthesis kit, as described above (Thermo Fisher, Waltham, MA, USA). The experiments also included untreated and scrambled controls to evaluate the unexpected effects of transfection. The effectiveness of the target knockdown or mimic was evaluated by performing qRT-PCR after 48 hours of RNA extraction with Tri-Reagent (Thermo Fisher, Waltham, USA). For confirming the miRNA induction or inhibition, we utilised TaqMan advanced microRNA assays (Thermo Fisher, Waltham, MA) with the same endogenous controls. TaqMan probe assays used in this study are presented table 2.2. Reaction conditions were2.5 µL TaqMan® Universal PCR mastermix II (Thermo Fisher, Waltham, MA, USA), 1.75 µL dH_2O, 0.5 µL cDNA, and 0.25 µL TaqMan® gene assay (Thermo Fisher, Foster City, USA) In a 5µL reaction volume. The following cycling temperatures were used: 50 °C for 2 minutes, 95 °C for 10 minutes, 50 cycles of 15 s each at 95 °C for 30 seconds, and 1 min at 60 °C.

5.2.6 Gene Ontology pathway analysis of dysregulated miRNA target genes

Because microRNAs exhibit tissue specificity, even legitimate targets might not be present in the cells of interest. We found 1836 verified targets of miR-15b-5p using the DNA intelligent analysis (DIANA) mirPath v3.0 database and miRTarBase (Huang *et al.*, 2020), which contains only experimentally validated target genes. Out of these, 429 genes were expressed in NHDF. EnrichR was used to perform gene set enrichment analysis (GSEA) to discover pathways that were enriched in verified miR-15b-5p target genes. EnrichR is a webtool that determines if candidate genes are more prevalent in biological or molecular function gene ontologies (GO) than one would predict at random, based on the adjusted p value (ranking determined from

Fisher's exact test for gene sets) significance (Chen *et al.*, 2013). The default configuration for thresholds was -1.0.

5.2.7 *C. elegans* growth and feeding with RNAi bacterial clone

C. elegans strains were grown at 20 °C on Petri plates with *Escherichia coli OP50* and nematode growth medium (NGM) agar. Gravity synchronisation was used to age-synchronize the animals for the research starting at the L1 stage, and they were then allowed to develop until the target day of adulthood, day 3. In this work, double-stranded RNA (dsRNA) expressing bacteria were provided to worms as part of the RNAi feeding technique (Timmons *et al.*, 2001). The strains of *C. elegans* utilised in this investigation were Bristol strain N2 (WT), and they were fed *Escherichia coli* OP50 producing double-stranded RNAi vectors against *anmt-3* and *fce-1*; table 5.1 showed the details of these RNAi clones. *ZMPSTE24/fce-1* was chosen to follow on with analysis *in vivo* due to a previous validation in our lab that *ZMPSTE24* is targeted and regulated by miR-15b-5p (Holly *et al.*, 2015). Also, *INMT/anmt-3* was used here to see the effect of this gene on system ageing. All clones for this study were obtained from the Ahringer library (Kamath & Ahringer, 2003) kindly donated from Tim Etheridge lab.

Table 5.1: Details showed the targeted genes of miRNAs studied in this chapter in human: *INMT* and *ZMPSTE24* and their orthologues in *C. elegans, anmt-3* and *fce-1*, respectively.

Gene Name *(Hs)*	Gene ID *(Hs)*	Gene Name *(C. elegans)*	Sequence ID *(C. elegans)*	Genetic position *(C. elegans)*	Protein Sequence Similarities
INMT	**ENSG00000241644**	***anmt-3***	**T07C12.9**	**V:2.22 +/- 0.000 cM**	**41.82 %**
ZMPSTE24	**ENSG00000084073**	***fce-1***	**C04F12.10**	**I:3.86 +/- 0.001 cM**	**25.00 %**

5.3.7.1 Lifespan and healthspan assays using the NemaLife microfluidic chips

The microfluidics-based Infinity Screening System (NemaLife Inc.) was used to study lifespan and healthspan of *C. elegans* strains upon deregulation of *anmt-3* and *fce-1* genes using RNAi. Worms were raised as explained in section 5.2.3 until day 0 of adulthood. Animals from day 0 were then collected in conical tubes after being cleaned off plates with 2 mL of M9. Young adults were allowed to settle at the bottom after the animals were rinsed three times with 14 mL of M9, and the supernatant was then drained to eliminate any bacterial debris. Worms were then picked in a 2.5-mL sterile syringe and 50 to 65 worms were placed onto each microfluidic chip (NemaLife Inc.'s Infinity chip) for whole-life culture as previously described (Rahman *et al.*, 2020). Every day, 20 mg/mL of *E. coli* OP50, *anmt-3*, or *fce-1* RNAi clones in liquid NGM was fed after the microfluidic culture chips had been cleaned to eliminate offspring and photographed for 90 seconds. Chips were then put in Petri plates with moist tissue coated in parafilm and refrigerated at 20 °C until the following day. The programme Infinity Code was used to score the obtained videos for live/dead and movement of animal content (NemaLife Inc.). Beginning on the first day of adulthood, survival analysis was performed every day until the last day of life. Movement was measured up to day 12 of adulthood as worms become mostly inactive and worm movement rates were assessed in three independent replicates for each treatment.

5.4 Results

5.4.1 Reduction in senescent cell load following increase in miR-15b-5p expression in late passage human primary dermal fibroblasts.

To determine whether miR-15b-5p, miR-92a-3p, or miR-125a-3p influence cellular senescence phenotypes, we treated primary senescent human dermal fibroblast cells with mimics to miR-15b-5p, miR-92a-3p, or miR-125a-3p. Transfection efficiencies were >95% (appendix V). We identified that increasing levels of miR-15b-5p in aged dermal fibroblast cells resulted in a 15.17% drop in the load of senescent cells in the culture (the load of senescent cells in cells treated with scramble was 76.91% (SD = 3.69%) compared with 61.74% (SD = 8.69%) in mimic treated cells; ($p = 0.0496$) (figure 5.1 A&B). There was also an increase in proliferation index (Ki67). The percentage of Ki67 positive cells in cells treated with scramble was 23.73% (SD = 2.97%) compared with 34.27% (SD = 5.02%) in miR-15b-5p mimic treated cells; ($p = 0.0353$) (figure 5.1 C&D). However, no significant change was observed in γH2AX staining cells (figure 5.1 E&F). No changes in senescence kinetics were noted for miR-92a-3p or miR-125a-3p (figure 5.2 and 5.3).

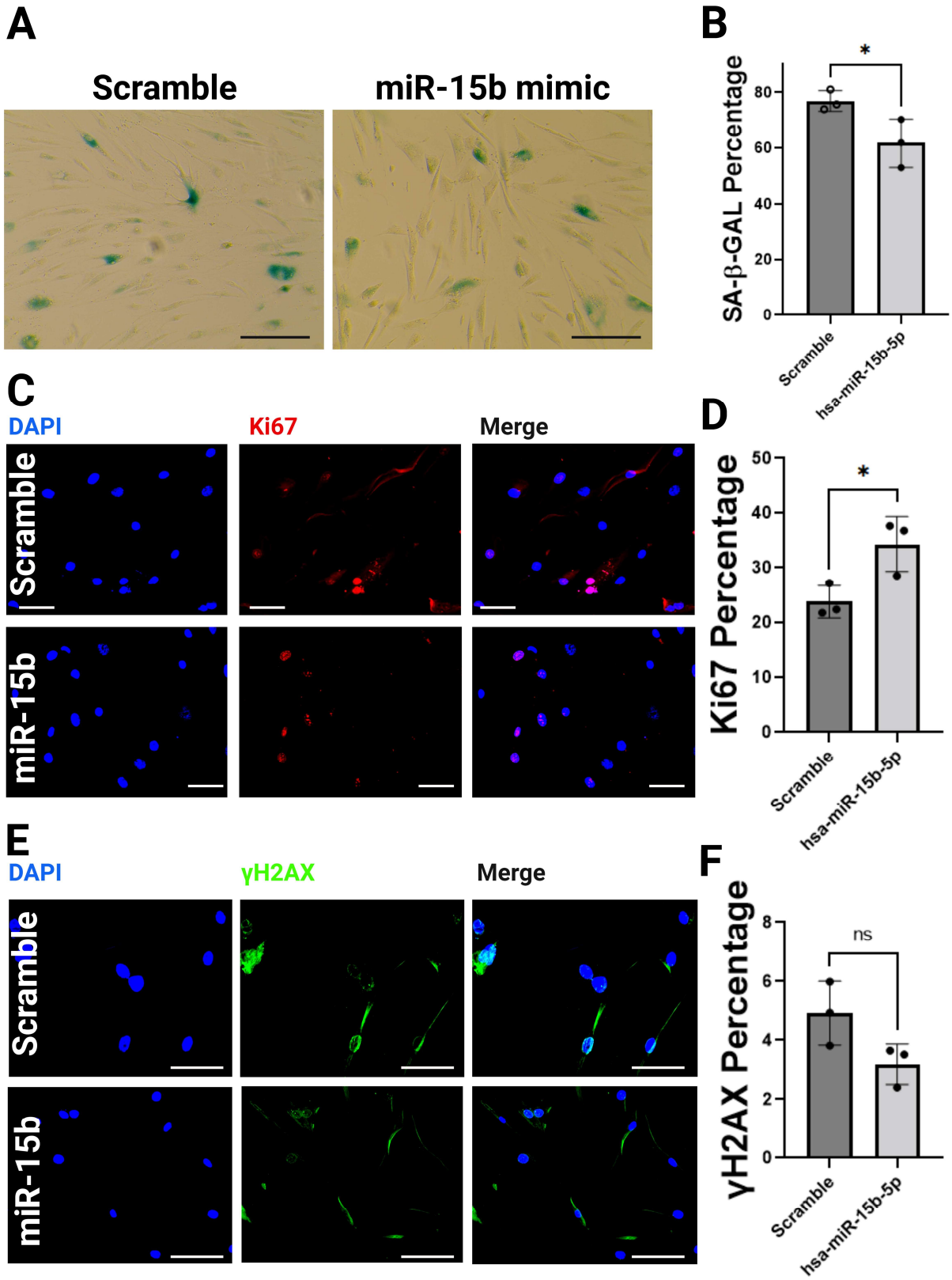
A
Scramble
miR-15b mimic
B
SA-β-GAL Percentage
0
20
40
60
80
*
Scramble
hsa-miR-15b-5p
C
DAPI
Ki67
Merge
Scramble
miR-15b
D
Ki67 Percentage
0
10
20
30
40
50
*
Scramble
hsa-miR-15b-5p
E
DAPI
γH2AX
Merge
Scramble
miR-15b
F
γH2AX Percentage
0
2
4
6
8
ns
Scramble
hsa-miR-15b-5p

Figure 5.1: Reduction of cellular senescence in aged fibroblast cells using a mimic to miR-15b-5p. The percentage of SA-β-Gal, Ki67, and γH2AX positive cells in cultures of late passage primary human dermal fibroblast cells treated with a mimic to miR-15b-5p or with scramble as a negative control are presented above. (A) Microscope fields illustrating representative senescence-associated beta galactosidase (SA-β-Gal) activity in scramble-treated late passage (PD = 95) human primary dermal fibroblast cells or late passage cells treated with a mimic to miR-15b-5p. (B) Graph showing change in SA-β-Gal activity in scramble-treated late passage (PD = 95) human primary dermal fibroblast cells or late passage cells treated with a mimic to miR-15b-5p. (C) Proliferation kinetics in scramble-treated late passage (PD = 95) human primary dermal fibroblast cells or late passage cells treated with a mimic to miR-15b-5p. Cells were stained for Ki67 activity. (D) Graph showing change in Ki67 staining in scramble-treated late passage (PD = 95) human primary dermal fibroblast cells or late passage cells treated with a mimic to miR-15b-5p. (E) DNA damage foci as identified by γH2AX staining in scramble-treated late passage (PD = 95) human primary dermal fibroblast cells or late passage cells treated with a mimic to miR-15b-5p. (F) Graph showing change in γH2AX staining in scramble-treated late passage (PD = 95) human primary dermal fibroblast cells or late passage cells treated with a mimic to miR-15b-5p. Dark grey bars represent senescent cell load in scramble treated cells, whilst the grey bars represent senescent cell load following treatment with a miR-15b-5p mimic. Transfection efficiency was >90%. Error bars indicate standard deviation of measurement. Statistical significance of effect as determined by independent t-test is indicated by a star * $p = <0.05$. Scale bar is 50 µm.

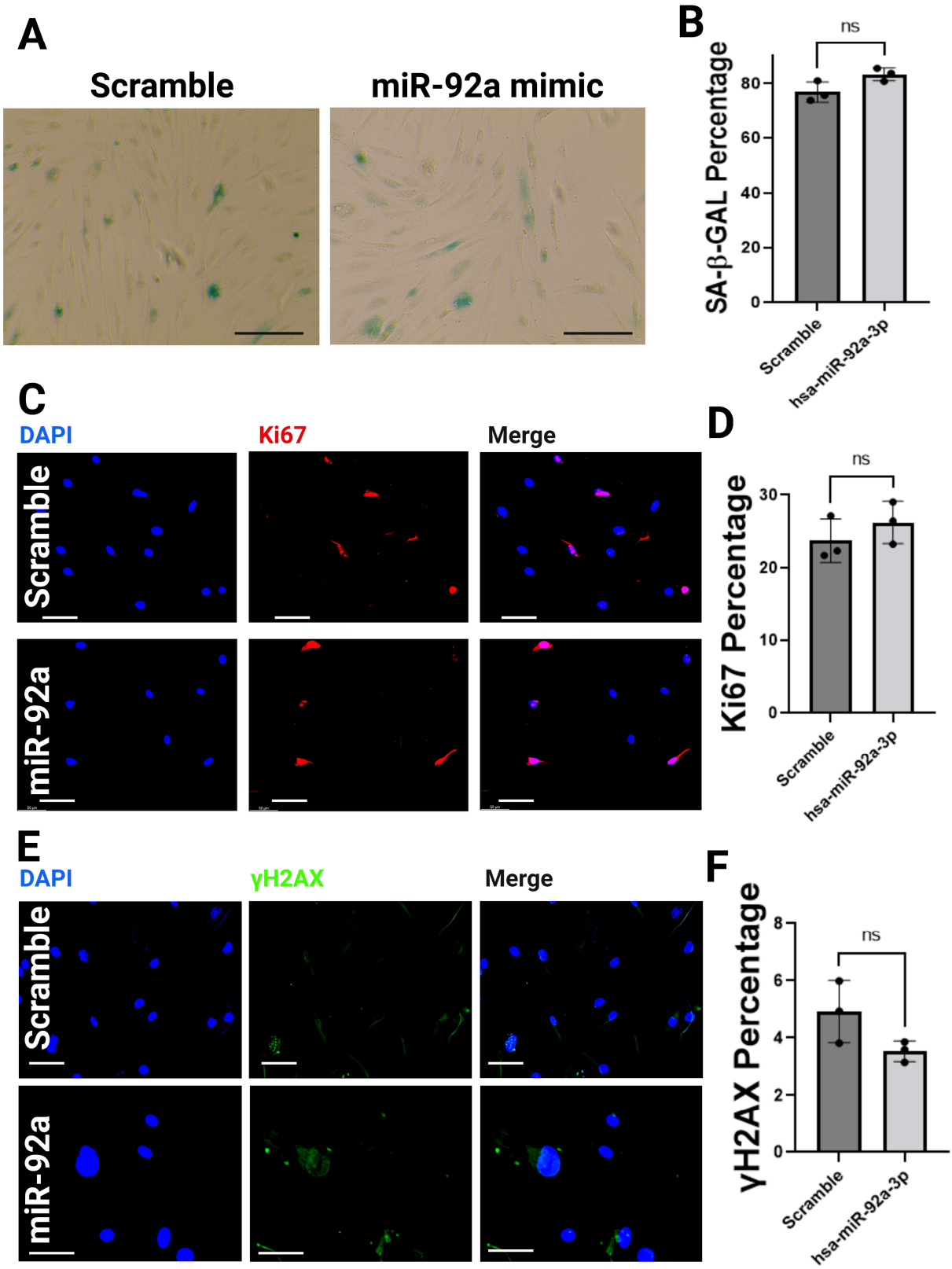
A
Scramble
miR-92a mimic
B
ns
SA-β-GAL Percentage
0
20
40
60
80
Scramble
hsa-miR-92a-3p
C
DAPI
Ki67
Merge
Scramble
miR-92a
D
ns
Ki67 Percentage
0
10
20
30
Scramble
hsa-miR-92a-3p
E
DAPI
γH2AX
Merge
Scramble
miR-92a
F
ns
γH2AX Percentage
0
2
4
6
8
Scramble
hsa-miR-92a-3p

Figure 5.2: Senescence kinetics of late passage human primary dermal fibroblast cells treated with scramble small RNA or mimic to miR-92a-3p. The percentage of SA-β-Gal, Ki67, and γH2AX positive cells in cultures of late passage primary human dermal fibroblast cells treated with a mimic to or with scramble as a negative control are presented above. (A) Microscope fields illustrating representative senescence-associated beta galactosidase (SA-β-Gal) activity in scramble-treated late passage (PD = 95) human primary dermal fibroblast cells or late passage cells treated with a mimic to miR-92a-3p. (B) Graph showing change in SA-β-Gal activity in scramble-treated late passage (PD = 95) human primary dermal fibroblast cells or late passage cells treated with a mimic to miR-92a-3p. (C) Proliferation kinetics in scramble-treated late passage (PD = 95) human primary dermal fibroblast cells or late passage cells treated with a mimic to miR-92a-3p. Cells were stained for Ki67 activity. (D) Graph showing change in Ki67 staining in scramble-treated late passage (PD = 95) human primary dermal fibroblast cells or late passage cells treated with a mimic to miR-92a-3p. (E) DNA damage foci as identified by γH2AX staining in scramble-treated late passage (PD = 95) human primary dermal fibroblast cells or late passage cells treated with a mimic to miR-92a-3p. (F) Graph showing change in γH2AX staining in scramble-treated late passage (PD = 95) human primary dermal fibroblast cells or late passage cells treated with a mimic to miR-92a-3p. The Dark grey bars represent senescent cell load in vehicle treated cells, whilst the grey bars represent senescent cell load following treatment with a miR-92a-3p mimic. Transfection efficiency was >90%. Error bars indicate standard deviation of measurement. Statistical significance of effect was determined by independent t-test and ns = not significant. Scale bar is 50 μm.

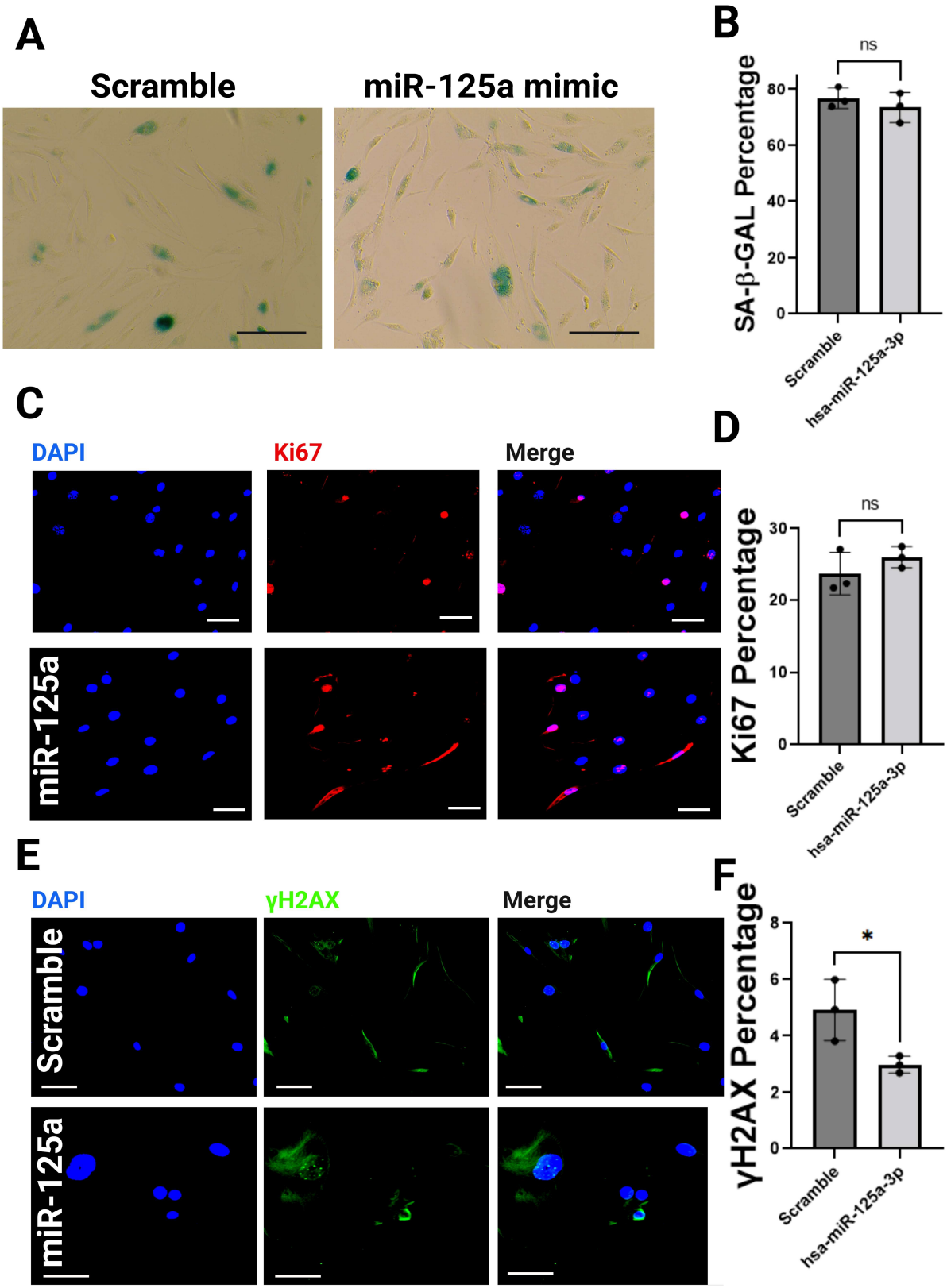
A
Scramble
miR-125a mimic
B
ns
SA-β-GAL Percentage
80
60
40
20
0
Scramble
hsa-miR-125a-3p
C
DAPI
Ki67
Merge
miR-125a
D
ns
Ki67 Percentage
30
20
10
0
Scramble
hsa-miR-125a-3p
E
DAPI
γH2AX
Merge
Scramble
miR-125a
F
*
γH2AX Percentage
8
6
4
2
0
Scramble
hsa-miR-125a-3p

Figure 5.3: Senescence kinetics of late passage human primary dermal fibroblast cells treated with scramble small RNA or mimic to miR-125a-3p. The percentage of SA-β-Gal, Ki67, and γH2AX positive cells in cultures of late passage primary human dermal fibroblast cells treated with a mimic to miR-125a-3p or with scramble as a negative control are presented above. (A) Microscope fields illustrating representative senescence-associated beta galactosidase (SA-β-Gal) activity in scramble-treated late passage (PD = 95) human primary dermal fibroblast cells or late passage cells treated with a mimic to miR-125a-3p. (B) Graph showing change in SA-β-Gal activity in scramble-treated late passage (PD = 95) human primary dermal fibroblast cells or late passage cells treated with a mimic to miR-125a-3p. (C) Proliferation kinetics in scramble-treated late passage (PD = 95) human primary dermal fibroblast cells or late passage cells treated with a mimic to miR-125a-3p. Cells were stained for Ki67 activity. (D) Graph showing change in Ki67 staining in scramble-treated late passage (PD = 95) human primary dermal fibroblast cells or late passage cells treated with a mimic to miR-125a-3p. (E) DNA damage foci as identified by γH2AX staining in scramble-treated late passage (PD = 95) human primary dermal fibroblast cells or late passage cells treated with a mimic to miR-125a-3p. (F) Graph showing change in γH2AX staining in scramble-treated late passage (PD = 95) human primary dermal fibroblast cells or late passage cells treated with a mimic to miR-125a-3p. Dark grey bars represent senescent cell load in vehicle treated cells, whilst the grey bars represent senescent cell load following treatment with a miR-125a-3p. Transfection efficiency was >90%. Error bars indicate standard deviation of measurement. Statistical significance of effect was determined by independent t-test where a star * $p = <0.05$ and ns = not significant. Scale bar is 50 μm.

5.4.2 Induction of miR-15b-5p levels in late passage human primary dermal fibroblast cells influence several markers of cellular senescence

Based on the kinetics results after induction of mimics of the three miRNAs in NHDF, I chose to further investigate the changes of miR-15b-5p knock-in on senescent markers and SASP factors. This experiment was performed on 11 independently cultured replicates (different vials) of NHDF cells to confidently validate the changes on senescent phenotypes. *LMNB1* expression was increased upon treatment with a miR-15b-5p mimic (p value = 0.005254) while *CDKN2A* was decreased (p value = 0.003) compared to scramble treated late fibroblast (figure 5.4, A). SASP factors IL6 (p value = 0.000004), IL8 (p value = 0.000010), *CXCL1* (p value = <0.000001), *CXCL10* (p value = <0.000001), and *IL2B* (p value = 0.004238) were significantly decreased in comparison to negative control (scramble) treated cells (figure 5.4, B). *IL12A* (p value = 0.41) showed no changes and *MMP3* (p value = 0.00001) was higher in miR-15b-5p mimics treated cells. DNA damage response elements, *ATM* (p value = 0.00002) and *ATR* (p value = 0.00003) were also altered (figure 5.4, D). Apoptotic markers activation genes *CASP1* (p value = 0.0003), *CASP3* (p value = 0.0001), and *CASP7* (p value = 0.03) and the antiapoptotic marker *BCL2* (p value = 0.01) (figure 5.4, D).

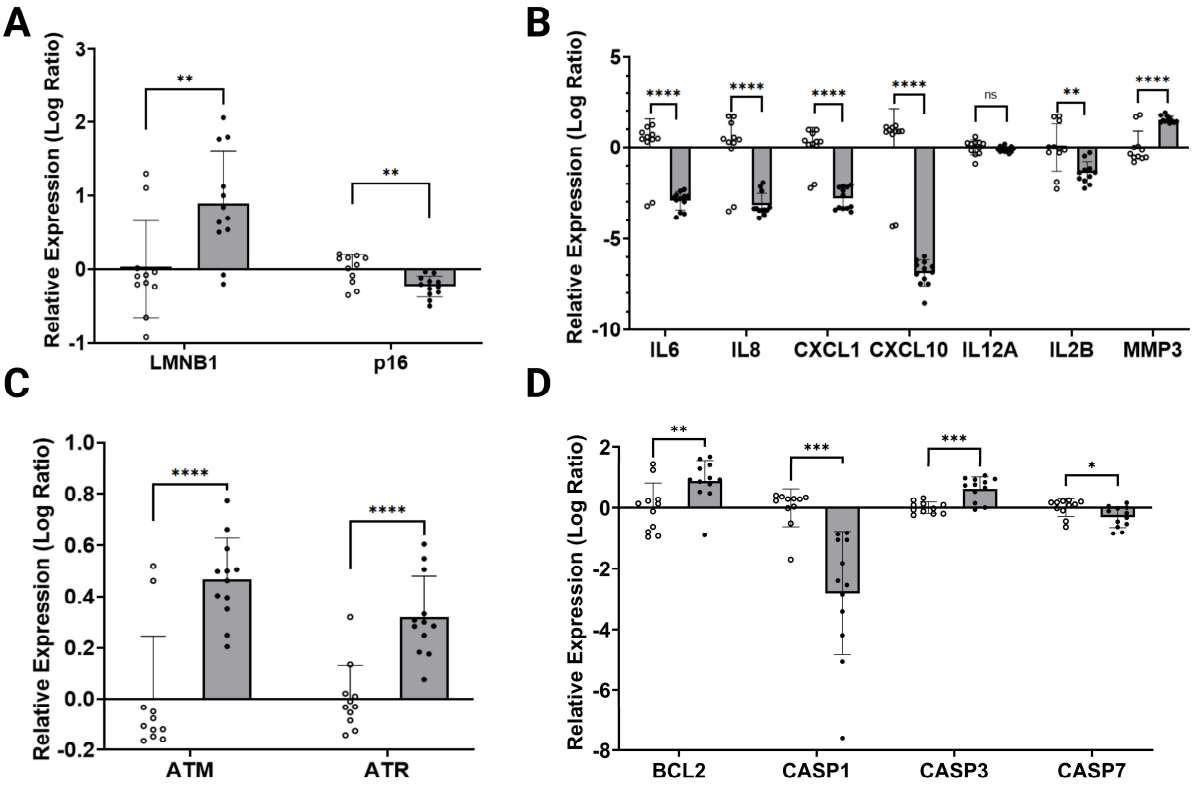

Figure 5.4: qRT-PCR to measure senescence markers alteration in response to induction of miR-15b-5p mimics compared to scramble in late passage human primary dermal fibroblast cells. (A) Two senescent markers were investigated, LMNB1 and P16 in scramble compared to miR-15b-5p mimics treated cells. (B) SASP factors as cytokines and chemokines: IL6, IL8, CXCL1, CXCL10, IL12A, IL2B, and MMP3 were measured in scrambled and miR-15b-5p mimics treated cells. (C) DNA damage response markers, ATM and ATR were examined in scrambled and miR-15b-5p mimics treated cells. (D) Apoptotic markers activation genes *CASP1*, *CASP3*, and *CASP7* and the antiapoptotic marker BCL2 expression were shown in scrambled and miR-15b-5p mimics treated cells. White bars indicate scramble treated cells; grey bars indicate late passage cells treated with miR-15b-5p mimics (n = 11 biological replicates). Error bars represent SD. Graph was created using GraphPad Prism 9.0. Statistical significance was determined by *t test* and * p = <0.05, ** p = <0.01, *** p = <0.001 and **** p = <0.0001. Where ns = not significant.

5.4.3 Expression and pathway analysis of induced miRNA and their target genes

Next, I assessed the genes expression patterns of genes targeted by miR-15b-5p in early and late passage NHDF. The miRTarbase database which provides only experimentally validated targets to miRNA (Vlachos *et al.*, 2015), indicates that miR-15b-5p can directly target and interact with 1836 genes in man, of which 307 have potential to affect the ageing process (Tacutu *et al.*, 2018). To select genes that may be influenced by miR-15b-5p in senescence in NHDF, I carried out a whole transcriptome evaluation of gene expression level in early (PD = 36) and late (PD = 95) passage NHDF. Out of 1836 validated target genes, only 16 genes demonstrating differential expression in NHDF (figure 5.5). A gene ontology (GO) terms analysis of experimentally validated miR-15b-5p target genes indicated that these genes were enriched in several pathways involved in regulating cellular senescence: pathways in cancer, cellular senescence, FOXO signaling pathway, p53 signaling pathway, microRNAs in cancer, PI3K-AKT signaling pathway, signaling pathways regulating pluripotency of stem cells, MAPK signaling pathway, apoptosis, chemokine signaling pathway, and RAS signaling pathway (table 5.2). For the complete analysed data please see the supplementary II file.

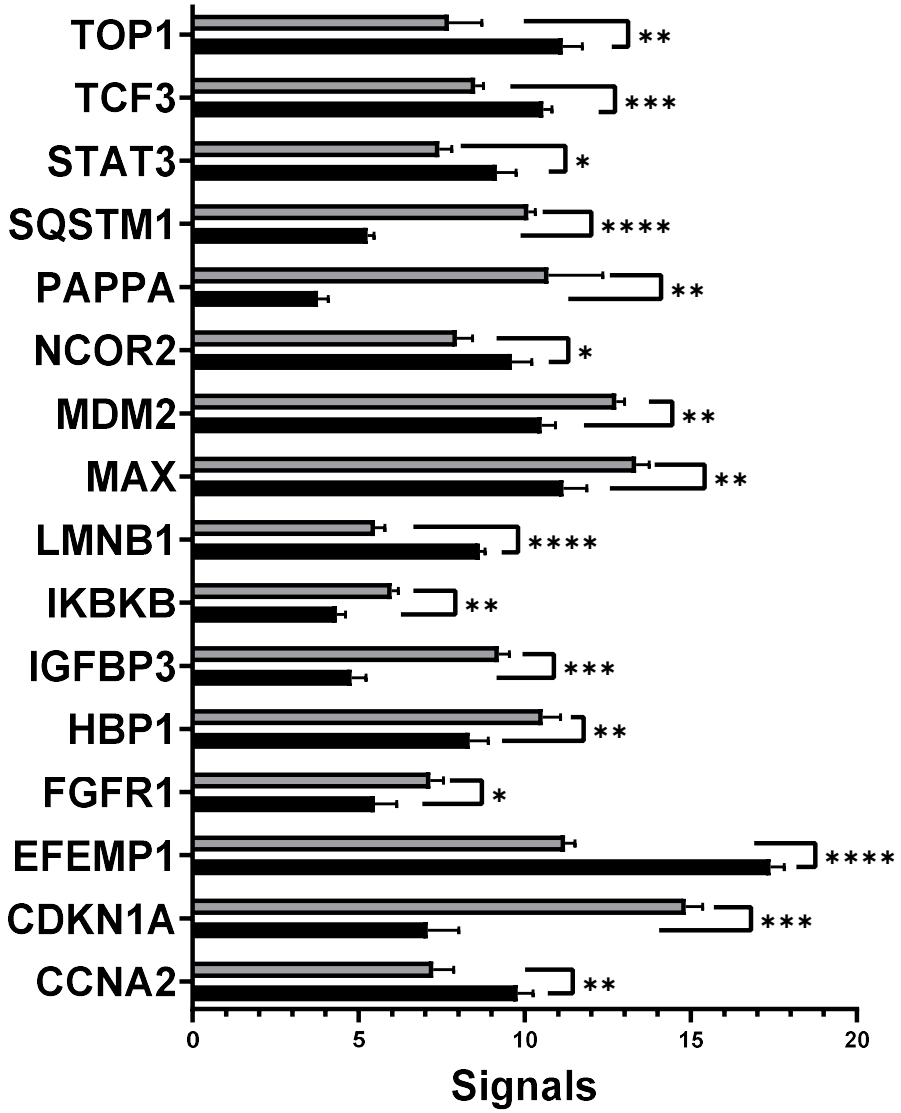

Figure 5.5 Differential expression of miR-15b-5p targets in early and late passage human primary dermal fibroblast cells. The expression patterns of 16 bioinformatically and experimentally validated target genes of miR-15b-5p in early (PD = 38) and late (PD = 95) passage human primary dermal fibroblast cells are given. Black bars indicate early passage cells, grey bars indicate late passage cells (n = 3 biological replicates). Error bars represent SD. Graph was created using GraphPad Prism 9.0. Statistical significance was determined by *t test* and * = p = <0.05, ** = p = <0.01, *** = p = <0.001 and **** = p = <0.0001.

Table 5.2 Gene Ontology (GO) biological enriched in miR-15b-5p target genes displaying differential expression in between early and late passage of primary human dermal fibroblast cells. Pathways implicated in cellular senescence are marked in bold type. P values and adjusted p values have been derived from KEGG exact test for gene set enrichment in each pathway.

Term	P-value	Adjusted P-value
Transcriptional misregulation in cancer	5.35E-09	3.74E-07
Epstein-Barr virus infection	7.25E-09	3.74E-07
Pathways in cancer	8.31E-08	2.84E-06
Cellular senescence	1.10E-07	2.84E-06
Prostate cancer	9.05E-07	1.86E-05
FoxO signaling pathway	3.01E-06	5.17E-05
Hepatitis B	7.00E-06	1.03E-04
Viral carcinogenesis	1.70E-05	1.83E-04
Proteoglycans in cancer	1.77E-05	1.83E-04
Acute myeloid leukemia	1.95E-05	1.83E-04
Human T-cell leukemia virus 1 infection	2.30E-05	1.83E-04
Melanoma	2.42E-05	1.83E-04
p53 signaling pathway	2.52E-05	1.83E-04
Human cytomegalovirus infection	2.55E-05	1.83E-04
Chronic myeloid leukemia	2.85E-05	1.83E-04
Pancreatic cancer	2.85E-05	1.83E-04
Small cell lung cancer	5.05E-05	3.06E-04
MicroRNAs in cancer	8.89E-05	5.09E-04
Human papillomavirus infection	1.15E-04	6.21E-04
Cell cycle	1.23E-04	6.32E-04
PI3K-Akt signaling pathway	1.48E-04	7.28E-04
Signaling pathways regulating pluripotency of stem cells	1.87E-04	8.76E-04
Hepatitis C	2.47E-04	0.001104024
Kaposi sarcoma-associated herpesvirus infection	4.52E-04	0.001938202
Bladder cancer	4.83E-04	0.001990527
Shigellosis	9.14E-04	0.003622399
Adipocytokine signaling pathway	0.001364325	0.005204646
Non-small cell lung cancer	0.001484374	0.005426197
MAPK signaling pathway	0.001527764	0.005426197

Glioma	0.001609305	0.005525282
PD-L1 expression and PD-1 checkpoint pathway in cancer	0.002256241	0.007496543
C-type lectin receptor signaling pathway	0.003064426	0.009612855
Parathyroid hormone synthesis, secretion and action	0.003181041	0.009612855
Th17 cell differentiation	0.003240123	0.009612855
Insulin resistance	0.003299721	0.009612855
HIF-1 signaling pathway	0.003359833	0.009612855
Toxoplasmosis	0.00354325	0.009863641
Growth hormone synthesis, secretion and action	0.003989094	0.010812544
Osteoclast differentiation	0.004528998	0.011961201
Fluid shear stress and atherosclerosis	0.005398787	0.013562806
Measles	0.005398787	0.013562806
Apoptosis	0.005627344	0.013800391
Breast cancer	0.00601805	0.014415329
Necroptosis	0.007005115	0.016398336
JAK-STAT signaling pathway	0.007262663	0.016623428
Chemokine signaling pathway	0.010070045	0.022548144
Lipid and atherosclerosis	0.01249992	0.027393442
Coronavirus disease	0.01444527	0.030364547
Ras signaling pathway	0.01444527	0.030364547

5.4.4 *in vivo* validation of miRNAs targeted genes involvement in healthspan

INMT, *LHFPL2*, *LYST*, and *ZMPSTE24* genes are validated target genes of miR-15b-5p, miR-92a-3p, and miR125a-5p, in human fibroblasts with potential to influence cellular senescence (Holly *et al.*, 2015). Here, I assessed whether RNAi gene knockdown of *C. elegans* orthologues of these genes had the potential to affect healthspan or lifespan in an invertebrate model, *C. elegans*. Of these 4 genes, only *INMT* and *ZMPSTE24* had known orthologues in *C. elegans,* which featured similar gene structures to their human counterparts (figure 5.6, A and D). (*anmt-3*) and *fce-1* respectively; figure 5.6, A and D). *C. elegans* treated with empty vector alone had a mean lifespan of 20 days, whereas knockdown of the *daf-16* and *age-1* positive control genes resulted in reduction of lifespan of 4 days and increase of lifespan of 6 days respectively. No significant changes in *C. elegans* lifespan was observed for both genes following RNAi knockdown of *anmt-3* or *fce-1* (P = 0.18 and 0.85 respectively; figure 5.6), but movement was reduced upon knocking down *fce-1* but not *anmt-3*.

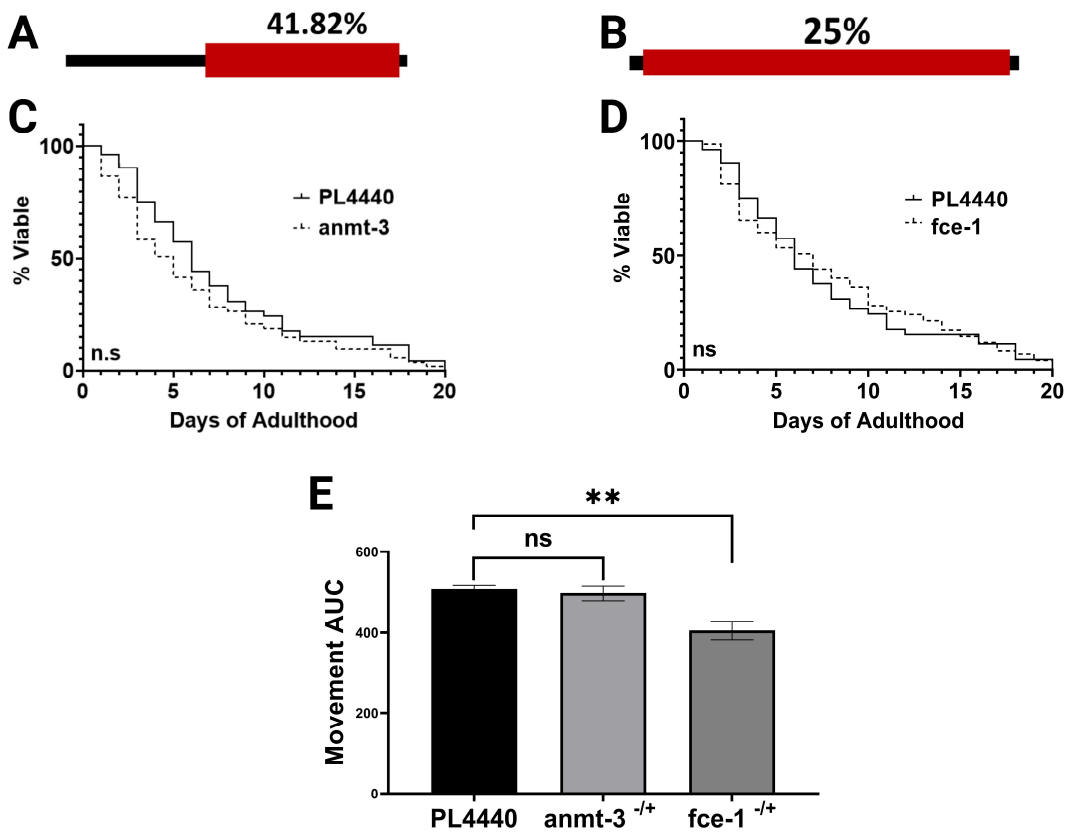

Figure 5.6: Knock down genes targeted by miR-15b-5p has effect on the survival and healthspan of *C. elegans*. (A and B) Amino acids sequence alignment analysis revealed high similarity between the human gene, *INMT* or *anmt-3* and *ZMPSTE24* with its orthologue *fce-1* genes from *C. elegans*. (C) Lifespan curves were obtained by using the NemaLife device microfluidic device. worms fed on *anmt-3* RNAi clone bacteria has no significant changes in term of survival compared to negative control (P = 0.1807). (D) Worms fed on *fce-1* RNAi clone bacteria has increase the median lifespan to 21 days but no significant changes in term of maximum lifespan compared to negative control PL4440 (P = 0.0357). (E) Movement analysis showed no changes between negative, and *anmt-1* (P = 0.498) treated worms, but movement was reduced in *fce-1* (P = 0.007). For all strains three biologically independent repeats were examined. Results were analysed by using Kaplan–Meier curves, with Bonferroni-corrected multiple comparisons and Welch's t-test for the movement AUC analysis. ** P = < 0.01 and ns where * P = > 0.05.

5.4 Discussion

The genes involved in the ageing process and senescence are regulated at least in part by a wide variety of microRNAs (miRNAs). In this chapter, three miRNAs (miR-15b-5p, miR-92a-3p, and miR-125a-3p), previously determined to be associated with senescence in human cells of multiple lineages and in blood isolated from old participants (Holly *et al.*, 2015), were assessed for functional roles in development of cellular senescence by targeted attenuation of their expression using miRNA mimics. Here, induction of miR-15b-5p level in late passage human primary dermal fibroblasts (NHDF) in *in vitro* cultured cells brought about a reduction in the senescent cell load of the culture, alter the proliferation index (Ki67) (figure, 5.1), and decreased the expression of several SASP factors. Attenuation of miR-92a-3p, and miR-125a-3p expression did not alter senescence kinetics in late passage primary dermal fibroblasts. Despite the effect on senescence phenotypes *in vitro*, RNAi gene knockdown of miR-15b-5p target genes did not yield any increase in lifespan or healthspan in a *C. elegans* model system. These data suggest that whilst miR-15b-5p may be involved in the establishment or maintenance of the senescent cell phenotype, this does not translate to increases in healthspan or lifespan when the expression of this miRNA target gene is manipulated in an *in vivo* systemic model.

MiR-15b has been previously reported to regulate several genes that are essential for development of ageing-related diseases and are involved in pathways that affect senescence (figure 5.5 and table 5.2) (Huang *et al.*, 2022; Kumari & Jat, 2021). These pathways include the FoxO signaling pathway, the p53 signaling pathway, the PI3K-Akt signaling pathway, the MAPK signaling pathway and the Ras signaling pathway (Morris *et al.*, 2015; Slack *et al.*, 2015). At normal conditions, suppression and silencing FoxOs promotes cellular growth (S. Du & Zheng, 2021). For example,

skeletal muscle proteins of old mice show a 25% drop in FoxO3 and an 18% reduction suggesting its roles in ageing (Furuyama *et al.*, 2002). Also, it has been shown that FoxO can regulate senescent cells through splicing factors, a key player in ageing mechanisms (Holly *et al.*, 2013; Latorre *et al.*, 2019; Lee *et al.*, 2020). miR-15b inhibits PI3K/AKT signalling pathway and promotes apoptosis of endothelial cell (Liu *et al.*, 2020). MKK4 (mitogen-activated protein kinase (MAPK) kinase 4) is downregulated by multiple miRNAs including miR-15b which results in p16 expression patterns and senescence phenotypes (Marasa *et al.*, 2009). In NHDF, I found reduction of senescent cells load, increase in ki67, and reduction in SASP factors. Controversy, Lang and colleagues showed miR-15b-5p negatively regulated *SIRT4* and upregulation of SIRT was associated with increase in SASP and ROS productions (Lang *et al.*, 2016). miR-15b-5p may have different roles based on cellular or tissue specific.

Senescence is a form of cell fate that function as stopping cancerous cells from progression. However, with ageing these senescent cells may convert to cancer or make other cells to senesce. Similarly, some genes may regulate miR-15b-5p plays a dual role by acting as proto-oncogene and tumor suppressor (Ghafouri-Fard *et al.*, 2022). Previous reports have shown that miR-15b-5p can both promote the cell growth and inhibit cellular proliferation (Chen *et al.*, 2018; Ghafouri-Fard *et al.*, 2022; Sun *et al.*, 2017; Tölle, Buckendahl, & Jung, 2019; Zhao *et al.*, 2017). Both the mRNA and protein levels of HPSE2 (heparanase-2) expression were considerably raised in breast tumor cells *in vitro* and *in vivo* using a xenograft model in mice when miR-15b-5p was knocked down (B. Wu et al., 2020). Furthermore, they demonstrated that knocking down miR-15b-5p greatly decreased tumour development in a mouse xenograft model. (Huang *et al.*, 2022; Kumari & Jat, 2021).

Previous research has linked miR-92a to the process of healthy ageing (Holly et al., 2015; H. Zhang et al., 2015); but mechanisms by which miR-92a may influence ageing have yet to be thoroughly investigated. In my experiments, miR-92a-3p did not show a significant effect on cellular kinetics, indicating that this miRNA may not be important in fibroblast senescence. However, miR-92a-3p has been described to play roles in several ageing-related diseases such as colorectal cancer (Yamada & Senda, 2021), hepatocellular carcinoma (Sorop *et al.*, 2020; Wang *et al.*, 2021), and breast cancer cells (Jinghua *et al.*, 2021). Also, in mice, exosomal miR-92a-3p was found to control the growth and degradation of cartilage through inhibition of *Wnt5a*. The substantial damage to the knee articular cartilage shown in the osteoarthritis mouse model was mitigated by inducing miR-92a-3p at an early stage of the disease (Mao *et al.*, 2018). Furthermore, miR-92a-3p suppressed *ATG-4A* expression in cardiomyocytes and improved rejuvenation *in vitro* (Xia *et al.*, 2020). miR-92a have been shown previously to be an effector in the wound healing process. On the contrary, inhibition of miR-92a-3p has been demonstrated to beneficially impact heart health, the development of new blood vessels, and enhanced blood circulation when administered intravenously (Abplanalp *et al.*, 2020). Although this miRNA showed no effects on senescence in dermal fibroblasts, it may play important roles in other cell types.

In late NHDF cells, induction of miR-125a-3p expression does not show any significant alterations in the senescent markers and phenotypes. Nanostring analysis of isolated miRNAs from young and senescent human lung diploid fibroblasts HFL-1 showed miR-125a-3p was significantly up-regulated (Markopoulos *et al.*, 2017). In hepatocellular carcinoma (HCC), miR-125a-3p and miR-125b was found to suppress *Sirtuin7* an oncogenic potential in HCC (J. K. Kim et al., 2013). Also, miR-125a-3p has been shown to play role in several ARDs including ovarian cancer (Ramirez *et al.*,

2022). multiple myeloma (Chu *et al.*, 2022), Heart failure (HF) (Dimitrakopoulou *et al.*, 2015; Ma *et al.*, 2021).

The invention of NemaLife microfluidic chips has overcome many limitations previously known to be challenging in using microfluidic chips in ageing studies (Rahman *et al.*, 2020). The limitations of previous methods include difficulties in consistent feeding regimes, transferring adults of *C. elegans*, and removing progeny to allow study ageing progression of adult worms which is better and easy to manipulate with NemaLife. Furthermore, NemaLife microfluidic chips consist of a micropillar structure that support worms to move normally, crawling, in case of washing steps to remove progeny and addition of food. However, as *C. elegans* are fed on bacterial culture, colonies could build up with time and that leading to stuck of progeny during the washing steps.

The gene *fce-1/ZMPSTE24* is known to be involved in progeroid syndromes (Spear *et al.*, 2018). Zinc metalloproteinase (*ZMPSTE24*) cleaves *LAMIN A*, an important element of nuclear membrane. The premature ageing condition Hutchinson-Gilford progeria syndrome is caused by the inability to cleave a shortened version of prelamin A, often known as progerin (Barrowman *et al.*, 2012; Messner *et al.*, 2020; Rivera-Torres *et al.*, 2013; Spear *et al.*, 2018). It is worth noting that *fce-1* knocked down *C. elegans* showed no changes in the lifespan of worms compared to control but had increased the production of progeny (Data is not shown). This was observed when the microfluidic chips were washed daily and despite of multiple washes, several progeny remained in the chips probably due to overproduction and aggregation of progeny. It would be interesting to examine the influence of gain-of-function and/or loss-of-function of the *fce-1* gene on ageing in future research. In human primary fibroblast cells and blood samples, the *fce-1* orthologue, *ZMPSTE24*, was downregulated in

young individuals and overexpressed in old people (Holly *et al.*, 2015). It remains unknown whether the *fce-1* gene has an antagonistic effect in worms. This gene probably may influence reproduction in the early years and may be more detrimental late in the life of *C. elegans*.

In conclusion, miR-15b-5p may possess an interesting regulatory role in senescence and its associated phenotypes. Here, we showed that miR-15b-5p reduced the senescent cells load *in vitro* in the primary human dermal fibroblast cells. Induction of miR-15b-5p expression led to reduction in multiple SASP factors which are known to act negatively on neighbouring cells in tissues through chronic production by senescent cells. miR-15b-5p may have a senomorphic effect on NHDF senescent cells. More studies are warranted to investigate the role of this miRNA in systematic ageing. These findings highlight the significance of miRNAs in the control of senescence; however, to show that attenuation of the targets of miR-15b-5p *ZMPSTE24/fce-1* may be more detrimental to the healthspan than beneficial.

Chapter 6
Discussion and Conclusion

6.1 Summary of thesis

Ageing is a complicated, multifactorial process that is influenced by a wide variety of factors. Age is known to be the most significant risk factor for many chronic diseases collectively known as ageing-related diseases. Given this, as the population ages, the number of morbidities and their social and economic effects will rise. The development of solutions to increase healthspan and reduce the negative consequences of age-related illness will depend on our ability to understand the interaction between these processes and their management. Cellular senescence is one of the hallmarks of ageing and plays an important role in the ageing process.

The process of cellular senescence, which is defined by irreversible growth arrest, has emerged as a key target for the treatment of a wide range of human disorders associated with ageing. Through autocrine and paracrine effectors, the SASP may act as a source of pro-inflammatory cytokines in surrounding tissues and organs. Several substances released by senescent cells can worsen the cellular microenvironment, encouraging tumour growth and aggravating disorders associated with ageing. Targeting and removing cellular senescence or SASP has received a great deal of interest due to its growing importance in the pathophysiology of age-related diseases.

The goal of the study was to find miRNAs that were not only associated with senescence but also potentially causal in human primary cultured cells *in vitro*. Then, to further assess these findings, I tried to validate the effects on ageing in a model organism after manipulation of the top dysregulated target genes of miRNAs. This may highlight the potential roles of these miRNAs and could influence longevity and healthspan in the ageing process.

6.2 Data chapters summaries

6.2.1 Chapter 3: miR-361-5p: A resveratrol-responsive miRNA associated with rescue from cellular senescence

6.2.1.1 Summary

I aimed to identify and assess miRNAs that were not only related to senescence but also to the response to senescence-reversing small molecules in human primary endothelial cells, a cell type that is involved in many human diseases. Senescence profiles alone reflect both the causes and consequences of senescence, while other miRNAs not implicated in senescence reversal may be changed by pharmacological therapy. A comparison of the two datasets, on the other hand, may help in the determination of miRNAs with a possible impact on senescence. In all datasets, three miRNAs (miR-5787, miR-3665, and miR-361-5p) showed dysregulated expression, although only one, miR-361-5p, showed opposite directionality. The pathways of protein transport, localization, and catabolism, as well as RNA metabolism and splicing, are concentrated among the targets of this miRNA, as shown by a GO keyword analysis. Lastly, changing the levels of miR-361-5p with a miRNA mimic for miR-361-5p led to a 24% drop in the number of senescent cells in late passage primary endothelial cells. I found no variations in cell count between the scramble-treated control and the mimic-treated cells, suggesting that the decrease in senescent cells was not caused by senolysis. This research supports earlier results that splicing dysregulation causes senescence rather than senolysis. The findings indicate that miR-361-5p may play a role in the onset of senescence in human primary endothelial cells.

Limitations to this chapter were that the findings were based on only three biological independently cultured cells *in vitro*, which may be affected by other stressors. Also, measurements were only carried out for genes at the mRNA level, and not at other posttranscriptional and posttranslational regulation steps.

6.2.1.2 Novelty of the finding

To the best of my knowledge, this miRNA, miR-361-5p, has been shown, here, for the first time to play a responsive role in rescuing human primary endothelial senescent cells *in vitro*. The purpose of this data is to show for the first time the entire miRNAome in RSV-treated cells and to identify a candidate miRNA with a causal potential role in reversing senescent cells. My data analysis suggested that miR-361-5p may be involved in attenuation of the senescence phenotype; however, it is unlikely to be a useful therapeutic candidate since its target mRNAs include those required for normal cellular function.

6.2.1.3 Future work

miR-361-5p has been shown here to reduce the senescent cell load in primary human endothelial cells. However, targets of miRNAs included many essential genes for normal growth of cells. Therefore, finding out the specific targets responsible for the senescence phenotype and how the manipulation of these targets might be targeted to attenuate senescence would be valuable.

6.2.2 Chapter 4: Determination of the role of miR-361-5p target genes in cellular senescence phenotypes *in vitro*, and on ageing and healthspan measures in *C. elegans*

6.2.2.1 Summary

miR-361-5p may reverse or reduce the load of senescent cells in an *in vitro* endothelial cell culture. Several of these genes targeted by miR-361-5p and are key players in the ageing process (Holly *et al.*, 2013; Latorre *et al.*, 2019; Latorre *et al.*, 2018; Lee *et al.*, 2019). It has been shown that reducing senescent cells benefits animals and reduces age-related disorders such as cancer and neurological diseases (Amor *et al.*, 2020; Baker *et al.*, 2016; Barnes *et al.*, 2019). In this chapter, I initially identified differentially regulated in senescence miR-361-5p targets by comparing the whole-transcriptome of early passage dividing versus late passage non-dividing endothelial *in vitro* cultured cells. This could aid in the identification of genes that may be causally involved in senescence phenotypes. To study their effect *in vivo*, I investigated how target gene knockdown affected lifespan and ageing phenotypes in the invertebrate animal model system, *C. elegans*. I identified 839 validated miR-361-5p target genes, of which 32 demonstrated evidence of altered expression in senescent human primary endothelial cells. The evaluation of the impact on lifespan and movement characteristics in *C. elegans* upon miR-361-5p target knockdown took place through the utilization of the Ahringer RNAi library (Kamath & Ahringer, 2003). There were *C. elegans* orthologues for 16 verified miR-361-5p target genes, and 9 of these genes decreased longevity and 12 of these genes had an impact on healthspan after reducing the expression of these genes. This suggests that, although miR-361-5p may have a role in the onset or maintenance of cellular senescence in human primary endothelial cells, knocking

down its target genes globally in *C. elegans* may be more deleterious than favorable *in vivo*.

The limitation of this study include that only investigated loss-of-function analysis similar to the function of miRNA; however, gain-of-function analysis might cause opposite effect on *C. elegans* ageing phenotypes as well. Since *C. elegans* does not possess replicative senescence as their cells are terminally differentiated unlike human primary endothelial cells which also lacked in *C. elegans*. However, it is nonetheless subject to other types of senescence. Studying the effect of loss-of-function in other animal models that their cells share similar fate as human could give more useful findings.

6.2.2.2 Novelty of the finding

While hundreds of genes in *C. elegans* have previously been associated with longevity, only a small number of miRNAs are known to regulate these genes and have functions in key ageing pathways (Elder & Pasquinelli, 2022). In this chapter, I reported that 12 of the 32 miR-361-5p target genes that display dysregulated expression in senescent human primary endothelial cells have detrimental effects on the lifespan and survival of *C. elegans* when RNAi was used. Given that, it may be concluded that although miR-361-5p is involved in the establishment or maintenance of the senescent cell phenotype, it is also essential for organismal growth and function.

6.2.2.3 Future work

Through a loss-of-function study, I discovered 12 genes in *C. elegans* that have a detrimental impact on longevity and/or healthspan. Many of these genes have yet to

be thoroughly investigated to determine how they may impact *C. elegans* health and movement. Using CRISPR/Cas9 activators to induce the expression of endogenous genes of interest is one method of investigating the role of genes in ageing phenotypes. It would be interesting to see how increasing the expression of these genes affects the processes of ageing and longevity in *C. elegans*. In *C. elegans*, the distribution of RNAi using bacterial feeding method is known to spread equally in the worm (Zhuang and Hunter 2012; Watts *et al.*, 2020). However, to reveal which cells are affected by this knock down, further research is needed.

6.2.3 Chapter 5: miR-15b-5p, miR-92a-3p, and miR-125a-3p miRNAs may have senescence maintenance roles

6.2.3.1 Summary

A diverse set of microRNAs (miRNAs) regulates the genes that are involved in the ageing and senescence processes. Three miRNAs (miR-15b-5p, miR-92a-3p, and miR-125a-3p) previously identified (Holly *et al.*, 2015) to be linked with senescence in human cells of diverse lineages and blood isolated from elderly, were investigated in this chapter. They were evaluated for functional contribution to the growth of cellular senescence by utilising miRNA mimics and inhibitors. By modulating miRNA levels in primary human fibroblasts, I investigated the roles of miR-15b-5p, miR-92a-3p, and miR-125a-3p on senescence phenotypes. Initially, the senescence-associated beta galactosidase assay (SA-β-Gal) (senescence), Ki67 (proliferation index), γH2AX (DNA damage marker), and TUNEL assay (apoptosis assay) were used to quantify senescent cell load. Senescence parameters were measured after miRNA knockdown or knock-in using miRNA inhibitors or mimics, depending on the directionality of the

change in senescence. Also, in senescent primary fibroblasts, the impact of siRNA-mediated suppression of the *INMT*, *LYST*, *LHFPL2*, and *ZMPSTE24* genes, which are known targets of miR-15b-5p, miR-92a-3p, or miR-125a-3p, was also studied. The expression levels of verified miRNA target genes were also measured. Finally, longevity and healthspan were evaluated in an invertebrate animal model, *C. elegans*, after knocking down the orthologues of the *ZMPSTE24* and *INMT* genes, *fce-1* and *anmt*, respectively, using the source Ahringer RNAi library. (Kamath & Ahringer, 2003).

Elevation of miR-15b-5p expression in late passage human primary dermal fibroblast (NHDF) cells cultured *in vitro* lowered senescent cell load, changed the proliferation index (Ki67), and decreased the expression of many SASP factors. Inhibition of miR-92a-3p and miR-125a-3p had no effects on senescence kinetics in late passage primary dermal fibroblasts. Also, RNAi gene suppression of miR-15b-5p target genes did not result in an increase in longevity or healthspan in a *C. elegans* model system, despite the influence on senescence symptoms *in vitro*. These findings suggest that whilst miR-15b-5p plays a role in the emergence or maintenance of senescence in human cells, effects on lifespan in *C. elegans* are probably not mediated via *fce-1* or *anmt-3*. However, reducing the expression of *fce-1*, a validated target of miR-15b-5p, gene in an *in vivo* systemic model did not result in an increase in healthspan or longevity.

Limitation of this work include the fact that miR-15b-5p does not exist in *C. elegans* genome. However, I looked for the genes that previously validated targets of miR-15b-5p and were dysregulated in late passage fibroblasts. These genes may be responsible for the reduction in senescent cells load and SASP factors in human cells, but knocking down these genes resulted in negative effects on the movement of *C. elegans* with no changes on healthspan. Manipulation of this miRNA may be better to

be performed *in vivo* in animal model that shares similar miR-15b-5p sequence and targets such as mice.

6.2.3.2 Novelty of the finding

MiR-15b-5p, miR-92a-3p, and miR-125a-3p have previously been linked to ageing and found to be dysregulated in senescent human primary fibroblast cells and blood from elderly people (Holly *et al.*, 2015). Here, through gain and loss-of function analysis, I showed that dysregulated miR-15b-5p may contribute to the establishment or maintenance of senescence, whereas miR-92a-3p or miR-125a-3p may represent senescence-related effects. However, reducing the expression of the validated target gene of miR-15b-5p *ZMPSTE24/fce-1* in *C. elegans* negatively influenced ageing phenotypes.

6.2.3.3 Future work

Induction of miR-15b-5p in fibroblast shows promising results in reducing the senescent cell load and expression of the SASP factors. Reduction in SASP factors and no changes in cell count may indicate that this miRNA may function as a senomorphic agent in human cells, *in vitro*. Further *in vivo* investigations in a more conserved animal model to study the effects of inducing miR-15b-5p on ageing and lifespan might provide new insights into the processes that underpin the emergence of age-related pathologies.

6.3 Discussion of thesis

miRNAs are major players in controlling gene expression in mammals at all cellular levels, and they have necessary roles in the healthspan and lifespan of organisms.

This thesis attempted to identify miRNAs that control, maintain, or reverse cellular senescence in primary fibroblast and endothelial cells as *in vitro* models and in *C. elegans* as an *in vivo* model organism. I identified miR-361-5p as a potential agent to attenuate senescence in human primary endothelial senescent cells. Similar effects were noted for miR-15b-5p in senescent human primary fibroblasts. In *C. elegans*, the top hits of validated targets and dysregulated genes were investigated to determine their impact on ageing phenotypes and survival. Multiple targets were identified to negatively affect the healthspan and lifespan of *C. elegans* which may mean that these miRNAs regulate crucial genes in the growth and development of worms.

These findings identify new miRNA players in senescence in human cells cultured *in vitro*. They show that miR-361-5p is highly expressed in reversed senescent cells where senescence phenotypes have been attenuated by exposure to the senotherapeutic resveratrol. I showed that miR-361-5p is able to reduce senescent cell load *in vitro* in human primary endothelial cells when cells are transfected with the miRNA mimics. Also, miR-15b-5p showed a reduction in senescent cell load and several SASP factors, indicating its potential regulatory role in senescence. However, RNAi that was used against dysregulated genes targeted by these miRNAs did not show positive effects on lifespan or healthspan; indeed, they showed more detrimental effects in *C. elegans*. These data suggest that these miRNAs are also regulating genes that are necessary for the normal development of worms.

This thesis demonstrates how miRNAs may regulate senescence *in vitro* and showed how the targeted genes are necessary for the normal growth, healthspan, and lifespan of *C. elegans*. Cellular senescence is defined primarily by a permanent inhibition of proliferation and secretion of SASP factors. Senescence is triggered by a variety of stimuli, including shortening in telomere length, oncogene activation, and DNA

damage among others. Although senescence contributes positively to a variety of physiological processes, including embryonic development, wound healing and tumour suppression, age-related accumulation of senescent cells is also associated with disease in later life. Elimination of senescent cells from tissue and organs has been shown to prolong healthy lifespan and ameliorate a variety of age-related phenomena. The p53*/CDKN1A*(p21) and *CDKN2A*(p16)/RB pathways and the SASP are essential for the development and maintenance of senescence. MiRNAs may influence ageing through, but not limited to, regulation of factors within the fundamental senescence pathways p16/p21, p53/pRB, and SASP.

Multiple miRNAs have also been identified as having interactions with genes in signaling cascades implicated in ageing. A few miRNAs have been demonstrated to influence lifespan and healthspan through targeting crucial genes in pathways known to influence ageing, such as the insulin/insulin-like growth factor signaling (IIS), Sirtuins and mechanistic target of rapamycin (mTOR) pathways (Pan & Finkel, 2017). Several of these miRNAs and their activities have been shown to be highly conserved in organisms (Dimmeler & Nicotera, 2013; Kinser & Pincus, 2020), showing a critical involvement in the modulation of these mechanisms. Numerous pathologies, both age-related and otherwise, have been reported to be affected by miRNAs (Piletič & Kunej, 2016; Sharma & Lu, 2018; Stolzenburg & Harris, 2018; Williams *et al.*, 2017), such as the premature ageing diseases Hutchinson-Gilford progeria (Frankel *et al.*, 2018) and Werner syndrome, where some miRNAs have been demonstrated to influence the expression of key genes in these diseases (Dallaire *et al.*, 2012). Furthermore, Harries (Harries, 2014) and Caravia and Lopez-Otin (Caravia & López-Otín, 2015) articles discussed miRNAs that are now known to be involved in the ageing processes. Several of the designated miRNAs may regulate targets linked to more than one

hallmark of ageing, presenting the prospect that networks of miRNAs may collaborate to give precise control over several components of the ageing process at the same time.

MiRNAs are markedly related to ageing and lifespan as illustrated in the previous and presented studies in this thesis. Here, the thesis showed that miR-361-5p, miR-15b-5p and their targets, for the first time, are linked to attenuation of the senescence phenotype in human primary cells cultured *in vitro*. Although longevity and lifespan experiments did not show beneficial effects upon reducing the expression of genes targeted by these miRNAs in *C. elegans*, further studies may be useful to identify genes that cause the reversal of senescent *in vitro*. These could lead to identification of the exact genes responsible for the observed phenotypes and that would be beneficial in reducing senescence and senescence phenotypes.

Weaknesses of these data include that I only used a single cell type for each analysis separately, primary fibroblast cells and primary endothelial cells, and they were isolated from different participants (PromoCell). Although I did not validate each gene empirically by method such as dual luciferase reporter system, I used my complete transcriptomic data that generated from proliferating and non proliferating fibroblast and endothelial cells to validate bioinformatically predicted targets of these miRNAs. *C. elegans* is a useful but imperfect model in that it does not undergo replicative senescence as our cells do, since it is post-mitotic. Also, in this study I assessed only in worms treated from L1 towards adulthood, while the effects of some genes may be in the early life of *C. elegans*.

Another limitation in this thesis is that the lack of using early passaging cells as a reference to the reversal senescent cells in resveratrol or miR treatment. This was not

performed here due to challenges in assessment of senescent cells in the early passage culturing cells. Early passage culture may give false positive SA-β-Gal cells due to clump of cells.

6.4 Future work

In this thesis, I found that two miRNAs have roles in reversing senescence phenotypes in primary human endothelial and normal human dermal fibroblast cells *in vitro*. However, when manipulating the validated target genes of miR-361-5p and miR-15b-5p *in vivo*, more damaging effects were observed on the model system, *C. elegans*. These data were generated from a single cell type and from one donor; it would be valuable to validate them from several participants of the same cell type. Studying the expression of these miRNAs in tissues or blood samples from young, old, and centenarian people will validate if these miRNAs are playing roles in senescence and ageing. This could be performed using a human blood cohort (InCHIANTI) or another accessible cohort for examining the expression of these miRNAs and their targets and how they might affect senescence markers and pathways. Additionally, it would be useful to validate the effect of induction of these miRNAs *in vivo* in animals that express these miRNAs and share similar targeted genes as mice. MiRNAs may target genes with opposite effects, and it could be a proto-oncogene or suppressor molecule depending on their targets. Thus, studying the induction of miR-361-5p and miR-15b-5p *in vivo* in cell-specific ways by testing their roles on lifespan and healthspan *in vivo* would be beneficial and could lead to the identification of precise targeted genes that are responsible for senescent cell reversal.

Three-dimensional tissue culture provides many benefits over typical two-dimensional cell culture, which was employed in this thesis. Materials used in 2D *in vitro* cell culture put other stresses on the cells such as plastics and nutrients which may results in

variability in results. However, 3D tissue culture is an innovative method with several applications. 3D culture resembles the natural environment of cells in the human body more precisely. To further evaluate the impact of the examined miRs in this thesis on rescuing senescent cells and other ageing parameters, they might be manipulated and analyzed in 3D culture. This will reduce the variability of SA-β-Gal, Ki67, and γH2AX positive cells. Also, I investigated the targets of miR-361-5p and miR-15b-5p in *C. elegans* and not the miRs themselves due to the lack of orthologs in this model which is a limitation. However, this miRs could be studied in *in vivo* models such as mice which has orthologs to these miRs and reveal the effects on ageing in terms of healthspan and lifespan.

6.5 Conclusion

This thesis explores the miRNAs that may paly causal roles in driving senescent cells in HAoECs and NHDF and investigates their targets genes on influencing longevity and healthspan in *C. elegans*. Additional *in vivo* experiments using animal models expressing miR-361-5p and/or miR-15b-5p should be conducted to evaluate their involvement in senescence processes via induction or reduction of miRNA expression. The research may highlight some miRNAs that have important roles in the maintenance of senescent cells, which accumulate in tissues as we age and disrupt the normal function of organs and worsen the age-related diseases. MiRNAs are a master regulator of the human genome and finding miRNAs that regulate, drive or reverse senescent cells could become future senotherapeutic agents to treat ageing-related diseases and improve human healthy ageing.

References

Abplanalp, W. T., Fischer, A., John, D., Zeiher, A. M., Gosgnach, W., Darville, H., … Dimmeler, S. (2020). Efficiency and Target Derepression of Anti-miR-92a: Results of a First in Human Study. *Nucleic Acid Therapeutics*, *30*(6), 335–345. https://doi.org/10.1089/nat.2020.0871

Acosta, Juan C., O'Loghlen, A., Banito, A., Guijarro, M. V., Augert, A., Raguz, S., … Gil, J. (2008). Chemokine Signaling via the CXCR2 Receptor Reinforces Senescence. *Cell*, *133*(6), 1006–1018. https://doi.org/10.1016/j.cell.2008.03.038

Acosta, Juan Carlos, Banito, A., Wuestefeld, T., Georgilis, A., Janich, P., Morton, J. P., … Gil, J. (2013). A complex secretory program orchestrated by the inflammasome controls paracrine senescence. *Nature Cell Biology*, *15*(8), 978–990. https://doi.org/10.1038/ncb2784

Aebersold, R., Agar, J. N., Amster, I. J., Baker, M. S., Bertozzi, C. R., Boja, E. S., … Zhang, B. (2018). How many human proteoforms are there? *Nature Chemical Biology*, *14*(3), 206–214. https://doi.org/10.1038/nchembio.2576

Ameling, S., Kacprowski, T., Chilukoti, R. K., Malsch, C., Liebscher, V., Suhre, K., … Völker, U. (2015). Associations of circulating plasma microRNAs with age, body mass index and sex in a population-based study. *BMC Medical Genomics*, *8*(1), 61. https://doi.org/10.1186/s12920-015-0136-7

Amor, C., Feucht, J., Leibold, J., Ho, Y. J., Zhu, C., Alonso-Curbelo, D., … Lowe, S. W. (2020). Senolytic CAR T cells reverse senescence-associated pathologies. *Nature*, *583*(7814), 127–132. https://doi.org/10.1038/s41586-020-2403-9

Armanios, M., de Cabo, R., Mannick, J., Partridge, L., Van Deursen, J., & Villeda, S. (2015, December). Translational strategies in aging and age-related disease. *Nature Medicine*. United States. https://doi.org/10.1038/nm.4004

Aubert, G., & Lansdorp, P. M. (2008). Telomeres and aging. *Physiological Reviews*, *88*(2), 557–579. https://doi.org/10.1152/physrev.00026.2007

Austad, S. N., & Hoffman, J. M. (2018). Is antagonistic pleiotropy ubiquitous in aging biology? *Evolution, Medicine and Public Health*, *2018*(1), 287–294. https://doi.org/10.1093/emph/eoy033

Baar, M. P., Brandt, R. M. C. C., Putavet, D. A., Klein, J. D. D. D., Derks, K. W. J. J., Bourgeois, B. R. M. M., … de Keizer, P. L. J. J. (2017). Targeted Apoptosis of Senescent Cells Restores Tissue Homeostasis in Response to Chemotoxicity and Aging. *Cell*, *169*(1), 132-147.e16. https://doi.org/10.1016/j.cell.2017.02.031

Baker, D. J., Childs, B. G., Durik, M., Wijers, M. E., Sieben, C. J., Zhong, J., … van Deursen, J. M. (2016). Naturally occurring p16(Ink4a)-positive cells shorten healthy lifespan. *Nature*, *530*(7589), 184–189. https://doi.org/10.1038/nature16932

Baker, D. J., Childs, B. G., Durik, M., Wijers, M. E., Sieben, C. J., Zhong, J., … Van Deursen, J. M. (2016). Naturally occurring p16 Ink4a-positive cells shorten healthy lifespan. *Nature*, *530*(7589), 184–189. https://doi.org/10.1038/nature16932

Baker, D. J., Dawlaty, M. M., Wijshake, T., Jeganathan, K. B., Malureanu, L., Van Ree, J. H., … Van Deursen, J. M. (2013). Increased expression of BubR1 protects against aneuploidy and cancer and extends healthy lifespan. *Nature Cell Biology*, *15*(1), 96–102. https://doi.org/10.1038/ncb2643

Baker, D. J., Wijshake, T., Tchkonia, T., Lebrasseur, N. K., Childs, B. G., Van De Sluis, B., … Van Deursen, J. M. (2011). Clearance of p16 Ink4a-positive senescent cells delays ageing-associated disorders. *Nature*, *479*(7372), 232–236. https://doi.org/10.1038/nature10600

Barnes, P. J., Baker, J., & Donnelly, L. E. (2019). Cellular Senescence as a Mechanism and

Target in Chronic Lung Diseases. *American Journal of Respiratory and Critical Care Medicine*, *200*(5), 556–564. https://doi.org/10.1164/rccm.201810-1975TR

Barresi, R., & Campbell, K. P. (2006). Dystroglycan: From biosynthesis to pathogenesis of human disease. *Journal of Cell Science*, *119*(2), 199–207. https://doi.org/10.1242/jcs.02814

Barrowman, J., Wiley, P. A., Hudon-Miller, S. E., Hrycyna, C. A., & Michaelis, S. (2012). Human ZMPSTE24 disease mutations: Residual proteolytic activity correlates with disease severity. *Human Molecular Genetics*, *21*(18), 4084–4093. https://doi.org/10.1093/hmg/dds233

Bartel, D. P. (2004). MicroRNAs: Genomics, Biogenesis, Mechanism, and Function. *Cell*, *116*(2), 281–297. https://doi.org/10.1016/S0092-8674(04)00045-5

Baur, J. A., Pearson, K. J., Price, N. L., Jamieson, H. A., Lerin, C., Kalra, A., … Sinclair, D. A. (2006). Resveratrol improves health and survival of mice on a high-calorie diet. *Nature*, *444*(7117), 337–342. https://doi.org/10.1038/nature05354

Baur, J. A., & Sinclair, D. A. (2006). Therapeutic potential of resveratrol: the in vivo evidence. *Nature Reviews. Drug Discovery*, *5*(6), 493–506. https://doi.org/10.1038/nrd2060

Bautista-Sánchez, D., Arriaga-Canon, C., Pedroza-Torres, A., De La Rosa-Velázquez, I. A., González-Barrios, R., Contreras-Espinosa, L., … Herrera, L. A. (2020). The Promising Role of miR-21 as a Cancer Biomarker and Its Importance in RNA-Based Therapeutics. *Molecular Therapy - Nucleic Acids*, *20*, 409–420. https://doi.org/10.1016/j.omtn.2020.03.003

Beauséjour, C. M., Krtolica, A., Galimi, F., Narita, M., Lowe, S. W., Yaswen, P., & Campisi, J. (2003). Reversal of human cellular senescence: roles of the p53 and p16 pathways. *The*

EMBO Journal, *22*(16), 4212–4222. https://doi.org/10.1093/emboj/cdg417

Ben-Zvi, A., Miller, E. A., & Morimoto, R. I. (2009). Collapse of proteostasis represents an early molecular event in Caenorhabditis elegans aging. *Proceedings of the National Academy of Sciences of the United States of America*, *106*(35), 14914–14919. https://doi.org/10.1073/pnas.0902882106

Benedetto, A., & Gems, D. (2019). Autophagy promotes visceral aging in wild-type C. elegans. *Autophagy*, *15*(4), 731–732. https://doi.org/10.1080/15548627.2019.1569919

Bernardes de Jesus, B., Vera, E., Schneeberger, K., Tejera, A. M., Ayuso, E., Bosch, F., & Blasco, M. A. (2012). Telomerase gene therapy in adult and old mice delays aging and increases longevity without increasing cancer. *EMBO Molecular Medicine*, *4*(8), 691–704. https://doi.org/10.1002/emmm.201200245

Boehm, M., & Slack, F. (2005). Physiology: A developmental timing microRNA and its target regulate life span in C. elegans. *Science*, *310*(5756), 1954–1957. https://doi.org/10.1126/science.1115596

Borja-Gonzalez, M., Casas-Martinez, J. C., McDonagh, B., & Goljanek-Whysall, K. (2020). Inflamma-MiR-21 negatively regulates myogenesis during ageing. *Antioxidants*, *9*(4). https://doi.org/10.3390/antiox9040345

Borodkina, A. V., Deryabin, P. I., Giukova, A. A., & Nikolsky, N. N. (2018). “Social life” of senescent cells: What is SASP and why study it? *Acta Naturae*, *10*(1), 4–14. https://doi.org/10.32607/20758251-2018-10-1-4-14

Boujemaa-Paterski, R., Martins, B., Eibauer, M., Beales, C. T., Geiger, B., & Medalia, O. (2020). Talin-activated vinculin interacts with branched actin networks to initiate bundles. *ELife*, *9*, 1–26. https://doi.org/10.7554/eLife.53990

Bramwell, L. R., & Harries, L. W. (2021). Targeting Alternative Splicing for Reversal of Cellular Senescence in the Context of Aesthetic Aging. *Plastic and Reconstructive Surgery*, *147*(1 2), 25S-32S. https://doi.org/10.1097/PRS.0000000000007618

Brenner, S. (1974). The genetics of Caenorhabditis elegans. *Genetics*, *77*(1), 71–94.

Bronze-Da-Rocha, E. (2014). MicroRNAs expression profiles in cardiovascular diseases. *BioMed Research International*, *2014*, 985408. https://doi.org/10.1155/2014/985408

Brown, J. P., Wei, W., & Sedivy, J. M. (1997). Bypass of senescenoe after disruption of p21(CIP1)/(WAF1) gene in normal diploid human fibroblasts. *Science*, *277*(5327), 831–834. https://doi.org/10.1126/science.277.5327.831

Bueno, M. J., & Malumbres, M. (2011). MicroRNAs and the cell cycle. *Biochimica et Biophysica Acta - Molecular Basis of Disease*, *1812*(5), 592–601. https://doi.org/10.1016/j.bbadis.2011.02.002

Bussian, T. J., Aziz, A., Meyer, C. F., Swenson, B. L., van Deursen, J. M., & Baker, D. J. (2018). Clearance of senescent glial cells prevents tau-dependent pathology and cognitive decline. *Nature*, *562*(7728), 578–582. https://doi.org/10.1038/s41586-018-0543-y

Calin, G. A., Dumitru, C. D., Shimizu, M., Bichi, R., Zupo, S., Noch, E., … Croce, C. M. (2002). Frequent deletions and down-regulation of micro-RNA genes miR15 and miR16 at 13q14 in chronic lymphocytic leukemia. *Proceedings of the National Academy of Sciences of the United States of America*, *99*(24), 15524–15529. https://doi.org/10.1073/pnas.242606799

Campisi, J. (2005). Senescent cells, tumor suppression, and organismal aging: Good citizens, bad neighbors. *Cell*, *120*(4), 513–522. https://doi.org/10.1016/j.cell.2005.02.003

Campisi, J., Kapahi, P., Lithgow, G. J., Melov, S., Newman, J. C., & Verdin, E. (2019). From discoveries in ageing research to therapeutics for healthy ageing. *Nature*, *571*(7764), 183–

192. https://doi.org/10.1038/s41586-019-1365-2

Caravia, X. M., & López-Otín, C. (2015). Regulatory roles of miRNAs in aging. *Advances in Experimental Medicine and Biology*, *887*, 213–230. https://doi.org/10.1007/978-3-319-22380-3_11

Cartegni, L., Chew, S. L., & Krainer, A. R. (2002). Listening to silence and understanding nonsense: Exonic mutations that affect splicing. *Nature Reviews Genetics*, *3*(4), 285–298. https://doi.org/10.1038/nrg775

Chakraborty, C., Sharma, A. R., Sharma, G., Doss, C. G. P., & Lee, S. S. (2017). Therapeutic miRNA and siRNA: Moving from Bench to Clinic as Next Generation Medicine. *Molecular Therapy - Nucleic Acids*, *8*, 132–143. https://doi.org/10.1016/j.omtn.2017.06.005

Chambers, C. R., Ritchie, S., Pereira, B. A., & Timpson, P. (2021). Overcoming the senescence-associated secretory phenotype (SASP): a complex mechanism of resistance in the treatment of cancer. *Molecular Oncology*, *15*(12), 3242–3255. https://doi.org/10.1002/1878-0261.13042

Chang, J., Wang, Y., Shao, L., Laberge, R. M., Demaria, M., Campisi, J., … Zhou, D. (2016). Clearance of senescent cells by ABT263 rejuvenates aged hematopoietic stem cells in mice. *Nature Medicine*, *22*(1), 78–83. https://doi.org/10.1038/nm.4010

Chen, E. Y., Tan, C. M., Kou, Y., Duan, Q., Wang, Z., Meirelles, G. V., … Ma'ayan, A. (2013). Enrichr: Interactive and collaborative HTML5 gene list enrichment analysis tool. *BMC Bioinformatics*, *14*(1), 1–14. https://doi.org/10.1186/1471-2105-14-128

Chen, R., Sheng, L., Zhang, H. J., Ji, M., & Qian, W. Q. (2018). miR-15b-5p facilitates the tumorigenicity by targeting RECK and predicts tumour recurrence in prostate cancer. *Journal of Cellular and Molecular Medicine*, *22*(3), 1855–1863.

https://doi.org/10.1111/jcmm.13469

Chen, Y. L., Sheu, J. J., Sun, C. K., Huang, T. H., Lin, Y. P., & Yip, H. K. (2020). MicroRNA-214 modulates the senescence of vascular smooth muscle cells in carotid artery stenosis. *Molecular Medicine*, *26*(1), 46. https://doi.org/10.1186/s10020-020-00167-1

Chendrimada, T. P., Gregory, R. I., Kumaraswamy, E., Norman, J., Cooch, N., Nishikura, K., & Shiekhattar, R. (2005). TRBP recruits the Dicer complex to Ago2 for microRNA processing and gene silencing. *Nature*, *436*(7051), 740–744. https://doi.org/10.1038/nature03868

Childs, B. G., Gluscevic, M., Baker, D. J., Laberge, R. M., Marquess, D., Dananberg, J., & Van Deursen, J. M. (2017). Senescent cells: An emerging target for diseases of ageing. *Nature Reviews Drug Discovery*, *16*(10), 718–735. https://doi.org/10.1038/nrd.2017.116

Chin, L., Tam, A., Pomerantz, J., Wong, M., Holash, J., Bardeesy, N., … DePinho, R. A. (1999). Essential role for oncogenic ras in tumour maintenance. *Nature*, *400*(6743), 468–472. https://doi.org/10.1038/22788

Chiu, C. G., St.-Pierre, P., Nabi, I. R., & Wiseman, S. M. (2008). Autocrine motility factor receptor: A clinical review. *Expert Review of Anticancer Therapy*, *8*(2), 207–217. https://doi.org/10.1586/14737140.8.2.207

Choi, S., & Anderson, R. A. (2016). IQGAP1 is a phosphoinositide effector and kinase scaffold. *Advances in Biological Regulation*, *60*, 29–35. https://doi.org/10.1016/j.jbior.2015.10.004

Chu, M., Fan, Y., Wu, L., Ma, X., Sao, J., Yao, Y., … Zhang, C. (2022). Knockdown of lncRNA BDNF-AS inhibited the progression of multiple myeloma by targeting the miR-125a/b-5p-BCL2 axis. *Immunity and Ageing*, *19*(1), 3. https://doi.org/10.1186/s12979-021-00258-5

Chung, C. Z., Seidl, L. E., Mann, M. R., & Heinemann, I. U. (2017). Tipping the balance of RNA stability by 3′ editing of the transcriptome. *Biochimica et Biophysica Acta - General*

Subjects, *1861*(11), 2971–2979. https://doi.org/10.1016/j.bbagen.2017.05.003

Clancy, D. J., Gems, D., Harshman, L. G., Oldham, S., Stocker, H., Hafen, E., … Partridge, L. (2001). Extension of life-span by loss of CHICO, a Drosophila insulin receptor substrate protein. *Science*, *292*(5514), 104–106. https://doi.org/10.1126/science.1057991

Collado, M., Gil, J., Efeyan, A., Guerra, C., Schuhmacher, A. J., Barradas, M., … Serrano, M. (2005). Tumour biology: Senescence in premalignant tumours. *Nature*, *436*(7051), 642. https://doi.org/10.1038/436642a

Corsi, A. K., Wightman, B., & Chalfie, M. (2015, June). A transparent window into biology: A primer on Caenorhabditis elegans. *Genetics*. https://doi.org/10.1534/genetics.115.176099

Cui, W., Li, Y., Xu, K., Chen, G., Lu, X., Duan, Q., & Kang, Z. (2016). miR-361-5p inhibits hepatocellular carcinoma cell proliferation and invasion by targeting VEGFA. *Biochemical and Biophysical Research Communications*, *479*(4), 901–906. https://doi.org/10.1016/j.bbrc.2016.09.076

Curran, S. P., & Ruvkun, G. (2007). Lifespan regulation by evolutionarily conserved genes essential for viability. *PLoS Genetics*, *3*(4), e56. https://doi.org/10.1371/journal.pgen.0030056

d'Adda di Fagagna, F. (2008). Molecular mechanisms of cellular senescence. In *European Journal of Cancer Supplements* (Vol. 6, p. 35). https://doi.org/10.1016/s1359-6349(08)71309-0

D'Adda Di Fagagna, F., Reaper, P. M., Clay-Farrace, L., Fiegler, H., Carr, P., Von Zglinicki, T., … Jackson, S. P. (2003). A DNA damage checkpoint response in telomere-initiated senescence. *Nature*, *426*(6963), 194–198. https://doi.org/10.1038/nature02118

Dallaire, A., Garand, C., Paquet, E. R., Mitchell, S. J., de Cabo, R. D., Simard, M. J., & Lebel,

M. (2012). Down regulation of miR-124 in both Werner syndrome DNA helicase mutant mice and mutant Caenorhabditis elegans wrn-1 reveals the importance of this microRNA in accelerated aging. *Aging*, *4*(9), 636–647. https://doi.org/10.18632/aging.100489

Dart, A. E., Donnelly, S. K., Holden, D. W., Way, M., & Caron, E. (2012). Nck and Cdc42 co-operate to recruit N-WASP to promote FcγR-mediated phagocytosis. *Journal of Cell Science*, *125*(12), 2825–2830. https://doi.org/10.1242/jcs.106583

de Magalhães, J. P., & Passos, J. F. (2018). Stress, cell senescence and organismal ageing. *Mechanisms of Ageing and Development*, *170*(March 2017), 2–9. https://doi.org/10.1016/j.mad.2017.07.001

Demaria, M., Ohtani, N., Youssef, S. A., Rodier, F., Toussaint, W., Mitchell, J. R., … Campisi, J. (2014). An essential role for senescent cells in optimal wound healing through secretion of PDGF-AA. *Developmental Cell*, *31*(6), 722–733. https://doi.org/10.1016/j.devcel.2014.11.012

Dimitrakopoulou, K., Vrahatis, A. G., & Bezerianos, A. (2015). Integromics network meta-analysis on cardiac aging offers robust multi-layer modular signatures and reveals micronome synergism. *BMC Genomics*, *16*(1), 147. https://doi.org/10.1186/s12864-015-1256-3

Dimmeler, S., & Nicotera, P. (2013). MicroRNAs in age-related diseases. *EMBO Molecular Medicine*, *5*(2), 180–190. https://doi.org/10.1002/emmm.201201986

Dimri, G. P., Lee, X., Basile, G., Acosta, M., Scott, G., Roskelley, C., … Campisi, J. (1995). A biomarker that identifies senescent human cells in culture and in aging skin in vivo. *Proceedings of the National Academy of Sciences of the United States of America*, *92*(20), 9363–9367. https://doi.org/10.1073/pnas.92.20.9363

Dreisbach, C. (2022). *Introduction to genetics and genomics*. (The C. elegans Research Community, Ed.), *Fast Facts on Genetics and Genomics for Nurses: Practical Applications*. WormBook. https://doi.org/10.1895/wormbook.1.17.1

Du, J., Li, M., Huang, Q., Liu, W., Li, W. qun, Li, Y. jian, & Gong, Z. cheng. (2019). The critical role of microRNAs in stress response: Therapeutic prospect and limitation. *Pharmacological Research*, *142*, 294–302. https://doi.org/10.1016/j.phrs.2018.12.007

Du, S., & Zheng, H. (2021). Role of FoxO transcription factors in aging and age-related metabolic and neurodegenerative diseases. *Cell and Bioscience*, *11*(1), 188. https://doi.org/10.1186/s13578-021-00700-7

Dyson, N. (1998). The regulation of E2F by pRB-family proteins. *Genes and Development*, *12*(15), 2245–2262. https://doi.org/10.1101/gad.12.15.2245

Elder, C. R., & Pasquinelli, A. E. (2022). New Roles for MicroRNAs in Old Worms. *Frontiers in Aging*, *3*. https://doi.org/10.3389/fragi.2022.871226

Elfenbein, A., & Simons, M. (2013). Syndecan-4 signaling at a glance. *Journal of Cell Science*, *126*(17), 3799–3804. https://doi.org/10.1242/jcs.124636

Ellwood, R. A., Hewitt, J. E., Torregrossa, R., Philp, A. A. M., Hardee, J. P., Hughes, S., … Szewczyk, N. J. (2021). Mitochondrial hydrogen sulfide supplementation improves health in the C. elegans Duchenne muscular dystrophy model. *Proceedings of the National Academy of Sciences of the United States of America*, *118*(9). https://doi.org/10.1073/pnas.2018342118

Elsharawy, A., Keller, A., Flachsbart, F., Wendschlag, A., Jacobs, G., Kefer, N., … Nebel, A. (2012). Genome-wide miRNA signatures of human longevity. *Aging Cell*, *11*(4), 607–616. https://doi.org/10.1111/j.1474-9726.2012.00824.x

Feng, Y. H., & Tsao, C. J. (2016). Emerging role of microRNA-21 in cancer (Review). *Biomedical Reports*, *5*(4), 395–402. https://doi.org/10.3892/br.2016.747

Fire, A., Xu, S., Montgomery, M. K., Kostas, S. A., Driver, S. E., & Mello, C. C. (1998). Potent and specific genetic interference by double-stranded RNA in Caenorhabditis elegans. *Nature*, *391*(6669), 806–811. https://doi.org/10.1038/35888

Fischer, B., Metzger, M., Richardson, R., Knyphausen, P., Ramezani, T., Franzen, R., … Hammerschmidt, M. (2014). p53 and TAp63 Promote Keratinocyte Proliferation and Differentiation in Breeding Tubercles of the Zebrafish. *PLoS Genetics*, *10*(1), e1004048. https://doi.org/10.1371/journal.pgen.1004048

Fischer, M., & Müller, G. A. (2017). Cell cycle transcription control: DREAM/MuvB and RB-E2F complexes. *Critical Reviews in Biochemistry and Molecular Biology*, *52*(6), 638–662. https://doi.org/10.1080/10409238.2017.1360836

Fougère, B., Boulanger, E., Nourhashémi, F., Guyonnet, S., & Cesari, M. (2019). Retraction: Chronic inflammation: Accelerator of biological aging (Journals of Gerontology - Series A Biological Sciences and Medical Sciences DOI: 10.1093/gerona/glw240). *Journals of Gerontology - Series A Biological Sciences and Medical Sciences*, *74*(3), 431. https://doi.org/10.1093/gerona/gly284

Frankel, D., Delecourt, V., Harhouri, K., De Sandre-Giovannoli, A., Lévy, N., Kaspi, E., & Roll, P. (2018). MicroRNAs in hereditary and sporadic premature aging syndromes and other laminopathies. *Aging Cell*, *17*(4), e12766. https://doi.org/10.1111/acel.12766

Furuyama, T., Yamashita, H., Kitayama, K., Higami, Y., Shimokawa, I., & Mori, N. (2002). Effects of aging and caloric restriction on the gene expression of Foxo1, 3, and 4 (FKHR, FKHRL1, and AFX) in the rat skeletal muscles. *Microscopy Research and Technique*, *59*(4), 331–334. https://doi.org/10.1002/jemt.10213

García-Palmero, I., Torres, S., Bartolomé, R. A., Peláez-García, A., Larriba, M. J., Lopez-Lucendo, M., … Casal, J. I. (2016). Twist1-induced activation of human fibroblasts promotes matrix stiffness by upregulating palladin and collagen α1(VI). *Oncogene*, *35*(40), 5224–5236. https://doi.org/10.1038/onc.2016.57

Georgi, L. L., Albert, P. S., & Riddle, D. L. (1990). daf-1, a C. elegans gene controlling dauer larva development, encodes a novel receptor protein kinase. *Cell*, *61*(4), 635–645. https://doi.org/10.1016/0092-8674(90)90475-T

Gerasymchuk, M., Cherkasova, V., Kovalchuk, O., & Kovalchuk, I. (2020). The role of micrornas in organismal and skin aging. *International Journal of Molecular Sciences*, *21*(15), 1–36. https://doi.org/10.3390/ijms21155281

Gershon, D. (1970). Studies on aging in nematodes. I. The nematode as a model organism for aging research. *Experimental Gerontology*, *5*(1), 7–12. https://doi.org/10.1016/0531-5565(70)90023-9

Geuens, T., Bouhy, D., & Timmerman, V. (2016). The hnRNP family: insights into their role in health and disease. *Human Genetics*, *135*(8), 851–867. https://doi.org/10.1007/s00439-016-1683-5

Ghafouri-Fard, S., Khoshbakht, T., Hussen, B. M., Jamal, H. H., Taheri, M., & Hajiesmaeili, M. (2022). A Comprehensive Review on Function of miR-15b-5p in Malignant and Non-Malignant Disorders. *Frontiers in Oncology*, *12*. https://doi.org/10.3389/fonc.2022.870996

Gorgoulis, V., Adams, P. D., Alimonti, A., Bennett, D. C., Bischof, O., Bishop, C., … Demaria, M. (2019). Cellular Senescence: Defining a Path Forward. *Cell*, *179*(4), 813–827. https://doi.org/https://doi.org/10.1016/j.cell.2019.10.005

Grassmann, F., Schoenberger, P. G. A., Brandl, C., Schick, T., Hasler, D., Meister, G., …

Weber, B. H. F. (2014). A circulating MicroRNA profile is associated with late- stage neovascular age-related macular degeneration. *PLoS ONE*, *9*(9), e107461. https://doi.org/10.1371/journal.pone.0107461

Grillari, J., Hackl, M., & Grillari-Voglauer, R. (2010). miR-17-92 cluster: Ups and downs in cancer and aging. *Biogerontology*, *11*(4), 501–506. https://doi.org/10.1007/s10522-010-9272-9

Guan, P., Sun, Z.-M., Wang, N., Zhou, J., Luo, L.-F., Zhao, Y.-S., & Ji, E.-S. (2019). Resveratrol prevents chronic intermittent hypoxia-induced cardiac hypertrophy by targeting the PI3K/AKT/mTOR pathway. *Life Sciences*, *233*, 116748. https://doi.org/https://doi.org/10.1016/j.lfs.2019.116748

Guarente, L., & Kenyon, C. (2000). Genetic pathways that regulate ageing in model organisms. *Nature*, *408*(6809), 255–262. https://doi.org/10.1038/35041700

Hagiwara, S., McClelland, A., & Kantharidis, P. (2013). MicroRNA in diabetic nephropathy: Renin angiotensin, AGE/RAGE, and oxidative stress pathway. *Journal of Diabetes Research*, *2013*, 173783. https://doi.org/10.1155/2013/173783

Hamdan, Y., Mazini, L., & Malka, G. (2021). Exosomes and micro-rnas in aging process. *Biomedicines*, *9*(8). https://doi.org/10.3390/biomedicines9080968

Hamilton, B., Dong, Y., Shindo, M., Liu, W., Odell, I., Ruvkun, G., & Lee, S. S. (2005). A systematic RNAi screen for longevity genes in C. elegans. *Genes and Development*, *19*(13), 1544–1555. https://doi.org/10.1101/gad.1308205

Hara, E., Smith, R., Parry, D., Tahara, H., Stone, S., & Peters, G. (1996). Regulation of p16CDKN2 expression and its implications for cell immortalization and senescence. *Molecular and Cellular Biology*, *16*(3), 859–867. https://doi.org/10.1128/mcb.16.3.859

Harley, C. B., Futcher, A. B., & Greider, C. W. (1990). Telomeres shorten during ageing of human fibroblasts. *Nature*, *345*(6274), 458–460. https://doi.org/10.1038/345458a0

Harries, L. W. (2014). MicroRNAs as mediators of the ageing process. *Genes*, *5*(3), 656–670. https://doi.org/10.3390/genes5030656

Harries, L. W. (2019). RNA biology provides new therapeutic targets for human disease. *Frontiers in Genetics*. https://doi.org/10.3389/fgene.2019.00205

Harries, L. W., Hernandez, D., Henley, W., Wood, A. R., Holly, A. C., Bradley-Smith, R. M., … Melzer, D. (2011). Human aging is characterized by focused changes in gene expression and deregulation of alternative splicing. *Aging Cell*, *10*(5), 868–878. https://doi.org/10.1111/j.1474-9726.2011.00726.x

Hatley, M. E., Patrick, D. M., Garcia, M. R., Richardson, J. A., Bassel-Duby, R., van Rooij, E., & Olson, E. N. (2010). Modulation of K-Ras-dependent lung tumorigenesis by MicroRNA-21. *Cancer Cell*, *18*(3), 282–293. https://doi.org/10.1016/j.ccr.2010.08.013

Hayflick, L. (1965). The limited in vitro lifetime of human diploid cell strains. *Experimental Cell Research*, *37*(3), 614–636. https://doi.org/10.1016/0014-4827(65)90211-9

Hayflick, L., & Moorhead, P. S. (1961). The serial cultivation of human diploid cell strains. *Experimental Cell Research*, *25*(3), 585–621. https://doi.org/10.1016/0014-4827(61)90192-6

He, L., Thomson, J. M., Hemann, M. T., Hernando-Monge, E., Mu, D., Goodson, S., … Hammond, S. M. (2005). A microRNA polycistron as a potential human oncogene. *Nature*, *435*(7043), 828–833. https://doi.org/10.1038/nature03552

He, S., & Sharpless, N. E. (2017). Senescence in Health and Disease. *Cell*, *169*(6), 1000–1011. https://doi.org/10.1016/j.cell.2017.05.015

Hernandez-Segura, A., Nehme, J., & Demaria, M. (2018). Hallmarks of Cellular Senescence. *Trends in Cell Biology*, *28*(6), 436–453. https://doi.org/10.1016/j.tcb.2018.02.001

Herrera-Carrillo, E., & Berkhout, B. (2017). Survey and summary: Dicer-independent processing of small RNA duplexes: Mechanistic insights and applications. *Nucleic Acids Research*, *45*(18), 10369–10379. https://doi.org/10.1093/nar/gkx779

Holly, A. C., Grellscheid, S., van de Walle, P., Dolan, D., Pilling, L. C., Daniels, D. J., … Harries, L. W. (2015). Comparison of senescence-associated miRNAs in primary skin and lung fibroblasts. *Biogerontology*, *16*(4), 423–434. https://doi.org/10.1007/s10522-015-9560-5

Holly, A. C., Melzer, D., Pilling, L. C., Fellows, A. C., Tanaka, T., Ferrucci, L., & Harries, L. W. (2013). Changes in splicing factor expression are associated with advancing age in man. *Mechanisms of Ageing and Development*, *134*(9), 356–366. https://doi.org/10.1016/j.mad.2013.05.006

Holzenberger, M., Dupont, J., Ducos, B., Leneuve, P., Géloën, A., Even, P. C., … Le Bouc, Y. (2003). IGF-1 receptor regulates lifespan and resistance to oxidative stress in mice. *Nature*, *421*(6919), 182–187. https://doi.org/10.1038/nature01298

Honda, Y., & Honda, S. (1999). The daf-2 gene network for longevity regulates oxidative stress resistance and Mn-superoxide dismutase gene expression in Caenorhabditis elegans . *The FASEB Journal*, *13*(11), 1385–1393. https://doi.org/10.1096/fasebj.13.11.1385

Hong, Y., He, H., Jiang, G., Zhang, H., Tao, W., Ding, Y., … Zhang, Y. (2020). miR-155-5p inhibition rejuvenates aged mesenchymal stem cells and enhances cardioprotection following infarction. *Aging Cell*, *19*(4), e13128. https://doi.org/10.1111/acel.13128

Hsu, P. H., Chen, Y. H., Huang, P. I., & Hwang, P. A. (2022). Skin proteomic profiling of irradiation-induced fibrosis and its modulation by low molecular weight fucoidan via tight

junction pathway. *Biomedicine and Pharmacotherapy*, *153*, 113417. https://doi.org/10.1016/j.biopha.2022.113417

Hu, Z., Klein, J. D., Mitch, W. E., Zhang, L., Martinez, I., & Wang, X. H. (2014). MicroRNA-29 induces cellular senescence in aging muscle through multiple signaling pathways. *Aging*, *6*(3), 160–175. https://doi.org/10.18632/aging.100643

Huan, T., Chen, G., Liu, C., Bhattacharya, A., Rong, J., Chen, B. H., … Levy, D. (2018). Age-associated microRNA expression in human peripheral blood is associated with all-cause mortality and age-related traits. *Aging Cell*, *17*(1), 1–10. https://doi.org/10.1111/acel.12687

Huang, H. Y., Lin, Y. C. D., Cui, S., Huang, Y., Tang, Y., Xu, J., … Huang, H. Da. (2022). MiRTarBase update 2022: An informative resource for experimentally validated miRNA-target interactions. *Nucleic Acids Research*, *50*(D1), D222–D230. https://doi.org/10.1093/nar/gkab1079

Huang, H. Y., Lin, Y. C. D., Li, J., Huang, K. Y., Shrestha, S., Hong, H. C., … Huang, H. Da. (2020). MiRTarBase 2020: Updates to the experimentally validated microRNA-target interaction database. *Nucleic Acids Research*, *48*(D1), D148–D154. https://doi.org/10.1093/nar/gkz896

Huang, W., Hickson, L. T. J., Eirin, A., Kirkland, J. L., & Lerman, L. O. (2022). Cellular senescence: the good, the bad and the unknown. *Nature Reviews Nephrology*, *18*(10), 611–627. https://doi.org/10.1038/s41581-022-00601-z

Huang, Y., He, Y., Makarcyzk, M. J., & Lin, H. (2021). Senolytic Peptide FOXO4-DRI Selectively Removes Senescent Cells From in vitro Expanded Human Chondrocytes. *Frontiers in Bioengineering and Biotechnology*, *9*. https://doi.org/10.3389/fbioe.2021.677576

Islam, M. R., Kaurani, L., Berulava, T., Heilbronner, U., Budde, M., Centeno, T. P., … Fischer,

A. (2021). A microRNA signature that correlates with cognition and is a target against cognitive decline. *EMBO Molecular Medicine*, *13*(11), e13659. https://doi.org/10.15252/emmm.202013659

Jia, G., Aroor, A. R., Jia, C., & Sowers, J. R. (2019). Endothelial cell senescence in aging-related vascular dysfunction. *Biochimica et Biophysica Acta (BBA) - Molecular Basis of Disease*, *1865*(7), 1802–1809. https://doi.org/https://doi.org/10.1016/j.bbadis.2018.08.008

Jin, C., Li, J., Green, C. D., Yu, X., Tang, X., Han, D., … Han, J. D. J. (2011). Histone demethylase UTX-1 regulates C. elegans life span by targeting the insulin/IGF-1 signaling pathway. *Cell Metabolism*, *14*(2), 161–172. https://doi.org/10.1016/j.cmet.2011.07.001

Jinghua, H., Qinghua, Z., Chenchen, C., Lili, C., Xiao, X., Yunfei, W., … Hui, H. (2021). MicroRNA miR-92a-3p regulates breast cancer cell proliferation and metastasis via regulating B-cell translocation gene 2 (BTG2). *Bioengineered*, *12*(1), 2033–2044. https://doi.org/10.1080/21655979.2021.1924543

Johnston, W. L., Krizus, A., Ramani, A. K., Dunham, W., Youn, J. Y., Fraser, A. G., … Dennis, J. W. (2017). C. elegans SUP-46, an HNRNPM family RNA-binding protein that prevents paternally-mediated epigenetic sterility. *BMC Biology*, *15*(1), 61. https://doi.org/10.1186/s12915-017-0398-y

Justice, J. N., Nambiar, A. M., Tchkonia, T., LeBrasseur, N. K., Pascual, R., Hashmi, S. K., … Kirkland, J. L. (2019). Senolytics in idiopathic pulmonary fibrosis: Results from a first-in-human, open-label, pilot study. *EBioMedicine*, *40*, 554–563. https://doi.org/10.1016/j.ebiom.2018.12.052

Kamath, R. S., & Ahringer, J. (2003). Genome-wide RNAi screening in Caenorhabditis elegans. *Methods (San Diego, Calif.)*, *30*(4), 313–321. https://doi.org/10.1016/S1046-2023(03)00050-1

Kapić, A., Helmbold, H., Reimer, R., Klotzsche, O., Deppert, W., & Bohn, W. (2006). Cooperation between p53 and p130(Rb2) in induction of cellular senescence. *Cell Death and Differentiation*, *13*(2), 324–334. https://doi.org/10.1038/sj.cdd.4401756

Kempers, L., Driessen, A. J. M., van Rijssel, J., Nolte, M. A., & van Buul, J. D. (2021). Review the rhogef trio: A protein with a wide range of functions in the vascular endothelium. *International Journal of Molecular Sciences*, *22*(18). https://doi.org/10.3390/ijms221810168

Kenessary, A., Zhumadilov, Z., Nurgozhin, T., Kipling, D., Yeoman, M., Cox, L., … Faragher, R. (2013). Biomarkers, interventions and healthy ageing. *New Biotechnology*, *30*(4), 373–377. https://doi.org/10.1016/j.nbt.2012.11.018

Kim, E. C., & Kim, J. R. (2019). Senotherapeutics: Emerging strategy for healthy aging and age-related disease. *BMB Reports*, *52*(1), 47–55. https://doi.org/10.5483/BMBRep.2019.52.1.293

Kim, J. K., Noh, J. H., Jung, K. H., Eun, J. W., Bae, H. J., Kim, M. G., … Nam, S. W. (2013). Sirtuin7 oncogenic potential in human hepatocellular carcinoma and its regulation by the tumor suppressors MiR-125a-5p and MiR-125b. *Hepatology*, *57*(3), 1055–1067. https://doi.org/10.1002/hep.26101

Kim, W., Underwood, R. S., Greenwald, I., & Shaye, D. D. (2018). Ortholist 2: A new comparative genomic analysis of human and caenorhabditis elegans genes. *Genetics*, *210*(2), 445–461. https://doi.org/10.1534/genetics.118.301307

Kim, Y. J., Cho, M. J., Yu, W. D., Kim, M. J., Kim, S. Y., & Lee, J. H. (2022). Links of Cytoskeletal Integrity with Disease and Aging. *Cells*, *11*(18). https://doi.org/10.3390/cells11182896

Kim, Y. K., Yeo, J., Kim, B., Ha, M., & Kim, V. N. (2012, June). Short Structured RNAs with Low

GC Content Are Selectively Lost during Extraction from a Small Number of Cells. *Molecular Cell*. United States. https://doi.org/10.1016/j.molcel.2012.05.036

Kinser, H. E., & Pincus, Z. (2020). MicroRNAs as modulators of longevity and the aging process. *Human Genetics*, *139*(3), 291–308. https://doi.org/10.1007/s00439-019-02046-0

Krishnamurthy, J., Torrice, C., Ramsey, M. R., Kovalev, G. I., Al-Regaiey, K., Su, L., & Sharpless, N. E. (2004). Ink4a/Arf expression is a biomarker of aging. *Journal of Clinical Investigation*, *114*(9), 1299–1307. https://doi.org/10.1172/JCI22475

Krtolica, A., Parrinello, S., Lockett, S., Desprez, P. Y., & Campisi, J. (2001). Senescent fibroblasts promote epithelial cell growth and tumorigenesis: A link between cancer and aging. *Proceedings of the National Academy of Sciences of the United States of America*, *98*(21), 12072–12077. https://doi.org/10.1073/pnas.211053698

Kumari, R., & Jat, P. (2021). Mechanisms of Cellular Senescence: Cell Cycle Arrest and Senescence Associated Secretory Phenotype. *Frontiers in Cell and Developmental Biology*, *9*. https://doi.org/10.3389/fcell.2021.645593

Lago, J. C., & Puzzi, M. B. (2019). The effect of aging in primary human dermal fibroblasts. *PloS One*, *14*(7), e0219165. https://doi.org/10.1371/journal.pone.0219165

Lang, A., Grether-Beck, S., Singh, M., Kuck, F., Jakob, S., Kefalas, A., … Piekorz, R. P. (2016). MicroRNA-15b regulates mitochondrial ROS production and the senescence-associated secretory phenotype through sirtuin 4/SIRT4. *Aging*, *8*(3), 484–505. https://doi.org/10.18632/aging.100905

LaPierre, M. P., & Stoffel, M. (2017). MicroRNAs as stress regulators in pancreatic beta cells and diabetes. *Molecular Metabolism*, *6*(9), 1010–1023. https://doi.org/10.1016/j.molmet.2017.06.020

Laplante, M., & Sabatini, D. M. (2009). mTOR signaling at a glance. *Journal of Cell Science*, *122*(20), 3589–3594. https://doi.org/10.1242/jcs.051011

Latorre, E., Birar, V. C., Sheerin, A. N., Jeynes, J. C. C., Hooper, A., Dawe, H. R., … Harries, L. W. (2017). Small molecule modulation of splicing factor expression is associated with rescue from cellular senescence. *BMC Cell Biology*, *18*(1), 31. https://doi.org/10.1186/s12860-017-0147-7

Latorre, E., Ostler, E. L., Faragher, R. G. A., & Harries, L. W. (2018). FOXO1 and ETV6 genes may represent novel regulators of splicing factor expression in cellular senescence. *FASEB Journal : Official Publication of the Federation of American Societies for Experimental Biology*, fj201801154R. https://doi.org/10.1096/fj.201801154R

Latorre, E., Ostler, E. L., Faragher, R. G. A., & Harries, L. W. (2019). FOXO1 and ETV6 genes may represent novel regulators of splicing factor expression in cellular senescence. *FASEB Journal*, *33*(1), 1086–1097. https://doi.org/10.1096/fj.201801154R

Latorre, E., Pilling, L. C., Lee, B. P., Bandinelli, S., Melzer, D., Ferrucci, L., & Harries, L. W. (2018). The VEGFA 156 b isoform is dysregulated in senescent endothelial cells and may be associated with prevalent and incident coronary heart disease. *Clinical Science*, *132*(3), 313–325. https://doi.org/10.1042/CS20171556

Latorre, E., Torregrossa, R., Wood, M. E., Whiteman, M., & Harries, L. W. (2018). Mitochondria-targeted hydrogen sulfide attenuates endothelial senescence by selective induction of splicing factors HNRNPD and SRSF2. *Aging*, *10*(7), 1666–1681. https://doi.org/10.18632/aging.101500

Lee, B. P., Smith, M., Buffenstein, R., & Harries, L. W. (2020). Negligible senescence in naked mole rats may be a consequence of well-maintained splicing regulation. *GeroScience*, *42*(2), 633–651. https://doi.org/10.1007/s11357-019-00150-7

Lee, B. Y., Han, J. A., Im, J. S., Morrone, A., Johung, K., Goodwin, E. C., … Hwang, E. S. (2006). Senescence-associated β-galactosidase is lysosomal β-galactosidase. *Aging Cell*, *5*(2), 187–195. https://doi.org/10.1111/j.1474-9726.2006.00199.x

Lee, Ben P, & Harries, L. W. (2021). Senotherapeutic Drugs: A New Avenue for Skincare? *Plastic and Reconstructive Surgery*, *148*(6S). Retrieved from https://journals.lww.com/plasreconsurg/Fulltext/2021/12001/Senotherapeutic_Drugs__A_New_Avenue_for_Skincare_.6.aspx

Lee, Benjamin P., Mulvey, L., Barr, G., Garratt, J., Goodman, E., Selman, C., & Harries, L. W. (2019). Dietary restriction in ILSXISS mice is associated with widespread changes in splicing regulatory factor expression levels. *Experimental Gerontology*, *128*, 110736. https://doi.org/10.1016/j.exger.2019.110736

Lee, Benjamin P., Pilling, L. C., Bandinelli, S., Ferrucci, L., Melzer, D., & Harries, L. W. (2019). The transcript expression levels of HNRNPM, HNRNPA0 and AKAP17A splicing factors may be predictively associated with ageing phenotypes in human peripheral blood. *Biogerontology*, *20*(5), 649–663. https://doi.org/10.1007/s10522-019-09819-0

Lee, Benjamin P., Pilling, L. C., Emond, F., Flurkey, K., Harrison, D. E., Yuan, R., … Harries, L. W. (2016). Changes in the expression of splicing factor transcripts and variations in alternative splicing are associated with lifespan in mice and humans. *Aging Cell*, *15*(5), 903–913. https://doi.org/10.1111/acel.12499

Lee, R. C., Feinbaum, R. L., & Ambros, V. (1993). the C. elegans\rheterochronic gene lin-4 encodes small RNAs with antisense\rcomplementarity to lin-14. *Cell* , *75: 843–85*, 843–854. https://doi.org/10.1016/0092-8674(93)90529-Y

Lee, S. J., Jung, Y. S., Yoon, M. H., Kang, S. M., Oh, A. Y., Lee, J. H., … Park, B. J. (2016). Interruption of progerin-lamin A/C binding ameliorates Hutchinson-Gilford progeria

syndrome phenotype. *Journal of Clinical Investigation*, *126*(10), 3879–3893. https://doi.org/10.1172/JCI84164

Lee, Y., Ahn, C., Han, J., Choi, H., Kim, J., Yim, J., … Kim, V. N. (2003). The nuclear RNase III Drosha initiates microRNA processing. *Nature*, *425*(6956), 415–419. https://doi.org/10.1038/nature01957

Lewis, B. P., Shih, I., Jones-Rhoades, M. W., Bartel, D. P., & Burge, C. B. (2003). Prediction of Mammalian MicroRNA Targets. *Cell*, *115*(7), 787–798. https://doi.org/10.1016/S0092-8674(03)01018-3

Lewis, S. A., Sureshchandra, S., Zulu, M. Z., Doratt, B., Jankeel, A., Ibraim, I. C., … Messaoudi, I. (2021). Differential dynamics of peripheral immune responses to acute SARS-CoV-2 infection in older adults. *Nature Aging*. https://doi.org/10.1038/s43587-021-00127-2

Li, T., Yan, X., Jiang, M., & Xiang, L. (2016). The comparison of microRNA profile of the dermis between the young and elderly. *Journal of Dermatological Science*, *82*(2), 75–83. https://doi.org/10.1016/j.jdermsci.2016.01.005

Liakou, E., Mavrogonatou, E., Pratsinis, H., Rizou, S., Evangelou, K., Panagiotou, P. N., … Kletsas, D. (2016). Ionizing radiation-mediated premature senescence and paracrine interactions with cancer cells enhance the expression of syndecan 1 in human breast stromal fibroblasts: The role of TGF-β. *Aging*, *8*(8), 1650–1669. https://doi.org/10.18632/aging.100989

Ling, J., & He, P. (2021). miR-361-5p regulates ovarian cancer cell proliferation and apoptosis by targeting TRAF3. *Experimental and Therapeutic Medicine*, *21*(3), 199. https://doi.org/10.3892/etm.2021.9632

Liu, D., Tao, T., Xu, B., Chen, S., Liu, C., Zhang, L., … Chen, M. (2014). MiR-361-5p acts as a

tumor suppressor in prostate cancer by targeting signal transducer and activator of transcription-6(STAT6). *Biochemical and Biophysical Research Communications*. https://doi.org/10.1016/j.bbrc.2014.01.140

Liu, J., Xu, H., Wang, N., & Sun, M. (2020). miR-15b, a diagnostic biomarker and therapeutic target, inhibits oesophageal cancer progression by regulating the PI3K/AKT signalling pathway. *Experimental and Therapeutic Medicine*, *20*(6), 1–1. https://doi.org/10.3892/etm.2020.9352

Loganantharaj, R., & Randall, T. A. (2017). The Limitations of Existing Approaches in Improving MicroRNA Target Prediction Accuracy. *Methods in Molecular Biology (Clifton, N.J.)*, *1617*, 133–158. https://doi.org/10.1007/978-1-4939-7046-9_10

Lopes-Paciencia, S., Saint-Germain, E., Rowell, M. C., Ruiz, A. F., Kalegari, P., & Ferbeyre, G. (2019). The senescence-associated secretory phenotype and its regulation. *Cytokine*, *117*, 15–22. https://doi.org/10.1016/j.cyto.2019.01.013

López-Otín, C., Blasco, M. A., Partridge, L., Serrano, M., & Kroemer, G. (2013). The hallmarks of aging. *Cell*, *153*(6), 1194. https://doi.org/10.1016/j.cell.2013.05.039

López-Otín, C., Blasco, M. A., Partridge, L., Serrano, M., & Kroemer, G. (2023). Hallmarks of aging: An expanding universe. *Cell*, *186*(2), 243–278. https://doi.org/10.1016/j.cell.2022.11.001

Lye, J. J., Latorre, E., Lee, B. P., Bandinelli, S., Holley, J. E., Gutowski, N. J., … Harries, L. W. (2019). Astrocyte senescence may drive alterations in GFAPα, CDKN2A p14 ARF, and TAU3 transcript expression and contribute to cognitive decline. *GeroScience*, *41*(5), 561–573. https://doi.org/10.1007/s11357-019-00100-3

Ma, Xiaodong, Choudhury, S. N., Hua, X., Dai, Z., & Li, Y. (2013). Interaction of the oncogenic

miR-21 microRNA and the p53 tumor suppressor pathway. *Carcinogenesis*, *34*(6), 1216–1223. https://doi.org/10.1093/carcin/bgt044

Ma, Xudan, Zhang, Q., Zhu, H., Huang, K., Pang, W., & Zhang, Q. (2021). Establishment and analysis of the lncRNA-miRNA-mRNA network based on competitive endogenous RNA identifies functional genes in heart failure. *Mathematical Biosciences and Engineering*, *18*(4), 4011–4026. https://doi.org/10.3934/mbe.2021201

Majeed Shah, I., Ahmad Dar, M., Ahmad Bhat, K., Ahmad Dar, T., Ahmad, F., & Mudasir Ahmad, S. (2022). Long Non-Coding RNAs: Biogenesis, Mechanism of Action and Role in Different Biological and Pathological Processes. In M. A. Dar (Ed.), *Recent Advances in Noncoding RNAs* (p. Ch. 7). Rijeka: IntechOpen. https://doi.org/10.5772/intechopen.104861

Majidinia, M., Mir, S. M., Mirza-Aghazadeh-Attari, M., Asghari, R., Kafil, H. S., Safa, A., … Yousefi, B. (2020). MicroRNAs, DNA damage response and ageing. *Biogerontology*, *21*(3), 275–291. https://doi.org/10.1007/s10522-020-09862-2

Mao, G., Zhang, Z., Hu, S., Zhang, Z., Chang, Z., Huang, Z., … Kang, Y. (2018). Exosomes derived from miR-92a-3poverexpressing human mesenchymal stem cells enhance chondrogenesis and suppress cartilage degradation via targeting WNT5A. *Stem Cell Research and Therapy*, *9*(1), 247. https://doi.org/10.1186/s13287-018-1004-0

Marasa, B. S., Srikantan, S., Masuda, K., Abdelmohsen, K., Kuwano, Y., Yang, X., … Gorospe, M. (2009). Increased MKK4 abundance with replicative senescence Is linked to the joint reduction of multiple microRNAs. *Science Signaling*, *2*(94), ra69–ra69. https://doi.org/10.1126/scisignal.2000442

Marei, H. E., Althani, A., Afifi, N., Hasan, A., Caceci, T., Pozzoli, G., … Cenciarelli, C. (2021). P53 Signaling in Cancer Progression and Therapy. *Cancer Cell International*, *21*(1), 703.

https://doi.org/10.1186/s12935-021-02396-8

Markopoulos, G. S., Roupakia, E., Tokamani, M., Vartholomatos, G., Tzavaras, T., Hatziapostolou, M., … Kolettas, E. (2017). Senescence-associated microRNAs target cell cycle regulatory genes in normal human lung fibroblasts. *Experimental Gerontology*, *96*, 110–122. https://doi.org/10.1016/j.exger.2017.06.017

Marthandan, S., Priebe, S., Hemmerich, P., Klement, K., Diekmann, S., & Hofmann, T. G. (2014). Long-term quiescent fibroblast cells transit into senescence. *PLoS ONE*, *9*(12), e115597. https://doi.org/10.1371/journal.pone.0115597

Matranga, C., Tomari, Y., Shin, C., Bartel, D. P., & Zamore, P. D. (2005). Passenger-strand cleavage facilitates assembly of siRNA into Ago2-containing RNAi enzyme complexes. *Cell*, *123*(4), 607–620. https://doi.org/10.1016/j.cell.2005.08.044

McHugh, D., & Gil, J. (2018). Senescence and aging: Causes, consequences, and therapeutic avenues. *Journal of Cell Biology*, *217*(1), 65–77. https://doi.org/10.1083/jcb.201708092

McMullan, R., & Nurrish, S. J. (2011). The RHO-1 RhoGTPase modulates fertility and multiple behaviors in adult C. elegans. *PLoS ONE*, *6*(2), e17265. https://doi.org/10.1371/journal.pone.0017265

Mendes-Silva, A. P., Pereira, K. S., Tolentino-Araujo, G. T., Nicolau, E. de S., Silva-Ferreira, C. M., Teixeira, A. L., & Diniz, B. S. (2016). Shared Biologic Pathways Between Alzheimer Disease and Major Depression: A Systematic Review of MicroRNA Expression Studies. *American Journal of Geriatric Psychiatry*, *24*(10), 903–912. https://doi.org/10.1016/j.jagp.2016.07.017

Meng, J., Li, Y., Wan, C., Sun, Y., Dai, X., Huang, J., … Yang, K. (2021). Targeting senescence-like fibroblasts radiosensitizes non-small cell lung cancer and reduces

radiation-induced pulmonary fibrosis. *JCI Insight*, *6*(23). https://doi.org/10.1172/jci.insight.146334

Messner, M., Ghadge, S. K., Maurer, T., Graber, M., Staggl, S., Christine Maier, S., … Zaruba, M. M. (2020). ZMPSTE24 Is Associated with Elevated Inflammation and Progerin mRNA. *Cells*, *9*(9). https://doi.org/10.3390/cells9091981

Mi, H., & Thomas, P. (2009). PANTHER pathway: an ontology-based pathway database coupled with data analysis tools. *Methods in Molecular Biology (Clifton, N.J.)*, *563*, 123–140. https://doi.org/10.1007/978-1-60761-175-2_7

Mijit, M., Caracciolo, V., Melillo, A., Amicarelli, F., & Giordano, A. (2020). Role of p53 in the regulation of cellular senescence. *Biomolecules*, *10*(3). https://doi.org/10.3390/biom10030420

Morimoto, R. I., & Cuervo, A. M. (2014). Proteostasis and the aging proteome in health and disease. *Journals of Gerontology - Series A Biological Sciences and Medical Sciences*, *69*(Suppl 1), S33–S38. https://doi.org/10.1093/gerona/glu049

Morris, B. J., Willcox, D. C., Donlon, T. A., & Willcox, B. J. (2015). FOXO3: A Major Gene for Human Longevity - A Mini-Review. *Gerontology*, *61*(6), 515–525. https://doi.org/10.1159/000375235

Morris, J. Z., Tissenbaum, H. A., & Ruvkun, G. (1996). A phosphatidylinositol-3-OH kinase family member regulating longevity and diapause in Caenorhabditis elegans. *Nature*, *382*(6591), 536–539. https://doi.org/10.1038/382536a0

Morrow, G., Samson, M., Michaud, S., & Tanguay, R. M. (2004). Overexpression of the small mitochondrial Hsp22 extends Drosophila life span and increases resistance to oxidative stress. *The FASEB Journal : Official Publication of the Federation of American Societies for*

Experimental Biology, *18*(3), 598–599. https://doi.org/10.1096/fj.03-0860fje

Mulrane, L., McGee, S. F., Gallagher, W. M., & O'Connor, D. P. (2013). miRNA dysregulation in breast cancer. *Cancer Research*, *73*(22), 6554–6562. https://doi.org/10.1158/0008-5472.CAN-13-1841

Muñoz-Espín, D., Cañamero, M., Maraver, A., Gómez-López, G., Contreras, J., Murillo-Cuesta, S., … Serrano, M. (2013). XProgrammed cell senescence during mammalian embryonic development. *Cell*, *155*(5), 1104. https://doi.org/10.1016/j.cell.2013.10.019

Muñoz-Espín, D., & Serrano, M. (2014). Cellular senescence: From physiology to pathology. *Nature Reviews Molecular Cell Biology*, *15*(7), 482–496. https://doi.org/10.1038/nrm3823

Narita, M., Narita, M., Krizhanovsky, V., Nuñez, S., Chicas, A., Hearn, S. A., … Lowe, S. W. (2006). A Novel Role for High-Mobility Group A Proteins in Cellular Senescence and Heterochromatin Formation. *Cell*, *126*(3), 503–514. https://doi.org/10.1016/j.cell.2006.05.052

Narita, M., Nũnez, S., Heard, E., Narita, M., Lin, A. W., Hearn, S. A., … Lowe, S. W. (2003). Rb-mediated heterochromatin formation and silencing of E2F target genes during cellular senescence. *Cell*, *113*(6), 703–716. https://doi.org/10.1016/S0092-8674(03)00401-X

Niccoli, T., & Partridge, L. (2012). Ageing as a risk factor for disease. *Current Biology*, *22*(17), R741–R752. https://doi.org/10.1016/j.cub.2012.07.024

Nikitenko, L., & Boshoff, C. (2006). Endothelial cells and cancer. *Handbook of Experimental Pharmacology*, *176*(PART2), 307–334. https://doi.org/10.1007/3-540-36028-x_10

Niklander, S., Bandaru, D., Lambert, D. W., & Hunter, K. D. (2020). ROCK inhibition modulates the senescence-associated secretory phenotype (SASP) in oral keratinocytes. *FEBS Open Bio*, *10*(12), 2740–2749. https://doi.org/10.1002/2211-5463.13012

Nikolajevic, J., Ariaee, N., Liew, A., Abbasnia, S., Fazeli, B., & Sabovic, M. (2022). The Role of MicroRNAs in Endothelial Cell Senescence. *Cells*, *11*(7). https://doi.org/10.3390/cells11071185

Novelle, M. G., Wahl, D., Diéguez, C., Bernier, M., & de Cabo, R. (2015). Resveratrol supplementation: Where are we now and where should we go? *Ageing Research Reviews*, *21*, 1–15. https://doi.org/10.1016/j.arr.2015.01.002

Nunes, A. D. C., Weigl, M., Schneider, A., Noureddine, S., Yu, L., Lahde, C., … Masternak, M. M. (2021). miR-146a-5p modulates cellular senescence and apoptosis in visceral adipose tissue of long-lived Ames dwarf mice and in cultured pre-adipocytes. *GeroScience*. https://doi.org/10.1007/s11357-021-00490-3

O'Connor, M. S., Safari, A., Xin, H., Liu, D., & Songyang, Z. (2006). A critical role for TPP1 and TIN2 interaction in high-order telomeric complex assembly. *Proceedings of the National Academy of Sciences of the United States of America*, *103*(32), 11874–11879. https://doi.org/10.1073/pnas.0605303103

O'Sullivan, R. J., & Karlseder, J. (2012). The great unravelling: Chromatin as a modulator of the aging process. *Trends in Biochemical Sciences*, *37*(11), 466–476. https://doi.org/10.1016/j.tibs.2012.08.001

Ogrodnik, M., Miwa, S., Tchkonia, T., Tiniakos, D., Wilson, C. L., Lahat, A., … Jurk, D. (2017). Cellular senescence drives age-dependent hepatic steatosis. *Nature Communications*, *8*, 15691. https://doi.org/10.1038/ncomms15691

Olivieri, F., Bonafè, M., Spazzafumo, L., Gobbi, M., Prattichizzo, F., Recchioni, R., … Testa, R. (2014). Age- and glycemia-related miR-126-3p levels in plasma and endothelial cells. *Aging*, *6*(9), 771–787. https://doi.org/10.18632/aging.100693

Ota, A., Tagawa, H., Karnan, S., Tsuzuki, S., Karpas, A., Kira, S., … Seto, M. (2004). Identification and Characterization of a Novel Gene, C13orf25, as a Target for 13q31-q32 Amplification in Malignant Lymphoma. *Cancer Research*, *64*(9), 3087–3095. https://doi.org/10.1158/0008-5472.CAN-03-3773

Othman, N., & Nagoor, N. H. (2019). Overexpression of miR-361-5p plays an oncogenic role in human lung adenocarcinoma through the regulation of SMAD2. *International Journal of Oncology*, *54*(1), 306–314. https://doi.org/10.3892/ijo.2018.4602

Owens, R. J., & Baralle, F. E. (1986). Mapping the collagen-binding site of human fibronectin by expression in Escherichia coli. *The EMBO Journal*, *5*(11), 2825–2830. https://doi.org/10.1002/j.1460-2075.1986.tb04575.x

Paez-Ribes, M., González-Gualda, E., Doherty, G. J., & Muñoz-Espín, D. (2019). Targeting senescent cells in translational medicine. *EMBO Molecular Medicine*, *11*(12), e10234. https://doi.org/10.15252/emmm.201810234

Pan, H., & Finkel, T. (2017). Key proteins and pathways that regulate lifespan. *Journal of Biological Chemistry*, *292*(16), 6452–6460. https://doi.org/10.1074/jbc.R116.771915

Paraskevopoulou, M. D., Georgakilas, G., Kostoulas, N., Vlachos, I. S., Vergoulis, T., Reczko, M., … Hatzigeorgiou, A. G. (2013). DIANA-microT web server v5.0: service integration into miRNA functional analysis workflows. *Nucleic Acids Research*, *41*(Web Server issue), W169-73. https://doi.org/10.1093/nar/gkt393

Park, J. Il, Venteicher, A. S., Hong, J. Y., Choi, J., Jun, S., Shkreli, M., … Artandi, S. E. (2009). Telomerase modulates Wnt signalling by association with target gene chromatin. *Nature*, *460*(7251), 66–72. https://doi.org/10.1038/nature08137

Partridge, L., Deelen, J., & Slagboom, P. E. (2018). Facing up to the global challenges of

ageing. *Nature*, *561*(7721), 45–56. https://doi.org/10.1038/s41586-018-0457-8

Petrova, N. V., Velichko, A. K., Razin, S. V., & Kantidze, O. L. (2016). Small molecule compounds that induce cellular senescence. *Aging Cell*, *15*(6), 999–1017. https://doi.org/10.1111/acel.12518

Pfaffl, M. W. (2001). A new mathematical model for relative quantification in real-time RT–PCR. *Nucleic Acids Research*, *29*(9), E45. https://doi.org/10.1093/nar/29.9.e45

Piletič, K., & Kunej, T. (2016). MicroRNA epigenetic signatures in human disease. *Archives of Toxicology*, *90*(10), 2405–2419. https://doi.org/10.1007/s00204-016-1815-7

Pitto, L., Rizzo, M., Simili, M., Colligiani, D., Evangelista, M., Mercatanti, A., … Rainaldi, G. (2009). miR-290 acts as a physiological effector of senescence in mouse embryo fibroblasts. *Physiological Genomics*, *39*(3), 210–218. https://doi.org/10.1152/physiolgenomics.00085.2009

Poblocka, M., Bassey, A. L., Smith, V. M., Falcicchio, M., Manso, A. S., Althubiti, M., … Macip, S. (2021). Targeted clearance of senescent cells using an antibody-drug conjugate against a specific membrane marker. *Scientific Reports*, *11*(1), 20358. https://doi.org/10.1038/s41598-021-99852-2

Provost, P. (2010). MicroRNAs as a molecular basis for mental retardation, Alzheimer's and prion diseases. *Brain Research*, *1338*, 58–66. https://doi.org/10.1016/j.brainres.2010.03.069

Qi, H., Liu, Z., Liu, B., Cao, H., Sun, W., Yan, Y., & Zhang, L. (2017). Micro-RNA screening and prediction model construction for diagnosis of salt-sensitive essential hypertension. *Medicine (United States)*, *96*(17), e6417. https://doi.org/10.1097/MD.0000000000006417

Qian, B., Zhang, D., Tao, R., Yu, G., Jia, B., Ye, K., … Wu, W. (2020). MiR-361-5p exerts

tumor-suppressing functions in gastric carcinoma by targeting syndecan-binding protein. *Anti-Cancer Drugs*, *31*(2), 131–140. https://doi.org/10.1097/CAD.0000000000000846

Raffaele, M., & Vinciguerra, M. (2022). The costs and benefits of senotherapeutics for human health. *The Lancet Healthy Longevity*, *3*(1), e67–e77. https://doi.org/10.1016/S2666-7568(21)00300-7

Rahman, M., Edwards, H., Birze, N., Gabrilska, R., Rumbaugh, K. P., Blawzdziewicz, J., … Vanapalli, S. A. (2020). NemaLife chip: a micropillar-based microfluidic culture device optimized for aging studies in crawling C. elegans. *Scientific Reports*, *10*(1), 1–19. https://doi.org/10.1038/s41598-020-73002-6

Raices, M., Maruyama, H., Dillin, A., & Kariseder, J. (2005). Uncoupling of longevity and telomere length in C, elegans. *PLoS Genetics*, *1*(3), 295–301. https://doi.org/10.1371/journal.pgen.0010030

Ramirez, J., Bitterman, P., Basu, S., & Barua, A. (2022). Changes in IL-16 Expression in the Ovary during Aging and Its Potential Consequences to Ovarian Pathology. *Journal of Immunology Research*, *2022*, 2870389. https://doi.org/10.1155/2022/2870389

Rani, A., O'Shea, A., Ianov, L., Cohen, R. A., Woods, A. J., & Foster, T. C. (2017). miRNA in circulating microvesicles as biomarkers for age-related cognitive decline. *Frontiers in Aging Neuroscience*, *9*(OCT), 323. https://doi.org/10.3389/fnagi.2017.00323

Reid, G., Pel, M. E., Kirschner, M. B., Cheng, Y. Y., Mugridge, N., Weiss, J., … van Zandwijk, N. (2013). Restoring expression of miR-16: A novel approach to therapy for malignant pleural mesothelioma. *Annals of Oncology*, *24*(12), 3128–3135. https://doi.org/10.1093/annonc/mdt412

Relitti, N., Saraswati, A. P., Federico, S., Khan, T., Brindisi, M., Zisterer, D., … Campiani, G.

(2020). Telomerase-based Cancer Therapeutics: A Review on their Clinical Trials. *Current Topics in Medicinal Chemistry*, *20*(6), 433–457. https://doi.org/10.2174/1568026620666200102104930

Rivera-Torres, J., Acín-Perez, R., Cabezas-Sánchez, P., Osorio, F. G., Gonzalez-Gómez, C., Megias, D., … Andrés, V. (2013). Identification of mitochondrial dysfunction in Hutchinson–Gilford progeria syndrome through use of stable isotope labeling with amino acids in cell culture. *Journal of Proteomics*, *91*, 466–477. https://doi.org/https://doi.org/10.1016/j.jprot.2013.08.008

Rodriguez, A., Griffiths-Jones, S., Ashurst, J. L., & Bradley, A. (2004). Identification of mammalian microRNA host genes and transcription units. *Genome Research*, *14*(10 A), 1902–1910. https://doi.org/10.1101/gr.2722704

Romo-García, M. F., Bastian, Y., Zapata-Zuñiga, M., Macías-Segura, N., Castillo-Ortiz, J. D., Lara-Ramírez, E. E., … Castañeda-Delgado, J. E. (2019). Identification of putative miRNA biomarkers in early rheumatoid arthritis by genome-wide microarray profiling: A pilot study. *Gene*, *720*, 144081. https://doi.org/10.1016/j.gene.2019.144081

Rorbach, G., Unold, O., & Konopka, B. M. (2018). Distinguishing mirtrons from canonical miRNAs with data exploration and machine learning methods /631/114/2397 /631/114/2785 /631/114/1305 /631/114/2415 /129 /139 /141 /45 article. *Scientific Reports*, *8*(1), 7560. https://doi.org/10.1038/s41598-018-25578-3

Rutledge, R. G. (2004). Sigmoidal curve-fitting redefines quantitative real-time PCR with the prospective of developing automated high-throughput applications. *Nucleic Acids Research*, *32*(22), e178. https://doi.org/10.1093/nar/gnh177

Ryu, S. J., Oh, Y. S., & Park, S. C. (2007). Failure of stress-induced downregulation of Bcl-2 contributes to apoptosis resistance in senescent human diploid fibroblasts. *Cell Death and*

Differentiation, *14*(5), 1020–1028. https://doi.org/10.1038/sj.cdd.4402091

Sabath, N., Levy-Adam, F., Younis, A., Rozales, K., Meller, A., Hadar, S., … Shalgi, R. (2020). Cellular proteostasis decline in human senescence. *Proceedings of the National Academy of Sciences of the United States of America*, *117*(50), 31902–31913. https://doi.org/10.1073/pnas.2018138117

Sadaie, M., Salama, R., Carroll, T., Tomimatsu, K., Chandra, T., Young, A. R. J., … Narita, M. (2013). Redistribution of the Lamin B1 genomic binding profile affects rearrangement of heterochromatic domains and SAHF formation during senescence. *Genes and Development*, *27*(16), 1800–1808. https://doi.org/10.1101/gad.217281.113

Saez, I., & Vilchez, D. (2014). The Mechanistic Links Between Proteasome Activity, Aging and Agerelated Diseases. *Current Genomics*, *15*(1), 38–51. https://doi.org/10.2174/1389202915011403061133 44

Salehi, B., Mishra, A. P., Nigam, M., Sener, B., Kilic, M., Sharifi-Rad, M., … Sharifi-Rad, J. (2018). Resveratrol: A Double-Edged Sword in Health Benefits. *Biomedicines*, *6*(3), 91. https://doi.org/10.3390/biomedicines6030091

Sanders, Y. Y., Liu, H., Zhang, X., Hecker, L., Bernard, K., Desai, L., … Thannickal, V. J. (2013). Histone modifications in senescence-associated resistance to apoptosis by oxidative stress. *Redox Biology*, *1*(1), 8–16. https://doi.org/10.1016/j.redox.2012.11.004

Sasaki, M., Kumazaki, T., Takano, H., Nishiyama, M., & Mitsui, Y. (2001). Senescent cells are resistant to death despite low Bcl-2 level. *Mechanisms of Ageing and Development*, *122*(15), 1695–1706. https://doi.org/10.1016/S0047-6374(01)00281-0

Schmauck-Medina, T., Molière, A., Lautrup, S., Zhang, J., Chlopicki, S., Madsen, H. B., … Fang, E. F. (2022). New hallmarks of ageing: a 2022 Copenhagen ageing meeting

summary. *Aging*, *14*(16), 6829–6839. https://doi.org/10.18632/aging.204248

Schneider, F., Metz, I., & Rust, M. B. (2023). Regulation of actin filament assembly and disassembly in growth cone motility and axon guidance. *Brain Research Bulletin*, *192*, 21–35. https://doi.org/10.1016/j.brainresbull.2022.10.019

Schroth, J., Thiemermann, C., & Henson, S. M. (2020). Senescence and the Aging Immune System as Major Drivers of Chronic Kidney Disease. *Frontiers in Cell and Developmental Biology*, *8*. https://doi.org/10.3389/fcell.2020.564461

Serrano, M., Hannon, G. J., & Beach, D. (1993). A new regulatory motif in cell-cycle control causing specific inhibition of cyclin D/CDK4. *Nature*, *366*(6456), 704–707. https://doi.org/10.1038/366704a0

Sharma, S., & Lu, H. C. (2018). microRNAs in Neurodegeneration: Current Findings and Potential Impacts. *Journal of Alzheimer's Disease & Parkinsonism*, *08*(01). https://doi.org/10.4172/2161-0460.1000420

Shay, J. W., & Wright, W. E. (2000). Hayflick, his limit, and cellular ageing. *Nature Reviews Molecular Cell Biology*, *1*(1), 72–76. https://doi.org/10.1038/35036093

Shen, B., Zhou, N., Hu, T., Zhao, W., Wu, D., & Wang, S. (2019). LncRNA MEG3 negatively modified osteosarcoma development through regulation of miR-361-5p and FoxM1. *Journal of Cellular Physiology*, *234*(8), 13464–13480. https://doi.org/10.1002/jcp.28026

Shimizu, I., & Minamino, T. (2019). Cellular senescence in cardiac diseases. *Journal of Cardiology*, *74*(4), 313–319. https://doi.org/10.1016/j.jjcc.2019.05.002

Shin, S. Y., Kim, T. H., Wu, H., Choi, Y. H., & Kim, S. G. (2014). SIRT1 activation by methylene blue, a repurposed drug, leads to AMPK-mediated inhibition of steatosis and steatohepatitis. *European Journal of Pharmacology*, *727*, 115–124.

https://doi.org/https://doi.org/10.1016/j.ejphar.2014.01.035

Smith-Vikos, T., Liu, Z., Parsons, C., Gorospe, M., Ferrucci, L., Gill, T. M., & Slack, F. J. (2016). A serum miRNA profile of human longevity: Findings from the Baltimore Longitudinal Study of Aging (BLSA). *Aging*, *8*(11), 2971–2987. https://doi.org/10.18632/aging.101106

Soriano-Arroquia, A., Mccormick, R., Molloy, A. P., Mcardle, A., & Goljanek-Whysall, K. (2016). Age-related changes in miR-143-3p: Igfbp5 interactions affect muscle regeneration. *Aging Cell*, *15*(2), 361–369. https://doi.org/10.1111/acel.12442

Sorop, A., Iacob, R., Iacob, S., Constantinescu, D., Chitoiu, L., Fertig, T. E., … Popescu, I. (2020). Plasma Small Extracellular Vesicles Derived miR-21-5p and miR-92a-3p as Potential Biomarkers for Hepatocellular Carcinoma Screening. *Frontiers in Genetics*, *11*, 712. https://doi.org/10.3389/fgene.2020.00712

Spear, E. D., Hsu, E. T., Nie, L., Carpenter, E. P., Hrycyna, C. A., & Michaelis, S. (2018). ZMPSTE24 missense mutations that cause progeroid diseases decrease prelamin a cleavage activity and/or protein stability. *DMM Disease Models and Mechanisms*, *11*(7). https://doi.org/10.1242/dmm.033670

Stavast, C. J., & Erkeland, S. J. (2019). The Non-Canonical Aspects of MicroRNAs: Many Roads to Gene Regulation. *Cells*, *8*(11), 1465. https://doi.org/10.3390/cells8111465

Stolzenburg, L. R., & Harris, A. (2018). The role of microRNAs in chronic respiratory disease: Recent insights. *Biological Chemistry*, *399*(3), 219–234. https://doi.org/10.1515/hsz-2017-0249

Storer, M., Mas, A., Robert-Moreno, A., Pecoraro, M., Ortells, M. C., Di Giacomo, V., … Keyes, W. M. (2013). Senescence is a developmental mechanism that contributes to embryonic growth and patterning. *Cell*, *155*(5), 1119. https://doi.org/10.1016/j.cell.2013.10.041

Su, M., Niu, Y., Dang, Q., Qu, J., Zhu, D., Tang, Z., & Gou, D. (2020). Circulating microRNA profiles based on direct S-Poly(T)Plus assay for detection of coronary heart disease. *Journal of Cellular and Molecular Medicine*, *24*(11), 5984–5997. https://doi.org/10.1111/jcmm.15001

Suh, N. (2018). MicroRNA controls of cellular senescence. *BMB Reports*, *51*(10), 493–499. https://doi.org/10.5483/BMBRep.2018.51.10.209

Sun, L. N., Zhi, Z., Chen, L. Y., Zhou, Q., Li, X. M., Gan, W. J., … Li, J. M. (2017). SIRT1 suppresses colorectal cancer metastasis by transcriptional repression of miR-15b-5p. *Cancer Letters*, *409*, 104–115. https://doi.org/10.1016/j.canlet.2017.09.001

Sun, Y., Coppé, J. P., & Lam, E. W. F. (2018). Cellular Senescence: The Sought or the Unwanted? *Trends in Molecular Medicine*, *24*(10), 871–885. https://doi.org/10.1016/j.molmed.2018.08.002

Tacutu, R., Thornton, D., Johnson, E., Budovsky, A., Barardo, Di., Craig, T., … De Magalhães, J. P. (2018). Human Ageing Genomic Resources: New and updated databases. *Nucleic Acids Research*, *46*(D1), D1083–D1090. https://doi.org/10.1093/nar/gkx1042

Takahashi, Y., Rayman, J. B., & Dynlacht, B. D. (2000). Analysis of promoter binding by the E2F and pRB families in vivo: Distinct E2F proteins mediate activation and repression. *Genes and Development*, *14*(7), 804–816. https://doi.org/10.1101/gad.14.7.804

Tentler, D., Lomert, E., Novitskaya, K., & Barlev, N. A. (2019). Role of ACTN4 in tumorigenesis, metastasis, and EMT. *Cells*, *8*(11). https://doi.org/10.3390/cells8111427

Timmons, L., Court, D. L., & Fire, A. (2001). Ingestion of bacterially expressed dsRNAs can produce specific and potent genetic interference in Caenorhabditis elegans. *Gene*, *263*(1–2), 103–112. https://doi.org/10.1016/S0378-1119(00)00579-5

Tölle, A., Buckendahl, L., & Jung, K. (2019). Plasma miR-15b-5p and miR-590-5p for distinguishing patients with bladder cancer from healthy individuals. *Oncology Reports*, *42*(4), 1609–1620. https://doi.org/10.3892/or.2019.7247

Tollervey, J. R., Wang, Z., Hortobágyi, T., Witten, J. T., Zarnack, K., Kayikci, M., … Ule, J. (2011). Analysis of alternative splicing associated with aging and neurodegeneration in the human brain. *Genome Research*, *21*(10), 1572–1582. https://doi.org/10.1101/gr.122226.111

Turk, M. A., Chung, C. Z., Manni, E., Zukowski, S. A., Engineer, A., Badakhshi, Y., … Heinemann, I. U. (2018). MiRAR — miRNA activity reporter for living cells. *Gene*. https://doi.org/10.3390/genes9060305

Tyczewska, A., Żywicki, M., Gracz, J., & Karłowski, W. (2016). Changes in expression of miRNAs involved in stress responses and senescence in glyphosate-treated maize. *New Biotechnology*, *33*, S160–S161. https://doi.org/10.1016/j.nbt.2016.06.1276

United Nations Department of Economic and Social Affairs/ Population Divisions. (2017). World Population Prospects - Key findings & advance tables World Population Prospects: The 2017 Revision. *Economic & Social Affairs*, *1–53*(December), 53. Retrieved from https://www.un.org/development/desa/publications/world-population-prospects-the-2017-revision.html#:~:text=The current world population of 7.6 billion is,a new United Nations report being launched today.

Uno, M., & Nishida, E. (2016). Lifespan-regulating genes in c. Elegans. *Npj Aging and Mechanisms of Disease*, *2*(1). https://doi.org/10.1038/npjamd.2016.10

van Deursen, J. M. (2014). The role of senescent cells in ageing. *Nature*, *509*(7501), 439–446. https://doi.org/10.1038/nature13193

van Willigenburg, H., de Keizer, P. L. J., & de Bruin, R. W. F. (2018). Cellular senescence as a therapeutic target to improve renal transplantation outcome. *Pharmacological Research*, *130*, 322–330. https://doi.org/10.1016/j.phrs.2018.02.015

van Zandwijk, N., Pavlakis, N., Kao, S. C., Linton, A., Boyer, M. J., Clarke, S., … Reid, G. (2017). Safety and activity of microRNA-loaded minicells in patients with recurrent malignant pleural mesothelioma: a first-in-man, phase 1, open-label, dose-escalation study. *The Lancet Oncology*, *18*(10), 1386–1396. https://doi.org/10.1016/S1470-2045(17)30621-6

Vander Ark, A., Cao, J., & Li, X. (2018). TGF-β receptors: In and beyond TGF-β signaling. *Cellular Signalling*, *52*, 112–120. https://doi.org/10.1016/j.cellsig.2018.09.002

Victoria, B., Dhahbi, J. M., Nunez Lopez, Y. O., Spinel, L., Atamna, H., Spindler, S. R., & Masternak, M. M. (2015). Circulating microRNA signature of genotype-by-age interactions in the long-lived Ames dwarf mouse. *Aging Cell*, *14*(6), 1055–1066. https://doi.org/10.1111/acel.12373

Vitulo, N., Forcato, C., Carpinelli, E. C., Telatin, A., Campagna, D., D'Angelo, M., … Valle, G. (2014). A deep survey of alternative splicing in grape reveals changes in the splicing machinery related to tissue, stress condition and genotype. *BMC Plant Biology*, *14*(1), 99. https://doi.org/10.1186/1471-2229-14-99

Vlachos, I. S., Zagganas, K., Paraskevopoulou, M. D., Georgakilas, G., Karagkouni, D., Vergoulis, T., … Hatzigeorgiou, A. G. (2015). DIANA-miRPath v3.0: Deciphering microRNA function with experimental support. *Nucleic Acids Research*, *43*(W1), W460–W466. https://doi.org/10.1093/nar/gkv403

Wang, A., Hu, N., Zhang, Y., Chen, Y., Su, C., Lv, Y., & Shen, Y. (2019). MEG3 promotes proliferation and inhibits apoptosis in osteoarthritis chondrocytes by miR-361-5p/FOXO1 axis. *BMC Medical Genomics*, *12*(1), 201. https://doi.org/10.1186/s12920-019-0649-6

Wang, L., Cui, M., Qu, F., Cheng, D., Yu, J., Tang, Z., … Liu, X. (2021). MiR-92a-3p Promotes the Malignant Progression of Hepatocellular Carcinoma by Mediating the PI3K/AKT/mTOR Signaling Pathway. *Current Pharmaceutical Design*, *27*(29), 3244–3250. https://doi.org/10.2174/1381612827666210612054156

Wang, Z., Gao, J., & Xu, C. (2022). Tackling cellular senescence by targeting miRNAs. *Biogerontology*, *23*(4), 387–400. https://doi.org/10.1007/s10522-022-09972-z

Watanabe, S., Kawamoto, S., Ohtani, N., & Hara, E. (2017). Impact of senescence-associated secretory phenotype and its potential as a therapeutic target for senescence-associated diseases. *Cancer Science*, *108*(4), 563–569. https://doi.org/10.1111/cas.13184

Wei, W., & Ji, S. (2018). Cellular senescence: Molecular mechanisms and pathogenicity. *Journal of Cellular Physiology*, *233*(12), 9121–9135. https://doi.org/10.1002/jcp.26956

Weinhouse, C., Truong, L., Meyer, J. N., & Allard, P. (2018). Caenorhabditis elegans as an emerging model system in environmental epigenetics. *Environmental and Molecular Mutagenesis*, *59*(7), 560–575. https://doi.org/10.1002/em.22203

Westerheide, S. D., Anckar, J., Stevens, S. M., Sistonen, L., & Morimoto, R. I. (2009). Stress-inducible regulation of heat shock factor 1 by the deacetylase SIRT. *Science*, *323*(5917), 1063–1066. https://doi.org/10.1126/science.1165946

Williams, G. C. (1957). Pleiotropy, Natural Selection, and the Evolution of Senescence. *Evolution*, *11*(4), 398. https://doi.org/10.2307/2406060

Williams, J., Smith, F., Kumar, S., Vijayan, M., & Reddy, P. H. (2017). Are microRNAs true sensors of ageing and cellular senescence? *Ageing Research Reviews*, *35*, 350–363. https://doi.org/10.1016/j.arr.2016.11.008

Wlaschek, M., Maity, P., Makrantonaki, E., & Scharffetter-Kochanek, K. (2021). Connective

Tissue and Fibroblast Senescence in Skin Aging. *Journal of Investigative Dermatology*, *141*(4), 985–992. https://doi.org/10.1016/j.jid.2020.11.010

Wood, J. G., Regina, B., Lavu, S., Hewitz, K., Helfand, S. L., Tatar, M., & Sinclair, D. (2004). Sirtuin activators mimic caloric restriction and delay ageing in metazoans. *Nature*, *430*(7000), 686–689. https://doi.org/10.1038/nature02789

Wrigley, J. D., Gavory, G., Simpson, I., Preston, M., Plant, H., Bradley, J., … Andrews, D. M. (2017). Identification and characterisation of dual inhibitors of the USP25/28 Deubiquitinating enzyme subfamily. *ACS Chemical Biology*, acschembio.7b00334. https://doi.org/10.1021/acschembio.7b00334

Wu, B., Liu, G., Jin, Y., Yang, T., Zhang, D., Ding, L., … Wei, Y. (2020). miR-15b-5p Promotes Growth and Metastasis in Breast Cancer by Targeting HPSE2. *Frontiers in Oncology*, *10*. https://doi.org/10.3389/fonc.2020.00108

Wu, S., Kim, T. K., Wu, X., Scherler, K., Baxter, D., Wang, K., … Dai, J. (2016). Circulating MicroRNAs and Life Expectancy Among Identical Twins. *Annals of Human Genetics*, *80*(5), 247–256. https://doi.org/10.1111/ahg.12160

Wu, X., Xi, X., Yan, Q., Zhang, Z., Cai, B., Lu, W., & Wan, X. (2013). MicroRNA-361-5p facilitates cervical cancer progression through mediation of epithelial-to-mesenchymal transition. *Medical Oncology*, *30*(4), 751. https://doi.org/10.1007/s12032-013-0751-0

Xia, W., Chen, H., Xie, C., & Hou, M. (2020). Long-noncoding RNA MALAT1 sponges microRNA-92a-3p to inhibit doxorubicin-induced cardiac senescence by targeting ATG4a. *Aging*, *12*(9), 8241–8260. https://doi.org/10.18632/aging.103136

Yamada, N. O., & Senda, T. (2021). Circulating microRNA-92a-3p in colorectal cancer: a review. *Medical Molecular Morphology*, *54*(3), 193–202. https://doi.org/10.1007/s00795-

021-00282-w

Yamakuchi, M., & Hashiguchi, T. (2018). Endothelial Cell Aging: How miRNAs Contribute? *Journal of Clinical Medicine*, *7*(7), 170. https://doi.org/10.3390/jcm7070170

Yang, D., Guo, P., He, T., & Powell, C. A. (2021). Role of endothelial cells in tumor microenvironment. *Clinical and Translational Medicine*, *11*(6), e450. https://doi.org/10.1002/ctm2.450

Yang, J., Huang, Q., Guo, Y., Wei, Z., Zhou, L., & Chen, H. (2021). DIAPH1 Promotes Laryngeal Squamous Cell Carcinoma Progression Through Cell Cycle Regulation. *Frontiers in Oncology*, *11*, 716876. https://doi.org/10.3389/fonc.2021.716876

Yang, N. C., & Hu, M. L. (2005). The limitations and validities of senescence associated-β-galactosidase activity as an aging marker for human foreskin fibroblast Hs68 cells. *Experimental Gerontology*, *40*(10), 813–819. https://doi.org/10.1016/j.exger.2005.07.011

Yang, W., & Xie, T. (2020). Hsa_circ_CSPP1/MiR-361-5p/ITGB1 Regulates Proliferation and Migration of Cervical Cancer (CC) by Modulating the PI3K-Akt Signaling Pathway. *Reproductive Sciences*, *27*(1), 132–144. https://doi.org/10.1007/s43032-019-00008-5

Yi, R., Qin, Y., Macara, I. G., & Cullen, B. R. (2003). Exportin-5 mediates the nuclear export of pre-microRNAs and short hairpin RNAs. *Genes and Development*, *17*(24), 3011–3016. https://doi.org/10.1101/gad.1158803

Yin, L. C., Xiao, G., Zhou, R., Huang, X. P., Li, N. L., Tan, C. L., … Liu, L. X. (2020). MicroRNA-361-5p Inhibits Tumorigenesis and the EMT of HCC by Targeting Twist1. *BioMed Research International*, *2020*, 8891876. https://doi.org/10.1155/2020/8891876

Yosef, R., Pilpel, N., Papismadov, N., Gal, H., Ovadya, Y., Vadai, E., … Krizhanovsky, V. (2017). p21 maintains senescent cell viability under persistent DNA damage response by

restraining JNK and caspase signaling . *The EMBO Journal*, *36*(15), 2280–2295. https://doi.org/10.15252/embj.201695553

Yosef, R., Pilpel, N., Tokarsky-Amiel, R., Biran, A., Ovadya, Y., Cohen, S., … Krizhanovsky, V. (2016). Directed elimination of senescent cells by inhibition of BCL-W and BCL-XL. *Nature Communications*, *7*, 11190. https://doi.org/10.1038/ncomms11190

Yoshida, K., Yokoi, A., Kato, T., Ochiya, T., & Yamamoto, Y. (2020). The clinical impact of intra- and extracellular miRNAs in ovarian cancer. *Cancer Science*, *111*(10), 3435–3444. https://doi.org/10.1111/cas.14599

Yu, G., Wang, L.-G., Han, Y., & He, Q.-Y. (2012). clusterProfiler: an R package for comparing biological themes among gene clusters. *Omics : A Journal of Integrative Biology*, *16*(5), 284–287. https://doi.org/10.1089/omi.2011.0118

Yu, X., Li, R., Shi, W., Jiang, T., Wang, Y., Li, C., & Qu, X. (2016). Silencing of MicroRNA-21 confers the sensitivity to tamoxifen and fulvestrant by enhancing autophagic cell death through inhibition of the PI3K-AKT-mTOR pathway in breast cancer cells. *Biomedicine and Pharmacotherapy*, *77*, 37–44. https://doi.org/10.1016/j.biopha.2015.11.005

Zhang, H. S., Gavin, M., Dahiya, A., Postigo, A. A., Ma, D., Luo, R. X., … Dean, D. C. (2000). Exit from G1 and S phase of the cell cycle is regulated by repressor complexes containing HDAC-Rb-hSWI/SNF and RB-hSWI/SNF. *Cell*, *101*(1), 79–89. https://doi.org/10.1016/S0092-8674(00)80625-X

Zhang, H., Yang, H., Zhang, C., Jing, Y., Wang, C., Liu, C., … Li, D. (2015). Investigation of MicroRNA expression in human serum during the aging process. *Journals of Gerontology - Series A Biological Sciences and Medical Sciences*, *70*(1), 102–109. https://doi.org/10.1093/gerona/glu145

Zhang, J. W., Zhang, D., & Yu, B. P. (2021). Senescent cells in cancer therapy: why and how to remove them. *Cancer Letters*, *520*, 68–79. https://doi.org/10.1016/j.canlet.2021.07.002

Zhang, R., Poustovoitov, M. V., Ye, X., Santos, H. A., Chen, W., Daganzo, S. M., … Adams, P. D. (2005). Formation of macroH2A-containing senescence-associated heterochromatin foci and senescence driven by ASF1a and HIRA. *Developmental Cell*, *8*(1), 19–30. https://doi.org/10.1016/j.devcel.2004.10.019

Zhang, S., Li, F., Zhou, T., Wang, G., & Li, Z. (2020). Caenorhabditis elegans as a Useful Model for Studying Aging Mutations. *Frontiers in Endocrinology*, *11*, 554994. https://doi.org/10.3389/fendo.2020.554994

Zhang, W., Chang, G., Cao, L., & Ding, G. (2021). Dysregulation of serum miR-361-5p serves as a biomarker to predict disease onset and short-term prognosis in acute coronary syndrome patients. *BMC Cardiovascular Disorders*, *21*(1), 74. https://doi.org/10.1186/s12872-021-01891-0

Zhang, X., Wei, C., Li, J., Liu, J., & Qu, J. (2017). MicroRNA-361-5p inhibits epithelial-to-mesenchymal transition of glioma cells through targeting Twist1. *Oncology Reports*, *37*(3), 1849–1856. https://doi.org/10.3892/or.2017.5406

Zhang, Z., Liu, X., Xu, H., Feng, X., Lin, Y., Huang, Y., … Gu, M. (2018). Obesity-induced upregulation of miR-361-5p promotes hepatosteatosis through targeting Sirt1. *Metabolism: Clinical and Experimental*, *88*, 31–39. https://doi.org/10.1016/j.metabol.2018.08.007

Zhao, C., Li, Y., Chen, G., Wang, F., Shen, Z., & Zhou, R. (2017). Overexpression of miR-15b-5p promotes gastric cancer metastasis by regulating PAQR3. *Oncology Reports*, *38*(1), 352–358. https://doi.org/10.3892/or.2017.5673

Zheng, S. R., Huang, Q. Di, Zheng, Z. H., Zhang, Z. T., & Guo, G. L. (2021). CircGFRA1 affects

the sensitivity of triple-negative breast cancer cells to paclitaxel via the miR-361-5p/TLR4 pathway. *Journal of Biochemistry*, *169*(5), 601–611. https://doi.org/10.1093/jb/mvaa148

Zhou, C., Jiang, X., Liang, A., Zhu, R., Yang, Y., Zhong, L., & Wan, D. (2020). COX10-AS1 Facilitates Cell Proliferation and Inhibits Cell Apoptosis in Glioblastoma Cells at Post-Transcription Level. *Neurochemical Research*, *45*(9), 2196–2203. https://doi.org/10.1007/s11064-020-03081-4

Zhou, M., Cai, J., Tang, Y., & Zhao, Q. (2013). MiR-17-92 cluster is a novel regulatory gene of cardiac ischemic/reperfusion injury. *Medical Hypotheses*, *81*(1), 108–110. https://doi.org/10.1016/j.mehy.2013.03.043

Zhu, J., Yang, S., Qi, Y., Gong, Z., Zhang, H., Liang, K., … Fang, X. (2022). Stem cell–homing hydrogel-based miR-29b-5p delivery promotes cartilage regeneration by suppressing senescence in an osteoarthritis rat model. *Science Advances*, *8*(13), eabk0011. https://doi.org/10.1126/sciadv.abk0011

Zhu, Y., Tchkonia, T., Fuhrmann-Stroissnigg, H., Dai, H. M., Ling, Y. Y., Stout, M. B., … Kirkland, J. L. (2016). Identification of a novel senolytic agent, navitoclax, targeting the Bcl-2 family of anti-apoptotic factors. *Aging Cell*, *15*(3), 428–435. https://doi.org/10.1111/acel.12445

Zhuang, Z. L., Tian, F. M., & Sun, C. L. (2016). Downregulation of miR-361-5p associates with aggressive clinicopathological features and unfavorable prognosis in non-small cell lung cancer. *European Review for Medical and Pharmacological Sciences*, *20*(24), 5132–5136.

Appendices

Appendix I Assessment of differentially regulated microRNAs in early and late passage human primary endothelial cells

The identity of each miRNA and the logged expression of each in early passage (PD = 36) and late passage cells (PD = 84) respectively are given (n = 3 biological replicates), along with the fold change, the raw p value and the FDR adjusted p value. The thresholds for nominal and FDR adjusted significance are indicated by grey bars.

miRNA	Old Avg (log2)	Young Avg (log2)	Fold Change	P-val	FDR-adj
hsa-miR-6850-5p	2.33	7.61	-38.69	5.71E-12	0.000247525
hsa-miR-4687-3p	2.15	7.03	-29.59	1.19E-10	0.00049505
hsa-miR-7108-5p	2.43	7.24	-28.03	1.29E-10	0.000742574
hsa-miR-4632-5p	1.43	4.82	-10.49	1.72E-10	0.000990099
hsa-miR-4530	1.77	5.78	-16.12	1.08E-09	0.001237624
hsa-miR-4505	1.32	4.96	-12.51	2.04E-09	0.001485149
hsa-miR-5001-5p	1.93	6.08	-17.67	2.05E-09	0.001732673
hsa-miR-1227-5p	2.24	5.75	-11.44	2.98E-09	0.001980198
hsa-miR-4270	1.81	4.3	-5.6	2.56E-08	0.002227723
hsa-miR-4486	1.4	3.95	-5.88	3.04E-08	0.002475248
hsa-miR-6821-5p	1.93	6.59	-25.29	3.36E-08	0.002722772
hsa-miR-6858-5p	2.23	6.3	-16.85	3.43E-08	0.002970297
U43	1.62	5.6	-15.76	3.79E-08	0.003217822
hsa-miR-4635	1.51	3.94	-5.39	4.41E-08	0.003465347
hsa-miR-101-5p	1.45	4.25	-6.94	4.49E-08	0.003712871
hsa-miR-3621	1.94	5.94	-16.07	4.80E-08	0.003960396
hsa-let-7i-5p	1.13	3.3	-4.51	6.12E-08	0.004207921
hsa-mir-6089-1	1.6	3.71	-4.33	7.01E-08	0.004455446
hsa-mir-6089-2	1.6	3.71	-4.33	7.01E-08	0.00470297
U43	2.06	6.02	-15.56	7.80E-08	0.004950495
hsa-miR-4739	1.7	5.04	-10.14	8.22E-08	0.00519802
hsa-miR-6880-5p	1.74	4.13	-5.22	9.79E-08	0.005445545
hsa-miR-4651	1.8	5.31	-11.39	1.49E-07	0.005693069
hsa-miR-4674	2.35	7.56	-36.95	1.52E-07	0.005940594
hsa-miR-3195	1.33	3.45	-4.35	1.64E-07	0.006188119
hsa-miR-6722-3p	1.49	4.83	-10.17	1.68E-07	0.006435644
hsa-miR-6791-5p	2.41	7.62	-36.91	1.70E-07	0.006683168
hsa-miR-6743-5p	2.17	5.64	-11.08	1.76E-07	0.006930693
hsa-miR-328-5p	2.02	5.31	-9.8	2.43E-07	0.007178218
hsa-miR-4741	1.56	4.81	-9.49	2.67E-07	0.007425743
hsa-miR-6805-5p	2.58	6.97	-21.07	3.20E-07	0.007673267
hsa-miR-8075	7.56	4.94	6.14	3.25E-07	0.007920792

hsa-miR-365b-5p	1.43	2.99	-2.95	3.34E-07	0.008168317
hsa-miR-3185	2.45	6.22	-13.64	4.35E-07	0.008415842
hsa-miR-6765-5p	2.53	6.13	-12.11	4.68E-07	0.008663366
hsa-miR-6771-5p	1.1	4.05	-7.73	5.23E-07	0.008910891
hsa-miR-2115-5p	9.29	7.62	3.18	6.18E-07	0.009158416
hsa-miR-4707-5p	2.52	6.87	-20.34	6.19E-07	0.009405941
hsa-miR-4763-3p	1.87	6.93	-33.56	6.63E-07	0.009653465
hsa-miR-1228-5p	2.79	7.19	-21.04	7.10E-07	0.00990099
hsa-miR-193a-5p	1.73	3.09	-2.58	7.30E-07	0.010148515
hsa-miR-4281	2.14	5.46	-9.95	9.86E-07	0.01039604
hsa-miR-3620-5p	1.55	4.41	-7.26	1.17E-06	0.010643564
hsa-miR-4758-5p	1.67	4.18	-5.7	1.42E-06	0.010891089
hsa-miR-6808-3p	7.46	6.14	2.49	1.73E-06	0.011138614
hsa-miR-4532	1.79	3.85	-4.18	1.78E-06	0.011386139
hsa-miR-4463	1.91	3.44	-2.9	1.85E-06	0.011633663
hsa-miR-1233-5p	1.66	3.82	-4.47	2.56E-06	0.011881188
hsa-miR-6781-5p	1.65	2.92	-2.41	2.63E-06	0.012128713
hsa-miR-4740-3p	1.27	2.88	-3.05	3.16E-06	0.012376238
hsa-miR-16-5p	1.36	3.58	-4.66	4.11E-06	0.012623762
hsa-miR-4492	1.52	4.22	-6.53	4.22E-06	0.012871287
hsa-miR-455-3p	9.46	7.33	4.37	5.09E-06	0.013118812
hsa-mir-320e	7.97	5.47	5.66	5.27E-06	0.013366337
hsa-miR-3663-3p	1.55	3.23	-3.21	5.50E-06	0.013613861
hsa-mir-6722	5.01	3.77	2.37	7.22E-06	0.013861386
hsa-miR-6775-5p	2.14	3.9	-3.38	7.92E-06	0.014108911
hsa-miR-4695-5p	1.84	4.62	-6.89	8.13E-06	0.014356436
hsa-miR-6732-5p	8.01	6.27	3.34	8.52E-06	0.01460396
hsa-miR-3180	1.76	3.75	-3.97	9.10E-06	0.014851485
hsa-miR-1909-3p	1.19	3.59	-5.27	1.15E-05	0.01509901
hsa-miR-214-3p	1.56	2.95	-2.63	1.17E-05	0.015346535
hsa-miR-1343-5p	1.82	4.57	-6.74	1.20E-05	0.015594059
hsa-miR-3180-3p	1.56	3.99	-5.38	1.24E-05	0.015841584
hsa-miR-1231	1.32	3.97	-6.27	1.39E-05	0.016089109
hsa-miR-4467	1.87	4.24	-5.19	1.45E-05	0.016336634
hsa-miR-1307-3p	1.66	2.84	-2.27	1.55E-05	0.016584158
hsa-miR-4454	2.02	5.21	-9.15	1.62E-05	0.016831683
hsa-miR-92b-5p	1.62	4.23	-6.1	1.62E-05	0.017079208
hsa-miR-3141	1.92	4.82	-7.48	2.11E-05	0.017326733
hsa-miR-26a-5p	1.98	4.81	-7.1	2.16E-05	0.017574257
hsa-miR-4787-5p	8.21	10.19	-3.93	2.39E-05	0.017821782
hsa-miR-4745-5p	3.1	7.82	-26.48	2.69E-05	0.018069307
hsa-miR-6803-5p	3.76	7.41	-12.61	2.73E-05	0.018316832
hsa-miR-4433b-3p	1.78	2.78	-1.99	2.96E-05	0.018564356
hsa-miR-6794-5p	2.22	3.34	-2.17	3.76E-05	0.018811881

hsa-miR-937-5p	1.67	3.61	-3.86	4.86E-05	0.019059406
hsa-miR-6752-5p	1.42	4.19	-6.84	6.05E-05	0.019306931
hsa-miR-6789-5p	1.58	7.04	-44.15	6.49E-05	0.019554455
hsa-miR-199a-5p	1.09	2.61	-2.86	7.14E-05	0.01980198
hsa-miR-149-3p	2.02	6.85	-28.47	7.18E-05	0.020049505
hsa-miR-6089	8.81	11.23	-5.35	8.08E-05	0.02029703
hsa-miR-212-5p	1.11	2.08	-1.96	8.67E-05	0.020544554
hsa-miR-6723-5p	1.53	2.65	-2.17	9.00E-05	0.020792079
hsa-miR-3665	9.21	11.34	-4.37	9.08E-05	0.021039604
hsa-miR-3940-5p	3.96	8.06	-17.06	9.56E-05	0.021287129
hsa-mir-101-1	1.21	1.82	-1.53	0.0001	0.021534653
hsa-miR-29a-3p	1.28	2.05	-1.7	0.0001	0.021782178
hsa-miR-4330	1.82	3.99	-4.52	0.0001	0.022029703
hsa-miR-4663	2.26	3.55	-2.45	0.0001	0.022277228
hsa-miR-6753-5p	1.81	2.72	-1.88	0.0001	0.022524752
hsa-miR-6798-5p	1.6	2.54	-1.92	0.0001	0.022772277
hsa-mir-6800	3.65	6.66	-8.1	0.0001	0.023019802
hsa-mir-6800	3.82	6.94	-8.69	0.0001	0.023267327
hsa-miR-93-5p	1.32	2.98	-3.15	0.0001	0.023514851
hsa-miR-1207-5p	1.5	3.35	-3.6	0.0002	0.023762376
hsa-mir-4466	1.23	2.17	-1.92	0.0002	0.024009901
hsa-miR-4507	1.34	3.36	-4.04	0.0002	0.024257426
hsa-miR-4734	1.99	7.76	-54.67	0.0002	0.02450495
U44	1.38	2.78	-2.63	0.0002	0.024752475
hsa-let-7e-5p	5.63	3.38	4.76	0.0003	0.025
hsa-miR-22-3p	1.31	3.98	-6.36	0.0003	0.025247525
hsa-miR-27a-3p	1.26	2.19	-1.9	0.0003	0.02549505
hsa-miR-3960	9.39	10.8	-2.65	0.0003	0.025742574
hsa-mir-3960	1.28	2.32	-2.06	0.0003	0.025990099
hsa-miR-574-3p	1.82	2.65	-1.78	0.0003	0.026237624
hsa-miR-5787	7.32	7.93	-1.53	0.0003	0.026485149
hsa-miR-6724-5p	2.37	7.82	-43.69	0.0003	0.026732673
hsa-miR-6756-5p	2.05	3.83	-3.45	0.0003	0.026980198
hsa-miR-8064	1.14	2.07	-1.91	0.0003	0.027227723
hsa-miR-106b-5p	1.36	2.04	-1.61	0.0004	0.027475248
hsa-miR-4508	2.38	7.85	-44.25	0.0004	0.027722772
hsa-miR-4649-5p	1.15	3.16	-4.03	0.0004	0.027970297
hsa-miR-6085	1.75	3.49	-3.35	0.0004	0.028217822
hsa-miR-6860	1.45	2	-1.47	0.0005	0.028465347
hsa-miR-1268a	1.27	2.85	-2.99	0.0006	0.028712871
hsa-miR-31-5p	1.48	2.93	-2.73	0.0006	0.028960396
hsa-miR-6090	9.05	10.64	-3.01	0.0006	0.029207921
hsa-miR-6786-5p	5.19	7.5	-4.97	0.0006	0.029455446
hsa-mir-6880	6.99	6.25	1.67	0.0006	0.02970297
hsa-miR-3178	4.17	7.5	-10.07	0.0007	0.029950495

hsa-miR-3613-3p	1.37	3.42	-4.14	0.0007	0.03019802
hsa-miR-3613-5p	7.96	1.71	75.76	0.0007	0.030445545
hsa-miR-4690-5p	1.09	3.04	-3.87	0.0007	0.030693069
hsa-miR-6800-5p	3.3	8.16	-28.97	0.0008	0.030940594
hsa-miR-8063	1.3	3.19	-3.71	0.0009	0.031188119
hsa-miR-338-5p	1.27	1.98	-1.64	0.001	0.031435644
hsa-miR-5189-3p	5.68	8.37	-6.46	0.001	0.031683168
hsa-miR-6790-5p	1.56	2.89	-2.5	0.001	0.031930693
hsa-mir-101-1	1.29	1.91	-1.54	0.0011	0.032178218
hsa-mir-924	1.63	1.21	1.34	0.0012	0.032425743
hsa-miR-4749-5p	1.46	3.02	-2.96	0.0013	0.032673267
hsa-miR-5189-5p	1.36	2.56	-2.3	0.0016	0.032920792
hsa-miR-6869-5p	7.74	9.17	-2.69	0.0016	0.033168317
hsa-miR-16-2-3p	1.27	2.68	-2.66	0.0017	0.033415842
hsa-miR-6816-5p	3.8	7.62	-14.05	0.0017	0.033663366
hsa-miR-6729-5p	7.12	9.61	-5.6	0.0018	0.033910891
hsa-miR-6806-3p	2.66	4.4	-3.32	0.002	0.034158416
hsa-miR-7704	8.42	10.52	-4.29	0.0021	0.034405941
hsa-mir-4537	1.28	2.1	-1.77	0.0023	0.034653465
hsa-miR-4516	4.89	9.16	-19.22	0.0024	0.03490099
hsa-miR-744-5p	1.34	2.81	-2.78	0.0024	0.035148515
hsa-miR-762	4	8.01	-16.09	0.0024	0.03539604
hsa-mir-7108	2.66	3.2	-1.46	0.0026	0.035643564
hsa-miR-2861	4.81	8.66	-14.4	0.0027	0.035891089
hsa-mir-4449	1.53	2.61	-2.12	0.0027	0.036138614
hsa-miR-6779-5p	1.61	2.72	-2.17	0.0027	0.036386139
hsa-miR-92a-3p	1.38	2.18	-1.74	0.0028	0.036633663
hsa-miR-4498	1.29	3.04	-3.37	0.0029	0.036881188
hsa-miR-4750-5p	1.54	2.85	-2.48	0.003	0.037128713
hsa-miR-663a	4.54	7.85	-9.94	0.0032	0.037376238
hsa-miR-191-5p	1.55	2.6	-2.07	0.0033	0.037623762
hsa-miR-127-3p	1.53	2.3	-1.71	0.0034	0.037871287
hsa-mir-592	1.82	1.33	1.41	0.0035	0.038118812
hsa-miR-3188	1.33	2.21	-1.84	0.0036	0.038366337
hsa-miR-4665-5p	1.58	2.84	-2.4	0.0037	0.038613861
hsa-miR-199a-3p	1.04	3.44	-5.27	0.0039	0.038861386
hsa-miR-199b-3p	1.04	3.44	-5.27	0.0039	0.039108911
hsa-miR-1908-5p	4.94	8.3	-10.26	0.004	0.039356436
hsa-miR-4668-5p	1.44	2.94	-2.82	0.004	0.03960396
hsa-miR-107	1.85	2.92	-2.09	0.0041	0.039851485
hsa-miR-23b-3p	1.58	3.84	-4.79	0.0043	0.04009901
hsa-mir-4750	1.68	1.16	1.43	0.0045	0.040346535
hsa-miR-8069	8.06	10.32	-4.77	0.0045	0.040594059
U32A	1.32	1.82	-1.41	0.0046	0.040841584
U74	1.08	2.32	-2.35	0.0048	0.041089109

hsa-miR-7641	1.18	1.7	-1.43	0.0051	0.041336634
hsa-miR-1237-5p	5.75	8.54	-6.89	0.0052	0.041584158
hsa-miR-221-3p	2.12	6.21	-17	0.0052	0.041831683
hsa-miR-3187-3p	1.38	3.02	-3.12	0.0054	0.042079208
hsa-miR-138-5p	0.87	2.45	-2.99	0.0058	0.042326733
hsa-miR-3190-5p	1.32	2.46	-2.21	0.0059	0.042574257
hsa-mir-330	1.56	1.19	1.3	0.0059	0.042821782
hsa-miR-6125	7.81	9.72	-3.77	0.0059	0.043069307
hsa-mir-885	2.04	2.49	-1.37	0.0059	0.043316832
hsa-miR-3127-5p	1.69	1.02	1.59	0.0061	0.043564356
hsa-miR-6126	1.41	2.07	-1.58	0.0065	0.043811881
hsa-miR-6132	1.18	2.01	-1.79	0.0065	0.044059406
hsa-miR-4466	7.92	9.71	-3.47	0.0066	0.044306931
hsa-miR-6087	7.81	9.55	-3.34	0.0066	0.044554455
hsa-mir-4469	1.47	1.99	-1.44	0.0067	0.04480198
hsa-miR-8072	5.89	7.79	-3.73	0.007	0.045049505
hsa-miR-6749-5p	1.96	3.51	-2.92	0.0076	0.04529703
hsa-mir-6776	2.92	2.49	1.35	0.0076	0.045544554
hsa-miR-125b-5p	2.91	5.85	-7.67	0.0078	0.045792079
hsa-miR-145-5p	0.89	2.15	-2.4	0.0081	0.046039604
hsa-miR-4488	7.67	9.37	-3.25	0.0082	0.046287129
hsa-mir-619	1.39	1.71	-1.25	0.0087	0.046534653
hsa-miR-6787-5p	1.54	3.04	-2.84	0.0093	0.046782178
hsa-mir-33b	1.65	1.31	1.26	0.0094	0.047029703
hsa-miR-4497	9.81	10.33	-1.43	0.0099	0.047277228
hsa-miR-6727-5p	7.59	9.58	-3.96	0.0104	0.047524752
hsa-mir-654	1.35	1.72	-1.29	0.0106	0.047772277
hsa-miR-3196	7.27	9.11	-3.58	0.0111	0.048019802
hsa-miR-361-5p	1.64	2.24	-1.52	0.0114	0.048267327
hsa-mir-3918	1.73	1.06	1.59	0.0114	0.048514851
hsa-miR-633	1.08	1.37	-1.22	0.0129	0.048762376
hsa-miR-222-3p	2.01	6.55	-23.26	0.0131	0.049009901
hsa-miR-1915-3p	7.51	9.39	-3.69	0.0134	0.049257426
U33	1.44	2.62	-2.27	0.0136	0.04950495
hsa-mir-5703	2.12	2.76	-1.56	0.0138	0.049752475
hsa-miR-3656	6.05	7.79	-3.34	0.014	0.05

Appendix II: Assessment of differentially regulated microRNAs in late passage human primary endothelial cells treated with resveratrol.

The identity of each miRNA and the logged expression of each in vehicle (DMSO) treated late passage cells (PD = 84) and late passage, but resveratrol-treated cells (PD = 84) are given, along with the fold change, the raw p value and the FDR adjusted p value. The thresholds for nominal and FDR adjusted significance are indicated by grey bars.

miRNA	Control (log2)	Resveratrol (log2)	Fold Change	P-val	FDR P-val
hsa-miR-5787	2.65	3.47	-1.76	1.80E-05	0.000495
hsa-miR-3665	1.8	3.55	-3.36	0.0007	0.00099
hsa-miR-361-5p	1.36	0.87	1.41	0.0011	0.001485

Appendix III: Validation of bioinformatically predicted miR-361-5p target genes in relation to cellular senescence in human primary endothelial cells.

The identity of the predicted gene, its fold change in late passage (PD = 84) human primary endothelial cells compared with early passage cells (PD = 36) is given, the raw p value and the FDR adjusted p value is given. ND = not determined NA = not applicable.

Gene	Fold change	p value	FDR
LUM	-1130.18	1.45E-08	0.001538
LPAR1	-136.53	4.59E-08	0.003077
PDCD4	-15.33	7.28E-08	0.004615
TGFBR1	-15.92	1.55E-07	0.006154
RAD23B	-18.2	3.76E-07	0.007692
LDLR	-13.34	1.07E-06	0.009231
DAG1	-8.99	1.60E-06	0.010769
DIAPH1	-6.29	2.64E-06	0.012308
SDC4	-14.9	5.53E-06	0.013846
CCND2	-13.22	5.67E-06	0.015385
RHOA	-10.51	5.91E-06	0.016923
RECK	-44.97	1.04E-05	0.018462
RAD23A	-16.13	1.43E-05	0.02
ARFGEF1	-4.6	2.15E-05	0.021538
EZR	19.35	2.84E-05	0.023077
PRPF8	-9.8	3.96E-05	0.024615
MDM2	-5.06	5.41E-05	0.026154
ZMAT3	-14.88	6.19E-05	0.027692
DHX16	-5.45	6.20E-05	0.029231
MSH6	-5.83	6.94E-05	0.030769
IQGAP1	-5.02	8.47E-05	0.032308
HNRNPM	-6.07	8.50E-05	0.033846
ARPC5L	3.92	8.69E-05	0.035385
PRKDC	-11.29	9.38E-05	0.036923
FN1	-8.79	0.0001	0.038462
TWIST1	-5.94	0.0001	0.04
VCL	-9.31	0.0001	0.041538
ACTN4	-5.13	0.0002	0.043077
VIM	-3.67	0.0002	0.044615
AMFR	-5.78	0.0003	0.046154
SNRNP200	-7.59	0.0003	0.047692
WASL	-5.08	0.0003	0.049231
FDR significance threshold			
SSR1	-3.21	0.0004	0.050769
MCL1	-2.23	0.0007	0.052308
HNRNPA1	-2.88	0.0009	0.053846
STAG2	-3.36	0.0009	0.055385

CCNG1	-4.92	0.0014	0.056923
CDC7	-1.97	0.0018	0.058462
SEL1L	-1.95	0.002	0.06
PDIA6	-5.65	0.0022	0.061538
SRSF1	-3.11	0.0022	0.063077
SEPT11	-1.99	0.0028	0.064615
ZFYVE16	-2.01	0.0029	0.066154
NEDD4L	3.01	0.0034	0.067692
XIAP	-5.72	0.0036	0.069231
VEGFA	-3.1	0.0045	0.070769
SNRPC	-2.74	0.0048	0.072308
UBE2E2	-2.98	0.0051	0.073846
UGGT1	-3.44	0.006	0.075385
RAB5B	-1.73	0.0063	0.076923
UBR5	-5.43	0.0063	0.078462
CHMP1B	-1.74	0.0066	0.08
STT3B	1.61	0.0067	0.081538
SAE1	-2.61	0.0069	0.083077
FRS2	-3.51	0.0074	0.084615
ACAP2	-1.99	0.0107	0.086154
KIF23	-1.79	0.0118	0.087692
CD2AP	1.98	0.0119	0.089231
HSPH1	2.93	0.0156	0.090769
E2F5	-1.83	0.0176	0.092308
NCKAP1	-2.02	0.0247	0.093846
LMAN1	-1.42	0.0361	0.095385
ORC6	-1.67	0.0437	0.096923
BIRC5	-1.28	0.0451	0.098462
YOD1	-1.64	0.0493	0.1

Appendix IV: Quantitative real-time PCR validation of changes in miR-361-5p expression with senescence.

Expression levels of miR-361-5p in early passage (PD = 36) and late passage (PD = 84) human primary fibroblasts is given. N = 3 biological replicates, each assessed in 3 technical replicates relative to the Geometric mean of expression of the endogenous control genes miR-24, miR-10b and miR-15. AU = arbitrary units. ** = p<0.01

A

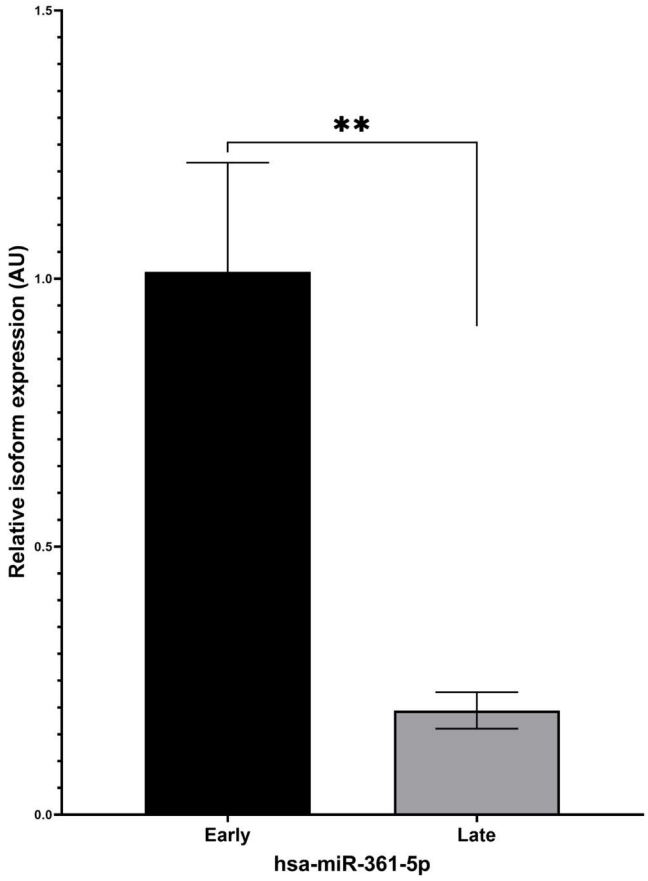

B

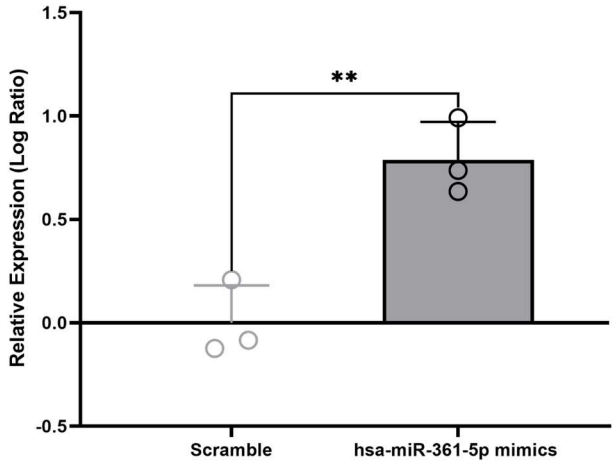

Appendix V: The transfection efficiency of NHDF and HAoECs using the lipofectamine 3000©. Error bar is 50 µm.

A

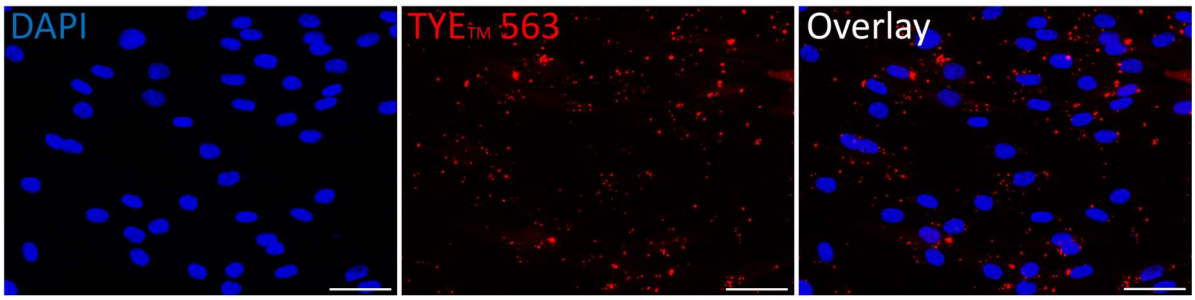

B

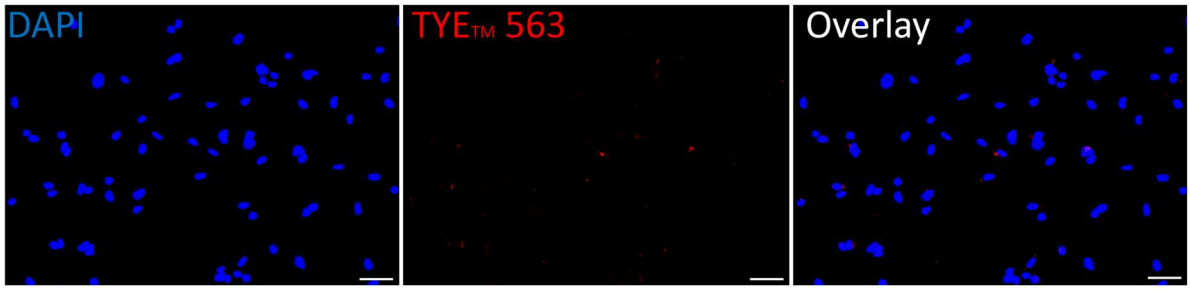

Appendix VI: Control for the *C. elegans* RNAi experiment. Daf-16 reduced the lifespan and age-1 increased the lifespan upon knocking down

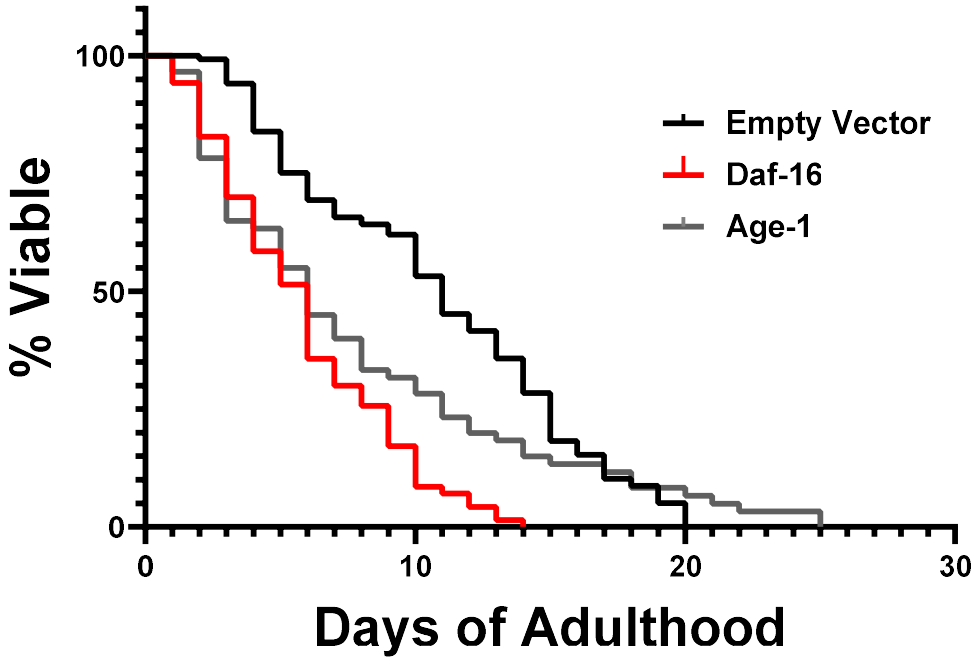

Appendix VII: The list of *C. elegans* orthologs of human genes and their RNAi used in this thesis that were targeted by the miR-361-5p and miR-15b-5p

Human		*C. elegans*			
Gene Name	Gene ID	Ortholog Gene Name	Sequence ID	Genetic position	Source Bioscience Location
ARPC5L	ENSG00000136950	C46H11.3	C46H11.3	I:-0.42 +/- 0.000 cM (interpolated)	I-2A18
EZR	ENSG00000092820	erm-1	C01G8.5	I:-0.16 +/- 0.005 cM	I-2I14
AMFR	ENSG00000159461	hrdl-1	F26E4.11	I:3.91 +/- 0.001 cM	I-4L12
HNRNPM	ENSG00000099783	sup-46	C25A1.4	I:4.72 +/- 0.000 cM	I-5G19
IQGAP1	ENSG00000140575	pes-7	F09C3.1	I:24.15 +/- 0.021 cM	I-7K17
CCND2	ENSG00000118971	cyd-1	Y38F1A.5	II:13.29 +/- 0.136 cM	II-8F09
FN1	ENSG00000115414	let-805	H19M22.2	III:-10.86 +/- 0.073 cM	III-1J01
DIAPH1	ENSG00000131504	cyk-1	F11H8.4	III:-0.83 +/- 0.009 cM	III-3P11
PRPF8	ENSG00000174231	prp-8	C50C3.6	III:-0.37 +/- 0.000 cM	III-4G10
TGFBR1	ENSG00000106799	daf-1	F29C4.1	IV:-26.90 +/- 0.008 cM	IV-1C09
WASL	ENSG00000106299	wsp-1	C07G1.4	IV:3.66 +/- 0.003 cM	IV-4K15
VCL	ENSG00000035403	deb-1	ZC477.9	IV:3.29 +/- 0.000 cM	IV-9A03
RHOA	ENSG00000067560	rho-1	Y51H4A.3	IV:15.09 +/- 0.001 cM	IV-9L11
ACTN4	ENSG00000130402	atn-1	W04D2.1	V:4.31 +/- 0.022 cM	V-8I08
TWIST1	ENSG00000122691	hlh-8	C02B8.4	X:-0.53 +/- 0.011 cM	X-4M03
VIM	ENSG00000026025	ifa-1	F38B2.1	X:2.87 +/- 0.001 cM	X-5M06
SDC4	ENSG00000124145	sdn-1	F57C7.3	X:2.31 +/- 0.010 cM	X-8E06
DAG1	ENSG00000173402	dgn-2	F56C3.6	X:-18.21 +/- 0.052 cM	X-8H06
INMT	ENSG00000241644	anmt-3	T07C12.9	V:2.22 +/- 0.000 cM	V-6N22
ZMPSTE24	ENSG00000084073	fce-1	C04F12.10	I:3.86 +/- 0.001 cM	I-4H24
FOXO3	ENSG00000118689	daf-16	R13H8.1	I:5.08 +/- 0.026 cM	I-5M24
PIK3CG	ENSG00000105851	age-1	B0334.8	II:3.61 +/- 0.011 cM	II-7J02

Appendix VIII: Submitted manuscript (Chapter 3 and Chapter 4)

An evaluation of the role of miR-361-5p in senescence and systemic ageing

Emad Manni[1], Nicola Jeffery[1], David Chambers[2], Luke Slade[3], Timothy Etheridge[3] and Lorna W. Harries[1*]

[1] University of Exeter Medical School, Faculty of Health and Life Sciences, Barrack Road, Exeter, EX2 5DW, UK

[2]Wolfson Centre for Age-Related Diseases, King's College London, London WC2R 2LS, UK

[3]Department of Sport and Health Sciences, College of Life and Environmental Sciences, University of Exeter, Exeter, EX1 2LU, UK

Corresponding Author

Professor L.W. Harries,

Institute of Biomedical and Clinical Sciences,

University of Exeter Medical School,

Barrack Road,

EX2 5DW,

UK.

Tel: 44-1392-406773

Email: L.W.Harries@exeter.ac.uk

Keywords: miRNA; miR-361-5p; human endothelial cells; senescence; lifespan; *C. elegans*

Abstract

Senescent cells are key regulators of ageing and age-associated disease. MicroRNAs (miRs) are a key component of the molecular machinery governing cellular senescence, with several known to regulate important genes associated with this process.

We sought to identify miRs associated with both senescence and reversal by pinpointing those showing opposing directionality of effect in senescence and in response to senotherapy. Cellular senescence phenotypes were assessed in primary human endothelial cells following targeted manipulation of emergent miRNAs. Finally, the effect of conserved target gene knockdown on lifespan and healthspan was assessed in a *C. elegans* system *in vivo*.

Three miRNAs (miR-5787, miR-3665 and miR-361-5p) demonstrated associations with both senescence and rejuvenation, but miR-361-5p alone demonstrated opposing effects in senescence and rescue. Treatment of late passage human endothelial cells with a miR-361-5p mimic caused a 14% decrease in the senescent load of the culture. RNAi gene knockdown of conserved miR-361-5p target genes in a *C. elegans* model however resulted in adverse effects on healthspan and/or lifespan.

Although miR-361-5p may attenuate aspects of the senescence phenotype in human primary endothelial cells, many of its validated target genes also play essential roles in the regulation or formation of the cytoskeletal network, or its interaction with the extracellular matrix. These processes are essential for cell survival and cell function. Targeting miR-361-5p alone would not represent a promising target for future senotherapy; more sophisticated approaches to attenuate its interaction with specific targets without roles in essential cell processes would be required.

Introduction

Organismal ageing and its associated biochemical and cellular changes are major risk factors for the development of common, complex disease [1]. It is now becoming apparent that age-related disorders share a common set of triggers [2]. The factors leading to ageing remain elusive, but there are consistent changes in cell biology that occur in ageing cells, which are known collectively as the 'hallmarks of ageing'. The original hallmarks include alteration of intracellular communication, stem cell exhaustion, genomic instability, shortening of telomere length, loss of proteostasis, epigenetic alteration, dysregulation of nutrient sensing, malfunction of mitochondria, and cellular senescence [3]. More recently, additional hallmarks including compromised autophagy, microbiome disturbance, altered mechanical properties, inflammation and splicing dysregulation have been proposed [4].

Cellular senescence is defined as the irreversible exit from cell cycle that occurs at the end of the replicative lifespan of a cell. Senescent cells are alive and metabolically active, but exhibit characteristic differences to their non-senescent counterparts [5]. These include morphological and functional changes, which in most cases include the secretion of the senescence-associated secretory phenotype (SASP); a cocktail of cytokines and remodelling proteins [6]. The most compelling evidence for senescent cells as drivers of ageing involve selective ablation of senescent cells in transgenic mice demonstrated elegantly that the presence of such cells shortened healthy lifespan [7] and the removal of these is able to prevent several age-associated diseases [8]. Follow on work has since demonstrated links between the presence of senescent

cells and multiple ageing phenotypes [9-11]. Accordingly, approaches to selectively ablate or regenerate senescent cells *in vivo* (senotherapeutics) are now the subject of intense study as future therapeutics which are already demonstrating promise in human systems [12,13].

Cellular senescence can arise from repeated and unresolved cellular stress [14]. Cells have a battery of molecular responses to stress, one of which is the microRNA (miRNA) response [15,16]. MicroRNAs are small RNA molecules of approximately 22 nucleotides in length that are pivotal regulators of gene expression and have roles in many aspects of cell development, proliferation, and apoptosis [17]. In accordance with their fundamental importance in complex cellular processes and in systemic ageing, studies have reported associations between miRNA profiles and age-related phenotypes [18-20], and between individual miRNA and cellular senescence itself [21,22]. The small size of miRNA, the relative ease of high throughput methods for measuring them and the ready availability of reagents for their evaluation *in vitro* has highlighted them as a promising therapeutic avenue [23].

In this study, we aimed to identify miRNAs contributory to the establishment of senescence, and to characterise the effect of targeted manipulation of candidate miRNAs *in vitro* and of their validated target genes *in vivo*. We first sought to identify miRNAs demonstrating opposing directionality of expression in senescent primary human endothelial cells, and in those that had undergone small-molecule induced partial rejuvenation. We then evaluated the effect of targeted manipulation of miRNAs displaying opposing direction of effect in senescence and rejuvenation on senescence

phenotypes in primary human endothelial cells *in vitro.* Finally, we determined the effect of knockdown of target genes of candidate miRs on lifespan and healthspan measures in an invertebrate model system *C. elegans*. We identified 3 miRNAs (miR-5787, miR-3665 and miR-361-5p) which demonstrated dysregulated expression in both datasets, but only one, miR-361-5p, exhibited opposing directionality. Treatment of primary senescent endothelial cell cultures with an miR-361-5p mimic to replicate expression levels in early passage cells brought about a reduction in senescent cell load of the culture. We determined that 65 validated miR-361-5p target genes were expressed in human primary endothelial cells, of which 32 demonstrated differential expression in senescent cells. 16 senescence-related miR-361-5p target genes had direct *C. elegans* orthologues, many of which were involved in regulation of cytoskeletal function and interaction with the extracellular matrix. Targeted RNAi gene knockdown of these revealed that 9/16 had statistically significant adverse effects on lifespan. Furthermore, 14/16 miR-361-5p target genes also reduced healthspan, as measured by decreased movement. Our work suggests that although miR-361-5p may be contributory to the senescent cell phenotype, it also targets multiple genes that are essential for cellular health and function, meaning that simply elevating its expression is not currently likely to be fruitful as a target for senotherapy.

Materials and Methods

Cell culture conditions and assessment of senescence kinetics

Commercially procured primary human aortic endothelial cells (HAoEC; C-12271, PromoCell, Germany) were cultured and propagated in C-22022 medium (Promocell,

Germany) with 1% penicillin and 1% streptomycin at 37˚C and 5% CO_2. Replicative senescence was induced by continuous culture as previously described until growth slowed to less than 0.5 population doublings per week[24,25]. Early and late passage cells were at PD= 36 and PD = 84 respectively. For assessment of miRNA response to partial rejuvenation, we assessed response to 5 μM of resveratrol , a polyphenol previously demonstrated to lead to reversal of multiple senescence phenotypes in human primary dermal fibroblasts [25] or with DMSO carrier alone for 48 hours. Cells were seeded at a density of 4.0×10^5 cell/cm^2 in 6-well plates and left to settle for 24 hr prior to treatment.

Senescence was evaluated at 80% confluence by the Senescence Cells Histochemical Staining Kit (Sigma, Aldrich, UK; CS0030) (SA-□-Gal) in 3 biological replicates. Proliferation index and DNA damage foci were also assessed by Ki67 and □H2AX immunofluorescence in 3 biological replicates. In brief, cells were grown on 13 mm coverslips prior to fixation with 4% paraformaldehyde. Primary antibodies were applied at 2.5 μg/ml for 24hrs. After washing, secondary antibodies were applied at 5 μg/ml and DAPI at 1 μg/ml for 1 hour. Coverslips were mounted using Dako mounting medium (S302380-2, Agilent). Antibodies were sourced from Abcam: Rb anti-Ki67 (ab15580, ab16667), Ms anti-γH2AX (ab26350), Alexa Fluor ® 555 Goat pAb to Rb (ab150078, ab150086) and Alexa Fluor ® 488 Goat pAb to Ms (ab150117). Images were captured using the Leica DM4 B Upright Microscope. Statistical significance was determined by one-way AVOVA in GraphPad Prism 8 (GraphPad Software, San Diego, California USA). A minimum of 5 representative image fields were manually counted for each assay, with a minimum of 400 cells assessed for each replicate.

RNA extraction and Purification

Prior to RNA extraction, cells were washed in Dulbecco's phosphate-buffered saline (DPBS) and harvested. Total RNA was then extracted from each biological replicate using 1 mL of Tri reagent® (Thermo Fisher, Waltham, MA, USA) according to the manufacturer's instructions. RNA samples destined for GeneChip miRNome and whole transcriptome analysis were purified further using a RNA Clean & Concentrator kit (Zymo Research, CA, USA) according to the manufacturer's instructions.

Whole miRNome profiling

Transcriptome-wide miRNA patterns of miRNA expression were assessed in early passage (PD = 36), late passage (PD = 84) cells, and in resveratrol or vehicle (DMSO) treated late passage cells (PD = 84) in 3 biological replicates using the GeneChip™ miRNA 4.0 system (Thermo Fisher, Waltham, MA, USA), which allows simultaneous assessment of all miRNAs in miRBase release 20. Sample preparation and gene chip cartridge arrays were performed by a commercial subcontractor (UK Bioinformatics Ltd, Caterham, UK). Data underwent quality control for probeset mean for hybridisation intensity, probeset residual mean which compares probeset signal to residual signal, poly-A positive spike in controls as control genes and positive versus negative area under the curve. SST-RMA was selected to reduce background and normalize intensity (46) following which a differential expression analysis was undertaken using the Transcriptomic Analysis Console (TAC) (Applied Biosystems) software (TAC 4.0.2.10) using the default settings (22, 47). Differences between two groups were identified by one-way ANOVA. Data analysis and statistical significance were completed using GraphPad Prism 8.0 software (GraphPad Software, La Jolla,

CA, USA). Data were adjusted for false discovery rate by Benjamini Hochberg correction.

qRTPCR validation of miR-361-5p expression in senescent cells

To validate our microarray results, we carried out quantitative PCR assessment of the expression of miR-361-5p in a previously untested set of early passage (PD = 36) and late passage (PD = 84) human primary endothelial cells. Assay details are available on request. Cells were assessed in three biological and three technical replicates. Quantitative RTPCR reaction mixes included 2.5 µL Taqman® Universal PCR mastermix II (no AmpErase® UNG) (Thermo Fisher, Waltham, MA, USA), 1.75 µL dH_2O, 0.5 µL cDNA and 0.25 µL Taqman® gene assay (Thermo Fisher, Foster City USA) in a 5 µL reaction volume. Cycling conditions were: 50 °C for 2 min, 95 °C for 10 min and 50 cycles of 15 seconds at 95 °C for 30 s and 1 minute at 60 °C. Reactions were carried out in 3 biological replicates and 3 technical replicates. Endogenous controls were chosen on the basis that they did not display expression change in senescent cells and were miR-24, miR-15 and miR-10b. The relative expression of each target miRNA was determined by the comparative Ct approach and was calculated relative to the geometric mean of the endogenous control genes.

Identification of miR-361-5p target genes and assessment of their expression in senescence

To assess the genuine gene targets of miR-361-5p, we used the DNA intelligent analysis (DIANA) mirPath v3.0 database [26,27], which identifies target genes across multiple prediction programs, and the miRTarBase version 9.0 platform, a database

containing only experimentally validated miRNA target genes [28,29]. All identified target genes were then assessed for expression in human primary endothelial cells and for expression changes in relation to cellular senescence in 3 biological replicates of early and late passage human primary endothelial cells (PDs 36 and 84 respectively). Expression levels of validated miR-361-5p target genes were assessed on the Clariom D Pico GeneChip platform (Thermo Fisher, Waltham, MA, USA) as described above. Sample preparation and gene chip cartridge arrays were performed by a commercial subcontractor (UK Bioinformatics Ltd, Caterham, Surrey). Data QC was carried out as described above to ensure data normality and clustering, and associations between the expression of validated target genes and cellular senescence was then analysed using TAC 4.0.2.10 (Applied Biosystems, Thermo Fisher, Waltham, MA, USA).

Manipulation of miR-361-5p levels using a miRNA mimic.

To determine whether restoring miR-361-5p levels in senescent primary endothelial cells was capable of attenuating senescence, aged cells at PD80 were seeded into 12 well plates at a density of 2 x 10^5 cells/ well and maintained until 70% confluence. Cells were then transfected with 50pmol of a MirVana mimic (Thermo Fisher, Waltham, MA, USA) to miR-361-5p for 24hrs. Transfections were carried out using Lipofectamine 3000 (Thermo Fisher, Waltham, MA, USA) and lipofectamine-only and scramble controls were also performed. The percentage of senescent cells in the culture was then assessed by senescence-associated beta galactosidase staining in duplicate fields of each of 3 biological replicates, with >400 cells per condition assessed. Differences between treated and control cultures assessed for statistical significance by unpaired t-test (SPSS v26, IBM statistics).

Gene Ontology pathway analysis of dysregulated miRNA target genes

Gene Set enrichment analysis (GSEA) was carried out using EnrichR [30] to identify pathways that were enriched in validated target genes of miR-361-5p that were associated with senescence. EnrichR is a webtool designed to determine whether candidate genes from a user-supplied list are present in specific pathways or processes than one would expect by chance. We identified miR-361-5p target genes demonstrating significant associations with cellular senescence in human endothelial cells and queried these for enrichment in Gene Ontology (GO) cellular, molecular, or biological function pathways based on the adjusted *p* value significance (ranking derived from Fisher exact test).

Assessment of the effect of targeted knockdown of miR-361-5p target genes on lifespan and healthspan in C. elegans

C. elegans orthologues corresponding to validated miR-361-5p target genes were identified by comparison of two different databases to maximise the chances of identifying the correct orthologue. Databases were the NCBI HomoloGene database (ncbi.nlm.nih.gov/homologene; Release 68) and the Ortholist 2 database (ortholist.shaye-lab.org), which is based on a meta-analysis of six different orthology-prediction algorithms. 16 miR-361-5p target genes had validated C. elegans orthologues. These were: *rho-1 (RHOA), deb-1 (VCL), daf1 (TGFBR1), ifa-1 (VIM), cyk-1 (DIAPH1), hlh-8 (TWIST1), erm-1 (EZR), atn-1 (ACTN4), let-805 (FN1), sdn-1 (SDC4), wsp-1 (WASL), C46H11.3 (ARPC5L), dgn-2 (DAG1), pes-7 (IQGAP1), hrdl-1 (AMFR)* and *sup-46 (HNRNPM)*. Wild-type Bristol nematodes (N2 Bristol) were obtained from the *Caenorhabditis* Genetics Centre and were maintained on nematode

growth media (NGM) plates plated with Escherichia coli OP50 at 20°C according to previously described methods. Animals were age-synchronised by gravity synchronisation from the L1 stage. RNAi clones were procured from the Ahringer repository and delivered to the animals in 20 mg/mL of *E. coli* OP50 bacteria in liquid NGM. Synchronised L1 larvae were plated on RNAi NGM plates containing (50 mM NaCl, 0.25% (w/v) bacto peptone, 1.7% (w/v) agar, 1 mM CaCl2, 1 mM MgSO4, 25 mM KH2PO4 (pH 6), 12.9μM cholesterol, 1 mM IPTG, 50 μg/mL ampicillin. Empty vector was included as a negative control, and *daf-16* was included as a positive control.

Microfluidic assessment of C. elegans lifespan and healthspan

The effects of knockdown of the C. elegans orthologues of validated miR-361-5p target genes on lifespan and healthspan parameters was measured using the microfluidics-based Infinity Screening System (NemaLife Inc.) [31] on RNAi-treated worms. Worms were grown to day 0 of adulthood on RNAi NGM plates according to established protocols and then washed 3 times with M9 buffer to allow separation of young adult animals from bacterial contaminants and collected in 2.5ml syringes. 60 - 70 worms were loaded onto each chip according to manufacturer's instructions. Survival and movement analysis was carried out daily; chips were washed to remove progeny prior to assessment of survival and movement for 90s. Survival and movement analysis was assessed from 3 still-image frames per chip taken at 30 second intervals using a 0 to 1 coefficient in the Infinity Systems software (NemaLife Inc, Texas) with dead animals indicated by a coefficient of 0 and inactive animals indicated with coefficients of 0.01 to 0.40. Animals scoring between coefficients of 0.40 and 1 were classified as

active, mobile animals. Data were normalised to the number of animals loaded on day 1 of adulthood.

Results

S*enescence kinetics of early passage, late passage and rejuvenated primary human endothelial cells*

Early passage human primary endothelial cells (PD = 36) demonstrated an average level of 10% SA-β-Gal positive cells, whereas late passage cells (PD = 84) demonstrated 64% positivity (p = 0.0001). This was accompanied by a 25% decrease in the number of cells staining positive for the cell proliferation marker Ki67 (p = 0.0008) and a 28% increase in the number of cells demonstrating □H2AX foci indicating increased levels of DNA damage (p =0.0155 01; figure 1). We have previously reported that resveratrol and related analogues are able to bring about attenuation of multiple senescence phenotypes in late passage human primary dermal fibroblasts [25]. We observed a similar effect in human primary endothelial cells with treated cells demonstrating an approximate 33% decrease in the number of cells staining positive for SA-□-Gal activity (p = 0.0016; figure 2).

miRNAs demonstrating dysregulated expression in senescence and upon resveratrol treatment

Whole miRNome profiling of early and late passage human primary endothelial cells revealed that 404 miRNAs were expressed in early and/or late passage primary human endothelial cells. Of these, 244 miRNAs demonstrated nominal significance for an association with senescence, and 202 demonstrated significance following adjustment for false discovery rate (figure 3; Online Resource 1). The most dysregulated miRNA were miR-6850-5p (fold change = -38.69; FDR adjusted p value = 0.0002), miR-4687-3p (fold change = -29.59; FDR adjusted p value; Online Resource 1 = 0.0005), miR-7108-5p (fold change = -28.03; FDR adjusted p value = 0.0007), miR-4632-5p (fold change = -10.49; FDR adjusted p value = 0.001) and miR-4530 (fold change = -16.12; FDR adjusted p value = 0.001). We have previously demonstrated that low dose resveratrol is capable of bringing about reversal of multiple senescent cell phenotypes in human primary dermal fibroblasts [25]. Accordingly, treatment of late passage human primary endothelial cells also showed a rescue phenotype when treated with low dose (5 □M) resveratrol (figure 2). We identified 202 miRNAs were expressed in senescent primary human endothelial cells treated with resveratrol, of which 35 demonstrated nominal associations with senescence, and 3 met multiple testing criteria (figure 3; Online Resource 2). These were miR-5787 (fold change -1.76; FDR adjusted p value = 0.0005), miR-3665 (fold change -3.36; FDR-adjusted p value = 0.001) and miR-361-5p; fold change 1.41; FDR adjusted p value = 0.001). The changes we identified in miR-361-5p expression we noted in our Clariom D data were also confirmed in a new culture of senescent cells by qRTPCR (Online Resource 3).

miR-361-5p demonstrates opposing differential expression in response to senescence and reversal

MiRNA differentially regulated with senescence comprise a mix of those that may induce senescence and those that are a result of it. Similarly, not all miRNA that are responsive to resveratrol will be directly involved in the reversal response, due to the pleiotropic nature of the molecule. To focus our analysis on those miRNAs which may be directly involved in the reversal response, we identified those that are present at the juxtaposition of both datasets, but with opposite direction of effect. One miRNA, miR-361-5p fulfilled these criteria (figure 3), demonstrating a 1.52-fold decrease in expression in senescent endothelial cells (FDR- adjusted p value = 0.05) and a 1.41-fold increase in expression following resveratrol treatment (FDR- adjusted p value = 0.001).

Identification of miR-361-5p target genes and assessment of their expression in senescent human primary endothelial cells

Identification of validated miR-361-5p target genes using miRTarBase version 9.0 revealed that miR-361-5p regulates 839 mRNA transcripts. Of these, we determined that 65 were expressed in human primary endothelial cells. 32 miR-361-5p target genes demonstrated an association with senescence below an Benjamini Hochberg corrected FDR p value threshold 0f 0.05 (figure 4; Online Resource 4). However, in contrast to our predictions, the vast majority of miR-361-5p target genes demonstrated reduced, rather than elevated levels of expression in senescent primary endothelial cells relative to their early passage counterparts. The most dysregulated miR-361-5p

target genes in senescent endothelial cells included *TMEM43* (fold change >-1000; FDR adjusted p value = 0.002), *LPAR1* (fold change = -136.53; FDR adjusted p value = 0.003), *RECK* (fold change = -44.98; FDR adjusted p value = 0.02), *RAD23B* (fold change = -18.2; FDR adjusted p value = 0.008), *RAD23A* (fold change = -16.1; FDR adjusted p value = 0.02) and *TGFBR1* (fold change = -15.92' FDR adjusted p value = 0.006). Only *EZR* (fold change 19.35; FDR adjusted p value = 0.02) and *ARPC5L* (fold change 3.92; FDR adjusted p value = 0.035) demonstrated an increase in senescent cells, which would be consistent with the most predominant mode of miRNA regulation.

Pathway analysis of restored miRNA and their target genes

We carried out a Cellular and Molecular Function and Biological Processes GO terms analysis of the 32 miR-361-5p target genes demonstrating differential expression in senescent primary human endothelial cells (table 1). We identified that the cellular function pathways that were enriched in miR-361-5p target genes included those involved in cytoskeletal remodelling (focal adhesion; adjusted p value = <0.0001, actin filament; adjusted p value = 0.004, polymeric cytoskeletal fibre; p = 0.008) or with the core splicing machinery with the splicing machinery (U5 snRNP; adjusted p value = <0.0001, U4/U6 x U5 tri snRNP complex; adjusted p value = 0.008, spliceosomal tri-snRNP complex; adjusted p value 0.008, spliceosomal complex; adjusted p value = 0.004). Molecular processes enriched in miR-361-5p target genes included processes involved in ubiquitination (polyubiquitin modification-dependent protein binding; adjusted p value = 0.001, and ubiquitin-specific protease binding; adjusted p value = 0.006). Biological processes enriched on miR-361-5p target genes included those

involved in movement of cellular cargoes (cellular component movement; adjusted p value = 0.001, positive regulation of cellular component movement; adjusted p value = 0.002, vesicle transport along actin filaments; adjusted p value = 0.004) and stress granule formation (positive regulation of stress fibre assembly; adjusted p value = 0.004).

Restoration of miR-361-5p levels in aged cells causes a decrease in SA-□-Gal positive cells

To determine whether miR-361-5p influences cellular senescence phenotypes, we treated primary senescent human endothelial cells with miR-361-5p mimic. Transfection efficiencies were >90%. We identified that increasing levels of miR-361-5p in aged endothelial cells resulted in an approximately 14% drop in the percentage of senescent cells in the culture (the percentage of senescent cells in cells treated with carrier only was 52% (SD = 8%) compared with 38% (SD = 7%) in mimic treated cells; p = 0.013; figure 5). We noted no differences in proliferation index (as measured by Ki67) or the number of DNA damage foci (measured by □H2AX), indicating that the reversal effect was only partial.

miR-361-5p target genes do not promote lifespan and healthspan phenotypes in C. elegans

We next sought to determine whether RNAi knockdown of the worm orthologues of the 16 *C. elegans* orthologues of validated miR-361-5p target genes with differential expression in senescent human endothelial cells were associated with altered lifespan or healthspan parameters *in vivo*. A miRNA demonstrating down-regulation in aged cells would be expected to lead to up-regulation of its target genes, if it is the predominant regulatory factor. Of the 16 genes tested however, only 2 (*erm-1/EZR* and *C46H11.3/ARPC5L)* demonstrated elevated expression in senescent primary endothelial cells, whereas the remainder demonstrated reduced levels of expression. However, since miRNAs have been known to positively regulate target genes under some circumstances [32,33], we elected to also assess the effect of targeted knockdown of all 16 miR361-5p target genes with worm orthologues in our *C. elegans* work. Of the 16 orthologues tested, 9/16 demonstrated effects on lifespan and 12/16 demonstrated effects on healthspan, as assessed by movement rate across the agieng trajectory. However, in all cases, targeted knockdown was associated with an adverse outcome for both measures; reduction in target gene expression was associated with decreased, not increased, lifespan and healthspan (figure 6).

Discussion

MicroRNAs are key components of the cellular stress response and are pivotal to a multitude of cellular processes. Here, we report the miRNA profiles associated with cellular senescence and those associated with polyphenol-induced rescue from

senescence, in human primary endothelial cells. We have identified one miRNA, miR-361-5p, which demonstrates antagonistic patterns of expression in response to senescence and rejuvenation. GO terms analysis reveals that validated targets of this miRNA are enriched in pathways involved in transport of materials and cellular components in the cytosol by actin filaments and vesicles, and with components of the core spliceosome. Manipulation of miR-361-5p levels using a miRNA mimic resulted in a reduction of the senescent cell load in aged primary endothelial cells. In contrast with these findings however, targeted knockdown of validated miR-361-5p target genes in an invertebrate model animal *C. elegans* was not associated with increased lifespan and healthspan; indeed, knockdown of these genes was detrimental. From this we conclude that although miR-361-5p may contribute to aspects of the senescent cell phenotype, targeted manipulation of it alone is not likely to bring about beneficial effects in systems.

Altered expression of miR-361-5p has previously been associated with multiple diseases with an age-related component in multiple tissue types. These include acute coronary syndrome and coronary artery disease [34], osteoarthritis [35], rheumatoid arthritis [36], hepatosteatosis [37], hypertension [38], Alzheimer Disease [39] and macular degeneration [40]. MicroRNA miR-361-5p also has known roles in epithelial-to-mesenchymal cell transition [41-43] which may underpin its associations with the development or progression of multiple cancers, including those of the reproductive [44-46], respiratory [47,48], digestive [49,50], skeletal [51] and nervous systems [52]. We identified that the expression of miR-361-5p was decreased in human primary endothelial cells, but upregulated in these cells in response to treatment with a polyphenol small molecule associated with cellular rejuvenation in our previous work [25]. Targeted

upregulation of miR-361-5p was able to attenuate some aspects of senescence in senescent endothelial cells. This suggests that miR-361-5p may be contributory to the establishment or maintenance of some aspects of the senescent cell phenotype in endothelial cells.

Despite this, targeted manipulation of validated miR-361-5p target genes in a *C. elegans* animal model was not able to extend lifespan or healthspan parameters systemically when manipulated in adulthood. Although *C. elegans* do not undergo replicative senescence in the conventional sense due to the post-mitotic nature of their adult somatic cells, they do undergo other forms of senescence [53]. Interventions designed to attenuate senescence phenotypes therefore have potential to extend healthspan and lifespan in this system. We identified two target genes (*erm-1/EZR* and *C46H11.3/ARPC5L)* that demonstrated up-regulation of expression, consistent with the action of a down-regulated miRNA in senescence. The direction of change for most of the other miR-361-5p targets observed in senescent primary human endothelial cells however was inconsistent with the proposed action of a miRNA; the majority of validated targets demonstrated reduced rather than elevated expression in senescent cells. Although there are examples where miRNA can upregulate their targets in the context of senescence [33], this probably indicates that the majority of miR-361-5p targets are regulated by factors other than miR-361-5p in senescence.

The miR-361-5p targets responsible for the observed effect on senescent cell load are not clear, but it is likely that these would demonstrate elevated, rather than reduced, expression in senescent cells in response to reduced miR-361-5p levels, and down-

regulation in response to a miR-361-5p mimic. Of the miR-361-5p target genes expressed in human endothelial cells, only 2 (*EZR* and *ARPC5L)* demonstrated elevated expression in senescent cells and only *EZR* in a direction that would be consistent with rescue upon miR_361-5p mediated rescue. *EZR* encodes Ezrin, an actin binding protein which acts downstream of RB1 and is known to be involved in the morphological changes accompanying senescence [54]. Increased phosphorylation of Ezrin by CDK5 results in disassociation o the Rho GDP disassociation inhibitor (Rho-GDI) and increases the inhibitory interaction of Ezrin with the Rac1 GTPase yielding the characteristic 'flat' morphology of senescent cells [55]. Despite this, targeted RNAi knockdown of the *C. elegans* orthologue of EZR (*erm-1*) was not associated with systemic improvement in healthspan or lifespan.

Of the remaining validated *C. elegans* orthologus of the validated miR-361-5p target genes identified, 13 are directly involved in the regulation or formation of the cytoskeletal network, or its interaction with the extracellular matrix. *rho-1/RHOA*, *sdn-1/SDC4*, *wsp-1/WASL, pes-7/IQGAP1*, and *hrdl-1/AMFR* are involved in transducing signals from the exterior of the cell to the interior to regulate cell motility, morphology, and survival [56-60]. *Deb-1/VCL, ifa-1/VIM, cyk-1D/IAPH1, C46H11.3/ARPC5L, hlh-8/TWIST1* and *atn-1*/*ACTN4* are involved with formation or regulation of microtubules, intermediate filaments or other cytoskeletal components to facilitate cell attachment, cell:cell or cell:matrix interactions and EMT [61-66]. *let-805*/*FN1* and *dgn-2*/*DAG1* are extracellular matrix glycoproteins involved in cell adhesion, migration and survival [67,68]. The cytoskeleton and the actin filament network is widely known to regulate many aspects of cellular behaviour, particularly in the nervous system [63], and has known involvement in the ageing process and its diseases [69]. The remaining two miR-361-5p

target genes we assessed *sup-46/HNRNPM* and *daf-1/TGFBR1* are also known to have associations with ageing and senescence. *TGFBR1* is part of the TGF signalling network and a major inducer of cell cycle arrest and senescence [70]. *HNRNPM* is a member of a gene family encoding multifunctional proteins involved in alternative splicing and other aspects of mRNA processing [71]. Dysregulation of mRNA processing has been suggested as a new hallmark of ageing [4], and dysregulation of *HNRNPM* expression has been associated with ageing, senescence and age-related phenotypes in humans and other species [25,72,73]. It is possible that the partial attenuation of the senescent cell phenotype we have described in response to elevation of miR-361-5p levels is due to consequent reduction in the expression of other genes that we have not assessed, but without knowledge of the identity of those target genes, and very specific approaches to influence their interaction with this miR, miR-361-5p is unlikely to represent a tractable senotherapeutic target.

Conclusions

In conclusion, we report here the identification of a miRNA (miR-361-5p) that displays antagonistic effects in cellular senescence and cellular rejuvenation in human primary endothelial cells. We have validated its predicted target genes and demonstrated that several display dysregulated expression in senescent primary human endothelial cells. Although targeted manipulation of miR-361-5p was able to bring about reversal of some aspects of the senescence phenotype in human primary endothelial cells *in vitro*, the consequences of unintended attenuation of other critical target genes *in vivo* such as those involved in maintenance of the cytoskeletal network renders it unsuitable as a future senotherapeutic target.

References

1 Fougere, B., Boulanger, E., Nourhashemi, F., Guyonnet, S. & Cesari, M. Chronic Inflammation: Accelerator of Biological Aging. *J Gerontol A Biol Sci Med Sci* 72, 1218-1225 (2017).

2 Kenessary, A. *et al.* Biomarkers, interventions and healthy ageing. *N Biotechnol* 30, 373-377 (2013).

3 Lopez-Otin, C., Blasco, M. A., Partridge, L., Serrano, M. & Kroemer, G. The hallmarks of aging. *Cell* 153, 1194-1217 (2013).

4 Schmauck-Medina, T. *et al.* New hallmarks of ageing: a 2022 Copenhagen ageing meeting summary. *Aging (Albany NY)* 14, 6829-6839 (2022).

5 Childs, B. G. *et al.* Senescent cells: an emerging target for diseases of ageing. *Nat Rev Drug Discov* 16, 718-735 (2017).

6 Watanabe, S., Kawamoto, S., Ohtani, N. & Hara, E. Impact of senescence-associated secretory phenotype and its potential as a therapeutic target for senescence-associated diseases. *Cancer Sci* 108, 563-569 (2017).

7 Baker, D. J. *et al.* Naturally occurring p16(Ink4a)-positive cells shorten healthy lifespan. *Nature* 530, 184-189 (2016).

8 Baker, D. J. *et al.* Clearance of p16Ink4a-positive senescent cells delays ageing-associated disorders. *Nature* 479, 232-236 (2011).

9 Bussian, T. J. *et al.* Clearance of senescent glial cells prevents tau-dependent pathology and cognitive decline. *Nature* 562, 578-582 (2018).

10 van Willigenburg, H., de Keizer, P. L. J. & de Bruin, R. W. F. Cellular senescence as a therapeutic target to improve renal transplantation outcome. *Pharmacol Res* 130, 322-330 (2018).

11 Ogrodnik, M. *et al.* Cellular senescence drives age-dependent hepatic steatosis. *Nat Commun* 8, 15691 (2017).

12 Justice, J. N. *et al.* Senolytics in idiopathic pulmonary fibrosis: Results from a first-in-human, open-label, pilot study. *EBioMedicine* (2019).

13 Paez-Ribes, M., Gonzalez-Gualda, E., Doherty, G. J. & Munoz-Espin, D. Targeting senescent cells in translational medicine. *EMBO Mol Med* 11, e10234 (2019).

14 He, S. & Sharpless, N. E. Senescence in Health and Disease. *Cell* 169, 1000-1011 (2017).

15 LaPierre, M. P. & Stoffel, M. MicroRNAs as stress regulators in pancreatic beta cells and diabetes. *Mol Metab* 6, 1010-1023 (2017).

16 Du, J. *et al.* The critical role of microRNAs in stress response: Therapeutic prospect and limitation. *Pharmacol Res* 142, 294-302 (2019).

17 Bartel, D. P. MicroRNAs: genomics, biogenesis, mechanism, and function. *Cell* 116, 281-297 (2004).

18 Grillari, J., Hackl, M. & Grillari-Voglauer, R. miR-17-92 cluster: ups and downs in cancer and aging. *Biogerontology* 11, 501-506 (2010).

19 Li, T., Yan, X., Jiang, M. & Xiang, L. The comparison of microRNA profile of the dermis between the young and elderly. *J Dermatol Sci* 82, 75-83 (2016).

20 Rani, A. *et al.* miRNA in Circulating Microvesicles as Biomarkers for Age-Related Cognitive Decline. *Front Aging Neurosci* 9, 323 (2017).

21 Pitto, L. *et al.* miR-290 acts as a physiological effector of senescence in mouse embryo fibroblasts. *Physiological genomics* 39, 210-218 (2009).

22 Chen, Y. L. *et al.* MicroRNA-214 modulates the senescence of vascular smooth muscle cells in carotid artery stenosis. *Mol Med* 26, 46 (2020).

23 Chakraborty, C., Sharma, A. R., Sharma, G., Doss, C. G. P. & Lee, S. S. Therapeutic miRNA and siRNA: Moving from Bench to Clinic as Next Generation Medicine. *Mol Ther Nucleic Acids* 8, 132-143 (2017).

24 Holly, A. C. *et al.* Changes in splicing factor expression are associated with advancing age in man. *Mech Ageing Dev* 134, 356-366 (2013).

25 Latorre, E. *et al.* Small molecule modulation of splicing factor expression is associated with rescue from cellular senescence *BMC Cell Biology* In press (2017).

26 Paraskevopoulou, M. D. *et al.* DIANA-microT web server v5.0: service integration into miRNA functional analysis workflows. *Nucleic Acids Res* 41, W169-173 (2013).

27 Vlachos, I. S. *et al.* DIANA-miRPath v3.0: deciphering microRNA function with experimental support. *Nucleic Acids Research* 43, W460-W466 (2015).

28 Huang, H. Y. *et al.* miRTarBase 2020: updates to the experimentally validated microRNA-target interaction database. *Nucleic Acids Res* 48, D148-D154 (2020).

29 Huang, H. Y. *et al.* miRTarBase update 2022: an informative resource for experimentally validated miRNA-target interactions. *Nucleic Acids Res* 50, D222-D230 (2022).

30 Chen, E. Y. *et al.* Enrichr: interactive and collaborative HTML5 gene list enrichment analysis tool. *BMC Bioinformatics* 14, 128 (2013).

31 Rahman, M. *et al.* NemaLife chip: a micropillar-based microfluidic culture device optimized for aging studies in crawling C. elegans. *Sci Rep* 10, 16190 (2020).

32 Cheng, H. P. *et al.* MicroRNA-362 negatively and positively regulates SMAD4 expression in TGF-beta/SMAD signaling to suppress cell migration and invasion. *Int J Med Sci* 18, 1798-1809 (2021).

33 Hong, Y. *et al.* miR-155-5p inhibition rejuvenates aged mesenchymal stem cells and enhances cardioprotection following infarction. *Aging Cell* 19, e13128 (2020).

34 Su, M. *et al.* Circulating microRNA profiles based on direct S-Poly(T)Plus assay for detection of coronary heart disease. *J Cell Mol Med* 24, 5984-5997 (2020).

35 Wang, A. *et al.* MEG3 promotes proliferation and inhibits apoptosis in osteoarthritis chondrocytes by miR-361-5p/FOXO1 axis. *BMC Med Genomics* 12, 201 (2019).

36 Romo-Garcia, M. F. *et al.* Identification of putative miRNA biomarkers in early rheumatoid arthritis by genome-wide microarray profiling: A pilot study. *Gene* 720, 144081 (2019).

37 Zhang, Z. *et al.* Obesity-induced upregulation of miR-361-5p promotes hepatosteatosis through targeting Sirt1. *Metabolism* 88, 31-39 (2018).

38 Qi, H. *et al.* micro-RNA screening and prediction model construction for diagnosis of salt-sensitive essential hypertension. *Medicine (Baltimore)* 96, e6417 (2017).

39 Mendes-Silva, A. P. *et al.* Shared Biologic Pathways Between Alzheimer Disease and Major Depression: A Systematic Review of MicroRNA Expression Studies. *Am J Geriatr Psychiatry* 24, 903-912 (2016).

40 Grassmann, F. *et al.* A circulating microrna profile is associated with late-stage neovascular age-related macular degeneration. *PLoS One* 9, e107461 (2014).

41 Yin, L. C. *et al.* MicroRNA-361-5p Inhibits Tumorigenesis and the EMT of HCC by Targeting Twist1. *Biomed Res Int* 2020, 8891876 (2020).

42 Zhang, X., Wei, C., Li, J., Liu, J. & Qu, J. MicroRNA-361-5p inhibits epithelial-to-mesenchymal transition of glioma cells through targeting Twist1. *Oncol Rep* 37, 1849-1856 (2017).

43 Wu, X. *et al.* MicroRNA-361-5p facilitates cervical cancer progression through mediation of epithelial-to-mesenchymal transition. *Med Oncol* 30, 751 (2013).

44 Ling, J. & He, P. miR-361-5p regulates ovarian cancer cell proliferation and apoptosis by targeting TRAF3. *Exp Ther Med* 21, 199 (2021).

45 Zheng, S. R., Huang, Q. D., Zheng, Z. H., Zhang, Z. T. & Guo, G. L. circGFRA1 affects the sensitivity of triple negative breast cancer cells to paclitaxel via the miR-361-5p/TLR4 pathway. *J Biochem* (2021).

46 Yang, W. & Xie, T. Hsa_circ_CSPP1/MiR-361-5p/ITGB1 Regulates Proliferation and Migration of Cervical Cancer (CC) by Modulating the PI3K-Akt Signaling Pathway. *Reprod Sci* 27, 132-144 (2020).

47 Othman, N. & Nagoor, N. H. Overexpression of miR3615p plays an oncogenic role in human lung adenocarcinoma through the regulation of SMAD2. *Int J Oncol* 54, 306-314 (2019).

48 Zhuang, Z. L., Tian, F. M. & Sun, C. L. Downregulation of miR-361-5p associates with aggressive clinicopathological features and unfavorable prognosis in non-small cell lung cancer. *Eur Rev Med Pharmacol Sci* 20, 5132-5136 (2016).

49 Qian, B. *et al.* MiR-361-5p exerts tumor-suppressing functions in gastric carcinoma by targeting syndecan-binding protein. *Anticancer Drugs* 31, 131-140 (2020).

50 Cui, W. *et al.* miR-361-5p inhibits hepatocellular carcinoma cell proliferation and invasion by targeting VEGFA. *Biochem Biophys Res Commun* 479, 901-906 (2016).

51 Shen, B. *et al.* LncRNA MEG3 negatively modified osteosarcoma development through regulation of miR-361-5p and FoxM1. *J Cell Physiol* 234, 13464-13480 (2019).

52 Zhou, C. *et al.* COX10-AS1 Facilitates Cell Proliferation and Inhibits Cell Apoptosis in Glioblastoma Cells at Post-Transcription Level. *Neurochem Res* 45, 2196-2203 (2020).

53 Benedetto, A. & Gems, D. Autophagy promotes visceral aging in wild-type C. elegans. *Autophagy* 15, 731-732 (2019).

54 Yang, H. S. & Hinds, P. W. Increased ezrin expression and activation by CDK5 coincident with acquisition of the senescent phenotype. *Mol Cell* 11, 1163-1176 (2003).

55 Yang, H. S. & Hinds, P. W. Phosphorylation of ezrin by cyclin-dependent kinase 5 induces the release of Rho GDP dissociation inhibitor to inhibit Rac1 activity in senescent cells. *Cancer Res* 66, 2708-2715 (2006).

56 Kempers, L., Driessen, A. J. M., van Rijssel, J., Nolte, M. A. & van Buul, J. D. The RhoGEF Trio: A Protein with a Wide Range of Functions in the Vascular Endothelium. *Int J Mol Sci* 22 (2021).

57 Elfenbein, A. & Simons, M. Syndecan-4 signaling at a glance. *J Cell Sci* 126, 3799-3804 (2013).

58 Choi, S. & Anderson, R. A. IQGAP1 is a phosphoinositide effector and kinase scaffold. *Adv Biol Regul* 60, 29-35 (2016).

59 Dart, A. E., Donnelly, S. K., Holden, D. W., Way, M. & Caron, E. Nck and Cdc42 co-operate to recruit N-WASP to promote FcgammaR-mediated phagocytosis. *J Cell Sci* 125, 2825-2830 (2012).

60 Chiu, C. G., St-Pierre, P., Nabi, I. R. & Wiseman, S. M. Autocrine motility factor receptor: a clinical review. *Expert Rev Anticancer Ther* 8, 207-217 (2008).

61 Boujemaa-Paterski, R. *et al.* Talin-activated vinculin interacts with branched actin networks to initiate bundles. *Elife* 9 (2020).

62 Yang, J. *et al.* DIAPH1 Promotes Laryngeal Squamous Cell Carcinoma Progression Through Cell Cycle Regulation. *Front Oncol* 11, 716876 (2021).

63 Schneider, F., Metz, I. & Rust, M. B. Regulation of actin filament assembly and disassembly in growth cone motility and axon guidance. *Brain Res Bull* 192, 21-35 (2022).

64 Hsu, P. H., Chen, Y. H., Huang, P. I. & Hwang, P. A. Skin proteomic profiling of irradiation-induced fibrosis and its modulation by low molecular weight fucoidan via tight junction pathway. *Biomed Pharmacother* 153, 113417 (2022).

65 Tentler, D., Lomert, E., Novitskaya, K. & Barlev, N. A. Role of ACTN4 in Tumorigenesis, Metastasis, and EMT. *Cells* 8 (2019).

66 Garcia-Palmero, I. *et al.* Twist1-induced activation of human fibroblasts promotes matrix stiffness by upregulating palladin and collagen alpha1(VI). *Oncogene* 35, 5224-5236 (2016).

67 Barresi, R. & Campbell, K. P. Dystroglycan: from biosynthesis to pathogenesis of human disease. *J Cell Sci* 119, 199-207 (2006).

68 Owens, R. J. & Baralle, F. E. Mapping the collagen-binding site of human fibronectin by expression in Escherichia coli. *EMBO J* 5, 2825-2830 (1986).

69 Kim, Y. J. *et al.* Links of Cytoskeletal Integrity with Disease and Aging. *Cells* 11 (2022).

70 Vander Ark, A., Cao, J. & Li, X. TGF-beta receptors: In and beyond TGF-beta signaling. *Cell Signal* 52, 112-120 (2018).

71 Geuens, T., Bouhy, D. & Timmerman, V. The hnRNP family: insights into their role in health and disease. *Hum Genet* 135, 851-867 (2016).

72 Lee, B. P. *et al.* The transcript expression levels of HNRNPM, HNRNPA0 and AKAP17A splicing factors may be predictively associated with ageing phenotypes in human peripheral blood. *Biogerontology* 20, 649-663 (2019).

73 Lee, B. P. *et al.* Changes in the expression of splicing factor transcripts and variations in alternative splicing are associated with lifespan in mice and humans. *Aging Cell* 15, 903-913 (2016).

Acknowledgments

The authors would like to thank Al Jouf University and the Saudi Arabia Cultural Bureau in UK for providing scholarship and funding for Emad Manni. The authors gratefully acknowledge Mr. Zhoufan (Fred) Mou for advice on the GO terms analysis. This study was supported by the National Institute for Health and Care Research Exeter Biomedical Research Centre. The views expressed are those of the author(s) and not necessarily those of the NIHR or the Department of Health and Social Care.

Author Contributions: Conceptualization, Lorna Harries; Data curation, Lorna Harries and Emad Manni; Formal analysis, Emad Manni, Nicola Jeffery, David Chambers, Luke Slade and Lorna Harries; Investigation, Emad Manni, Luke Slade and David Chambers; Methodology, Emad Manni; Project administration, Lorna Harries; Resources, Lorna Harries; Supervision, Nicola Jeffery, Tim Etheridge and Lorna Harries, draft, Emad Manni; Writing – review & editing, Nicola Jeffery, David Chambers, Luke Slade, Tim Etheridge and Lorna Harries.

Data Availability Statement: The data presented in this study are available upon reasonable request from the corresponding author. The data are not publicly available for reasons of intellectual property.

Competing interests Section: LWH holds a position as Co-founder, Co-director and CSO of SENISCA Ltd

Figure Legends

Figure 1: fields illustrating representative senescence-associated beta galactosidase (SA-β-Gal) activity in early (PD = 36) and late passage (PD = 84) human primary endothelial cells. (B) Graph showing change in SA-□-Gal activity in early and late passage human primary endothelial cells. (C) Proliferation kinetics in early (PD = 36) and late passage (PD = 84) human primary endothelial cells stained for Ki67 activity. (D) Graph showing change in Ki67 staining in in early and late passage human primary endothelial cells. (E) DNA damage foci as identified by γH2AX staining in early and late passage human primary endothelial cells. (F) Graph showing change in γH2AX staining in in early and late passage human primary endothelial cells. Early passage cell counts are shown in black, late passage cell counts are given in grey. Cell counts were obtained by manual counting of multiple fields in 6-well plates from 3 biological replicates. N > 300 cells for each replicate. Error bars represent standard deviation of measurement. Statistical significance was determined by one-way ANOVA with * = $p \leq 0.05$, *** = ≤ 0.001 and **** = $p \leq 0.0001$.

Figure 2: Senescence-associated beta galactosidase activity in late passage (PD = 84) human primary endothelial cells treated with 5mM resveratrol for 48 hours. (A) Microscope fields illustrating representative senescence-associated beta galactosidase (SA-β-Gal) activity in late passage (PD = 84) human primary endothelial cells treated with resveratrol (RSV) or with vehicle (DMSO) alone. (B) Graph showing change in SA-□-Gal activity in early and late passage human primary endothelial cells. Vehicle treated cells are shown in black, resveratrol treated cells in grey. Cell counts

were obtained by manual counting of multiple fields in 6-well plates from 3 biological replicates. N > 400 cells for each replicate. Error bars represent standard deviation of measurement. Statistical significance was determined by one-way ANOVA with ** = ≤0.001.

Figure 3 Analysis of miRNAs expression profiles associated with endothelial cell senescence and rescue. (A) Volcano plot illustrating differentially-expressed miRNAs in senescent human primary endothelial cells. (B) Volcano plot illustrating differentially-expressed miRNAs in rejuvenated senescent human primary endothelial cells. (C) Venn diagram to summarize overlap between miRNA datasets differentially expressed in senescence and those differentially expressed in rejuvenation. (D) Expression pattern of miR-361-5p in senescent (black bars) and rejuvenated (grey bars) human primary endothelial cells expressed as a fold change compared with young or vehicle treated cells. Statistical significance was determined by Benjamini FDR. ** = ≤0.001.

Figure 4: Differential expression of miR-361-5p targets in early and late passage human primary endothelial cells. The expression patterns of 35 validated miR-361-5p target genes in early (PD = 36) and late (PD – 84) passage human primary endothelial cells are given. Black bars indicate early passage cells (PD = 36), lighter grey bars indicate late passage cells (PD = 84; n = 3 biological replicates for each). The Y axis refers to relative quantification arbitrary units (AU). Error bars represent standard deviation of measurement. Statistical significance was determined by t test and * = p ≤ 0.05, ** = ≤0.001 and *** = p ≤ 0.0001.

Figure 5: Attenuation of cellular senescence in aged endothelial cells using a mimic to miR-361-5p. The percentage of SA-β-Gal positive cells in cultures of senescent primary human endothelial cells treated with a mimic to miR-361-5p, or with lipofectamine alone are presented above. The black bars represent senescent cell load in vehicle treated cells, whilst the grey bars represent senescent cell load following treatment with a miR-361-5p mimic. Transfection efficiency was >90%. Error bars indicate standard deviation of measurement. Statistical significance of effect as determined by independent t-test is indicated by a star * = <0.05.

Figure 6: Attenuation of miR-361-5p target genes in a *C. elegans* model system. A. Survival curves illustrating the effect of targeted RNAi knockdown of 16 validated miR-361-5p target genes with known *C. elegans* orthologues. Probability of survival is given on the Y axis and days from start of analysis is given on the X axis. Data from control animals is given by solid black lines, data from treated animals is given by dashed grey lines. B. Area under the curve (AUC) measurements for a measure of healthspan (animal movement) following targeted RNAi knockdown of 16 validated miR-361-5p target genes with known *C. elegans* orthologues are given on the Y axis, and the identity of the gene on the X axis. Error bars represent standard deviation of measurement. In each case, data are from 3 biological replicates of 60-70 animals per replicate. * = $p \leq 0.05$, ** = ≤ 0.01, *** = $p \leq 0.001$ and **** = $p \leq 0.0001$.

Tables

Table 1:. Gene Ontology (GO) cellular, molecular and Biological processes enriched in miR-361-5p target genes displaying differential expression in senescent primary human endothelial cells. Adjusted p values have been derived from Fisher exact test for gene set enrichment in each pathway. Odds ratio refers to the probability that gene sets are enriched in a particular pathway and combined score is the Fisher exact test p-value multiplied by the z-score for deviation from expected rank.

	p value	Adj p value	Odds ratio	Combined Score
GO Cellular function				
focal adhesion (GO:0005925)	0.000	<0.001	18.79	310.3
actin filament (GO:0005884)	0.000	0.004	39.62	368.12
U5 snRNP (GO:0005682)	0.001	0.008	63.32	468.27
U4/U6 x U5 tri-snRNP complex (GO:0046540)	0.001	0.008	57.81	417.77
Golgi lumen (GO:0005796)	0.001	0.008	21.64	164.04
spliceosomal complex (GO:0005681)	0.001	0.008	18.51	132.13
polymeric cytoskeletal fiber (GO:0099513)	0.000	0.008	13	101.44
spliceosomal tri-snRNP complex (GO:0097526)	0.001	0.010	45.84	311.42
spliceosomal snRNP complex (GO:0097525)	0.004	0.024	23.29	128.53
filopodium (GO:0030175)	0.004	0.024	22.89	125.56
ficolin-1-rich granule membrane (GO:0101003)	0.004	0.024	22.5	122.69
platelet alpha granule lumen (GO:0031093)	0.005	0.025	20.41	107.6
endocytic patch (GO:0061645)	0.011	0.043	107.32	482.58

actin cortical patch (GO:0030479)	0.011	0.043	107.32	482.58
GO Molecular function				
polyubiquitin modification-dependent protein binding (GO:0031593)	0.000	0.001	51.54	517.04
ubiquitin-specific protease binding (GO:1990381)	0.000	0.006	95.02	772.86
protein kinase A regulatory subunit binding (GO:0034237)	0.000	0.006	83.13	656.15
disordered domain specific binding (GO:0097718)	0.001	0.009	63.32	468.27
GO Biological Processes				
regulation of cellular component movement (GO:0051270)	0.000	0.001	67.78	948.18
positive regulation of cellular component movement (GO:0051272)	0.000	0.002	114.66	1402.93
positive regulation of stress fiber assembly (GO:0051496)	0.000	0.004	60.65	636.13
vesicle transport along actin filament (GO:0030050)	0.000	0.004	266.17	2626.53
cytoskeletal anchoring at plasma membrane (GO:0007016)	0.000	0.006	190.1	1773.82
actin filament-based transport (GO:0099515)	0.000	0.007	166.33	1515.06
negative regulation of DNA damage response, signal transduction by p53 class mediator (GO:0043518)	0.000	0.008	133.05	1161.23
embryonic cranial skeleton morphogenesis (GO:0048701)	0.000	0.011	102.33	845.92
negative regulation of signal transduction by p53 class mediator (GO:1901797)	0.000	0.011	102.33	845.92
cardiac epithelial to mesenchymal transition (GO:0060317)	0.000	0.011	95.02	772.86

Figure 1

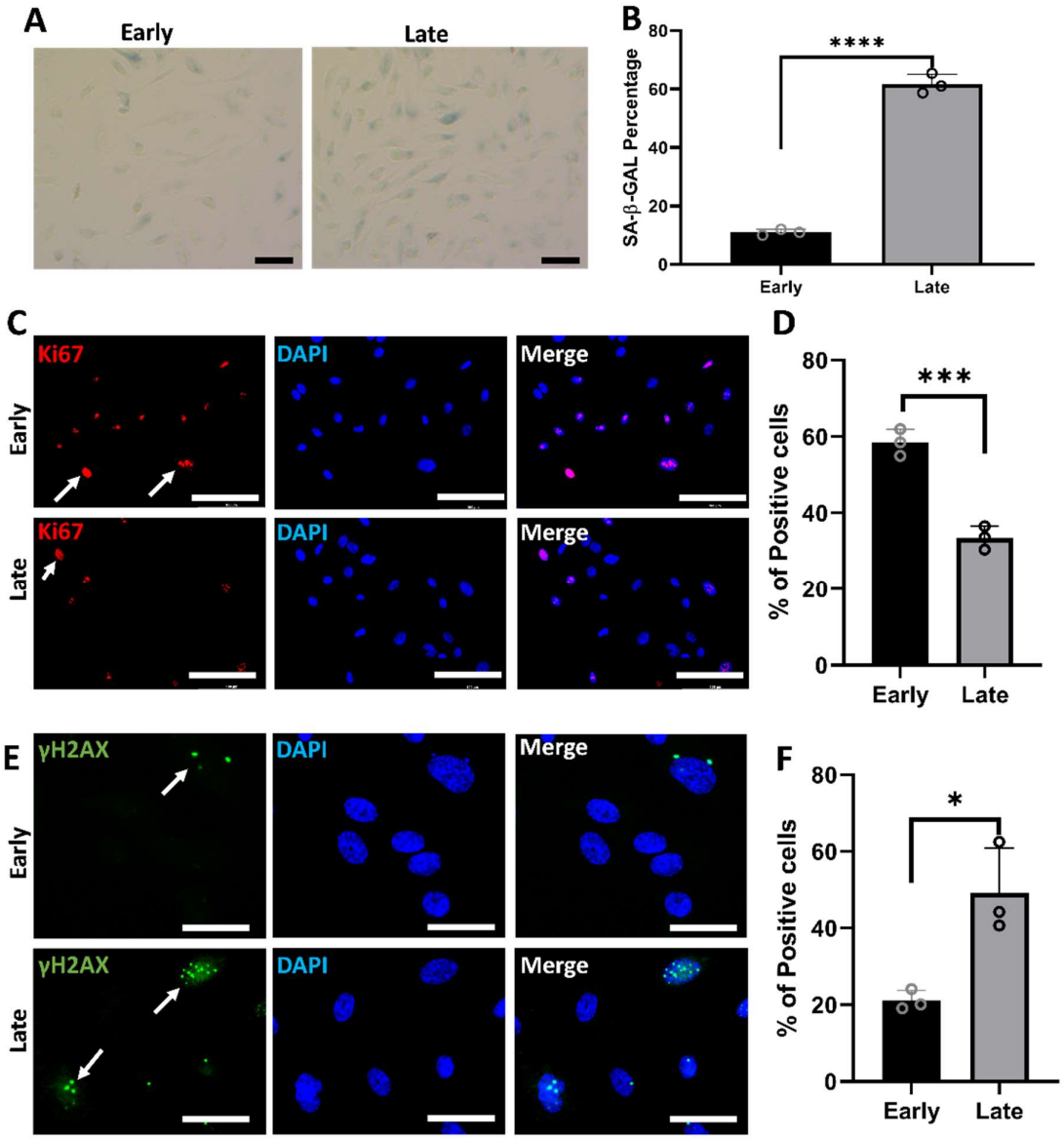
A
Early
Late
B
SA-β-GAL Percentage
80
60
40
20
0
****
Early
Late
C
Ki67
DAPI
Merge
Early
Late
D
% of Positive cells
80
60
40
20
0
***
Early
Late
E
γH2AX
DAPI
Merge
Early
Late
F
% of Positive cells
80
60
40
20
0
*
Early
Late

Figure 2

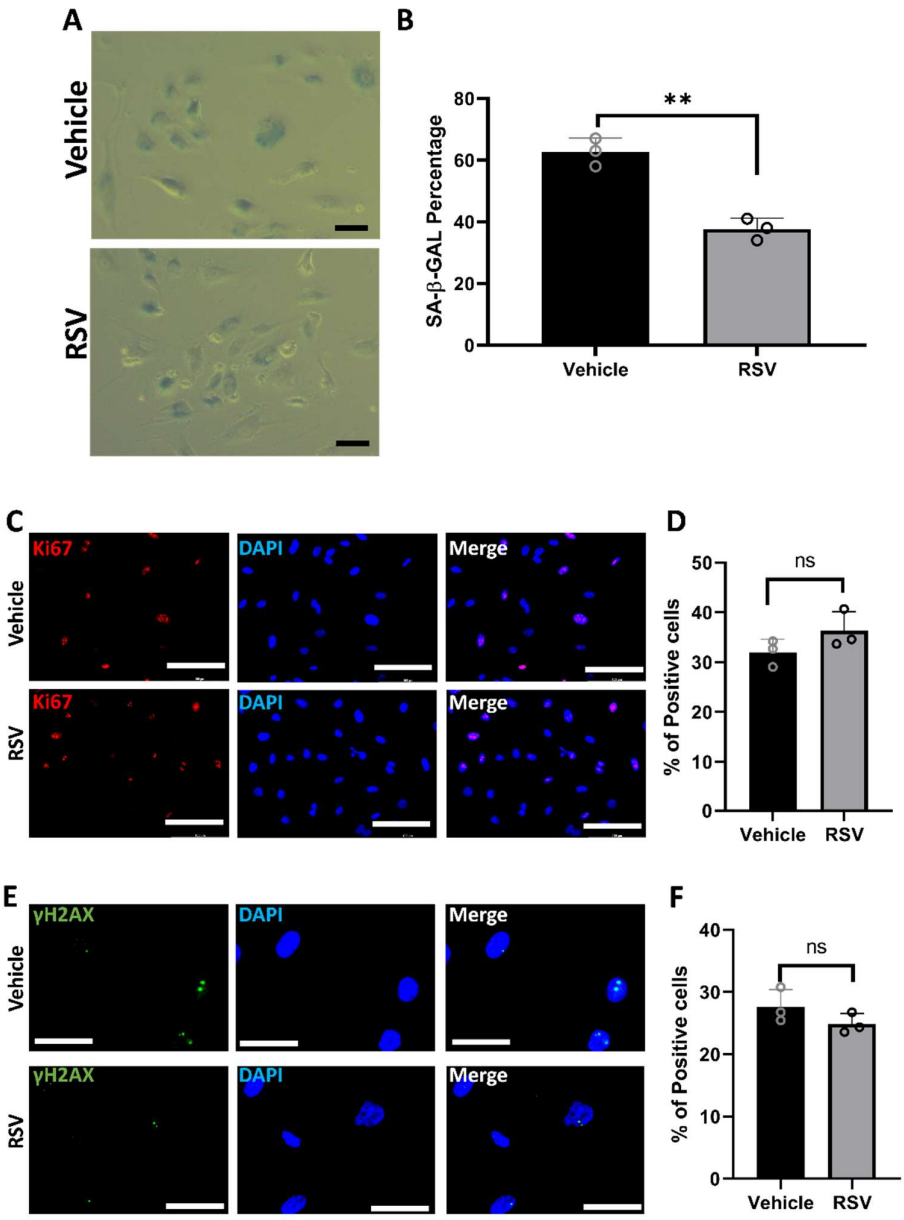
A
Vehicle
RSV
B
SA-β-GAL Percentage
80
60
40
20
0
**
Vehicle
RSV
C
Ki67
DAPI
Merge
Vehicle
RSV
D
% of Positive cells
50
40
30
20
10
0
ns
Vehicle
RSV
E
γH2AX
DAPI
Merge
Vehicle
RSV
F
% of Positive cells
40
30
20
10
0
ns
Vehicle
RSV

Figure 3

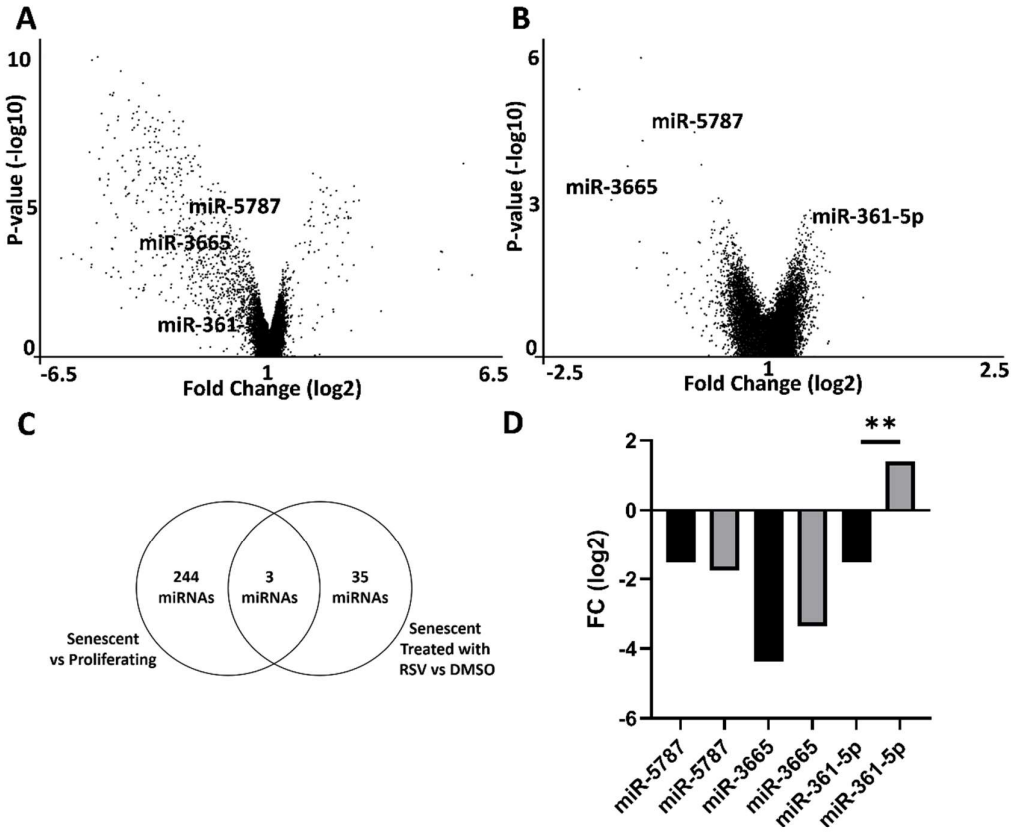
A
10
5
0
P-value (-log10)
miR-5787
miR-3665
miR-361
-6.5
1
6.5
Fold Change (log2)
B
6
3
0
P-value (-log10)
miR-5787
miR-3665
miR-361-5p
-2.5
1
2.5
Fold Change (log2)
C
244 miRNAs
3 miRNAs
35 miRNAs
Senescent vs Proliferating
Senescent Treated with RSV vs DMSO
D
**
2
0
-2
-4
-6
FC (log2)
miR-5787
miR-5787
miR-3665
miR-3665
miR-361-5p
miR-361-5p

Figure 4

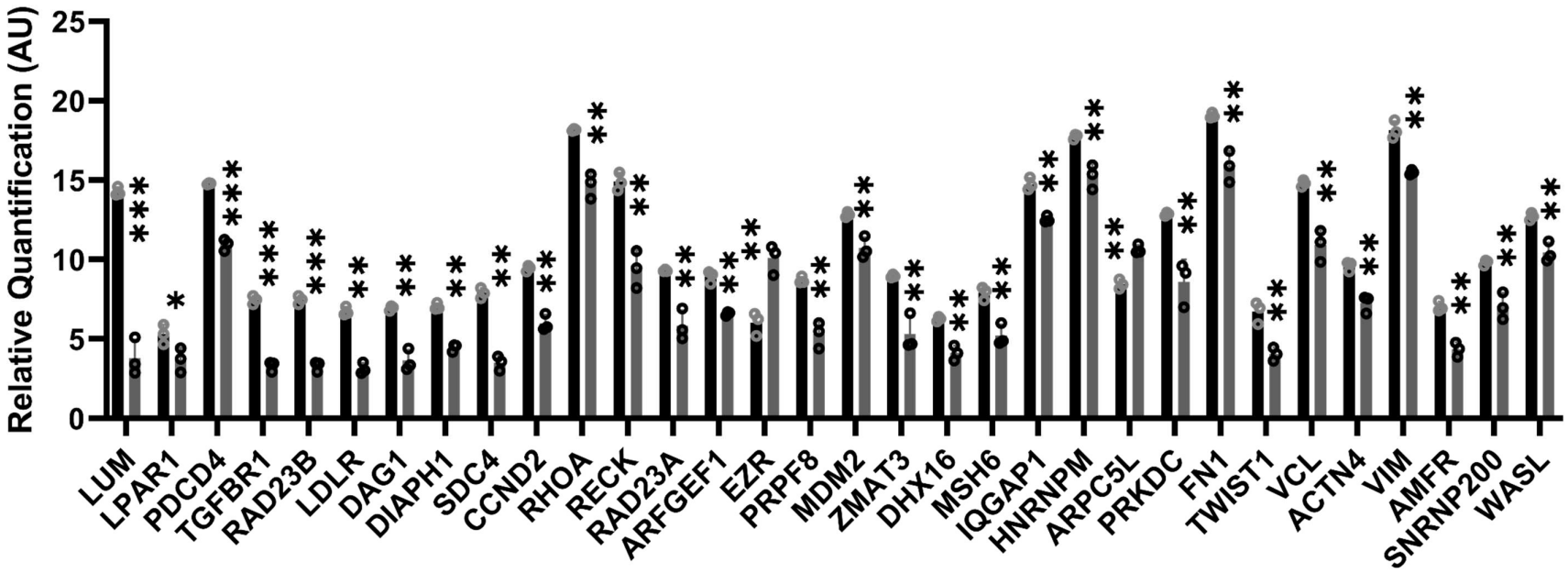
Relative Quantification (AU)
25
20
15
10
5
0
LUM
LPAR1
PDCD4
TGFBR1
RAD23B
LDLR
DAG1
DIAPH1
SDC4
CCND2
RHOA
RECK
RAD23A
ARFGEF1
EZR
PRPF8
MDM2
ZMAT3
DHX16
MSH6
IQGAP1
HNRNPM
ARPC5L
PRKDC
FN1
TWIST1
VCL
ACTN4
VIM
AMFR
SNRNP200
WASL

Figure 5

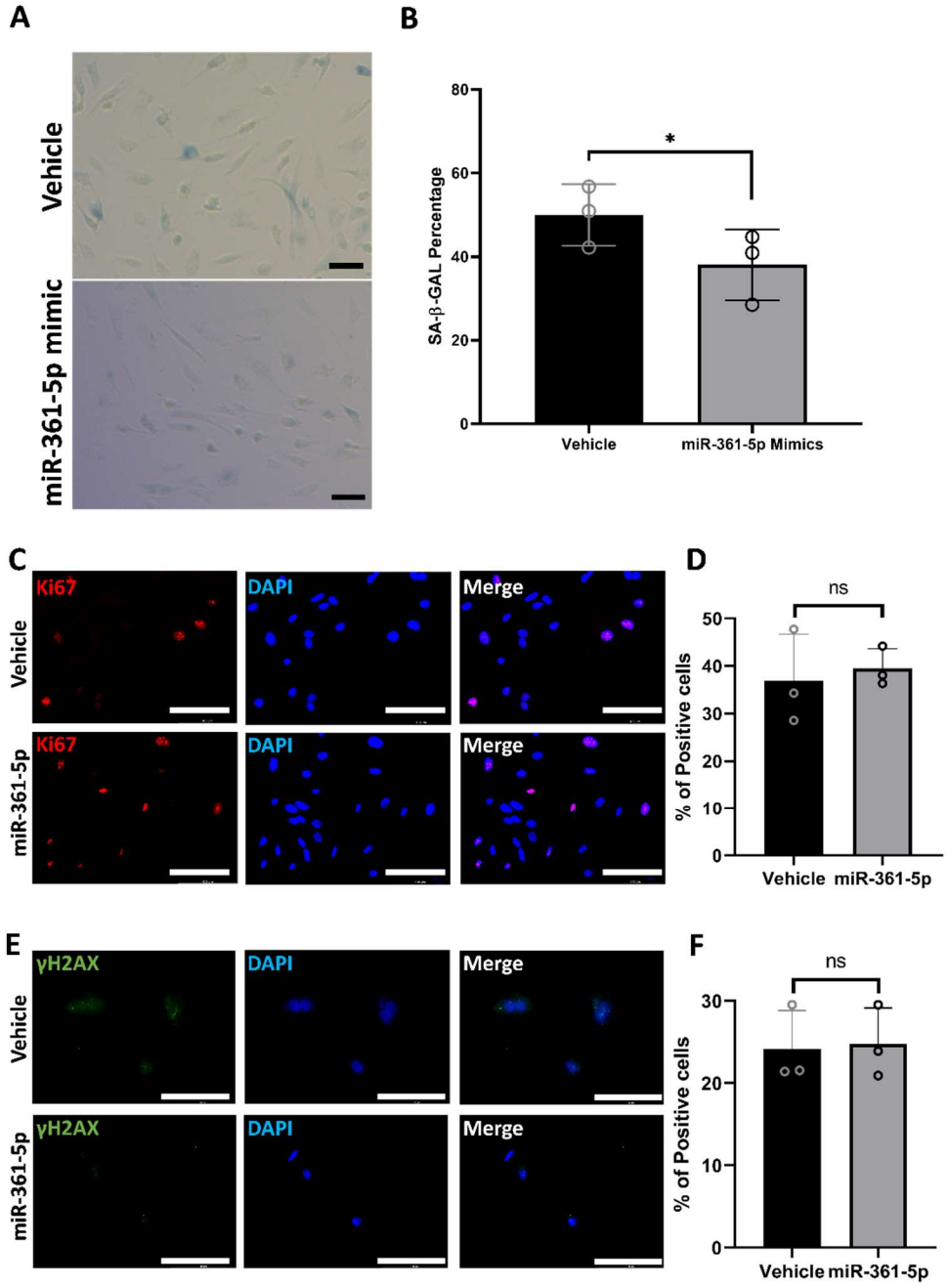
A
Vehicle
miR-361-5p mimic
B
SA-β-GAL Percentage
80
60
40
20
0
*
Vehicle
miR-361-5p Mimics
C
Ki67
DAPI
Merge
Vehicle
miR-361-5p
D
ns
% of Positive cells
50
40
30
20
10
0
Vehicle
miR-361-5p
E
γH2AX
DAPI
Merge
Vehicle
miR-361-5p
F
ns
% of Positive cells
30
20
10
0
Vehicle
miR-361-5p

Figure 6

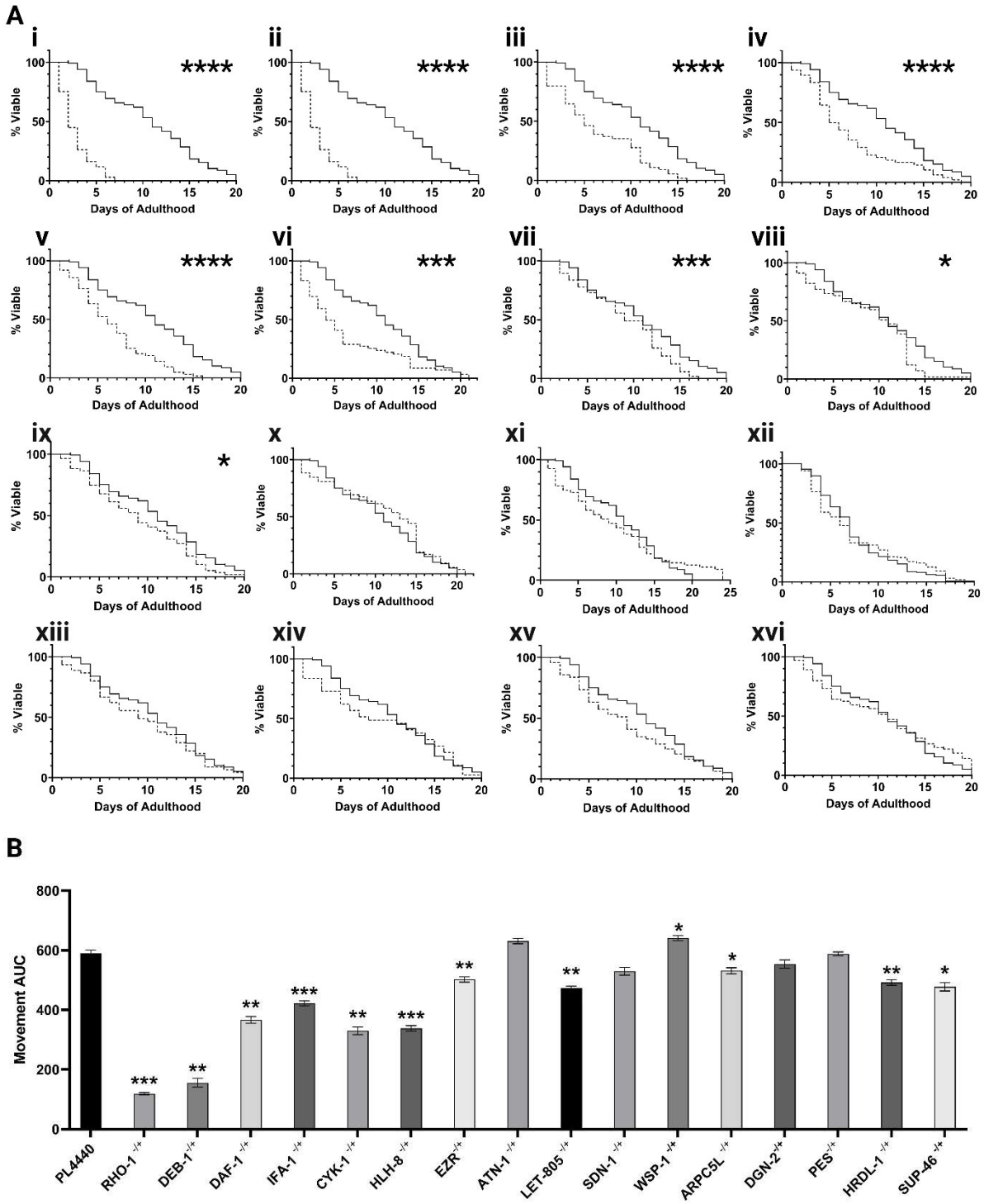
A
i
ii
iii
iv
v
vi
vii
viii
ix
x
xi
xii
xiii
xiv
xv
xvi
% Viable
Days of Adulthood
****
***
*
B
Movement AUC
PL4440
RHO-1 -/+
DEB-1 -/+
DAF-1 -/+
IFA-1 -/+
CYK-1 -/+
HLH-8 -/+
EZR -/+
ATN-1 -/+
LET-805 -/+
SDN-1 -/+
WSP-1 -/+
ARPC5L -/+
DGN-2 -/+
PES -/+
HRDL-1 -/+
SUP-46 -/+

Appendix IX: List of Publications

This is the list of publications of thesis author:

Manni, Emad, Nicola Jeffery, David Chambers, Luke Slade, Timothy Etheridge, and Lorna W Harries. 2023. “An Evaluation of the Role of MiR-361-5p in Senescence and Systemic Ageing.” *Experimental Gerontology* 174 (April): 112127. https://doi.org/10.1016/j.exger.2023.112127.

Roscoe, S., **Manni, E.**, Roberts, M., & Ananvoranich, S. (2020). Formation of mRNP granules in Toxoplasma gondii during the lytic cycle. *Molecular and Biochemical Parasitology*, *242*, 111349. https://doi.org/10.1016/j.molbiopara.2020.111349

Abdelhameed, M., Aly, S., Maity, P., **Manni, E.**, Mohammed, O. F., & Charpentier, P. A. (2019). Impact of the chemical nature and position of spacers on controlling the optical properties of silicon quantum dots. *Physical Chemistry Chemical Physics : PCCP*, *21*(31), 17096–17108. https://doi.org/10.1039/c9cp03537k

Chung, C. Z., Balasuriya, N., **Manni, E.**, Liu, X., Li, S. S.-C., O’Donoghue, P., & Heinemann, I. U. (2019). Gld2 activity is regulated by phosphorylation in the N-terminal domain. *RNA Biology*, *16*(8), 1022–1033. https://doi.org/10.1080/15476286.2019.1608754

Turk, M. A., Chung, C. Z., **Manni, E.**, Zukowski, S. A., Engineer, A., Badakhshi, Y., … Heinemann, I. U. (2018). MiRAR — miRNA activity reporter for living cells. *Gene*. https://doi.org/10.3390/genes9060305

Crater, A. K., **Manni, E.**, & Ananvoranich, S. (2015). Utilization of inherent mirnas in functional analyses of toxoplasma gondii genes. *Journal of Microbiological Methods*, *108*, 92–102. https://doi.org/10.1016/j.mimet.2014.11.014